THE INTERPLAY BETWEEN MICROBIAL DYSBIOSIS AND IMMUNE DYSFUNCTION WITH AGE

Netusha Thevaranjan

McMaster University, thevan2@mcmaster.ca

THE INTERPLAY BETWEEN MICROBIAL DYSBIOSIS AND IMMUNE DYSFUNCTION WITH AGE

BY

NETUSHA THEVARANJAN, B.SC.

A Thesis

Submitted to the School of Graduate Studies in

Partial Fulfillment of the Requirements

For the Degree

Master of Science

McMaster University

MASTER OF SCIENCE (2016) **McMaster University**

Medical Sciences (Infection and Immunity) **Hamilton, ON, Canada**

TITLE: The interplay between gut microbial dysbiosis and immune dysfunction with age

AUTHOR: Netusha Thevaranjan, B.Sc. (McMaster University, Hamilton, Ontario, Canada)

SUPERVISOR: Dr. Dawn M.E. Bowdish

NUMBER OF PAGES: 195

Abstract

It is well known that the elderly often manifest chronic low-grade inflammation. This phenomenon, called "inflamm-aging," is postulated to contribute to increased susceptibility towards infectious diseases and an overall increase in frailty. We have proposed examining the gut microbiome as a potential mediator of these changes. Gut microbial communities influence the host immune system; often dictating an individual's health status. Thus, harmful gut microbiome changes, termed dysbiosis, are associated with poor health in the elderly. We first sought to understand the key immunological, physiological and microbiome changes occurring with age (Chapter 3). Our data reveals immune impairments in aged mice, with increased intestinal permeability, systemic inflammation and alterations in the functions of myeloid cell populations. However, our aged germ-free (GF) mice are protected from these outcomes, indicating that the old microbiome may play a strong role in these age-associated impairments. To study this further, we have colonized young and old GF mice with the "young" or "old" microbiota in order to determine whether the relationship between microbial dysbiosis with age and health status is correlative or causative (Chapter 4). Interestingly, young GF mice colonized with old microbiota have significantly increased permeability, systemic inflammation and an influx of Ly6C^{high} monocytes when compared to those colonized with the young microbiota. By using transgenic mice (TNF$^{-/-}$ mice), or by reducing systemic TNF levels via therapeutics, we were able to reduce some aspects

of microbial dysbiosis and age-associated inflammation (Chapter 5). Our data suggests that harmful changes to the gut microbiome composition with age initiate a cycle of negative events that ultimately result in increased inflammatory myeloid cell recruitment, increased intestinal permeability and an overall increase in systemic inflammation in old mice. By identifying these key changes, we can work towards developing effective therapeutics that promotes healthy aging and protection against infectious diseases.

Acknowledgements

I have been a part of the Bowdish Laboratory for four years now and the experiences that I have gathered along with the wonderful people that I have met will forever be cherished. Although the first couple months here involved a huge learning curve, I had an enormous amount of support and guidance from my supervisor and fellow lab members. Having Dr. Bowdish as my supervisor was a true gift as she was always patient, encouraging and supportive. Whether it was praising my successes or providing feedback on my failures, I would not have come this far without her guidance. By providing me with the opportunity to leave my comfort zone and present at lab meetings as well as national and international conferences, I was able to build my confidence and present my work with ease. With her support, I have been involved in a number of publications that are either in submission or accepted. By giving me the opportunity to expand my project in aspects that interested me, and providing me with unlimited resources, I believe that I have experienced a truly fulfilling Master's degree.

I must also thank my committee members, Dr. Mike Surette and Dr. Elena Verdu. They have both provided me with enormous support and feedback during my committee meetings. Their helpful questions and suggestions always encouraged me to expand my knowledge on a variety of topics. Dr. Surette has supported me like I was one of his own students, by providing with helpful advice on data analysis and experimental design. He has also helped with manuscript edits to help me present

my best work and has allowed me to use his laboratory resources on numerous occasions. Dr. Elena Verdu has also played a key role in all of the successes I have experienced throughout my Master's degree. Her expertise helped us better design germ-free mouse experiments and edit manuscripts to ensure success. She has also been extremely generous in allowing us to use her laboratory resources, space and personnel for our experiments, which I am forever grateful for.

My fellow lab members have also been a huge support as for without them; I would not have enjoyed working in this laboratory setting as much as I did. They were all so kind and patient while I learned new techniques and would always offer me their time if I needed help. I must especially thank Patrick Schenck as he played an enormous role during each of my large mouse experiments and was always willing to stay long hours to help. Even though we started early in the morning, he would always show up with a positive attitude, some puns and many "fun-facts of the day" to help us get through a stressful day. I must also thank Avee Naidoo and Dessi Loukov for their helpful suggestions and assistance during experiments, and for patiently teaching me flow cytometry staining and analysis. Finally, I must thank the remainder of the Bowdish lab for their enormous support. I have met a huge group of friends and shared numerous memories that I will never forget.

Finally, I must thank those individuals that played key roles throughout the progress of my project. I thank Laura Rossi and Michelle Shah for patiently helping me through all the obstacles I encountered during my lab work. They helped answer questions and facilitated all of my sequencing experiments. Jen Jury from the Verdu

Lab has also been a tremendous help throughout my Master's degree. Even though I am not a member of her lab, she always took time out of her schedule to help me during experiments. I must thank Fiona Whelan and Jake Szamosi for patiently helping me understand and troubleshoot bioinformatic analyses. Finally, I must thank Dr. Mark McDermott for providing me with guidance throughout my thesis and dedicating so much of his personal time towards helping me.

I must also thank the McMaster Immunology Research Center and the School of Graduate Studies for providing me with this opportunity as I have gained so many valuable experiences and memories throughout the past years and am positive that these experiences will aid me in my future endeavors as well.

List of Figures

List of Tables

List of Abbreviations

The following abbreviations were used in addition to those abbreviations commonly accepted for units of measure and quantities.

Ab	Antibody
APC	Antigen-presenting cell
CCR	C-C chemokine receptor
CFU	Colony forming units
CRP	C-reactive protein
DC	Dendritic cell
DNA	Deoxyribonucleic acid
DSS	Dextran sulfate sodium
DTT	Dithiothreitol
EDTA	Ethylene Diamine Triacetic Acid
ELISA	Enzyme-linked immunosorbent assay
FBS	Fetal bovine serum
GALT	Gut-associated lymphoid tissue
GF	Germ-free
HEPES	4-(2-hydroxyethyl)-1-piperazineethanesulfonic acid
HIV	Human immunodeficiency virus
IBD	Intestinal bowel disease
IFN	Interferon
Ig	Immunoglobulin
IL	Interleukin
i.p.	Intraperitoneal
i.n.	Intranasal
KO	Knockout

LPS	Lipopolysaccharide
Ly6C	Lymphocyte antigen 6 complex
MALT	Mucosal associated lymphoid tissue
MCP	Macrophage chemoattractant protein
MDP	Muramyl dipeptide
MHC	Major histocompatibility complex
MIP	Macrophage inflammatory protein
mo	Month old
NF- κb	Nuclear factor kappa-light-chain-enhancer of activated B cells
NK	Natural killer
NO	Nitric oxide
PBS	Phosphate-buffered saline
PGE	Prostaglandin
RANTES	Regulated on Activation, Normal T Expressed and Secreted
ROS	Reactive oxygen species
rRNA	Ribsomal ribonucleic acid
SPF	Specific pathogen free
TLR	Toll-like receptor
TNF	Tumor necrosis factor
URT	Upper respiratory tract
WT	Wildtype

Declaration of Academic Achievement

In accordance with the *Guide for the Preparation of Theses at McMaster University,* this Master's thesis is presented with three chapters. The data and analysis present in Chapters 3, 4 and 5 represent work that I have completed between May 2014 and June 2016. Many of these experiments required assistance from fellow lab members and collaborators. As a result, in the following pages, I have outlined my contributions.

Chapter 3 Characterizing the physiological and microbiological changes in aging SPF mice

I completed all of the experiments mentioned in this chapter with a few exceptions. Dr. Alicja Puchta initially completed Figure 4B and I reproduced the data at a later time point. All of the data pertaining to Ussing chambers were completed with the assistance of Jen Jury. In Figure 6, Dr. Christian Schultz completed the liposomal clodronate injections. Dr. Dawn Bowdish and myself designed all experiments.

Chapter 4 Deciphering the role of age versus the composition of the microbiome physiological and immunological outcomes

I completed the majority of the experiments present in chapter 4 with the following exceptions. The images and data collected in Figure 8A and 8B were completed by Dr. Puchta. Patrick Schenck assisted with tissue processing during all of the experiments involving germ-free colonizations. The experiments and data analysis following Figure 9A and 10 were completed by Avee Naidoo. A. Naidoo completed the i.p injections for the NK cell depletion experiment carried out in Figure 11. Following the

injections, I completed the tissue collection, flow cytometry staining and data analysis for the experiment. All of the 16S Illumina sequencing data present throughout the chapters were completed in collaboration with the McMaster Sequencing Facility and Laura Rossi from the Surette Laboratory. I completed the analyses after obtaining the files from these individuals. Figure 16 was completed in collaboration with the Schertzer laboratory. Brittany Duggan from the Schertzer laboratory completed the insulin ELISA. Processing of the lung tissue in Figure 19B for flow cytometry was carried out by P. Schenck and the staining and data analysis was completed by me. Dr. Bowdish and myself designed all experiments.

Chapter 5 Combatting age-associated inflammatory defects in old mice by targeting the pro-inflammatory cytokine, TNF

I completed all of the experiments carried out in Chapter 5. P. Schenck assisted in the processing of tissues for histology, permeability studies and flow cytometry. I reproduced the data presented in Figure 25 that was originally completed by Dr. Puchta. Dr. Dawn Bowdish, Dr. Puchta and myself designed all experiments.

Appendix I *Streptococcus pneumoniae* Colonization Disrupts the Microbial Community within the Upper Respiratory Tract of Aging Mice

This manuscript was published in Infection and Immunity in 2016 and I am the primary author. The samples used for the preparation of this manuscript were obtained from experiments completed by Dr. Alicja Puchta. Dr. Dawn Bowdish, Dr. Alicja Puchta and myself carried out the experimental design. I completed the tissue

processing and analysis with the following exceptions. Figure 1A and parts of Figure 3 were completed by Fiona Whelan. Dr. Bowdish and myself wrote the manuscript. Dr. Bowdish, Dr. Surette and Fiona Whelan aided in the editing and submission of the manuscript.

Appendix II New evidence of Metchnikoff's hypothesis of aging: microbiota drive age-associated immune impairment

The data presented in this manuscript is a compilation of experiments presented in Chapters 3, 4 and 5 along with work completed by Dr. Puchta. Dr. Puchta and myself are the primary authors for this manuscript. Dr Bowdish, Dr. Pucta and myself conceived the ideas and wrote this manuscript. I contributed to portions of each of the figures. Dr. Puchta completed all of the *in vitro* experiments presented in this manuscript with the help of other members of the laboratory (Dr. Chris Verschoor, Avee Naidoo and Dessi Loukov). I completed the majority of murine experiments. I also completed the analysis for the 16S rRNA sequencing data presented in collaboration with Jake Szamosi from the Surette Laboratory. Dr. Elena Verdu provided us with the germ-free mouse colony and Jen Jury helped us completed the permeability assays. Dr. Bowdish, Dr. Surette, Dr. Verdu and Dr. Davidson provided guidance for experimental design and manuscript edits for submission. This manuscript is currently under revision.

Table of Contents

Chapter 1. Introduction

A) IMMUNOSENESCENCE

Aging and immune dysfunction

Immunosenescence is a growing topic of interest as the elderly population continues to expand within our community. In fact, the number of Americans >65 years old is estimated to double between 2000 and 2040 with an estimated growth in this age group from 12% to 20% within this time frame (1). Furthermore, by the year 2050, the number of individuals greater than 85 years old is expected to increase by an estimated 350% (2). This is of interest to us because these individuals are also at an increased risk of requiring health care services. This increase can be largely attributed to the decrease in fertility in most countries, along with the increase lifespan of elderly. As a result, we can expect an increase in health care costs related to this demographic shift. These shifts in the demographic population affect the incidence of both acute and chronic inflammatory conditions in this population. The elderly have increased susceptibility towards infectious diseases. For example, with regards to pneumococcal pneumonia, elderly individuals (>65 years) accounted for 60% of hospitalizations in United States in 2004 (1). Pneumococcal infections have detrimental outcomes in the elderly population and it was estimated that the 2004 costs for treating patients with such infections totaled 3.5 billion dollars (3). Epidemiologic studies have shown that the aging population will continue to increase and as a result, we can expect an increased burden on the health care system in the future. In order to prepare for these changes, it is important to study the changes that occur within the elderly in order to understand

and ultimately prevent some of the detrimental immune changes that occur with age.

The aging process is accompanied by a number of negative consequences including elevated levels of low-grade chronic inflammation (4), thymic involution, microbial dysbiosis (5, 6), and attenuated immune responses, resulting in an overall deterioration in the ability to combat infectious diseases (7). This process, coined immunosenescence, is believed to contribute to many age-related pathologies and as such, is a key phenomenon to study with regards to the elderly population. In addition to immune-related changes contributing to disease vulnerability, the elderly encounter a number of other risk factors as well. For instance, nursing home residents are at an increased risk of developing infections due to their close contact with other "at-risk" individuals. Furthermore, tube-fed elderly patients are an increased risk of mortality due to pneumonia when compared to those who are orally fed (8). In hospitals, the elderly have a higher chance of developing ventilator-associated pneumonia. Finally, functional ability also plays a role in the predisposition towards infectious diseases. Although there are several risk factors for disease, the research described in this thesis will be focused on increased infection susceptibility caused by the onset of immune-related changes with age.

Numerous studies have investigated the changes in immune parameters with age. Although some of these results are contradictory, the general consensus is that there is an overall increase in chronic systemic inflammation, termed "inflamm-aging," and this ultimately results in the overall physical decline with age (9). In fact,

serological changes seen with age include a 2-4 fold increase in inflammatory mediators including pro- inflammatory cytokines and acute phase proteins (10). These changes are believed to contribute to the immune dysfunction seen within the elderly. Indeed, our laboratory has demonstrated impairment of immune functions in aged mice, judged by increased plasma levels of IL-6, decreased macrophage function, increased intestinal permeability, and increased systemic inflammation (11) (Appendix II). Our data suggests that this phenomenon, termed age- associated inflammation (AAI), contributes to immune dysfunction with age.

The aging process is accompanied with increased levels of inflammatory mediators including tumor necrosis factor-alpha (TNF), interleukin (IL)-6, and interleukin (IL)-1 (12). These increases appear to correlate with the increased frailty and incidence of diseases including dementia, atherosclerosis, type 2 diabetes, Parkinson's disease and much more (8). As well, these cytokines have been shown to further upregulate production of chemokines including RANTES, MIP-1α, IL-8, MCP-1 and C reactive protein (CRP) (12). TNF and IL-1 have been studied in detail as they play crucial roles within the elderly. They are involved in the upregulation of IL-6 and also play key roles in energy metabolism and acute responses to infections (13). IL-6 has been shown to be involved with bone reabsorption, and has been previously identified to induce osteoporosis in animal models. As well, it produces acute phase proteins such as CRP (13). IL-6 is suppressed by estrogen and androgens. Consequently, it is believed that the increase in IL-6 observed within the elderly can partially be explained by the decrease in sex hormones with age (13).

TNF on the other hand is a pro-inflammatory cytokine that is produced mainly by macrophages and monocytes (14). It plays major roles within the body, particularly in terms of fighting against infectious diseases (15, 16). As such, TNF is an important immune modulator within the body as it has roles with regards to cytotoxic defense against tumours, infectious disease control, growth modulation and helps with cellular differentiation. For that reason, TNF has often been referred to as a pleiotropic cytokine (14). However, if present at continually high concentrations, as measured in our elderly populations, it can be detrimental towards cell function (15). Excessive TNF can play a role in the development of cachexia (or wasting syndrome), and lead to muscle atrophy, weakness and frailty within the elderly.

B) THE IMPORTANCE OF THE GUT MICROBIOME

The structure and function of the gut

The human gastrointestinal tract extends from the mouth to the anus and is able to release a number of enzymes and hormones, aid in the process of food digestion and nutrient absorption and contains a number of protective factors to help prevent the onset of infection. The gut is composed for four main components: the esophagus, the stomach, the small intestine and the large intestine. Along with the gut-associated lymphoid tissue, the gastrointestinal tract is also home to a diverse microbiome. The gut is the most heavily colonized region of the body and is home to approximately 1000 different bacterial species that encode more than 5 million genes (17). The upper intestines are approximated to contain around 10^1-

10^3 cells per gram and the colon is more densely inhabited, containing between 10^{11}-10^{12} bacteria per gram (18). *Firmicutes* (including *Lactobacillus, Clostridium,* and *Enterococcus*) and *Bacteroidetes* (including *Bacteroides*) phyla comprise the majority of bacteria found in the gut. Other phylas like *Actinobacteria, Proteobacteria, Fusobacteria, Verrucomicrobia,* and *Cyanobacteria* are present at lower concentrations. These bacteria function to maintain health and integrity within the gut (18).

The intestinal epithelial barrier functions to contain the bacterial contents in the luminal environment of the GI tract, regulate digestive processes, and promote absorption of nutrients and electrolytes (18, 19).The epithelial barrier contains a number of key features that help maintain these functions. For example the mucus layer contains antimicrobial peptides and secretory immunoglobulin (Ig) A that function to limit the contact between bacteria inside the lumen and immune cells present along the barrier and in mucosal tissues. Furthermore, the epithelial barrier is composed of a monolayer of epithelial cells that are connected via tight junctions, adheren junctions and desmosomes (19). Tight junction proteins are composed of protein complexes containing transmembrane proteins like claudins and occludin (19). They are located at the apical end of intestinal epithelial cells (closer to the gut lumen) (19). Tight junctions play crucial roles in determining the selective paracellular permeability of the epithelial barrier to solutes, ions and water molecules.

Structural changes within the gut with age

The intestinal epithelial layer plays a crucial barrier role as it is able to selectively allow the passage of nutrients and water while preventing antigens and the enteric flora from entering circulation to cause immune activation (20). However, the onset of a number of diseases can cause the integrity of the gut epithelium to be impaired, allowing it to become leaky and cause systemic inflammation (21). The changes in gut integrity with age are an important aspect to understand for a number of reasons. Firstly, increases in intestinal permeability have been proposed to contribute to the increased inflammation observed within the elderly (20). Since this phenomenon has been linked to increasing immune dysfunction within these individuals, it is important to understand how permeability changes with age (20). Second, increases in intestinal permeability would affect how aged individuals are able to absorb the drugs and nutrients they consume (20). Understanding how the gut becomes permeable will allow for the creation of more effective drugs and dietary supplements. Finally, if increases in intestinal permeability promote systemic inflammation, this can increase the risk towards a number of cardiovascular- related diseases. For example, in the context of obesity, mild inflammation caused by CRP increases the risk of suffering from a cardiac arrest or stroke by 2-folds (22). In the context of aging however, approximately 50% of elderly individuals suffer from low-grade inflammation (20). As a result it is important to understand how permeability changes with age and how this may affect systemic inflammation within these individuals. A disruption in the gut barrier

integrity can allow for the translocation of endotoxins, pro-inflammatory molecules and antigens to enter circulation and potentially trigger systemic inflammation as well (23). If the increase in intestinal permeability is contributing to the low-grade inflammation within the elderly, it is one aspect that should be targeted in terms of therapies.

Although some studies have examined the age-related changes in intestinal permeability using animal models, there is still much uncertainty around this topic. One particular study was conducted using baboons and it suggests that gastrointestinal dysfunction might occur within the elderly as a consequence of increased intestinal permeability. Colonic tissue isolated from old baboons had increased permeability, decreased amounts of tight junction proteins and had an increase in pro-inflammatory cytokines. In humans however, there are only four major studies completed to date (24–26). However, these studies are limited in the number of participants included and they mainly focused on the small intestinal permeability changes with age. As a result, it is difficult to definitively draw conclusions to answer this question. Therefore, the current data available to understand whether or not intestinal permeability increases with age and how this process may be mediated is limited. By understanding this phenomenon, we can begin to understand the potential routes to keep in mind when trying to reduce systemic inflammation within the elderly.

The role of the intestinal microbiome

Gut microbiome compositions have profound effects on an individual's health

(27). It is involved with the regulation of metabolic and physiological functions and as well, contributes to the overall mucosal immunity within the body (5). The microbiome helps extract energy from food sources and produces important nutrients that the host would not be able to produce otherwise, including short-chain fatty acids, certain vitamins and amino acids (5). Aside from producing helpful substances within the host, the intestinal microbiome also helps defend against harmful pathogens by producing antimicrobial compounds and providing a rigid intestinal barrier to prevent the colonization of pathogenic bacteria (5). Furthermore, the intestinal microbiome plays a key role in the production of IgA antibodies. These antibodies are necessary to help keep bacteria within the intestinal lumen to prevent leakage and tissue damage (28).

The temporal stability and variability of the gut microbiome with age

At approximately 36 months of age, the microbiome undergoes one final temporal shift in the composition of the microbiome. This shift is largely due to the introduction of novel food items to the diet. However, during adulthood, the gut microbiome composition has been characterized as relatively stable over time. In fact, unless there is a major disturbance, the overall composition does not change (29). A study conducted by Faith et al., followed 37 adults up to five years in order to study the stability of the microbiome over time (30). They concluded that after one year into the study, approximately 70% of the microbial composition remained stable. At the end of five years, only a few other recorded changes occurred (30). Furthermore, they found more variability in the microbiome composition of samples

taken in shorter time frames. However, when the overall composition was studied over a longer time period, stability was observed (30). The major factors known to temporarily alter the gut microbiome include changes in the diet, weight loss, physiological changes, drug administration or living conditions (29). In general, the adult gut microbiome is fairly resilient to changes and remain stable until the elderly years.

The changes in the gut microbiome composition in the elderly often correlate with their health status. In fact, the decline in health has been linked to the reduction in the stability and diversity of the gut microbiome (29, 31). Resilience in the gut microbiome composition is lost with age as the microbiome becomes largely skewed based on factors such as frailty, co-morbidities, use of antibiotics and residence (community-dwellers or residents in long-term care facilities) (29, 32).

Gut microbiome changes in the elderly

The intestinal microbiota undergoes drastic changes near the beginning and end of life. Children are exposed to microbial colonization immediately following birth. During the initial stages of life, the fecal microbiome is primarily composed of *Bifidobacteria* (28). Following weaning and the introduction of a solid food diet, their microbiome continues to diversify and expand until approximately the age of two, at which point, the microbial community is similar to that observed in adults (33). The adult microbiome has been described to be fairly stable in its composition and begins to change once again within the elderly. At this stage, harmful intestinal microbiome changes, termed dysbiosis, alter the host's susceptibility to infectious

disease (33–35). These changes have been associated with some of the negative consequences seen within the elderly including increased frailty and inflammation (36). For instance, elderly individuals with reduced levels of *Lactobacilli, Bacteroides, Bifidobacteria* and *Prevotella* groups tended to score higher on the frailty index. These individuals also had an increased abundance of *Enterobacteriaceae* (28). As well, the general consensus is that there is an overall decrease in the amount of facultative anaerobes and an overall increase in obligate anaerobes within fecal samples of aged individuals (Figure 1) (37). They have been shown to contain a larger abundance of *Enterobacteriacea* and other endotoxin-producing, Gram-negative bacteria (36). The composition of the intestinal microbiome can amplify or dampen local and systemic inflammation depending on the specific microbes present (36). For example, the presence of Bifidobacterial species within feces has been correlated with decreased levels of serum IL-10 and TNF (33). Thus, changes within the microbial community might contribute to the increased inflammation observed within elderly individuals (36).

Furthermore, several studies have suggested that there is an increase in bacterial/ endotoxin translocation with age as a result of a deteriorated intestinal barrier. This may also be allowing for increased translocation of bacterial products from the lumen of the GI tract into systemic circulation. This phenomenon would in turn lead to the activation of the immune system, and consequent production of a number of pro-inflammatory cytokines and molecules including TNF, IL-1, IL-6 and NO. Continual bacterial translocation and immune activation within the elderly

could lead to systemic inflammation and ultimately cause tissue destruction and overall immune dysfunction (38).

Development and immune deficiencies in germ-free mice

Since the development of germ-free mice in the 1950s, researchers have used them widely to compare regularly housed mice to those raised without the influence of any microbiome. Germ-free mice allow researchers to manually introduce one or two specific species or one entire microbial composition in order to understand what changes are specifically being caused by the microbiome (39, 40). In fact, by 1959, researchers had germ-free forms of mice, rats, guinea pigs, and chicks (39). Although being extremely beneficial in understanding the role of the microbiome in disease progression, germ-free mice do have their drawbacks, both from a developmental and immunological perspective.

The indigenous bacteria in the gut have co-evolved with the immune system in order to provide robust immune protection against pathogens and enhance survival. Therefore, it is of no surprise that germ-free mice inherently experience a number of developmental defects that contribute to alterations in their innate and adaptive immune responses. A number of changes have been identified in the development of the gut-associated lymphoid tissue (GALT) (41). With regards to the innate immune system, paneth cells from germ-free mice have reduced production of anti-microbial peptides like angiogenin 4 and REG3 y (28, 41). These proteins have bactericidal activity and can target specific groups of bacteria. For example, angiogenin 4 preferentially binds to gram-positive bacteria (28). However, these

deficiencies are reversible as conventionalized germ-free mice restore the anti-microbial peptide secretions soon after colonization. Commensal bacteria also play a strong role in the development of the adaptive immune system as germ-free mice have fewer peyers patches in the small intestine, thinner lamina propria and fewer plasma cells in the germinal center. These changes culminate to a reduction in antibody production (particularly with regards to IgA) and reduced/altered function of adaptive immune cells. In particular, germ-free mice have B cell developmental defects, fewer $CD8^+$ with reduced cytotoxicity and fewer $CD4^+$ cells which ultimately results in fewer TH17 cells as well (41). Interestingly, these defects in germ-free mice cannot be completely reversed by colonization with one particular species from the commensal microbiome. This suggests that in fact, a large and diverse microbiome composition is necessary to ensure proper immune development and function in the gut (28).

C) MONOCYTE/MACROPHAGE FUNCTION IN THE GUT

Gut-associated lymphoid tissue (GALT)

The mucosal surfaces within our body are the primary route of infection used by many pathogens. In particular, the gastrointestinal tract has thin, permeable membranes to allow for food absorption. However, this also increases its vulnerability towards infection. The gut is constantly being exposed to a number of foreign antigens in the form of food antigens. As well, it contains a diverse microbiota composed of approximately 10^{14} commensal bacteria that are able to reside within this region. As a result, it is important that an effective immune

response is present within this region to effectively differentiate between harmful and harmless substances (42). Within the gut, the mucosa-associated lymphoid tissues are referred to as the gut-associated lymphoid tissue (GALT). Major sites for the induction of immune responses within the gut occur within the Peyer's patches, the appendix and lymphoid follicles near the large intestine and rectum. In particular, the peyer's patches are follicles of immune cells present on the mucosa of the ileum. The cellular composition of murine Peyer's patches include mainly B cells, but also T cells, dendritic cells, macrophages and polymorphonuclear neutrophils (43).

Colonic macrophages and monocytes

The intestine encounters more antigens than any other part of the body and therefore it is no surprise that it is home to the largest compartment of the immune system. Tissue resident macrophages throughout the body often stem from the progenitors arising from the yolk sac and/or fetal liver during embryonic development. This is the case for resident macrophages found within the liver, lungs, peritoneal cavity and central nervous system. In these regions, circulating blood monocytes do not play a strong role in giving rise to macrophages (44). In the intestine however, recent publications have suggested that during inflammation monocytes are able to replenish the intestinal macrophage pool (45). In fact, monocytes can have a dual role in the intestines. During a healthy state, monocytes often differentiate into tissue macrophages that produce IL-10, have good

phagocytic ability and are resistant to TLR stimulation (features that are characteristic of intestinal macrophages under a non-inflamed state) (46). Under these circumstances, monocytes differentiate into CX3CR1+ macrophages and contribute to the overall balance of immune cells within the gut. However, during inflammation, a particular subset of monocytes called Ly6C^{high} monocytes can also be recruited. These monocytes, often called "inflammatory monocytes," preferentially migrate to the inflamed tissue in a CCR2-dependent manner, are able to contribute to local or systemic inflammation and are more likely to differentiate into pro-inflammatory effector cells (47, 48). Furthermore, during inflammation macrophage phenotype and function can also be altered to express increased numbers of TLR, CD14, co-stimulatory molecules and other pro-inflammatory receptors (49). At this time, intestinal macrophages may produce large quantities of pro-inflammatory cytokines and mediators like TNF, IL-1, IL-6, nitric oxide and reactive oxygen species (49).

D) Colonization with *Streptococcus pneumoniae*

The bacterium

Streptococcus pneumoniae is a gram-positive, alpha-hemolytic, facultative anaerobe that is commonly found within the upper respiratory tract (URT) (50). Although nasal passage colonization is often asymptomatic, access to the airways can result in pneumonia, with further dissemination causing invasive pneumococcal disease (i.e., otitis media, bacteremia, and meningitis) (51). Colonization rates are highest among young children and the elderly (52). Since colonization precedes

infection, it is important to understand the factors that either enhance or promote colonization in these cohorts as this may be the most effective way to limit infections and improve herd immunity (52).

Colonization outcomes with age

Children are highly susceptible to pneumococcal colonization and infection. Approximately one million children (<5 years of age) succumb to pneumococcal related infections annually (52). In fact, most children are colonized by this bacterium by 3 months of age (53). Colonization with *S. pneumoniae* tends to increase rapidly throughout the first few years of life and then begins to decline after about the age of 5 (53). Many factors contribute to the nasopharyngeal carriage rates and thus, pneumococcal carriage among children can range between 5-89%. Some factors that contribute to these differences include age, ethnicity, residence, and differences in sampling techniques (53). On average approximately 53% of children carry *S. pneumoniae* within their URT, as opposed to only 4-11% of adults (54, 55). Interestingly, even though carriage rates remain low in the elderly, colonization of the bacterium within the URT of the elderly likely leads to disease progression and infection. This makes the elderly population vulnerable to pneumococcal infections. In fact, elderly individuals (>65 years) have a pneumococcal infection incidence rate between 25-44 per 1000 population every year, this is approximately four times higher than the incidence in younger adults (56).

Age-associated URT microbiome changes that impact colonization

The elderly are at a increased rate of acquiring pneumococcal infections, particularly because of the gradual deterioration of their immune system with age, a process termed immunosenescence (4). We have recently published a study that focused on identifying the microbial communities present in the URT in order to identify their role against infectious diseases. In particular, we hypothesized that the composition of the upper respiratory tract (URT) microbiota changes with age and subsequently can contribute to sustained colonization and inefficient clearance of *S. pneumoniae* (57) *(*Appendix I). The publication is present in this thesis (Appendix 1). Briefly, the findings from our study indicates that alterations in the URT microbiome with age impact the ability of old mice to clear *S. pneumoniae* in an effective manner. In fact, after 21 days of colonization with the bacterium, we found that young mice were able to clear the majority of the bacteria. However, old mice still contained high levels of *S. pneumoniae* within their nasal wash. Furthermore, we found that upon colonization, *S. pneumoniae* is able to interact with other resident populations within the host in a synergistic or competitive manner to impact their abundance as well. These data suggest that studying the host-microbe interactions at the site of entry may be important as the resident microbiome may play a key role in facilitating colonization and disease progression in the elderly.

CENTRAL QUESTION:

Does chronic age-associated inflammation alter the intestinal microbiome, to increase microbial dysbiosis and ultimately result in immune dysfunction within the elderly?

HYPOTHESIS:

Gut microbial communities influence the host immune system; often dictating an individual's health status. Thus, harmful gut microbiome changes, termed dysbiosis, are associated with poor health in the elderly. Our pilot data reveals immune impairments in aged mice, with increased paracellular permeability, systemic inflammation and alterations in the phenotype and function of myeloid-derived cells. However, our aged germ-free (GF) mice are protected from these outcomes, thereby indicating that the old microbiome plays a strong role in these age-associated immune impairments. **I hypothesize that microbial dysbiosis with age contributes to increased intestinal permeability within old mice. Furthermore, age-related microbial dysbiosis contributes to the recruitment of inflammatory monocytes and macrophages within the gut, impairs barrier function and ultimately results in increased bacterial translocation across the intestinal barrier and increased systemic inflammation in old mice.**

Chapter 2. Methods

Mice

C57BL/6J female mice were from The Jackson Laboratory and were housed under specific-pathogen free (SPF) conditions at the McMaster University Central Animal Facility. Young (2-4 month old) and old (18-24 month old) mice were used for the studies. Germ-free mice were housed within the gnotobiotic facility at the McMaster University Central Animal Facility. Germ-free mice were placed on a vitamin enriched diet until they are exported out of the facility. To protect from age-related obesity aging SPF mice are fed with a low protein diet (Teklad Irradiated Global 14% protein Maintenance Diet) and provided with an exercise wheel, as were young controls. Germ-free mice were also placed in the same conditions once exported into SPF conditions. The average weight of a young mouse in this study was 20g+/-1g and the old mice are on average, 27g+/-2.5g. TNF knockout mice ($TNF^{-/-}$) mice (C57BL/6J background) were bred in the barrier unit at the McMaster University Central Animal Facility as previously described (58). All mice were housed in specific pathogen-free conditions. Continual monitoring of the health status of mice was performed (58).

Colonization of germ-free mice

Young and old germ-free (GF) mice were conventionalized with a specific microbiota using the co-housing method. They were individually co-housed with either a young or old SPF mouse for a total of six weeks in order to colonize them with that specific microbiota. Young germ-free mice are individually housed with old SPF mice in order to conventionalize them with the old microbiota. Likewise, old

germ-free mice are co- housed with young SPF mice to conventionalize them with the young microbiota. Control GF mice are also co-housed with either young or old SPF mice. For the first two weeks of colonization, mice remain in their cages without disturbance. Following the two- week period, three fecal pellets are collected from each mouse, every week until sacrifice (Supplementary Figure 1).

Measurements of intestinal permeability

Following four weeks of colonization, a fluorescent (FITC)-dextran gavage is completed on both the GF and SPF mice in order to observe differences in their intestinal permeability. Mice are fasted for four hours in a new cage without food and water. Following the 4-hour fast, mice are orally gavaged with 200 µl of FITC-dextran [80mg/ml in saline]. Four hours after the gavage, mice are bled into heparinized tubes. In order to measure the fluorescence intensity, 25 µl of whole blood is added to 25 µl of PBS. Fluorescence is measured at an excitation wavelength of 493 nm and emission wavelength of 518 nm using the SpectraMax i3 fluorescent plate reader.

In order to examine paracellular permeability within the colon, a portion of the gut is collected. Sections of colon and ileum were excised, opened along the mesenteric border, and mounted in Ussing chambers (World Precision Instruments, Sarasota, Florida). Recordings were performed as described in (59–61). Briefly, tissues were allowed to equilibrate for 15-25 min before baseline values for potential difference (PD) and short circuit current (Isc) were recorded. Tissue conductance (G) was calculated by Ohm's law using the PD and Isc values. Mucosal

to serosal flux of the small inert probe (360 Da) 51-chromium-ethylenediaminetetraacetic acid (^{51}Cr-EDTA) was used to assess paracellular permeability. After equilibration, samples were taken from the serosal buffer and 6µCi/ml ^{51}CR-EDTA was added to the mucosal compartment. A "hot sample" was taken from the mucosal buffer then samples were then taken every 30 minutes from the serosal buffer for 2 hours and counted in a liquid scintillation counter (Beckman). Counts from each 30 mins were averaged and compared to the "hot sample"(100%). Data expressed as mucosal-to-serosal flux (%flux/cm^2/hr). Each sample was completed in duplicates (11).

Flow-cytometry

In order to characterize the phenotype and quantity of immune cells within the gut, lungs and blood, the following monoclonal antibodies were used: F4/80 (APC or BV650), Ly6C (FITC), CD45 (eFluor 450), CD11b (PE-Cy7 or PerCPCy5.5), MHC II (PerCP eFluor 710), CD3 (Alexa Fluor 700 or APC-efluor 780), CD19 (Alexa Fluor 700), NK1.1 (Alexa Fluor 700), CCR2 (PE), CD64 (APC), Zombie (APC efluor 780), IL-6 (PerCP efluor 710) or TNF (BV605) (Supplementary Figure 2). Blood and single cell suspensions of lung were stained according to previously published procedures (58). Briefly, one lobe of the lung was collected and dissociated using the Miltenyi Biotec Lung Dissociation Kit (Cat#: 130-095-927) along with the gentleMACS Octo-Dissociator with Heaters (Cat#: 130-096-427) (58). After complete dissociation of the tissue, live cells were counted using trypan blue and 1x10^6 cells were used for the staining procedure and then processed for flow

cytometry. A gating strategy to distinguishing Ly6C^{high} monocytes in the lungs is provided in Supplementary Figure 3.

In order to characterize the immune cells present within the colon, a protocol was adapted from Dr. John Grainger's laboratory. Briefly, the colon was isolated from the murine gastrointestinal tract, cut open laterally and was washed with cold PBS twice. After thorough washing, it was cut into roughly 1.5 cm sections and placed in cold RPMI media containing 3% fetal bovine serum (FBS), penicillin and streptomycin, HEPES buffer, EDTA and DTT. The tissue was then incubated at 37 degrees while undergoing constant stirring. Following several washing steps, the colons were cut into smaller sections and incubated with digestion enzymes (Liberase) for 30 minutes at 37 °C. After the digestion, the tissues underwent several filtering steps involving 70 µm (3 filtering steps) and 40 µm filters (1 filtering step). Live cells were counted manually using trypan blue and $5x10^5$ cells were stained in a 50 µl volume to analyze using flow cytometry. A complete gating strategy to differentiate between colonic macrophages and monocytes is present in Supplementary Figure 4.

Measurement of plasma cytokines

Plasma levels of TNF and IL-6 were measured using mouse cytokine/chemokine magnetic bead panel (Millipore MCYTOMAG-70K). Plasma samples were collected using heparin as an anti-coagulant. Samples were centrifuged at 1000 xg for 10 minutes within half an hour of collection. Plasma was removed and stored at -80 degrees. Samples were vortexed and centrifuged prior to

use in the assay according to the manufacturer's protocol. The plasma concentrations of these cytokines were then measured using the Luminex 200 analyzer (Millipore).

Analysis of tissue integrity by histology

Histopathological analysis was carried out on samples from the lungs and colon of old WT, TNF KO and germ-free mice, and their young controls. Upon collection in formalin, tissues were paraffin-embedded. Tissue blocks were cut into 4-µm sections that were stained with hematoxylin-eosin (HE). Images were acquired with a Leica DM LB2 microscope at a magnification of 20X and captured using a Leica DFC 280 camera (11). Tissues were blinded and scored for architectural damage and cellular infiltration using previously published standards. In order to quantify the inflammation within the lungs, the total area of the cellular infiltration pockets within the lungs were represented as a percentage of the total lung area.

Antibody administration

Young and old wildtype mice (n=6/group) were treated with either Humira or human IgG isotype control for a total of 3.5 weeks. Intraperitoneal injections were given twice a week at a concentration of 40 ug/g. Before the experiment began, fecal pellets were collected from each mouse in order to be able to study microbiome changes before and after drug treatment. As well, prior to injections, a FITC- dextran gavage was completed in order to compare the differences in intestinal permeability before and after drug treatment. Following completion of the five injections, fecal pellets were collected once again for Illumina sequencing of the 16S rRNA region

and a final FITC-dextran gavage was completed as well. Mice were monitored for a week following the final injection and were sacrificed after a total of 4.5 weeks after the initial injection. Fecal pellets were also collected immediately before sacrifice.

For studies involving NK cell depletions, old wildtype mice (n = 5 mice/group) were given either anti-NK1.1 or an IgG control intraperitoneally. Two back-to-back doses of 200 ug of anti-NK1.1 (BioXcell) or IgG was administered. Following this, one last injection was administered two days later.

DNA extraction from fecal samples

The following protocol was followed to extract DNA from the fecal samples. Guanidine thiocynate (GES) buffer was prepared using 60g of guanidine thiocyanate (Sigma-Aldrich), 20 ml of 0.5M EDTA (pH 8) (Life Technologies), and 20 ml of sterile distilled H_20 (Life Technologies). This preparation was heated with mixing to 65°C, and cooled to room temperature. 1 g of N-lauroyl sarkosine (Sigma Aldrich) was added, the mixture was adjusted to 100 ml, and filter sterilized before use. 2 ml plastic screw top tubes (Fisher Scientific) containing 0.2 g of 0.1 mm glass beads were using for the extractions. After adding 800 µl of 200 mM $NaPO_4$ (pH8) and 100 µl of GES, the samples were added in 120-160 µl aliquots. The samples were homogenized using a bead beader (Mo Bio) for three minutes at 2500 rpm. 50 µl of lysozyme (100 mg/ml in water) (Sigma Aldrich), 50 µl of mutanolysin (10 U/ul) (Sigma Aldrich), and 10 µl of RNase A (10 mg/ml in water) (Qiagen) were added to the homogenized solution for an enzymatic digestion. The samples were vortexed briefly and incubated for 1-1.5 hours in a 37°C waterbath. Following the incubation,

25 µl of sodium dodecyl sulfate (SDS) (25%) (Life Technologies), 25 µl of proteinase K (Sigma Aldrich), and 100 µl of NaCl (5M) were added to each sample. The samples were vortexed briefly and were incubated 0.5-1.5 hours in a 65°C waterbath.

All samples were centrifuged for five minutes at maximum speed (35280 xg) and 900µl of the supernatant was transferred to a 2 ml tube (Diamed). Each sample was vortexed for ten seconds to shear the DNA. To this solution, an equal volume (900 µl) of 25:24:1 phenol-chloroform-isoamyl alcohol (Sigma Aldrich) was added, vortexed and centrifuged (35280 xg) for ten minutes. After centrifugation, the upper layer was carefully transferred into a 1.5 ml tube. DNA was isolated using the (Zymo Research) according to the manufacturer's recommendations. Briefly, 200 µl of DNA binding buffer was added to the solution which was transferred to a DNA column in 500 ul aliquots and centrifuged for one minute at 35280 xg; discarding the flow-through each time. To wash the column, 200 µl of wash buffer was added; repeating the same centrifugation steps. The column was washed two times. The DNA column was then transferred to a new 1.5 ml tube and the DNA was eluted with 50 µl of sterile DNase/RNase free ddH_20. Finally, DNA was quantified using a nanodrop spectrophotometer (Thermo Scientific).

PCR amplification of the 16S Region

The principles used to create this protocol were gathered from a previous publication (17). Each reaction mixture contained the following: 5 µl of 10x buffer (Life Technologies), 1.5 µl of $MgCl_2$ (50mM) (Life Technologies), 1 µl of dNTPs (10 mM) (Invitrogen), 2 µl of bovine serum albumin (BSA) (10 mg/mL made in pure

water, aliquoted and irradiated for 30 minutes) (Life Technologies), 5µl of V3F primer (1 uM), 5 µl of V3R primer (1 uM) (18), 0.5 µl of Taq polymerase (Life Technologies), and 200 ng of DNA. The reaction volume was then adjusted to 50µl using sterile DNase/RNase free ddH20. 30-50 ng of DNA was sufficient to conduct a successful PCR reaction. The reaction was made into triplicates by dividing the mixture into three tubes, each containing 16.7µl. The reaction was then run for 30 cycles; at 94 °C for 2 minutes, 94°C for 30 seconds, 50 °C for 30°C, 72 °C for 30 seconds and 72 °C for 10 minutes using a thermo cycler (Eppendorf). The products were visualized using a 2% agarose gel, operated for 30 minutes at 100 V. A 100 bp ladder was used to estimate the size of the bands. Products that appeared around 300 base pairs were excised and the bands were visualized under a UV transilluminator light (Protein Simple).

Illumina Sequencing

After each of the gel samples was purified, each sample was placed into a 96-well plate and sequenced using an Illumina genome analyzer in the McMaster DNA Sequencing Facility as mentioned previously (57). The steps taken before analysis have been previously described in a number of our laboratory's publications (57, 62). Briefly, the completed run was demultiplexed with Illumina's Casava software. The resulting sequenced data were processed as previously described (62, 63). Briefly, Cutadapt was used to trim the forward and reverse paired-end reads at the opposing primers for input into PANDAseq for assembly (64, 65). Sequences were organized into operational taxonomic units (OTUs) with a clustering threshqold of 97% using

AbundantOTU (65). Single-sequence OTUs (single- tons) were removed prior to all analyses using Quantitative Insights into Microbial Ecology (QIIME) (66). All beta diversity plots and taxonomic summaries were prepared using Quantitative Insights into Microbial Ecology (QIIME) (57).

Frailty Measures

To quantitate healthy aging in our mice, a frailty score was generated. This test is a validated and non-invasive method that utilizes clinical features in order to quantify frailty within our young and old mice (67). The index includes a total of 31 health-related parameters in order to measure factors like the quality of their coat, physical/musculoskeletal changes, ocular/nasal changes, digestive/urogenital, respiratory, level of discomfort, their overall weight, body temperature (Supplementary Figure 5). In addition to these parameters, we have modified the frailty test in order to add a cage-hang test, which is used to measure muscle strength in our young and old mice.

Liposomal clodronate depletion

In order to deplete macrophages from within the gut of our mice, we conducted a liposomal clodronate depletion (68). Briefly, mice were injected intraperitoneally with 200 µl of clodronate liposomes or PBS-control on two consecutive days. Mice were sacrificed on the third day in order to examine the depletion of macrophage populations within the gut. The spleen was collected and used as a positive control. Macrophage populations were identified using flow cytometry as previously described (58).

Chapter 3: Characterizing the physiological and microbiological changes of aging in SPF mice

INTRODUCTION

The inflammatory response is the primary innate response to tissue damage, injury and the identification of bacterial products. The acute inflammatory response is characterized by pain, redness, heat and swelling at the site of injury (69). Resident and recruited innate immune cells become activated, resulting in an increase of pro-inflammatory cytokines and mediators (70). In general, acute inflammation is transient. However, when the inflammation is not resolved, or the insult is not removed, the inflammation can become chronic.

In the context of aging, inflammation is present for extended periods of time and is chronically affecting tissues within the host. Elderly humans (>65 years old) experience a state of chronic, low-grade inflammation (71). This can contribute to a number of negative outcomes within the elderly, including reduced immune responses, reduced vaccine-induced responses and increased susceptibility to infections (72). Although there are several theories suggesting possible causes and contributors to age-associated inflammation, the precise etiology behind this inflammation is still undetermined.

We are proposing that negative changes in the gut microbiome within old mice, termed microbial dysbiosis, are contributing to increases in inflammation and decreases in immune function with age. Previously documented clinical studies have shown that the changes in the gut microbiome composition correlate with changes in overall frailty, or health status, within these individuals as well (32, 73, 74). However, these studies are often limited by confounding factors that can affect the

microbiome. For instance, an individual's diet, residence, social interactions and medications can all affect their microbiome composition differently (75). As a result, we have chosen to complete a more controlled experiment with young and old specific-pathogen free (SPF) mice which are all given the same diet (low-fat), housed within the same environment and interact specifically with other mice that fall with their same age group. By doing so, we are able to eliminate a number of confounding variables that are found in many microbiome studies and examine the effects of solely the age on the composition of the microbiome.

By comparing young (3-4mo) and old (18-22mo) mice, we were able to measure a variety of parameters that have shown to change with age. Using Illumina sequencing of the 16S rRNA gene, we were able to characterize the composition of the gut microbiome within young and old mice. We show that the composition of the gut microbiome differs between young and old mice and these changes can be identified globally or by looking at specific genera. Old mice also experience increased intestinal permeability with age, specifically within the colon. Phenotypes of colonic immune cells change with age as well. Specifically, gut monocyte and macrophage populations within the colons of aged mice appear more "inflammatory" in nature. In this chapter, we have characterized the microbiome, immune and structural changes occurring in old mice in order to begin to understand the components contributing to age-associated inflammation.

RESULTS

Old mice experience age-associated inflammation (AAI) and frailty

In order to determine if aged SPF mice experience age-associated inflammation (AAI), we measured plasma levels of TNF and IL-6 using high-sensitivity Luminex ELISA kits (Millipore) in our young (3-4 month old) and old (18-22 month old) mice. We hypothesized that our aged mice would have increased systemic inflammation with age. Measuring the plasma levels of pro-inflammatory cytokines revealed that old mice have higher levels of TNF (Figure 1A) and IL-6 (Figure 1B) within circulation when compared to their younger counterparts.

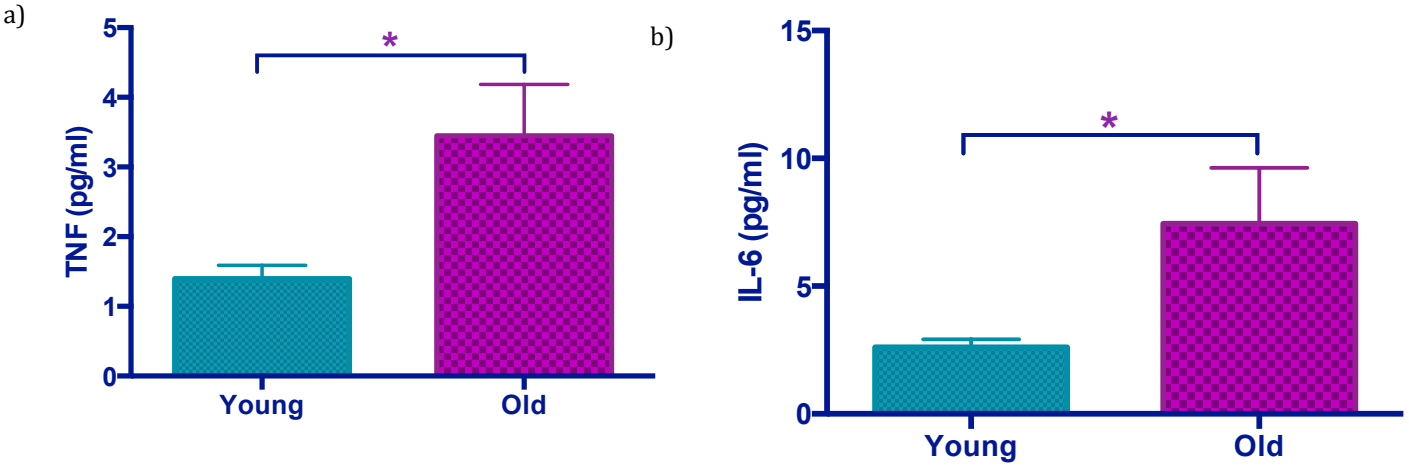

Figure 1: Old mice experience increased systemic inflammation.
Circulating levels of pro-inflammatory cytokines were measured in the plasma of young and old wildtype mice using a Luminex assay. Old mice have an increase in systemic levels of a) TNF and b) IL-6. Each sample was measured in duplicates. Values are the mean +/- SEM of samples within each category. Statistical significance was determined using unpaired t-tests where appropriate [n = 15- 20/group]. $P<0.05$ was considered to be significant.

Frailty, commonly defined as a decrease in the overall health and reduced ability to endure adversity, is a common feature of the geriatric population (67, 72). The aging process is often characterized by a loss of resilience to physical,

psychological and environmental stressors. Therefore, the frailty index is an effective method to measure this resilience within our aged mice. To quantify the differences in health status between our young and old mice, we utilized a frailty index as previously described (67). This index includes a variety of markers that effectively score the integument, physical/ musculoskeletal, vestibulocochlear/ auditory, ocular/nasal, digestive/urogenital, respiratory, and overall discomfort that may occur in aged mice (Supplementary Figure 5). We have also modified this frailty index in order to include the wire-hang test. This test allows us to measure motor function and muscle strength in our mice. (76). Sarcopenia, the loss of muscle tissue with age, has been identified as a major contributor to disability and frailty within the elderly (77). Thus, the result from our modified frailty score provides us with a holistic understanding of the mouse's overall health.

Using this frailty index, we found that our old mice were frailer than young mice (Figure 2A). We found that the majority of contributors to a high frailty score were the measures of integument. Specifically, this section focused on physical changes on the skin or fur (e.g. alopecia, poor grooming, loss in fur colour, presence of lesions etc.). Over 50% of old mice had a mild or very poor coat condition. Old mice generally also scored poorly in measures of physical/ musculoskeletal health and in certain measures of the digestive and ocular health. For example, about 20% of old mice experienced a rectal prolapse and about 10% experienced ocular changes such as the presence of cataracts, corneal opacity, microphthalmia or eye discharge. We did not observe any differences in nasal discharge, gait disorders,

breathing rates or their core body temperatures (Figure 2B). We did not collect measures of the auditory health, because we were not able to measure hearing loss and vestibular disturbance accurately and consistently. Data collected from 26 different measures included within the frailty index, indicate that old mice are significantly frailer than their younger counterparts.

We next examined muscle strength using the wire-hang test. This test involved placing the mouse on a wire rack approximately 30cm from the top of their cage and inverting the rack. Following inversion, the duration of time that the mouse can grip onto the rack without falling into the cage was measured. This test revealed that our old mice have reduced muscle strength (Figure 2C). Around 78% of young mice and 45% of old mice were able to grip onto the wire rack for the maximum length (60 seconds) at least once out of the 3 trials. On average, old mice were only able to grip onto the wire rack for 23.4 seconds. Thus, these data conclude that old mice have reduced health statuses and experience loss in muscle strength.

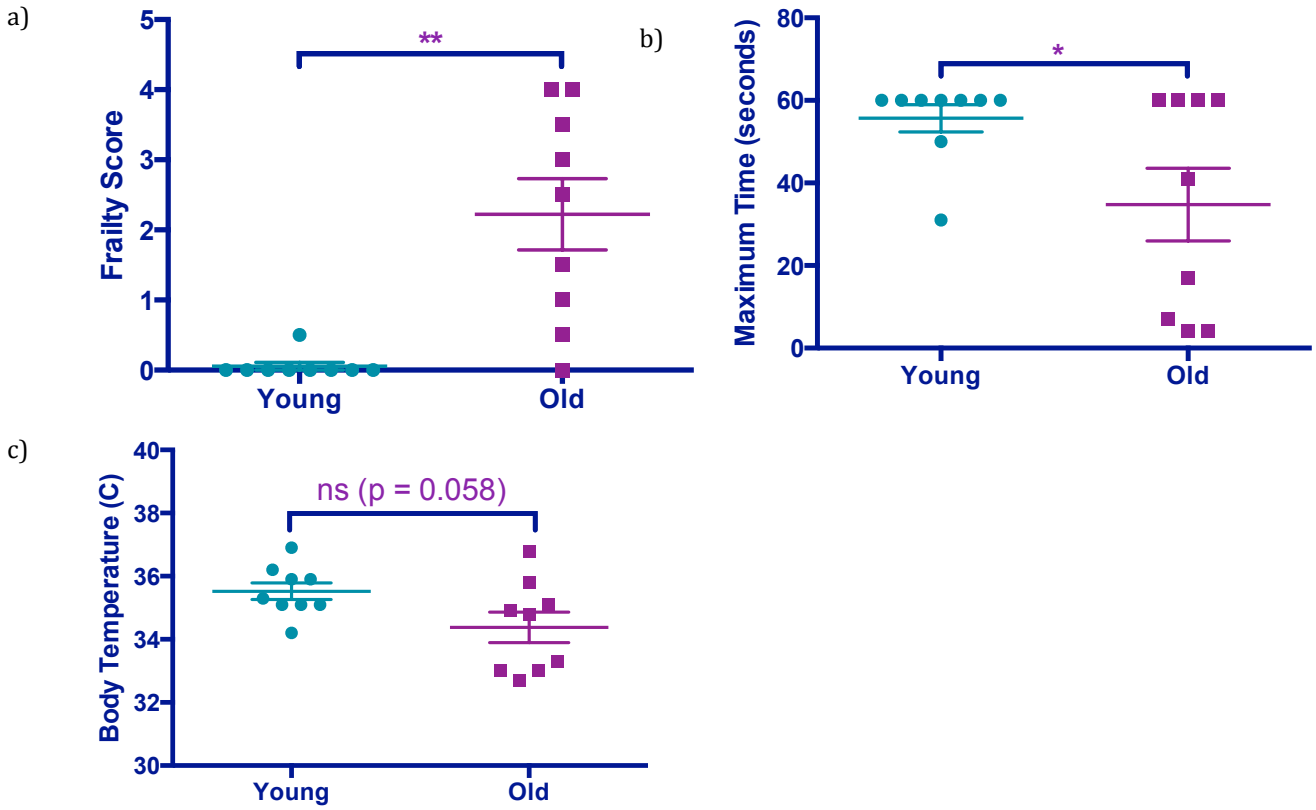

Figure 2: Old mice present clinical differences with age when compared to their younger counterparts.

The health statuses of young (<3mo) and old (>18mo) mice were measured using various parameters, as outlined by the frailty index. Old mice had a) increased frailty, b) decreased muscle strength, and c) no change in their core body temperature compared to young mice [n = 9/group]. Frailty score was measured using a validated method to quantify the overall health status of a mouse under 26 clinical parameters. Muscle strength was measured using the four limb-hanging test. Mice were placed on a grid and given 5 seconds to grasp onto the grid. Then, the grid was inverted and the length of time that the mouse can hold onto the grid is measured. Maximum time was reached when the mouse was able to grip on for 60 seconds. Each mouse was measured in triplicates. Body temperature was measured using a rectal thermometer. Values are the mean +/- SEM of samples within each category. Statistical significance was determined using unpaired t-tests where appropriate. P<0.05 was considered to be significant.

Microbial dysbiosis occurs with age

The differences in systemic inflammation and health statuses within our old mice prompted us to investigate the aged gut microbiome as a potential source for this inflammation. The composition of the gut microbiome is extremely diverse. In

fact, a healthy gut microbiome can contain more than a 1000 different species of bacteria and these inhabitants play key roles in protecting against harmful pathogens, mediating immune responses, and in some cases, can even contribute to disease (78). The gut microbiome has been shown to alter with age (75, 79, 80). We hypothesized that microbial dysbiosis within the aging gut microbiome may be negatively impacting the health outcomes within aged mice. In order to test this hypothesis, fecal pellets were collected from young and old wildtype mice and sequenced for the 16S rRNA gene. By doing so, we were able to characterize the composition of the gut microbiome within our young and old mice. Visualizing the beta-diversity within these mice on a Principle-coordinate analysis plot using the Bray-Curtis calculations indicate that young and old mice cluster distinctively within their own age groups (Figure 3A). Further examining the bacterial differences at the genus level using taxonomic summary plots indicates substantial differences in the microbial composition of young and old mice (Figure 3B). In particular, old wildtype mice have a significant reduction in bacteria belonging to the *Alistipes, Akkermansia* and *Blautia* genera (Table 1). They also have a significant increase in a number of bacterial groups, including *Clostridrium*, *Bifidobacteria* and *Lactobacillus* (Table 2). Although more work is required in order to understand the effect of each specific change, these data suggest that the gut microbiome significantly changes with age and these changes may be contributing to the negative health outcomes in old mice.

Table 1: OTUs that were significantly changed in old SPF and TNF$^{-/-}$ mice

Increased

Family	Genus	# of OTUs (WT)	Old>Young (WT)	Old>Young (TNF KO)	# of OTUs (TNF KO)
Ruminococcaceae	*Ruminococcus*	6	****	NS	7
Lachnospiraceae	*Clostridium*	34	****	a **	34
Ruminococcaceae	*Clostridium*	14	****	NS	16
Prevotellaceae	*Prevotella*	39	**	**	44
Erysipelotrichaceae	*Allobaculum*	54	****	*	60
Lachnospiraceae	Many identified	354	*	a *	343
Bifidobacteriaceae	*Bifidobacterium*	17	***	**	17
Ruminococcaceae	*Oscillospira*	54	****	NS	56
Lactobacillaceae	*Lactobacillus*	53	***	a****	57
Bacteroidaceae	*Bacteroides*	52	**	***	71
Coriobacteriaceae	*Adlercreutzia*	22	***	NS	23
Peptococcaceae	Not identified	14	*	NS	15
Catabacteriaceae	Not identified	51	****	a**	65
Coriobacteriaceae	Not identified	14	***	NS	14

Decreased

Family	Genus	# of OTUs (WT)	Old<Young (WT)	Old<Young (TNF KO)	# of OTUs (TNF KO)
Rikenellaceae	*Alistipes*	48	**	NS	52
Verrucomicrobiaceae	*Akkermansia*	41	****	b *	49
Lachnospiraceae	*Blautia*	11	****	b*	10

[a]OTUs that were significantly decreased in Old TNF$^{-/-}$ mice are underlined
[b]OTUs that were significantly increased in Old TNF$^{-/-}$ mice are underlined

Table 2: OTUs altered by anti-TNF treatment in old mice

Increased

Family	Genus	Old>Young	Decreased by anti-TNF treatment
Erysipelotrichaceae	Not identified	****	NS
Ruminococcaceae	*Ruminococcus*	****	NS
Lachnospiraceae	*Clostridium*	****	NS
Ruminococcaceae	*Clostridium*	****	NS
Prevotellaceae	*Prevotella*	**	NS
Erysipelotrichaceae	*Allobaculum*	****	NS
Lachnospiraceae	Many identified	*	NS
Bifidobacteriaceae	*Bifidobacterium*	***	NS
Ruminococcaceae	*Oscillospira*	****	NS
Lactobacillaceae	*Lactobacillus*	***	NS
Bacteroidaceae	*Bacteroides*	**	*
Coriobacteriaceae	*Adlercreutzia*	***	*
Peptococcaceae	Not identified	*	**
Catabacteriaceae	Not identified	****	* (Increased)
Coriobacteriaceae	Not identified	***	*
Ruminococcaceae	*Subdoligranulum*	NS	*

Decreased

Family	Genus	Old<Young	Increased by anti-TNF treatment
Rikenellaceae	*Alistipes*	**	NS
Verrucomicrobiaceae	*Akkermansia*	****	NS
Lachnospiraceae	*Blautia*	****	NS
Lachnospiraceae	*Roseburia*	NS	*
Eubacteriaceae	*Anaerofustis*	NS	*

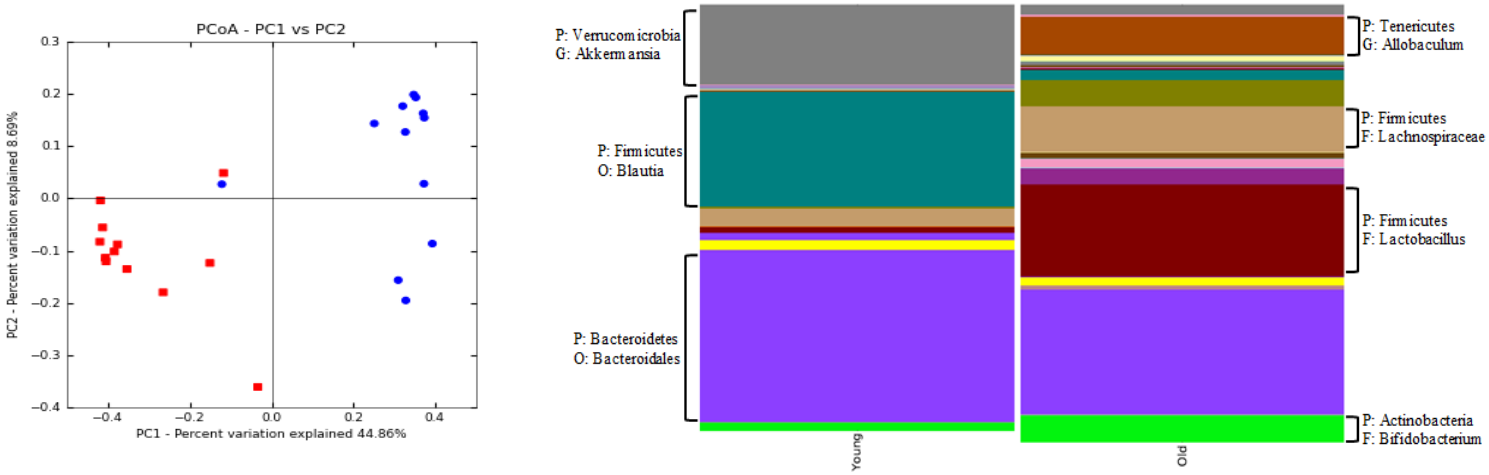

Figure 3: 16S rRNA sequencing of fecal pellets isolated from young and old wildtype mice under naïve conditions reveal differences within the overall bacterial composition. Bacterial communities were examined under naïve conditions to examine the differences between age groups. A) Communities clustered using Principal coordinate analyses (PCoA) of the Bray Curtis distance matrix. Each point represents one sample and is differentiated by colour to indicate their age. Blue = Young WT; Red = Old WT. Plots represent the microbial composition as indicated by the β-diversity between each nasal wash sample. Clustering was observed between the young and old mice [n=12 mice/group]. B) Averaged taxa summary plots of all the samples within the particular group [n=5- 7/group]. The bacterial groups are labeled according to phylum and then specified to highest assigned taxonomic group. The height of the bar represents the relative abundance of the associated genus within young and old mice. Most abundant genera are labeled on the group.

Old mice have increased intestinal permeability with age

Previous studies in our lab have shown that circulating bacterial products like muramyl dipeptide (MDP), increase with age in the frail elderly (81). We have reproduced this data in our old mice (11). Within the frail elderly, circulating MDP appears to be negatively associated with systemic levels of IL-10 (81). Interestingly, high levels of IL-10 correlate with robust intestinal barrier function (82). These data suggests an indirect relationship between intestinal permeability and circulating levels of bacterial products. Thus, we hypothesized that a loss in intestinal barrier integrity might occur with age, resulting in a "leaky" membrane. Increases in intestinal permeability, along with microbial dysbiosis with age might be facilitating the translocation of bacterial products from the intestinal tract into circulation. In

order to determine whether intestinal permeability changes within the entire intestinal tract with age, we used a FITC-dextran gavage. Mice were gavaged with a solution of 3-5kDa of fluorescein- isothiocyanate (FITC). Translocation of FITC into the blood was quantitated as a measure of permeability (11, 83, 84). These studies reveal that old WT mice have significantly increased intestinal permeability compared to their younger counterparts (Figure 4A).

Although the FITC-dextran gavages inform us about the permeability along the entire intestinal tract, it does not provide information on where or how the changes are occurring specifically. The paracellular barrier is formed by a collection of tight junction proteins and allows for the effective translocation of water, solutes, immune cells (85, 86). However, loss of integrity within this barrier can lead to leakiness within the gut. We hypothesized that the increased leakiness with age from the loss of tight junction proteins, results in the translocation of bacterial products from the gut lumen into circulation. This can activate the immune system and contribute to inflammation in the elderly. In order to narrow down the geographic location of these changes, paracellular permeability was measured in two segments of the small and large intestine (the ileum and colon). Once the tissue is mounted on an Ussing chamber, chromium labeled EDTA is placed on the mucosal side of the tissue. Paracellular permeability can then be determined by measuring the amount of EDTA present within the serosal side after various time points. Transepithelial tissue conductance (G), a measure of ion transport in the gut, also informs us about the gut integrity in our mice. Briefly, it can be measured using

ohm's law where the short circuit ion (Isc) value is divided by the transmural potential difference (PD) [G = Isc/PD] (87). By completing these experiments, we are able to identify the differences in paracellular permeability and tissue conductance in various segments throughout the gut (88). These studies revealed that although old WT mice do not have changes in paracellular permeability within the ileum, they do have significant increases within the distal colon (Figure 4B). Furthermore, we observed increased transpithelial conductance in the colons of our old mice (Figure 4C). These data conclude that the physical integrity of the gastrointestinal tract is altered with age. Old mice experience increased paracellular permeability within their colon and these changes may contribute to the translocation of bacterial products seen with age.

a)

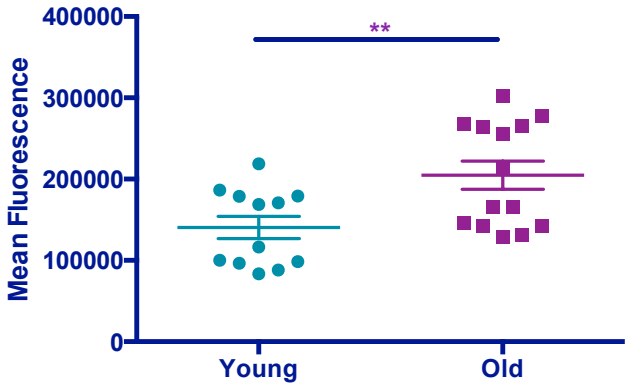

b)

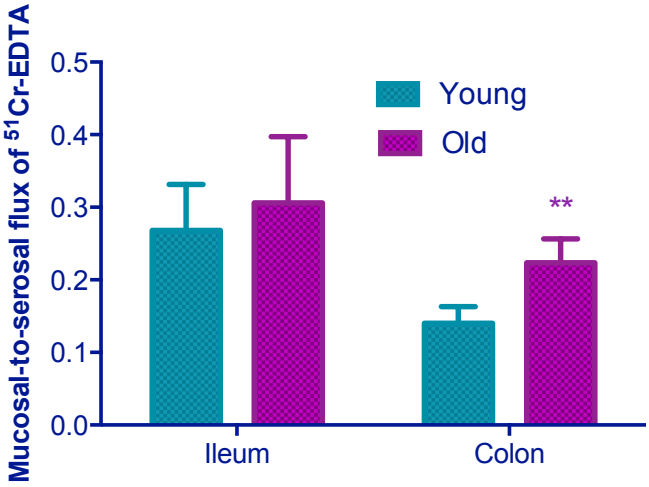

c)

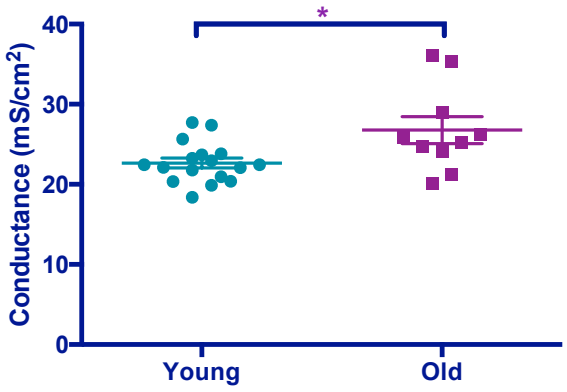

Figure 4: Old mice have significantly increased permeability compared to young mice.
Old mice have increased a) intestinal permeability and more specifically, have b) increased paracellular permeability within their colons, but not in the ileum. Old mice also have c) increased tissue conductance within the colon. Intestinal permeability was measured with a fluorescent-dextran gavage (average molecular weight, 3000 – 5000) [n=13-15/group]. A portion of the distal colon was removed from the mouse and mounted on an Ussing chamber in order to study permeability changes within the colon [n=8 mice/group]. Values are the mean +/- SEM of samples within each category. Statistical significance was determined using unpaired t-tests where appropriate. $P<0.05$ was considered to be significant.

Changes in gut immunity with age

The relationship between the microbiome and the host immune system are closely knit with a bidirectional relationship as these two aspects within the host interact continuously (89, 90). Immune cells within the host gut can be affected by environmental cues such as changes in the surrounding structure and cytokine levels (45). They can also be phenotypically altered by the surrounding microbiome (91–93). In models of disease, immune cells like monocytes and macrophages in the gut have been demonstrated to either contribute to or change phenotypically in response to increased permeability or exposure to a dysbiotic microbiota (90, 94, 95). In fact, the release of IL-1b, IL-18 and TNF by monocytes and M1 macrophages have been shown to contribute to a loss in gut integrity and intestinal inflammation

in Crohn's disease patients (94). In order to decipher the relationship between the immune system and the changing gut microbiome with age, we examined the abundance, phenotype and functions of specific immune cells present within the gut. We focused on the colon, as major differences were identified within the fecal microbiome (which we used as a proxy for the colon) as well as increases in paracellular permeability within this region. Specifically, the macrophage and monocyte populations were examined within this region as these innate cells are the primary producers of inflammatory cytokines and mediators of intestinal integrity in the gut and help protect against potential pathogens.

To explore the differences in macrophage populations within young and old wildtype mice, immune cells were isolated from the colon. For these studies, a total of $5x10^5$ cells were stained for flow cytometry and macrophage populations were identified within the live population as $CD3^-$ $CD19^-$ $CD45^+$ SSC^{lo} $CD11b^+$ $CD64^+$ cells (complete gating strategy in chapter 2). This population can be identified as negative for T cells, B cells, and neutrophils and positive for leukocytes and intestinal macrophages as previously described (44). There was no significant difference in the abundance of macrophages within the colon with age (Figure 5A). Even though the numbers of these macrophages were not changed, we hypothesized that their phenotype might be altered with age, causing them to become more pro-inflammatory. To test this, colonic macrophages isolated from young and old WT mice were stimulated with lipopolysaccharide (LPS) *in vitro* for 2.5 hr and the production of pro- and anti-inflammatory cytokines (TNF, IL-6, IL-10) were

measured using intra-cellular staining. Unstimulated colonic macrophages isolated from old mice produce significantly greater TNF compared to young mice (Figure 5B). Furthermore, when stimulated with LPS, colonic macrophages from old WT mice produce higher levels of TNF than young mice (Figure 5B). However, no significant changes were seen in the production of IL-6 (Figure 5C) or IL-10 (Figure 5D).

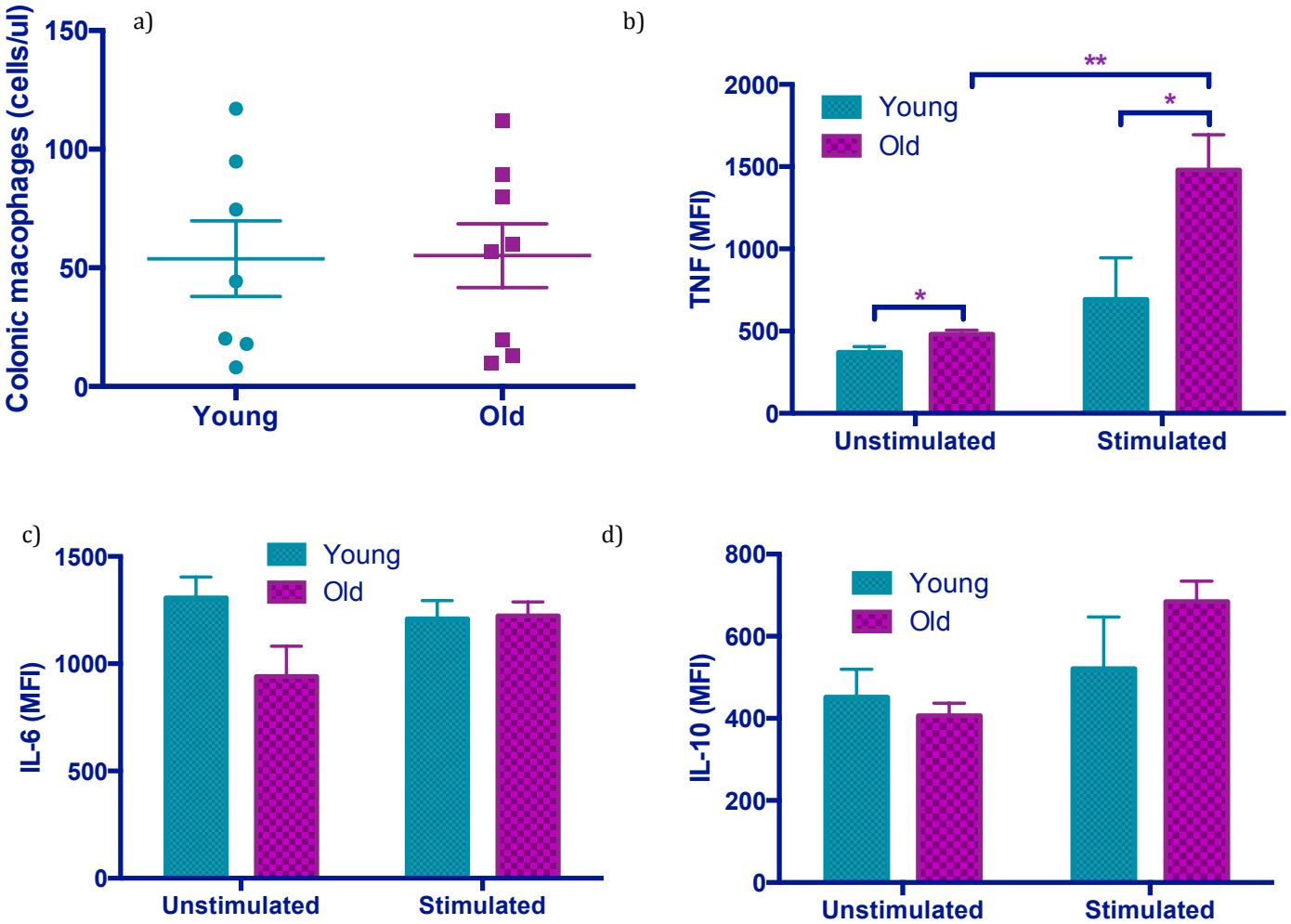

Figure 5: Colonic macrophages isolated from old mice have a hyper-inflammatory response to a bacterial product.

Young and old colonic macrophages were either stimulated with lipopolysaccaride (LPS) or unstimulated for 2.5 hours [n=4/group]. Productions of pro- and anti-inflammatory cytokines were

measured using flow cytometry. When stimulated with LPS, macrophages from old mice have a) a significant increase in TNF production, and b) have no changes in IL-6 or c) IL-10. Values are the mean +/- SEM of samples within each category. Statistical significance was determined using unpaired t-tests where appropriate. $P<0.05$ was considered to be significant. YWT = young wildtype; OWT = old wildtype; US = unstimulated; S = stimulated.

We hypothesized that if macrophages were the key producers of inflammatory cytokines within the gut, then depleting them within old mice would lead to reduced inflammation. To this this, we attempted to deplete the intestinal macrophages from this region using intra-peritoneal injections of liposomal clodronate. In a pilot study, clodronate depleted young WT mice showed significant reductions in macrophages within the spleen (Figure 6A). However, we did not see significant reductions within the colon (Figure 6B). As a result, this protocol needs to be optimized further in order to successfully deplete the macrophages within the gut. There are couple different factors that can be altered within the protocol (68). For instance, the route of administration can be changed. We utilized the intra-peritoneal route of administration as we hypothesized that this would be an effective way to deplete macrophages within the gut. Some other routes of administration that may be more efficient include intrarectal administration or intravenous injections. Other factors that can be optimized for greater success of macrophage depletion can be the dose of administration as well as the frequency/duration of administration. This protocol must be optimized for use in future studies.

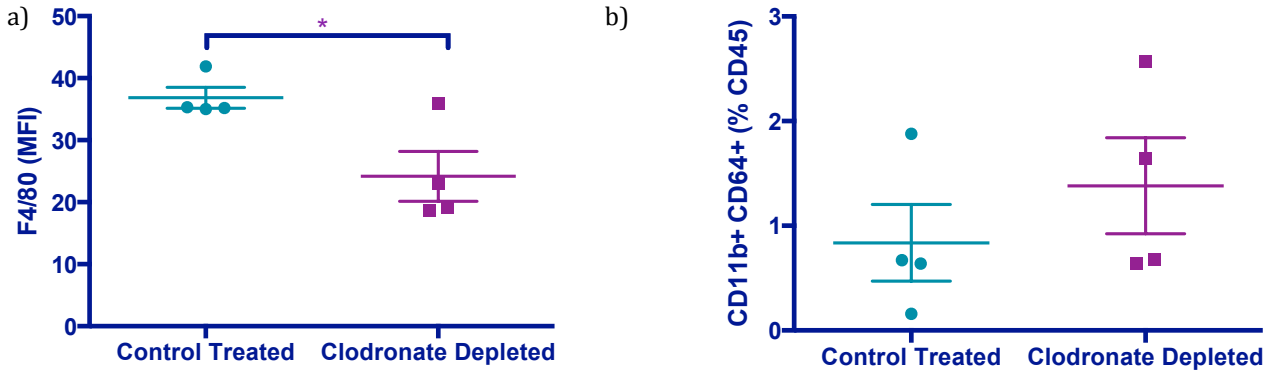

Figure 6: Clodronate liposome injections were administered to young mice in order to deplete the macrophage populations within the colon.
Mice were given two i.p. injections with 200 ul of clodronate liposomes. Control mice were treated with PBS. Macrophage populations were identified using flow cytometry. A significant reduction in the macrophage population was observed with the a) spleen, but not in the b) colon. n = 4 mice/group. Values are the mean +/- SEM of samples within each category. Statistical significance was determined using unpaired t-tests where appropriate. $P<0.05$ was considered to be significant.

Monocytes are the precursors to macrophages and are believed to have a role in colon integrity (94). Studies have shown that specifically, Ly6C^{high} monocytes replenish intestinal macrophages during times of inflammation within the gut (46). We have previously shown that systemic levels of Ly6C^{high} monocytes increase with age, due to increased CCR2 expression (96). Since CCR2 expression has been demonstrated to be required for inflammatory monocyte recruitment to the gut, we hypothesized that old mice would also have higher numbers of Ly6C^{high} monocytes in their colons. Although the numbers of colonic macrophages are not altered with age, the increase in inflammatory monocytes may contribute to functional changes in the macrophages, causing them to become more inflammatory in nature. Preliminary data suggests that old WT mice have increased Ly6C^{high} monocytes

within their colon compared to their young WT counterparts (Figure 7A). However, CCR2 expression was not increased in the gut (data not shown).

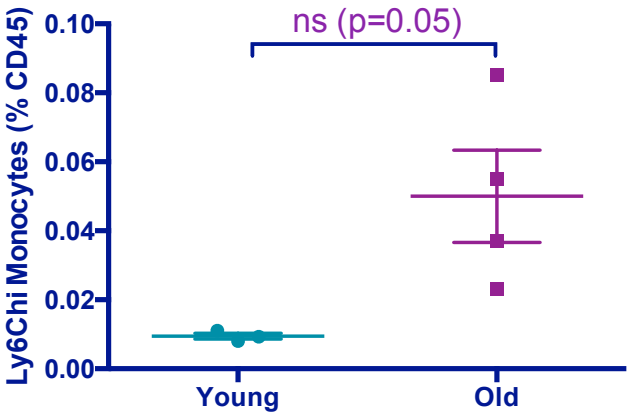

Figure 7: Ly6C^{high} monocytes in the colon increase with age.
Immune cells were isolated from the colon of young and old wildtype mice and stained for flow cytometry. Monocytes were identified in the live population as CD45^{+} CD3^{-} CD19^{-} SSC^{lo} CD11b^{+} Ly6C^{+} cells. Ly6C^{high} monocytes were identified based on their expression of Ly6C^{+} in this gated population. n = 4-5 mice/group. This data is representative of one technical replicate. Statistical significance was determined using unpaired t-tests where appropriate. $P<0.05$ was considered to be significant.

DISCUSSION

The aging process is often associated with an increase in systemic inflammation as well as a decrease in protection against stressors (97). Age-associated inflammation is characterized by increased peripheral white blood cell counts and accumulation of pro-inflammatory mediators within circulation (72, 98). Specifically, increases in systemic levels of IL-6, TNF, IL-1 and CRP have been documented (99). These cytokines have the ability to trigger age-associated pathology and are associated with mortality within the elderly (100). In fact, one study examining 333 healthy elderly individuals (>80 years) over a span of six years indicated that those who died during the course of the study had elevated serum levels of IL-6 (100). Increased IL-6 has also been linked to the likelihood of developing bacterial and viral infections and age-associated diseases like dementia

and atherosclerosis (96, 101, 102). Increases in TNF have been shown to be predictive of the development of atherosclerosis and dementia with age, while CRP has been linked to cardiovascular diseases, diabetes and rheumatoid arthritis (98, 103, 104). Since the elderly are at a higher risk of experiencing comorbid health conditions as a result of this chronic age-associated inflammation, it is important that we first characterize these changes in order to understand their etiology (10, 105, 106).

Data examining the plasma levels of pro-inflammatory cytokines within our aged mice mirror data from clinical studies. Although we did not test whether the degree of inflammation correlated with the degree of frailty, others have shown that these two are positively correlated using mouse models (72). Frailty correlates with immunosenescence in humans and can be used to predict responses to pathogens in the elderly (72, 107). In fact, in-depth analysis comparing the gene expression of various inflammatory pathways in purified monocytes from frail and non-frail adults show that monocytes isolated from frail individuals have increased expression of stress-responsive inflammatory pathway genes (72). LPS-stimulated monocytes from frail individuals showed higher expression of 116 genes involved in inflammatory pathways. These data suggest that increased expression of inflammatory genes with age and may be facilitating the progression of frailty in aged mice (72).

Our aged mice have also obtained reduced maximum times from their cage-hang tests, indicating that they experience muscle wasting with age. Sarcopenia, is

an inevitable consequence with age (108). However, the underlying mechanism behind this is currently unknown. Muscle wasting in our old mice may be a result of a loss in muscle fibres; loss of muscle strength due to increases in fat and non-contractile material or changes in muscle metabolism. In old mice, muscles are more prone to injury and are less likely to be repaired in an efficient manner (109). Muscle atrophy is an important measure when examining the overall frailty of a mouse as it directly contributes to its mobility, strength and health status (109).

Early studies of intestinal permeability studied the decrease in barrier function using absorption of polyethylene glycol in young and old rats (110). Furthermore, studies completed in young and old baboons have shown that increases in intestinal permeability with age may be a result of the remodeling of tight junction proteins (111). Colonic biopsies from old baboons reveal a decrease in the expression of tight junction proteins, specifically, zonula occluden-1, occludin, and junctional adhesion molecule-A. These samples also had increased expression of IFN-γ, IL-6 and IL-1β (111). These data suggest a possible correlation between decreased barrier function and increased inflammation in the gastrointestinal tract. Consistent with these findings, our aged mice experience increased paracellular permeability within their colons. Paracellular transport refers to the passing of substances between cells making up the epithelial barrier. Our data suggests that barrier integrity is lost with age and these changes are specifically found within the colon of aged mice. We hypothesized that the decrease in barrier function with age may be facilitating the transport of bacterial products from the intestinal lumen out

into circulation. Old mice have increased levels of muramyl dipeptide within their plasma (81). Whether the relationship between increased intestinal permeability and increased bacterial products within circulation is correlative or causative is yet to be determined within our old mice.

The observation that intestinal permeability and systemic inflammation increases with age led us to hypothesize that the immune cells within the gut may be altered with age as well. Under steady-state conditions, intestinal macrophages are highly phagocytic, but do not respond to TLR stimulation by releasing pro-inflammatory cytokines or nitric oxide (45). Instead, intestinal macrophages produce anti-inflammatory IL-10. Although this may seem counterintuitive at first, this dual personality of macrophages within the gut prevents them from creative excessive inflammation (45). Since numerous commensal bacteria inhabit the gut, it is important that the innate immune cells in this region are tolerogenic (112). Resident macrophages within the healthy gut also play and important role in maintaining epithelial integrity (45). Furthermore, intestinal macrophages are able to up-regulate the expression of PPAR-y in order to limit pro-inflammatory gene expression and prevent the entry of CCR2-expressing inflammatory monocytes into the gut (49, 113).

Our data suggests that intestinal macrophages isolated from the colons of old mice are more inflammatory under baseline conditions than those isolated from young mice. Furthermore, when exposed to a bacterial stimulus like LPS, intestinal macrophages isolated from old mice reveal a hyper-inflammatory phenotype as

measured by their production of TNF. These data suggest that macrophages become more inflammatory with age and produce a hyper-inflammatory response to bacterial stimuli. In models of IBD, the microbiome has been linked to inducing inflammation within the gut by altering the phenotype of intestinal lamina propria macrophages. It has been suggested that the microbiome has the potential to induce pro-inflammatory gene expression and increase the accumulation of $Ly6C^{+}$ monocytes within the colon. Our aged mice also experience a significant increase in the colonic $Ly6C^{high}$ population. We are suggesting that these increases in old mice may be a result of the change in the microbiome composition with age.

The intestinal microbiome is a large, and diverse community that has the ability to determine the health status of the host. The microbiome can communicate with the immune system and maintain a bidirectional relationship that can help initiate or suppress immune responses to various stimuli. However, studies have shown that under certain circumstances, negative changes in the microbiome, termed microbial dysbiosis, can contribute to increased inflammation. An abnormal proportion of beneficial to pathogenic bacteria characterizes this phenomenon (114). Particularly, in models of intestinal bowel diseases (IBD), the intestinal microbiome has been intimately linked to the onset of disease. In fact, the altered balance between bacteria within the gastrointestinal (GI) tract has been shown in the progression and severity of Crohn's disease and ulcerative colitis (UC) (115). Although the precise mechanism behind this is currently undetermined, the general consensus is that changes in the microbiome are able to provide antigenic

stimulation (115). This can in turn cause the activation of innate immune cells as well as pathogenic T cells, leading to increased intestinal inflammation and injury (115). Other studies have identified key species that may be playing a role in the pathogenesis of disease. For example, decreased abundance of *F. prausnitzii* and *B. fragilis* have been correlated with increased severity of ileal Crohn's disease (115). Abundance of other symbiotic bacteria like *Fecalibacterium* and *Roseburia* appear reduced in IBD patients. These bacteria are large producers of short-chain fatty acids and help maintain intestinal health to combat disease (115). In general, the gut microbiota of IBD patients contains more gram-negative bacteria, which may be contributing to intestinal inflammation within these patients as well (116).

The physiology of the intestinal tract changes tremendously with age, with increased intestinal permeability, and decreased motility (117). Decreased motility can impact gut fermentation and excretion, altering the homeostasis in this environment. In both human and mouse models of aging, changes in the gut microbiome composition have been correlated with frailty and immunosenescence (74, 75, 117). Frailty has been negatively associated with microbiota diversity in the elderly (73). Furthermore, parallel analyses completed in centenarians have concluded a positive relationship between the change in gut microbiome composition and the increase in inflammatory mediators within circulation (117). Although these results do not conclusively indicate whether these two changes occur simultaneously or independently, it does suggest that the gut microbiome composition plays a role in inflamm-aging and the progression of diseases in the

elderly. Early studies that characterized the aging gut microbiome in humans identified a decrease in the total number of anaerobes and an increase in *Enterobacteria* and other gram-negative bacteria (118). The elderly also have a decrease in *Faecalibacterium prauznitzii* and other butyrate-producing bacteria which are associated with promoting intestinal epithelial integrity and have anti-inflammatory properties (117). Findings from these studies suggest that the composition of the old gut microbiome might either contribute to or be affected by age-associated inflammation (117).

We have characterized the fecal microbiome of young and old mice using Illumina sequencing of the 16S rRNA gene. The findings from our study are consistent with previous studies, which demonstrate that the fecal microbiome is different between young and old mice. We observed a significant increase in the abundance of OTUs belonging to the *Oscillibacter, Clostridium, Allobaculum, Ruminococcus* and *Bacteroides* genera (a complete list of changes is provided in Table 1). There was a significant reduction in the OTUs belonging to the *Akkermansia, Alistipes* and *Blautia* genera.

Gut microbial dysbiosis with age has been associated with changes in short-chain fatty acid producers, and increases in the abundance of facultative anaerobes and opportunistic pathogens (75). It has been suggested that these changes may be cumulatively contributing to an increase in overall frailty and intestinal inflammation (75). Studies focusing on this potential relationship have indicated that frailer individuals have a higher prevalence of genera belonging to the

Oscillibacter and *Alistipes* groups. These individuals also have a reduction in bacteria belonging to the *Eubacteriaceae, Faecalibacterium* and *Lactobacillus* genera (75). Other bacterial groups like *Akkermansia* are also commonly found within the intestinal tract. The abundance of *Akkermansia* increases significantly throughout the early stages of life to adulthood. However, its abundance is significantly reduced in the elderly. *Akkermansia* is a mucin-degrading bacteria that plays a role in producing the mucus layer within the GI tract, which serves as a source of nutrients for other residents as well as provides a barrier to prevent the entrance of pathogens (119). In fact, *in vitro* studies have further shown that *Akkermansia muciniphila* has the capacity to strengthen enterocyte monolayer integrity and induce a less pro-inflammatory response. These data suggest that *Akkermansia* has the ability to increase gut barrier integrity and reduce inflammation (120–122). Reduction of this bacterial group in our aged mice, along with all of the other microbial changes, suggest that defects may be present in the development of the mucosa within the intestinal tract - ultimately contributing to increased intestinal permeability and inflammation with age.

This study characterized the physiological and microbiological changes in aged mice, in order to decipher the relationship between these factors in chapter 4. The overall findings suggest that old mice experience age-associated inflammation as measured by plasma levels of TNF and IL-6 and have increased paracellular permeability with age. Furthermore, our old mice experience microbial dysbiosis within their colons. By understanding the differences occurring between young and

old mice, we can begin to unravel the relationship between the altered microbiome and immune dysfunction in order to better understand how to promote healthy aging within the elderly.

Chapter 4: Deciphering the role of age versus the composition of the microbiome on physiological and immunological outcomes

INTRODUCTION

The gut is home to a diverse population, including resident microflora, foreign food antigens and the extensive repertoire of immune cells contained within the gut-associated lymphoid tissue (GALT) (42). The anatomical proximity of these components within the gut makes it crucial for them to maintain a symbiotic relationship. The gut is particularly exposed to infection and challenge by pathogenic bacteria because of its structure. The thin permeable membranes present within the mucosal tract are necessary for food absorption. The entry of foreign antigens also occurs readily as it is a portal of entry for food. As a result, it is important that the resident flora and the immune system are able to effectively maintain a healthy microbiome and gut integrity. Changes to either of these components, as occurs with age, can have detrimental outcomes in the host.

We have previously shown that old mice experience age-associated defects, including increased systemic inflammation, decreased paracellular permeability, and phenotypic changes in the immune cells of the myeloid lineage, along with an overall change in the composition of the gut microbiome. In this chapter, we have utilized gnotobiology in order to study the role of the microbiome in influencing these changes in old mice. Furthermore, by being able to manipulate the microbiome compositions of young and old GF mice, we are able to determine whether the composition of the old microbiota directly contributes to the negative changes with age. Furthermore, we can investigate the ability of the young microbiota to promote healthy outcomes within aged mice. Colonization of young GF mice with the old

microbiota resulted in increased systemic inflammation, decreased gut integrity and increased recruitment of Ly6C^{high} monocytes within the blood and colon when compared to young GF mice colonized with the young microbiota. These data suggest that the composition of the old microbiome directly contributes to age-associated inflammation in old mice. This chapter provides a comprehensive look at the relationship between the aging microbiome and the immune defects seen with age.

RESULTS

Germ-free mice are protected from age-associated inflammation

In order to investigate the contribution of the microbiome in age-associated inflammation, we utilized germ-free (GF) mice. Since GF mice do not have a microbiome, we hypothesized that aged germ-free mice (>18 months old) may be protected from some age-associated changes. Old SPF mice commonly experience alopecia, decreased body condition, poor posture/mobility, and develop grey fur. Visually, our old GF mice seldom show signs of greying fur or alopecia (Figure 8A), and live longer (Figure 8B). Old GF mice do not have increased plasma levels of TNF (Figure 8C) and IL-6 with age (Figure 8D). Finally, old GF mice do not have significantly increased paracellular permeability when compared to their young GF controls. In fact, old GF mice have lower paracellular permeability than their old SPF counterparts ($p = 0.06$) (Figure 8E). Taken together, these data suggest, that in the absence of the microbiome, old germ-free mice are protected from at least some of the age-associated changes observed within our SPF mice.

a)

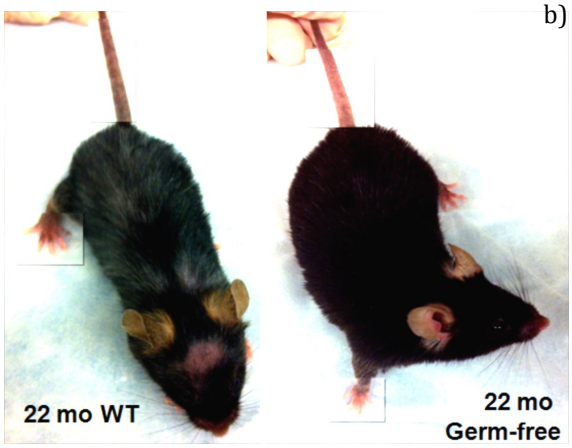
22 mo WT
22 mo
Germ-free

b)

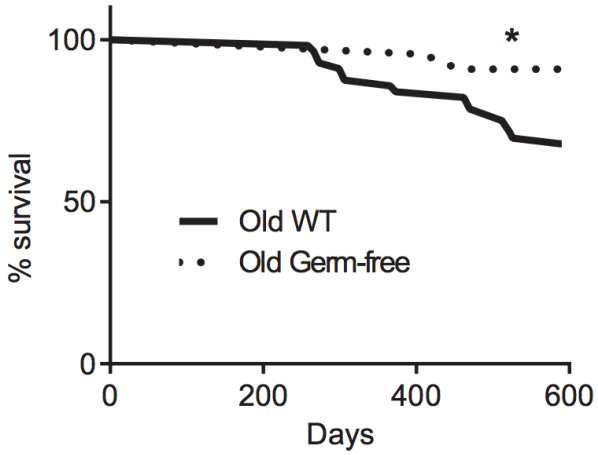
100
50
0
% survival
*
Old WT
Old Germ-free
0
200
400
600
Days

c)

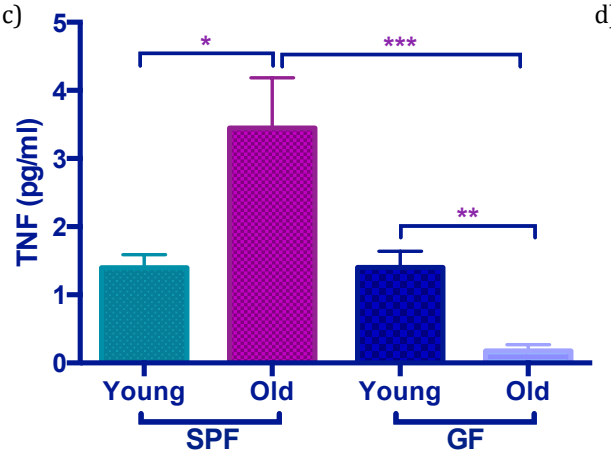
TNF (pg/ml)
5
4
3
2
1
0
*
***
**
Young
Old
Young
Old
SPF
GF

d)

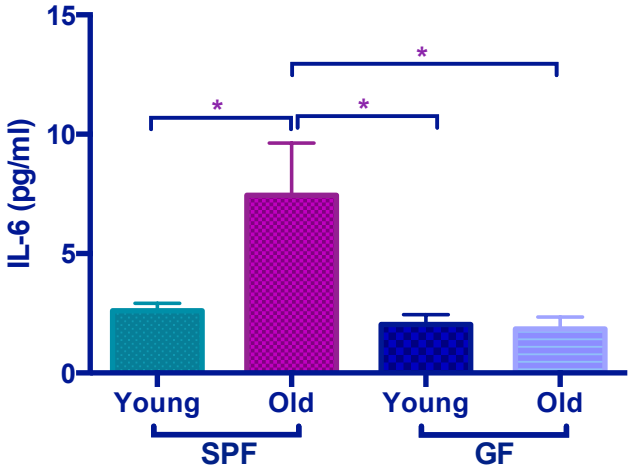
IL-6 (pg/ml)
15
10
5
0
*
*
*
Young
Old
Young
Old
SPF
GF

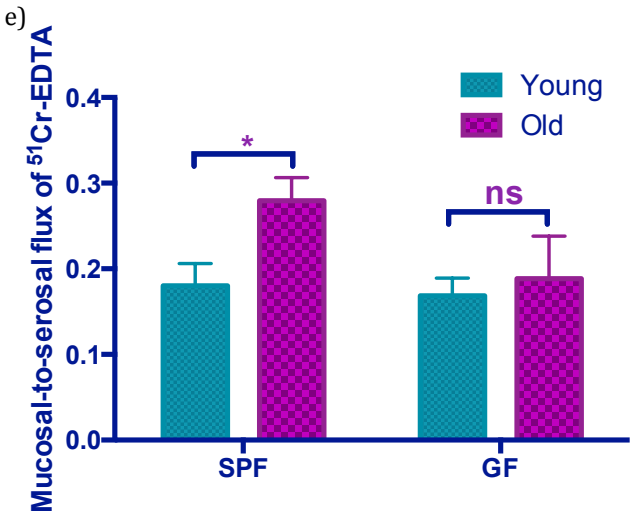

Figure 8: Old germ-free mice are protected from age-associated inflammation and have reduced intestinal permeability.
Old germ-free mice (>18mo) were compared to old SPF mice (>18mo) in terms of their visual appearance, total life span, systemic inflammation, as well as their barrier integrity. Old germ-free mice show a) decreased physical signs of aging, including have less hair-loss, improved posture, and decreased grey fur. Furthermore, old germ-free mice b) live significantly longer, and are protected from increases in their circulating levels of c) TNF and d) IL-6. Finally, aged germ-free mice also have e) reduced permeability within the colon compared to old SPF mice. Survival analysis showing all-cause mortality of WT and GF mice up to 600 days of life. Differences in the survival curves were analyzed by Log-rank (Mantel-Cox) test. Circulating levels of pro-inflammatory cytokines were measuring in young and old wildtype plasma using a Luminex assay. Each sample was measured in duplicates [n=5-15/group]. For Ussing chamber studies, a portion of the distal colon was removed from the mouse and mounted on the chamber in order to study permeability changes within the colon [n= 3-8 mice/group]. Values are the mean +/- SEM of samples within each category. Statistical significance was determined using unpaired t-tests where appropriate [n = 15- 20/group]. $P<0.05$ was considered to be significant.

The microbiota influences the development and function of myeloid lineage cells

To determine the influence of the microbiome on the immune system within the host, we compared the abundance of cells belonging to the myeloid lineage in young and old germ-free and SPF mice. Specifically, we examined the macrophage and monocyte populations within these groups. Our pilot data suggested that

Ly6C^{high} monocytes are increased in the colon of old SPF mice ($p = 0.05$). Thus, we next investigated whether the recruitment of these Ly6C^{high} monocytes are influenced by the presence of the microbiome. Immune cells were isolated from the colons of young and old GF mice. Our aged GF mice do not have an increase in Ly6C^{high} monocytes when compared to their younger counterparts (Figure 9A). In fact, old GF mice have significantly reduced Ly6C^{high} monocytes when compared to their old SPF controls, suggesting that the microbiome plays a role in the recruitment of more monocytes within the intestines with age. Analysis of the monocyte population within the colon mirrors the trend seen in the blood (Figure 9B). These data suggest that the microbiome plays a role in the recruitment of Ly6C^{high} monocytes within the colon and the blood in young and old SPF mice.

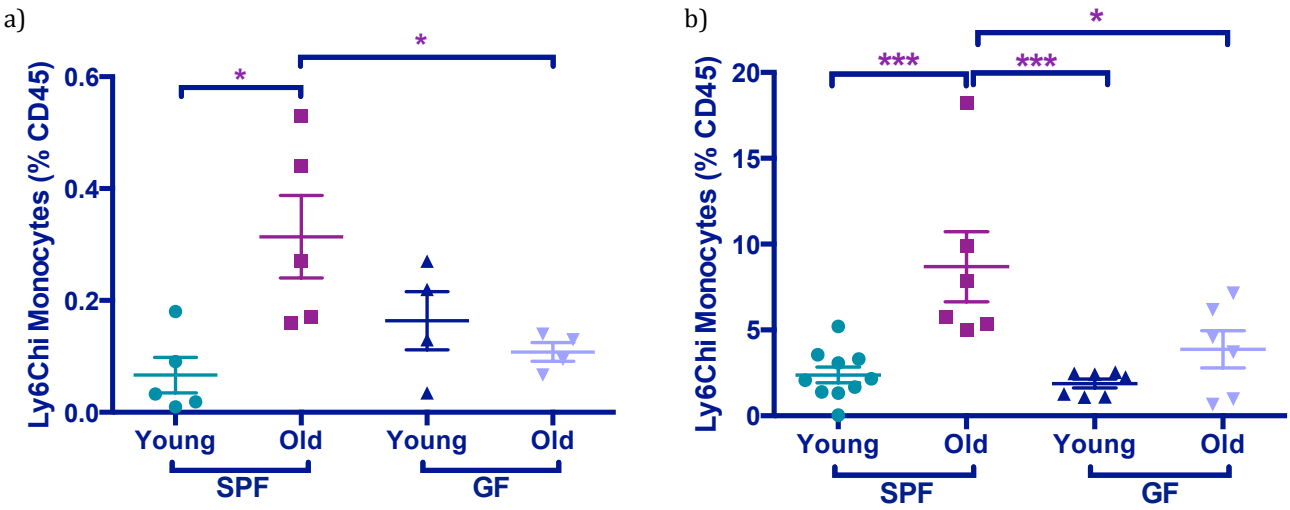

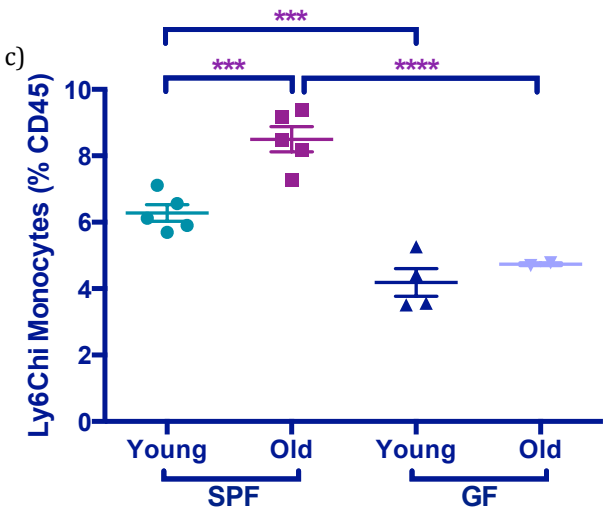

Figure 9: Increase of Ly6C^{high} monocytes with age may be mediated by the presence of the microbiome.
Abundance of Ly6C^{high} monocytes as a population of the CD45% population was determined using flow cytometry. Ly6Chi monocytes are increased with age in old mice within the a) Bone marrow, b) Blood and c) Colon. However, naïve old germ-free mice are protected from this phenomenon. Old SPF mice (>18mo) were compared to young SPF (<3mo) [n=5-8 mice/group]. As well, young and old GF mice [n=4-7 mice/group] were compared to their SPF counterparts. Values are the mean +/- SEM of samples within each category. Statistical significance was determined using unpaired t-tests where appropriate. * indicates $p < .05$, ** indicates $p < 0.005$, *** indicates $p < 0.0005$ and **** indicates $p < 0.00005$.

It has been reported that the hematopoietic stem cell compartment changes with age (123, 124). Specifically, they experience a decrease in lymphopoiesis and a marked increase in myelopoiesis (123). Thus, we next examined the bone marrow for changes in the monocyte population. Here, we were able to see that the Ly6C^{high} population within the bone marrow is also significantly reduced in old germ-free mice when compared to their old SPF controls (Figure 9C). This suggests that changes in the monocyte population within the colon and circulation may be preceded by changes occurring in the bone marrow.

We next examined the functionality of Ly6C^{high} monocytes in the blood, as monocytes are potent producers of inflammatory cytokines in response to bacterial stimuli (125). We have previously shown that when blood monocytes are stimulated with a bacterial product such as LPS, those isolated from old SPF mice produce a hyper-inflammatory response compared to their young controls (58). Thus, we decided to investigate whether this phenomenon in our aged germ-free mice. Using flow cytometry, blood monocytes from young and old GF mice (and their age-matched SPF controls) were stimulated with LPS and examined for TNF production. Monocytes from old GF mice produce higher amounts of TNF in comparison to monocytes from young GF mice in response to LPS. This suggests that the functionality of monocytes is not altered with age in the absence of the microbiome (Figure 10).

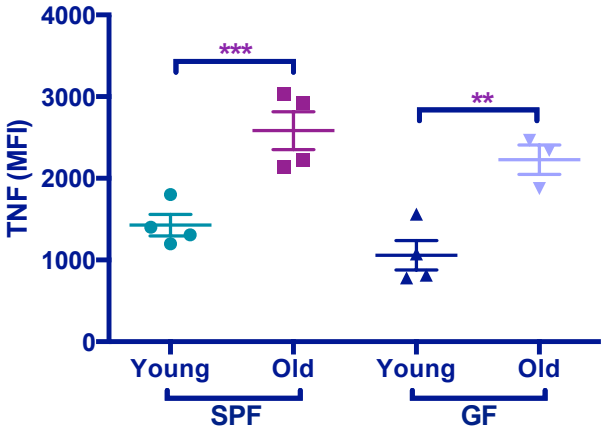

Figure 10: Ly6C^{high} monocytes within circulation of old SPF and GF mice produce increased levels of TNF in response to a bacterial product.
Whole blood was stimulated with lipopolysaccharide (LPS) for 4 hours, after which the production of TNF by Ly6Chi monocytes was quantified using flow cytometry. Values are the mean +/- SEM of samples within each category [n= 3-4 mice/group]. Statistical significance was determined using unpaired t-tests where appropriate. $P<0.05$ was considered to be significant.

Investigating the role of the aging microbiota on monocyte reprogramming

Monocytes are multi-functional innate cells that have the capacity to assist in tissue repair and maintenance, as well as help fight pathogens during infection. Local signals from the environment direct what effector functions are acquired by monocytes once they reach the tissue (126). Although early work suggests that only the adaptive immune system maintains the capacity to build immunological memory, recent studies have established innate cells to possess this memory as well. For instance, plants and invertebrates are protected against re-infection against pathogens even though they do not possess an adaptive immune response (127). Early studies performed in the 1960s suggested that exposure to bacterial stimuli can lead to the production of IFN-y by NK cells and this in turn can activate local macrophages. Not only does this help combat the initial infection, it can also contribute to a form of trained immunity within the innate immune system, resulting in a heightened response against a secondary infection (127). The memory exhibited in this scenario is different from the classically defined immunological memory acquired by cells within the adaptive immune system. In this case, the memory acquired is broad and can be used against a secondary infection with the same pathogen or a different one (127).

In a model of *Candida albicans* infection, it has been shown that memory towards reinfection with the fungi can occur via monocytes, independent of T and B cell populations (128). *In vitro* studies have shown that training monocytes via incubation with *C. albicans* results in increased TNF and IL-6 in response to a

secondary infection (128). Specifically, β-glucans derived from the cell wall of *C. albicans* can induce epigenetic changes involving histone methylations that result in the training of monocytes (128). Such epigenetic changes can train monocytes to become better suited to tackle secondary infections and provide non-specific protection against future infections. In depth analysis of the epigenetic changes occurring within trained human monocytes against β-glucan reveal that training resulted in altered metabolism of monocytes, leading to increased glucose consumption, lactate production and a general increase in glycolysis (129, 130). Histone H3 methylation has been specifically identified as the mechanism involved in the epigenetic training of monocytes to elicit robust long-term innate inflammatory responses (129).

Recent studies have shown that monocytes can be trained early on in development within the bone marrow to respond to bacterial products with regulatory functions, particularly within the gut (126). This phenomenon is called "monocyte reprogramming," and occurs when bacterial products from the gut microbiome directly or indirectly alter monocyte development in the bone marrow. In models of *T. gondii* infection, IL-12 produced within the MALT during infection can provide signals necessary for NK cells in the bone marrow to produce IFN-γ (126). This contributes to the education of myeloid progenitors and subsequently affects the inflammatory potential of $Ly6C^{high}$ monocytes towards stimuli received from the gut microbiome. Furthermore, depletion of NK cells also resulted in reduced changes to monocyte phenotype within the blood (126). These data

suggested that NK cells are the primary producers of IFN-γ in the bone marrow and thus, NK cells might be influencing the fate and function of monocytes within the gut during an infection.

Our previous thus far has shown that old mice experience age-associated inflammation and have increased Ly6C^{high} monocytes within the blood, colon and bone marrow. We have further shown that in the absence of the microbiome, our aged germ-free mice do not experience these effects. We hypothesized that cues presented by the aging gut microbiome might have the capacity to prime monocytes to take on an inflammatory phenotype even prior to egress from the bone marrow. In order to test this hypothesis, we depleted the NK cell population intraperitoneally and examined the blood and colon monocyte populations in old mice. If signals provided by the aging gut microbiota activated NK cells in the bone marrow to trigger monocyte reprogramming and result in increased Ly6C^{high} monocytes, then depletion of this population would result in a reduction of the Ly6C^{high} population in our old mice. Following intraperitoneal injections of NK1.1 antibody, the NK cell population was successfully depleted within the blood. However, we did not see any differences in the Ly6C^{high} population between the NK cell depleted group and IgG treated controls (data not shown). Furthermore, in the colon, we did not see a reduction of NK cells (Figure 11). These data suggest that the abundance of NK cells in old mice does not directly contribute to monocyte reprogramming with age. Thus, further experiments are required to fully elucidate the mechanism behind this phenomenon.

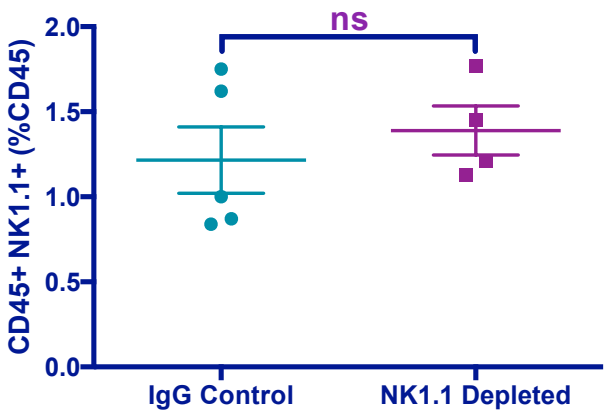

Figure 11: Intraperitoneal injection of anti-NK1.1 antibody did not result in a significant reduction in the NK cell population in the colon.
Mice were intraperitoneally injected with anti-NK1.1 antibody every other day for a week (receiving a total of three injections). Following depletion, the NK cell population was examined using flow cytometry. Within the live population, NK cells were gated as the $CD45^+$ $CD3^-$ $CD11b^-$ $MHCII^-$ $Ly6C^-$ $NK1.1^+$ cells. Values are represented as a percentage of the total $CD45^+$ population. n = 4-5 mice/group.

The composition of the old microbiota promotes age-associated inflammation

To determine whether the relationship between the age-related microbial dysbiosis and systemic inflammation in old mice is correlative or causative, we performed microbiota transfers in young and old germ-free mice. Briefly, we have colonized young and old GF mice with either the young or old microbiota in order to determine whether it is the age of the mouse or the composition of the microbiota that impacts the changes seen with age. Following colonization with a specific microbiota, we did not observe any global changes in the visual appearance of the donor SPF and recipient GF mice (data not shown).

a) i]

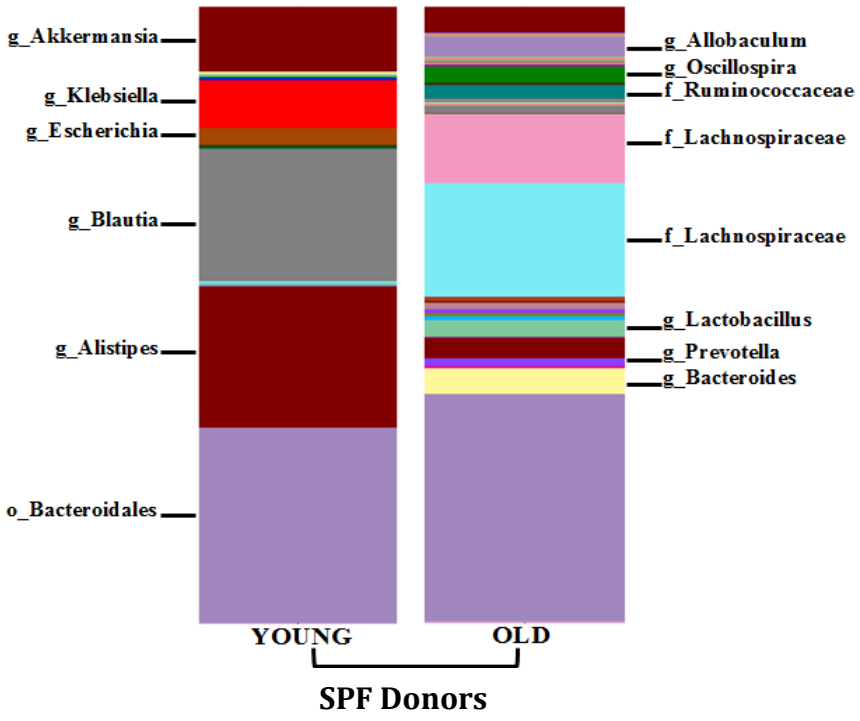
g_Akkermansia
g_Klebsiella
g_Escherichia
g_Blautia
g_Alistipes
o_Bacteroidales
g_Allobaculum
g_Oscillospira
f_Ruminococcaceae
f_Lachnospiraceae
f_Lachnospiraceae
g_Lactobacillus
g_Prevotella
g_Bacteroides
YOUNG
OLD
SPF Donors

a) ii]

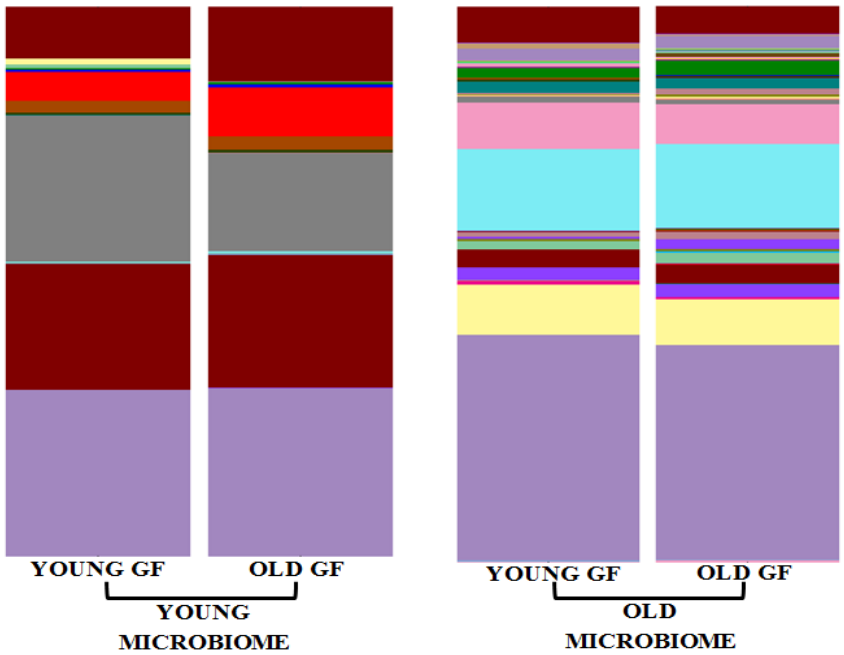
YOUNG GF
OLD GF
YOUNG MICROBIOME
YOUNG GF
OLD GF
OLD MICROBIOME

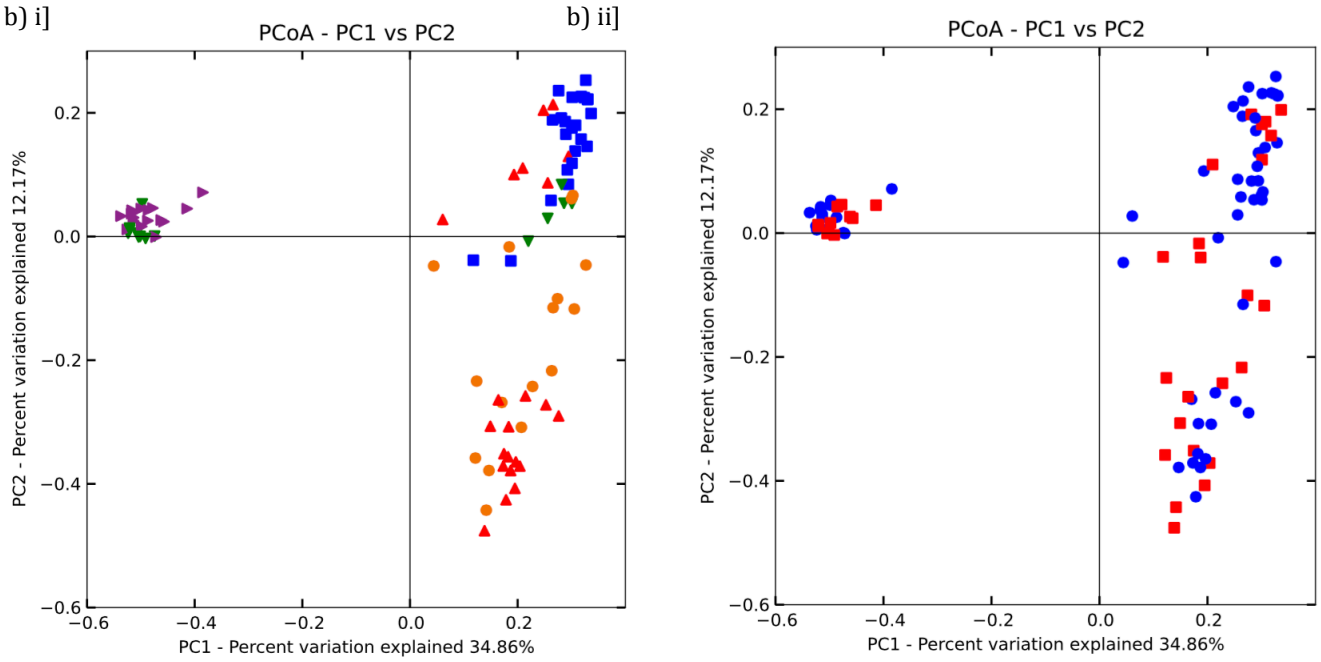

Figure 12: Germ-free mice have acquired the microbial compositions of their donor at the end of the colonization.
Germ-free mice were individually co-housed with either a young or old specific-pathogen free mouse for a total of six weeks. At the end of the colonization, fecal pellets were collected in order to complete 16S rRNA sequencing. A) The averaged taxa summary plots of all the samples within the particular group [n=5-16/group] are shown for the i] SPF Donors and ii] GF colonized recipients. The bacterial groups are labeled according to phylum and then specified to highest assigned taxonomic group. The height of the bar represents the relative abundance of the associated genus within young and old mice. Most abundant genera are labeled on the group. B) Bacterial communities of the donor and recipient mice clustered according to i] the age of the microbiome (Orange = old SPF, Blue = OGF + Old, Red = YGF + Old, Purple = YGF + Young, Green = OGF + Young) and ii] did not cluster in terms of the differing housing conditions using principal coordinate analyses (PCoA) of the Bray-Curtis distance matrix (Blue = SPF, Red = GF). For example, GF and SPF mice did not cluster separately. Each point represents one sample and is differentiated by color to indicate the age of the mouse. Plots represent the microbial composition as indicated by the -diversity between each nasal wash sample.
GF = Germ-free, SPF = Specific pathogen free, OGF = Old germ-free, YGF = Young germ-free

Following six weeks of colonization via co-housing, fecal pellets were collected from the donor SPF and recipient mice in order to examine their bacterial profiles. Taxa summary plots reveal that the compositions of the fecal microbiota of

young and old SPF donor mice are different (Figure 12A). In order to further determine if the composition of the fecal microbiome changed with age, the β-diversity metric, calculated based on the Bray-Curtis distance, was visualized using a principal coordinate analysis (PCoA) plot. This revealed that the young and old donor mice clustered distinctly from one another. (Figure 12C). Furthermore, our germ-free mice were able to successfully acquire the specific SPF donor microbiota regardless of their age (Figure 12B). This indicates that the composition of the microbiome is not influenced by the age of the recipient mouse, but rather, the age of the donor mouse. Under Bray-Curtis calculations, SPF and GF mice did not cluster separately from one another. In fact, visualizing the microbial compositions of the mice on a PCoA plot revealed that they could only be differentiated based on the donor microbiome given to them (Figure 12D). We have previously identified unique differences between the young and old gut microbiome. In order to investigate whether these changes was transferred to the colonized germ-free mice, we analyzed some of the major differences. The increase in *Firmicutes/Bacteroidetes* ratio was transferred with the old microbiota as this was seen in young GF mice colonized with the old microbiota as well (Figure 13A). Furthermore, decreases in the abundance of *Akkermansia* and *Alistipes* genera were transferred with the old microbiota in both young and old GF mice (Figure 13B and C). This suggests that colonization of young and old mice was successful and as a result, we were able to distinguish between the effects of age and microbiome composition in the subsequent experiments.

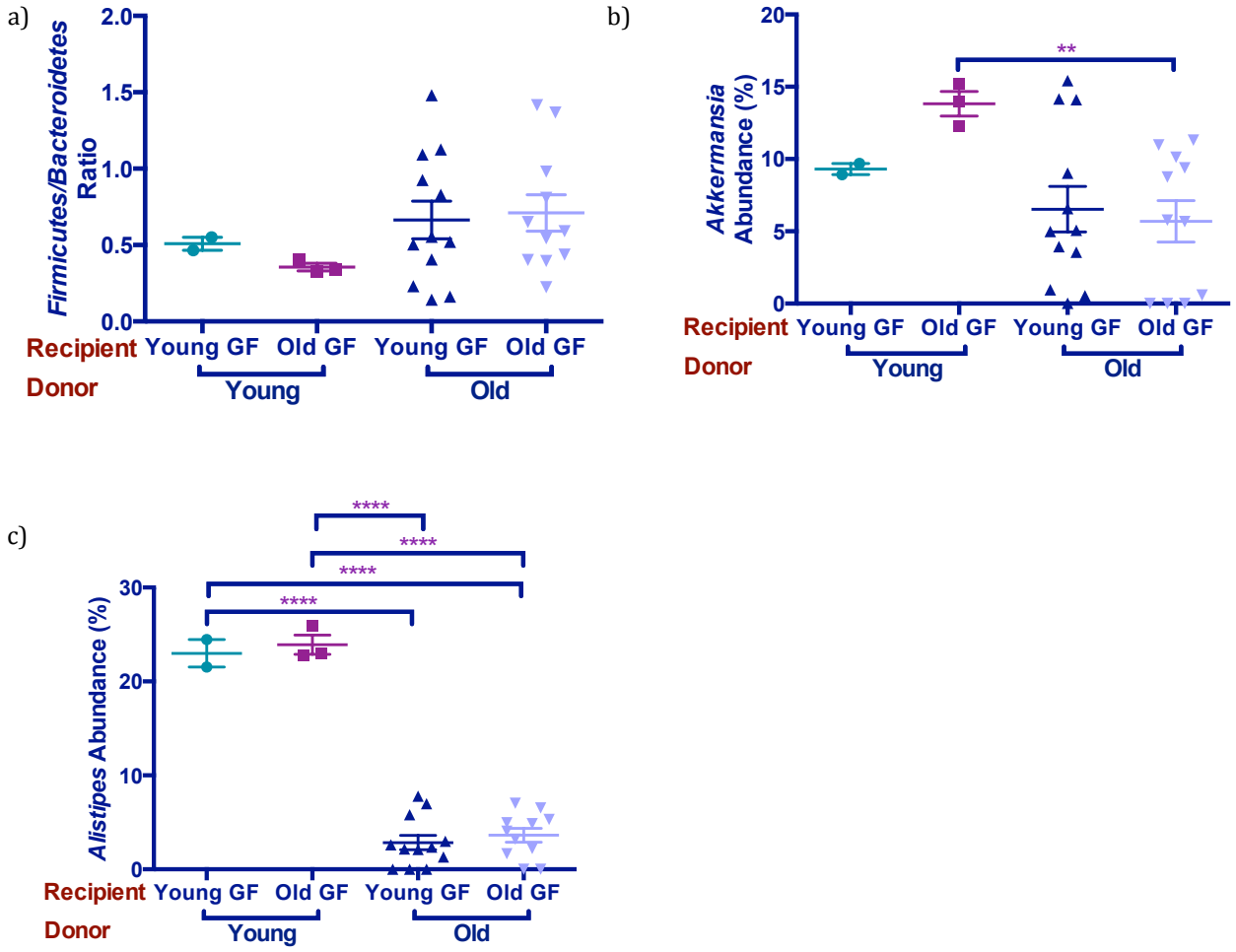

Figure 13: Colonized germ-free mice successfully acquire microbiome characterized that are similar to their donor microbiome.
Key microbial changes known to occur with the old microbiome were examined in the colonized germ-free mice in order to determine the success of the colonization. Mice colonized with the old microbiome had an A) increase in the *Firmicutes/Bacteroidetes* ratio, B) have reductions in the number of OTUs representing the *Akkermansia* genus as well as the C) *Alistipes* genus. The panels represent the mean relative abundance of each bacterial group in each category. Statistical significance was determined using multiple *t* test where appropriate (n = 3 to 12/group). P = 0.05 was considered significant.

Young GF mice colonized with the old microbiota have significantly increased paracellular permeability in their colon (Figure 14A) and systemic inflammation (Figure 14B) when compared to young GF mice colonized with the young

microbiome. Since the ages of these mice are the same, this indicates that the age of the microbiome is sufficient to induce these changes.

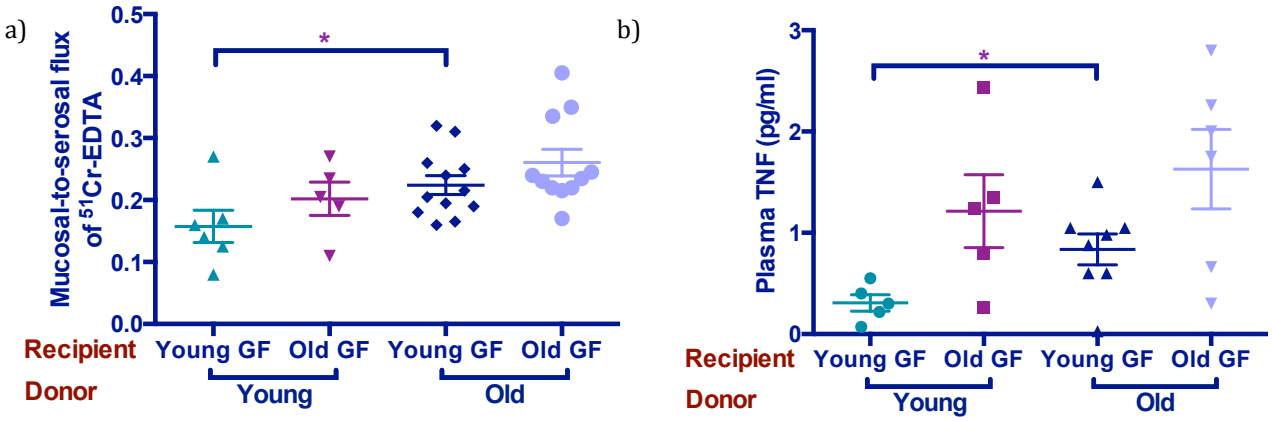

Figure 14: The old microbiome composition induces increased immune impairments in germ-free mice.
Germ-free mice were individually co-housed with either a young or old specific-pathogen free mouse for a total of six weeks. Following colonization, A) Intestinal permeability differences and B) Systemic levels of TNF were measured. A portion of the distal colon was removed from the mouse and mounted on an Ussing chamber in order to study intestinal permeability changes [n=5-12 mice/group]. Circulating levels of TNF in plasma were measured using a Luminex assay. Each sample was measured in duplicates [n = 5-8/group]. Values are the mean +/- SEM of samples within each category. Statistical significance was determined using multiple t-tests where appropriate. $P<0.05$ was considered to be significant.

We next wanted to examine whether the composition of the aging microbiome is sufficient to induce the recruitment of more inflammatory monocytes. We examined the immune populations within the blood and colon of young GF mice colonized with either the young or old microbiome. Young GF mice colonized with the old microbiome have significantly increased $Ly6C^{high}$ populations within the blood (Figure 15A) and colon (Figure 15B). These data reveal that even though the age of the mice in both of these populations are the same (<4 months old), the

composition of the microbiome alone is sufficient to induce the recruitment of inflammatory monocytes. Put together, the old microbiome has the ability to influence the phenotype of immune cells within circulation and within the gastrointestinal tract.

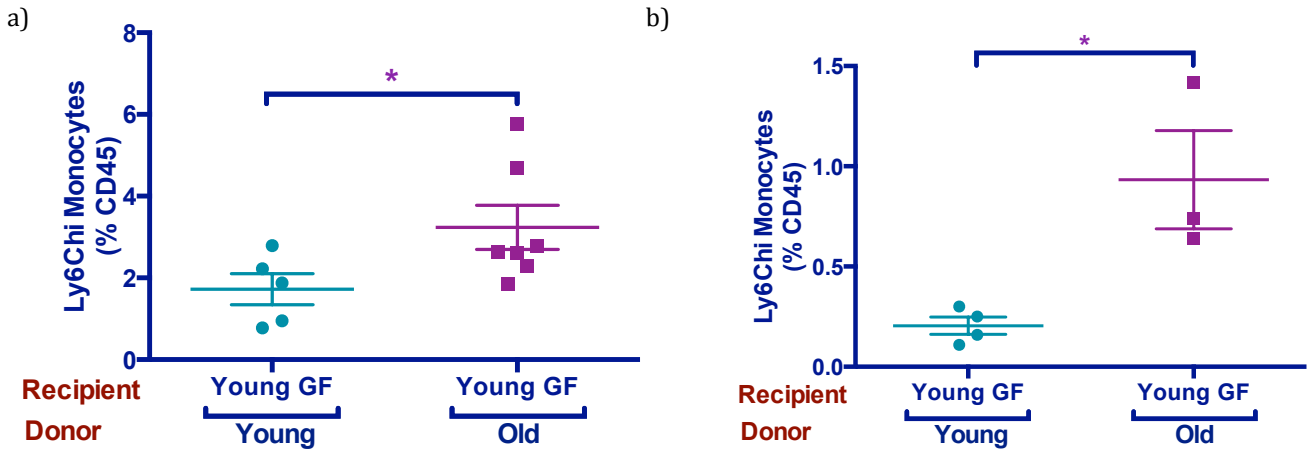

Figure 15: Colonization of germ-free mice with the old microbiome leads to the increased recruitment of Ly6Chi monocytes.
Ly6Chi monocyte populations were quantified as a population of the CD45+ population within the a) Blood and b) Colon of young germ-free mice (<3mo) that were colonized with either a young SPF microbiome or an old SPF microbiome for a total of six weeks. Values are the mean +/- SEM of samples within each category [n= 2-7 mice/group]. Statistical significance was determined using unpaired t-tests where appropriate. $P<0.05$ was considered to be significant.

The relationship between the aging gut microbiome and insulin resistance in old mice

Along with decreased protection against infectious diseases and age-associated inflammation, metabolic dysfunction is also common among the elderly. In particular, the elderly often experience glucose intolerance and insulin resistance (131–134). Insulin resistance is defined as the inability of insulin to effectively increase the uptake of glucose and inability of the tissues to use the glucose in times of need (135). Previous data has suggested that aged mice experience a post-

receptor defect in insulin action (131). Although no differences were observed in the fasting serum glucose levels between both age groups, fasting insulin levels are elevated within the elderly cohort (131). Even though the elderly have elevated insulin levels within the serum at baseline levels, and continue to have higher levels upon glucose challenge, they still maintain high levels of glucose upon challenge. This suggests that the elderly may be experiencing resistance against insulin (131). Although this phenomenon has been observed in a number of studies, the mechanism behind it is still undetermined. We hypothesized that the change in the composition of the microbiome with age may be contributing to the onset of insulin resistance with age. In order to study this, we measuring insulin resistance in our young and old germ-free mice that were colonized with either the young or old microbiota.

We did not observe any differences in the fasting blood glucose between young and old SPF donor mice (Figure 16A) or the recipient germ-free mice (Figure 16B). Germ-free mice colonized with the old microbiota however, showed slighted elevated insulin resistance compared to those mice colonized with the young microbiome (figure 16C). Although this data was not significant, it suggests a possible contribution of both the age and composition of the microbiome on insulin resistance with age.

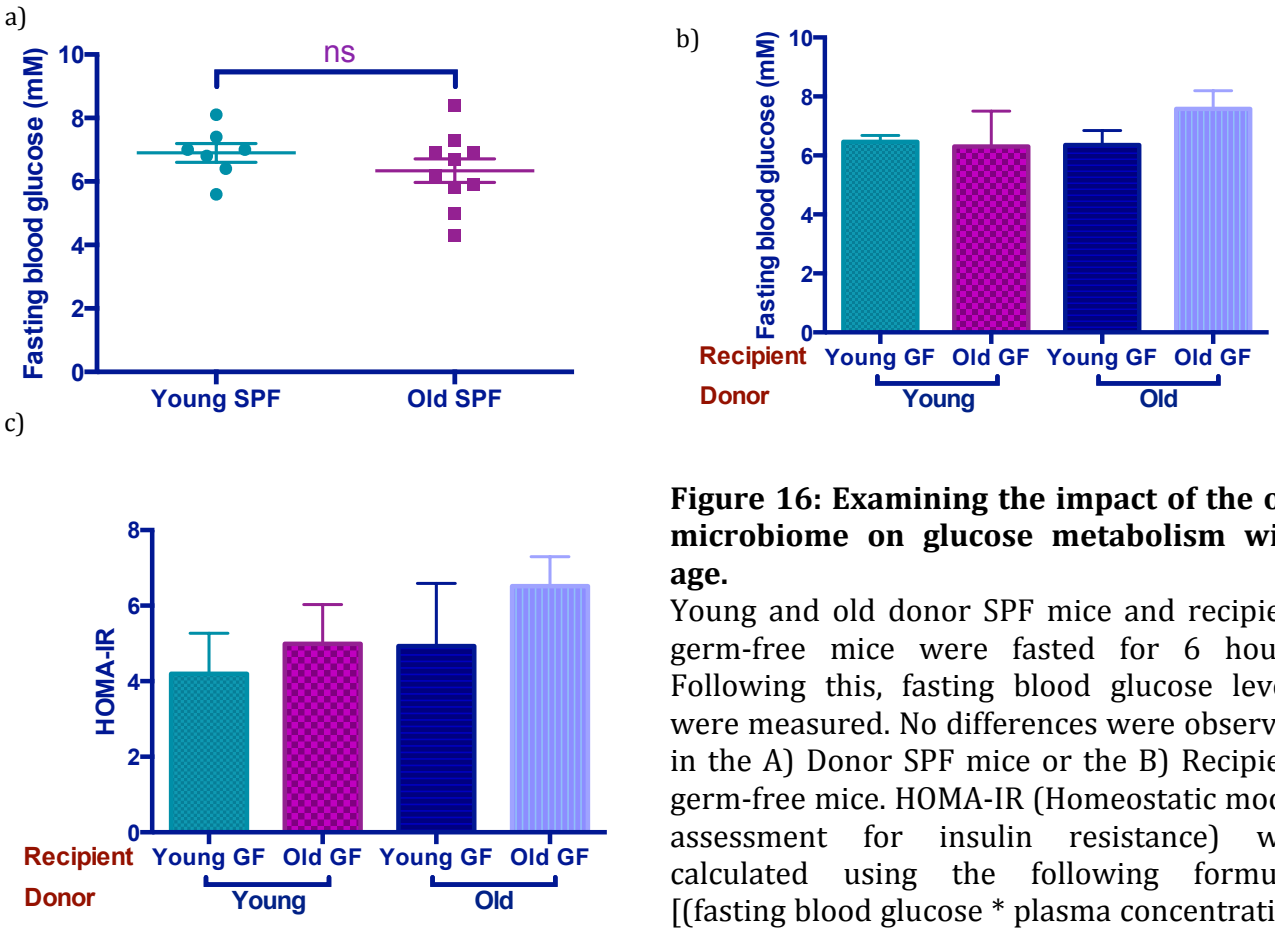

Figure 16: Examining the impact of the old microbiome on glucose metabolism with age.
Young and old donor SPF mice and recipient germ-free mice were fasted for 6 hours. Following this, fasting blood glucose levels were measured. No differences were observed in the A) Donor SPF mice or the B) Recipient germ-free mice. HOMA-IR (Homeostatic model assessment for insulin resistance) was calculated using the following formula: [(fasting blood glucose * plasma concentration of insulin) / 22.5]. Statistical significance was determined using multiple *t* test where appropriate (n = 2-7/group). P = 0.05 was considered significant.

Microbiome composition influences anti-pneumococcal immunity

We have thus far shown that systemic inflammation and monocyte mobilization seen in our aged mice can be, at least partly, explained by the composition of the gut microbiota. Previous work in our lab has shown that old mice are more susceptible to pneumococcal infections (96). In fact, when young and old mice are intranasally colonized with *Streptococcus pneumoniae*, the majority of young mice are able to clear the bacteria from their upper respiratory tract 21 days

after colonization. However, old mice have a decreased ability to clear the bacteria (57, 96). Our lab has previously demonstrated that old mice have delayed clearance of *S. pneumoniae* because of defects in Ly6C^{high} monocytes. Since we have shown that the composition of the microbiota alters the number of Ly6C^{high} monocytes in circulation, we hypothesized that it might also alter susceptibility to *S. pneumoniae*.

Thus, we wanted to examine whether the composition of the microbiome could influence the response against a bacterial stressor. In order to do so, we colonized young GF mice with either the young or old microbiome. Following six weeks of colonization, all donors and recipients were intranasally colonized with *S. pneumoniae*. Following five days of colonization with the bacteria, we did not notice any significant changes in mortality or weight loss (data not shown). Quantifying the bacterial CFUs within the nasal wash of the infected mice revealed an increase in bacterial CFUs within the young GF mice colonized with the old microbiome (Figure 17). However, this increase was not significant.

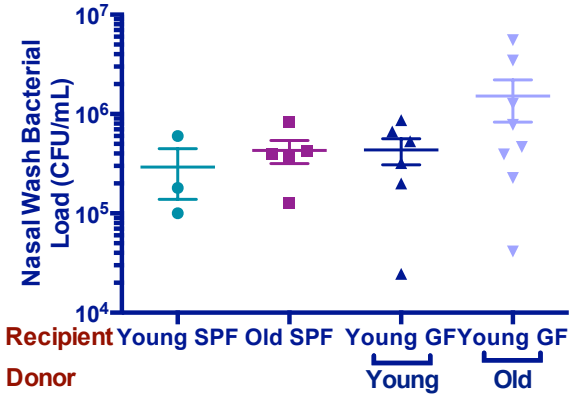

Figure 17: Colonization of young germ-free mice with the young microbiome does not lead to complete protection against a *S. pneumoniae* bacterial challenge when compared to young germ-free mice colonized with the old microbiome.
Young germ-free mice were colonized with either the young [n = 8] or old [n = 8] microbiome using the co-housing method for a total of six weeks. Following co-housing, mice were intranasally colonized with 10^7 CFU/mL of *S. pneumoniae* (strain P1547). Following five days of colonization with the bacterium, bacterial CFU's from the nasal washes were quantified within the mice to measure their ability to clear the bacteria five days after colonization. Statistical significance was determined using unpaired t-tests where appropriate.

Plasma levels of TNF and IL-6 were measured within the donors and recipients in order to determine whether bacterial challenge in the presence of the old microbiome induced a hyper-inflammatory response. We hypothesized that mice colonized with the old microbiome would have significantly elevated levels of pro-inflammatory cytokines within their plasma following *S. pneumoniae* challenge. However, we did not observe any differences in plasma levels of TNF (Figure 18A) or IL-6 (Figure 18B).

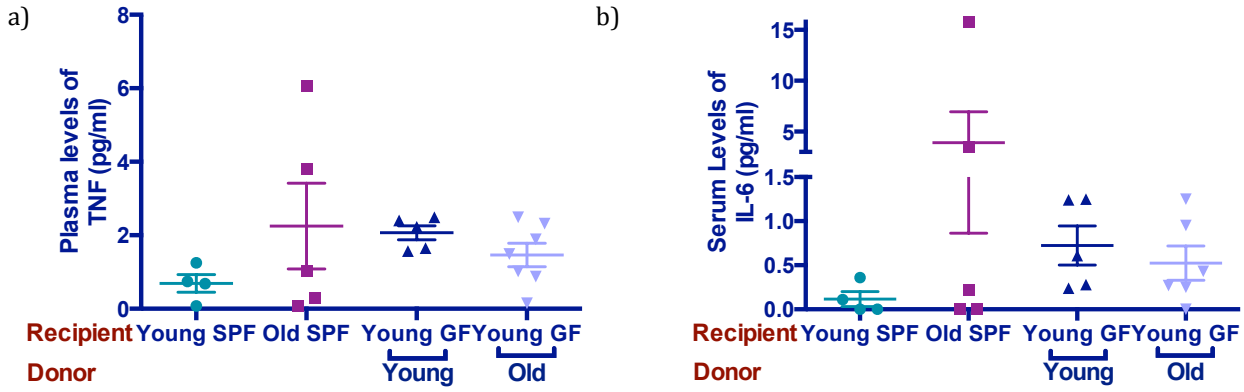

Figure 18: Colonization of young germ-free mice with the old microbiome does not result in the induction of a hyper-inflammatory response when colonized with *S. pneumoniae*. Young germ-free mice were intranasally colonized with either the young [n = 8] or old [n = 8] microbiome using the co-housing method for a total of six weeks. Following co-housing, mice were intranasally colonized with 10^7 CFU/mL of *S. pneumoniae* (strain P1547). Following five days of colonization with the bacterium, plasma was collected from all four groups in order to measure the circulating levels of pro-inflammatory cytokines. We did not observe a significant increase in the circulating levels of A) TNF and B) IL-6 in young germ-free colonized with the old microbiome. Statistical significance was determined using unpaired t-tests where appropriate (n = 4-7 mice/group).

In order to examine the influx of inflammatory monocytes within circulation, we quantified the Ly6C^{high} population within the blood using flow cytometry. The Ly6C^{high} population, quantified as a percentage of the total leukocyte population, was significantly higher within old SPF mice, when compared to their young controls (Figure 19A). Furthermore, we observed a significant increase in Ly6C^{high} monocytes within young GF mice colonized with the old microbiota compared to those colonized with the young microbiome. These data suggest that the old microbiome promotes the recruitment of more inflammatory monocytes within circulation following a bacterial challenge. We did not observe any differences within the lungs (Figure 19B).

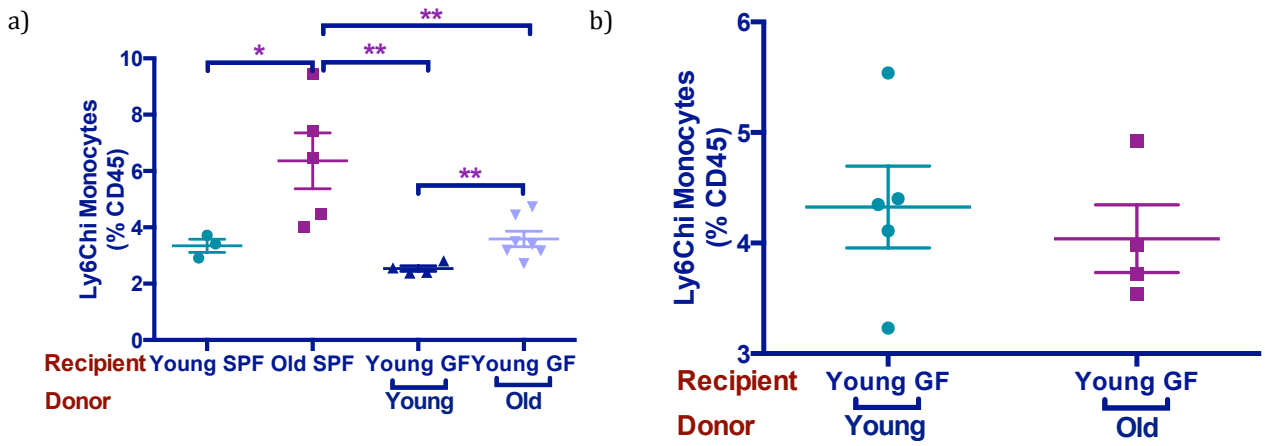

Figure 19: Young germ-free mice colonized with the old microbiota have increased Ly6C^{high} monocytes in circulation, but not within the lungs, following *S. pneumoniae* challenge compared to young germ-free mice colonized with the young microbiome.
Ly6C^{high} monocyte populations were quantified as a population of the CD45^{+} population within the a) Blood and b) Lungs of young germ-free mice (<3mo) that were colonized with either a young SPF microbiome or an old SPF microbiome and then challenged with *S. pneumoniae*. Values are the mean +/- SEM of samples within each category [n= 5-8 mice/group]. Statistical significance was determined using unpaired t-tests where appropriate. P<0.05 was considered to be significant.

DISCUSSION

The idea that the intestinal microbiome could potentially influence the health of an individual and contribute to the onset of senility within the elderly was suggested early in the 1900s by Elie Metchnikoff (136). Since then, the idea that microbial translocation across the intestinal barrier could cause immune activation, and subsequent systemic inflammation has been studied in the context of other diseases like HIV (137–140). Work conducted in our lab has shown that naïve germ-free mice are protected from a number of age-associated defects when compared to aged SPF mice, indicating that the presence of the aging microbiome drives these changes in old mice. We have investigated the relationship between the aging microbiome and its impact on the immune system of the elderly by colonizing young

and old germ-free mice with an age-specific microbiota. Furthermore, when young GF mice are colonized with the aged microbiome, we observed changes within these mice that were similar to that observed within the old SPF donors. These data suggest that the composition of the old microbiome facilitates the onset of age-associated inflammation and the accompanying defects.

Tissue resident intestinal macrophages have highly plastic functions within the intestines. Their functional diversity allows them to perform various activities during healthy and inflamed conditions. The intestinal macrophage pool requires constant replenishment via the circulating blood monocytes (44). Although monocyte recruitment to the intestinal mucosa is dependent on CCR2, the source of this chemokine is still unclear. Others and we have proposed that signals provided by the composition of the microbiome might be playing a role in the recruitment of monocytes to the intestine and this in turn may be impacting the differentiation and abundance of macrophages within this region as well (44) .

We have observed an increase in Ly6C^{high} monocytes within the colon. This population is often referred to as "inflammatory" monocytes because of their tendency to migrate towards regions of inflammation, their likelihood to develop into pro-inflammatory macrophages, produce more pro-inflammatory cytokines and less PGE2 and IL10. Furthermore, the balance between resident and pro-inflammatory macrophages within the colon are influenced by the recruitment of monocyte subsets via CCR2 (141). During times of inflammation, the phenotype and abundance of resident macrophages has not been shown to change. They tend to

maintain function by producing high levels of IL10 and remain hyporesponsive to TLR stimulation. Inflammation within the colon however, is partly mediated via recruited Ly6C^{high} monocytes that are able to differentiate into pro-inflammatory macrophages and contribute to inflammation within the colon. The increase in Ly6C^{high} monocytes within the colon with age may be contributing indirectly to negative consequences, like increased paracellular permeability, within the gut. In an inflamed gut, Ly6C^{high} monocytes have shown to upregulate TLR2 and NOD2, which make them more susceptible to recognize and become activated by bacterial products. This in turn skews their differentiation pattern and promotes pro-inflammatory effector cells in models of acute inflammation (48). Furthermore, other studies have shown that reducing the abundance of Ly6C^{high} monocytes within the intestine by either using models of CCR2-/- mice or by administrating anti-CCR2 antibody, results in the reduction of susceptibility towards colitis and as well, reduces colonic inflammation as measured by IL-6 and IL1b (48, 141). Ly6C^{high} monocytes are effectively recruited to inflamed tissues within the intestine. Furthermore, inflammation has been shown to promote the differentiation of these monocytes from anti-inflammatory macrophages to more pro-inflammatory dendritic cells (142). In models of IBD, data suggest that the inflammation mediated by monocytes are the key contributors to colitis following DSS treatment (143). In such models, monocyte derived lamina propria dendritic cells were examined as the source of pathology. Reconstitution of TNF-deficient monocytes into lamina propria DC depleted mice resulted in only mild pathology upon DSS treatment when

compared to wildtype monocyte recipients (143). Put together, these data suggest that inflammation can promote the recruitment of Ly6C^{high} monocytes and influence their differentiation into macrophages as well. This constant recruitment of Ly6C^{high} monocytes and expansion of intestinal macrophages during an inflamed state may lead to excessive inflammation and intestinal damage as well.

Intestinal macrophages are geographical positioned to mediate the relationship between the host intestinal epithelium as well as the diverse intestinal microbiome. Within this particular region, macrophages are constantly scavenging for bacterial products, pathogens and other foreign particles that can be detrimental to the host. Under the steady state, intestinal macrophages are able to effectively remove debris without provoking excessive inflammation or epithelial disruption. However, in cases of chronic inflammation, as seen with the aging process, differentiation of this cell type can be disrupting, leading to the differentiation of pro-inflammatory macrophages within this region (144). Although the mechanisms behind what may be contributing to disruption in balance between homeostatic and pro-inflammatory macrophages within the colon are unclear, we have proposed that the composition of the aging resident microbiome might be a contributing factor.

Within the large intestine, the resident microbiome has been shown to influence the homeostatic function of macrophages. Specifically, IL10 production by intestinal macrophages has been shown to be largely dependent on the presence of the microbiome (145). Lamina propria macrophages isolated from germ-free mice have been shown to have significant reductions in the production of IL10 compared

to those isolated from SPF mice (145). Furthermore, stimulation of these macrophages from GF mice with LPS resulted in an increased production of TNF and IL-6, suggesting that the LPS hyporesponsiveness seen in resident lamina propria macrophages in the steady state is partly mediated by the gut microbiome. Specific members of the gut microbiome like Bacteroides fragilis, have also been shown to play a role in mediating the adaptive immune system within the gut as well (145). In particular, polysaccharide A that is derived from B. fragilis is able to promote the development of IL10 - producing T regulatory cells (145, 146). Moreover, the presence of the microbiome itself is necessary for the efficient recruitment of Ly6C^{high} monocytes within the colonic mucosa. This has been shown following the depletion of the microbiome using broad spectrum antibiotics (46). We and others have also shown that the abundance of Ly6C^{high} monocytes are also markedly reduced within the colons of adult germ-free mice (46). This suggests that the microbiome influences the recruitment of Ly6C^{high} monocytes within the colon and can also determine the phenotype and function of the differentiated macrophages within these tissues.

In models of IBD, both the presence and the composition of the microbiome have been associated with the onset and severity of disease. GF mice have been shown to be more resistant to the development of colitis upon treatment with DSS (147). Furthermore, transfer of a specific microbiome into germ-free mice has been able to recapitulate the disease state in a number of IBD models. For example, colonization of GF mice with microbiome samples isolated from ulcerative colitis

patients have shown to increase the susceptibility towards intestinal inflammation (147). In our mouse model of aging, we wanted to determine whether the age-associated effects seen within our old mice were in part mediated by the composition of the aging microbiome. Thus, we have utilized gnotobiology in order to determine the relationship between these two. Colonization of young GF mice with the old microbiome resulted in increased systemic levels of TNF, increased intestinal permeability and increased recruitment of $Ly6C^{high}$ monocytes within the blood and colon when compared to young GF mice colonized with the young microbiome. This reveals that regardless of the age of the mouse, colonization with the aged microbiome is sufficient to induce some of the age-related changes observed within our old mice. We are suggesting that intestinal microbial dysbiosis occurring with age contributes to the chronic inflammation observed within old mice. Systemic inflammation, as discussed in the previous chapter, has been associated with decreased barrier integrity in a number of studies. This increase in paracellular permeability within the colon may be resulting in the translocation of bacterial products into circulation, ultimately feeding back to the cycle of increasing inflammation with age.

Ultimately, our goal is to determine whether the change in the microbiome with age has a physiological relevance in old mice. Upon infection with S. pneumoniae, our pilot data suggested that young GF mice colonized with the old microbiome may have increases in the total bacterial CFU numbers within the nasal wash. However, we did not find a hyper-inflammatory response in the plasma of

mice colonized with the old microbiota. This experiment needs to be replicated in order to fully elucidate the role of the aging gut microbiome on anti-pneumococcal immunity in the elderly.

The old gut microbiome contributes to age-associated inflammation in aged mice. Transferring the old microbiota composition to a young germ-free mouse was able to recapitulate various outcomes observed in old SPF mice. We are suggesting that components of the aging gut microbiome may be contributing to increased paracellular permeability within the colons of old mice. This in turn may be leading to increased systemic inflammation and decreased immune function with age. This work provides a broad understanding of how the composition of the old microbiome causes immune dysfunction in old mice. By understanding what changes occur within old mice and determining the effects of these changes, we are able to better target aspects that can be modified in old mice and promote healthy aging and protection against infectious diseases.

Chapter 5: Combating age-associated inflammatory defects in old mice by targeting the pro-inflammatory cytokine, TNF.

INTRODUCTION

Tumor necrosis factor (TNF) is a multi-functional pro-inflammatory cytokine that is produced by a broad range of cell types including macrophages, monocytes, and endothelial cells (148). Release of this cytokine in response to an injury or insult is crucial for its clearance and recovery processes. However, chronic exposure to TNF, as occurs with age, has detrimental effects on the host, including gut microbial dysbiosis and immunosenesence (10, 96, 100). Our lab has previously identified immune dysfunctions due to TNF using $TNF^{-/-}$ mice (58). Specifically we have shown changes in the monocyte and macrophage phenotype and function in old $TNF^{-/-}$ mice. Old $TNF^{-/-}$ mice have fewer $Ly6C^{high}$ monocytes in the blood. In accordance with this, stimulation of whole blood from old WT mice with LPS for 24 hours results in a significant increase in IL-6 production. However, old $TNF^{-/-}$ mice do not show these changes. Furthermore, we have shown that the deficiency of TNF with age contributes to improved immunity against pneumococcal colonization (58).

In this chapter, we have shown that that aged $TNF^{-/-}$ mice are protected from age-associated inflammation as measured by systemic levels of IL-6. We also observed a lack of gut microbial dysbiosis in $TNF^{-/-}$ mice which we hypothesize may contribute to protection against increases in paracellular permeability in the colon. Reduction of TNF using anti-TNF in old mice resulted in an overall decrease in systemic inflammation and reduced the degree of microbial dysbiosis. Understanding the effects of elevated TNF levels in old mice will allow us to identify

and target components of the inflammatory cascade that ultimately result in immune dysfunction with age.

RESULTS

$TNF^{-/-}$ mice are protected from age-associated inflammation, barrier defects and the degree of microbial dysbiosis with age

In order to investigate the role of TNF in age-associated inflammation, we examined young and old TNF knockout ($TNF^{-/-}$) mice, which are inherently deficient in the TNF gene. We hypothesized that aged $TNF^{-/-}$ mice would be protected by some of the defects, caused by chronic age-associated inflammation, as a result of their knockout status. Using a Luminex ELISA kit (Millipore), we found that old $TNF^{-/-}$ mice have significantly lower systemic levels of IL-6 (Figure 20). This is presumably due to the fact that IL-6 functions downstream of TNF (149). This suggested that old $TNF^{-/-}$ mice do not experience chronic inflammation and thus, we sought to investigate whether our old $TNF^{-/-}$ mice were protected from the age-associated defects that we have previously identified.

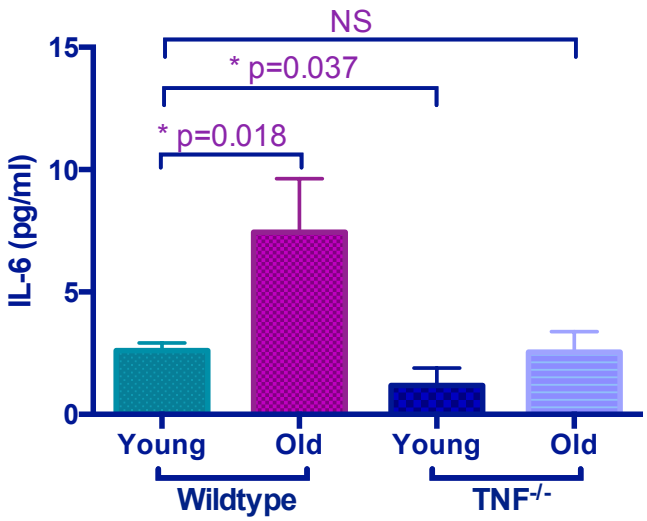

Figure 20: TNF$^{-/-}$ mice are protected from increases in systemic levels of IL-6.
Circulating levels of IL-6 was measured in the plasma of young and old wildtype and TNF$^{-/-}$ mice using a Luminex assay. Each sample was measured in duplicates. Values are the mean +/- SEM of samples within each category. Statistical significance was determined using unpaired t-tests where appropriate [n = 3- 13/group]. P<0.05 was considered to be significant.

a)

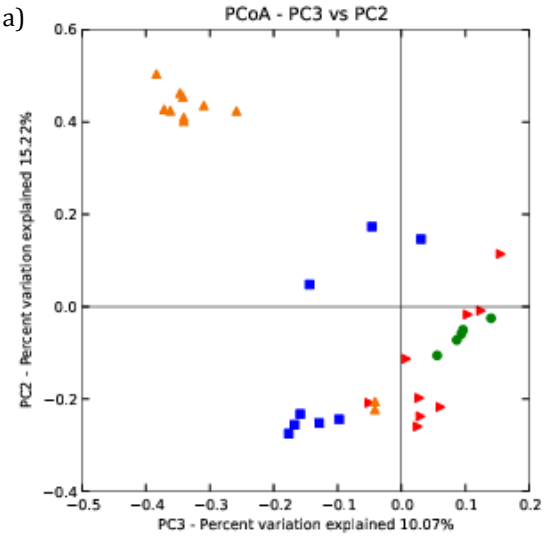

b)

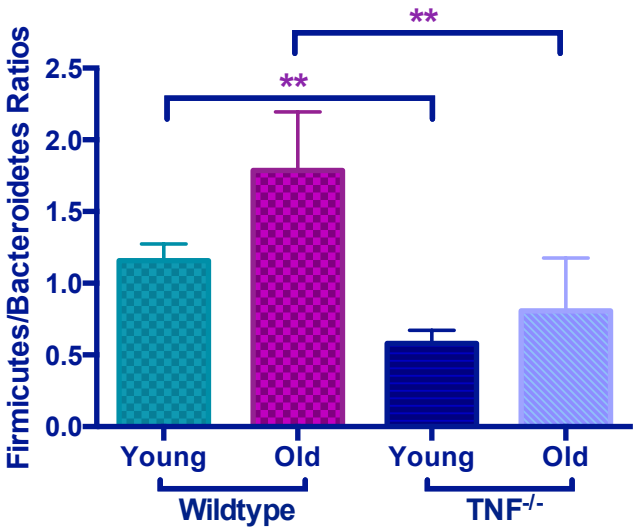

c)

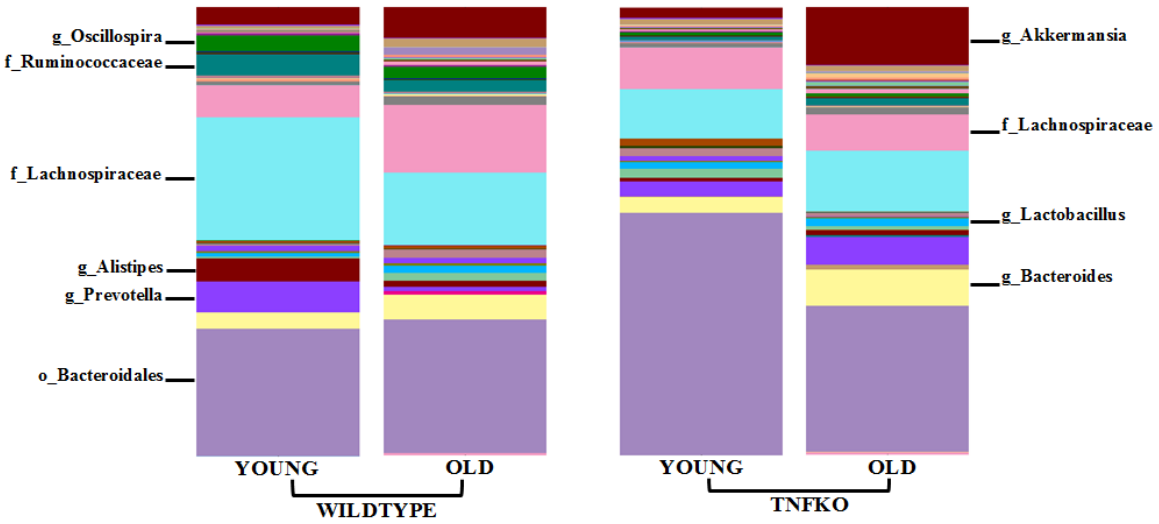

Figure 21: 16S sequencing of the gut microbiome from young and old WT and TNF$^{-/-}$ mice reveals differences in the old TNF$^{-/-}$ microbiome.
Bacterial communities were analyzed using Qiime software. A) Communities clustered using principal coordinate analyses (PCoA) of the Bray-Curtis distance matrix. Each point represents one sample and is differentiated by color to indicate the group. Plots represent the microbial composition as indicated by the β-diversity between each fecal sample. Communities of old TNF$^{-/-}$ mice clustered closely with young WT mice. [Green = young WT, Blue = old WT, Red = old TNF$^{-/-}$, Orange = young TNF$^{-/-}$. B) The *Firmicutes/Bacteroidetes* ratio was quantified in all four groups. C) Average taxa summary plot of all samples within a particular group (*n* = 5 to 16/group). The bacterial groups are labeled according to phylum and then specified to the highest assigned taxonomic group. The height of the bar represents the relative abundance of the associated genus. The most abundant genera are labeled on the group.

In the previous chapters, we have extensively characterized the role of the microbiome in contributing to age-associated inflammation. By colonizing germ-free mice with microbiota derived from young and old mice, we have demonstrated that the old microbiota significantly increases systemic inflammation and paracellular permeability. In order to determine if the microbial dysbiosis that we observe with age is a result of immune defects attributable to age-associated inflammation, we compared microbial dysbiosis in young and old TNF$^{-/-}$ mice to that of young and old WT mice. If microbial dysbiosis occurs as a result of age-associated inflammation,

then the old TNF$^{-/-}$ mice should not experience the same degree of dysbiosis as old SPF mice. If age related microbial dysbiosis is independent of TNF, then old TNF$^{-/-}$ mice should have the same degree of dysbiosis as old WT mice. We examined the fecal microbiome composition using Illumina sequencing of the 16S rRNA gene. Examining the β-diversity of young and old WT and TNF$^{-/-}$ mice using Principle Coordinate Analyses Plots under the Bray-Curtis calculations revealed that, wild-type mice clustered distinctly between their age groups (Figure 21A). Furthermore, the β-diversity of old TNF$^{-/-}$ mice clustered closely with young WT mice.

In order to observe these characteristics in more details, we examined the microbial community using taxa summary plots. When examining the composition of the microbiome at the genus level, it is evident that although the general compositions of the microbiome in old WT and TNF-/- mice are the same, the abundances of specific bacterial groups change (Figure 21C). One such difference is the ratio between the *Firmicutes/Bacteroides* phylas. We have observed increases in this ratio with age in our old wild-type mice; however, the ratio of these two phylas does not change with age in our old TNF$^{-/-}$ mice (Figure 21B).

In chapter 3, we extensively characterized the composition of the old microbiota and identified which bacterial groups are altered with age (Table 1 and 2). Interestingly, old TNF$^{-/-}$ mice may not experience some of these age related changes in the microbial composition. Several OTUs representing bacterial groups that are increased or decreased in old WT mice, but not old TNF$^{-/-}$ mice are tabulated in Table 1 and 2. Examples of bacterial genera that were decreased with age in the

WT mice but unaffected in TNF-/- mice include *Akkermansia* and *Blautia* (Table 2). Furthermore, the old WT mouse microbiome had a significant increase in OTUs belonging to the *Lactobacilli, Clostridium, Allobaculum, Bifidobacterium*, and *Oscillospira* groups (Table 1). $TNF^{-/-}$ mice did not have age-associated increases in the OTUs representing these genera. Therefore, although we observe age-related microbial changes in the WT microbiome, our data suggests that old $TNF^{-/-}$ mice do not experience the same degree of microbial dysbiosis when compared to their young $TNF^{-/-}$ counterparts.

In this chapter, we have thus far shown that $TNF^{-/-}$ mice are protected from increases in systemic inflammation and do not experience age-related microbial dysbiosis. Since our aged $TNF^{-/-}$ mice are protected from these two common age-associated defects, we hypothesized that they would as a result be protected from the structural changes observed in the gut as well. Specifically, if microbial dysbiosis drives intestinal permeability than old $TNF^{-/-}$ mice should be protected from intestinal permeability increases, as they do not experience the same degree of microbial dysbiosis observed in old WT mice. In another manner, if intestinal permeability is driven by systemic inflammation, then aged $TNF^{-/-}$ mice will be protected as well. In order to test these hypotheses, we first examined whether old $TNF^{-/-}$ mice experience increase intestinal permeability. After examining this, we tested the effects of blocking TNF on both microbial dysbiosis and barrier integrity. Old $TNF^{-/-}$ mice do not have increased paracellular permeability in the colon (Figure 22), and as a result, there was no detectable MDP within circulation (11).

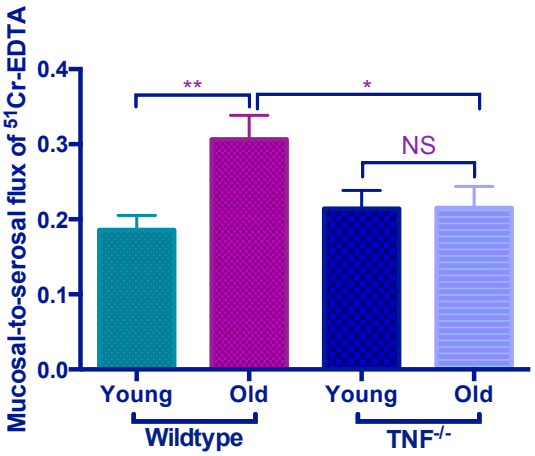

Figure 22: Old TNF$^{-/-}$ mice have significantly reduced paracellular permeability in the colon when compared to old wildtype mice.
A portion of the distal colon was removed from the mouse and mounted on an Ussing chamber in order to study intestinal permeability changes [n = 4- 11/group]. Values are the mean +/- SEM of samples within each category. Statistical significance was determined using multiple t-tests where appropriate. P<0.05 was considered to be significant.

With a reduction in microbial dysbiosis and age-associated inflammation, we hypothesized that old TNF$^{-/-}$ mice would also be protected from the phenotypic changes observed in the myeloid cell lineage with age. Old TNF$^{-/-}$ mice have a significant reduction in the abundance of Ly6C^{high} monocytes within the colon (Figure 23A). Others in our lab have shown that these mice are also protected from an increase in Ly6C^{high} monocytes within circulation (58). Interestingly, fewer colonic macrophages were found in mice presumed to be protected from gut microbial dysbiosis (ie. young and old TNF$^{-/-}$ and GF mice) (Figure 23B). Put together, these data suggest that without the constant exposure to TNF throughout life, old TNF$^{-/-}$ mice are protected from a number of the physiological, immunological and microbiome changes observed in aging wild-type mice.

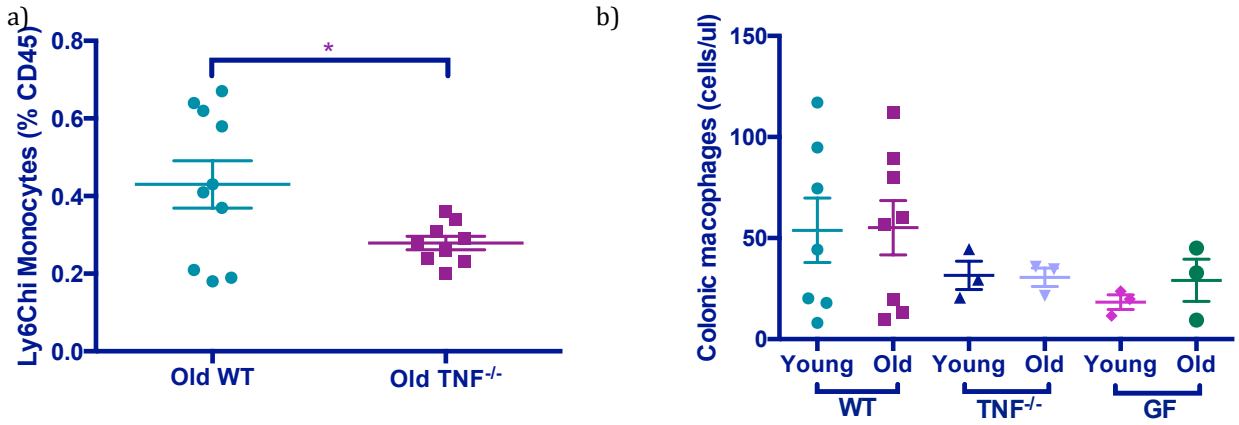

Figure 23: Monocyte and macrophage numbers are elevated in wildtype mice.
A) Abundance of Ly6C^{high} monocytes as a population of the CD45% population was determined using flow cytometry. Ly6C^{high} monocytes are significantly reduced in old TNFKO mice compared to their old WT counterparts within the colon. Old SPF mice (>18mo) were compared to old TNFKO mice (>18mo) [n = 9-10 mice/group]. B) Colonic macrophage population was quantified in young and old wildtype, TNF$^{-/-}$ and germ-free mice using flow cytometry. Macrophages were gated in the live cell population as CD45^{+} CD3^{-} CD11b^{+} SSC^{lo} CD64^{+} cells. Values are the mean +/- SEM of samples within each category. Statistical significance was determined using unpaired t-tests where appropriate. * indicates $p < .05$.

Anti-TNF therapy helps reduce some of the age-associated changes in old mice

We next investigated whether removing systemic TNF by administering anti-TNF therapy to our young and old mice would reduce age-associated microbial dysbiosis. We administered the anti-TNF drug, Adalimumab (Humira) or an isotype control i.p. to young and old mice at a concentration of 40ug/g. Since Humira is a human monoclonal antibody that functions to bind to TNF and inhibit its function, we hypothesized that administering this drug would result in an overall decrease in TNF and systemic inflammation in old mice. Previous work in our laboratory has shown that administration of Humira to old mice results in a reduction in the circulating levels of Ly6C^{high} monocytes (58). Furthermore, the number of Ly6C^{high} monocytes in the blood was reduced with Humira treatment, suggesting that fewer

monocytes are egressing from the bone marrow in response to reduced TNF. Intracellular staining on blood monocytes from Humira-treated old mice had reduced production of TNF and IL-6 in comparison to isotype-treated old controls as well (58). In our Humira-treated old mice, we found a decrease in the plasma levels of TNF (Figure 24A) and IL-6 (Figure 24B), suggesting that anti-TNF therapy was not only able to specifically target systemic levels of TNF, but it was able to reduce the overall levels of inflammation as well.

In order to determine if the microbiome composition was altered in old mice treated with Humira, fecal pellets were collected following the last day of injections and sequenced using Illumina sequencing. We hypothesized that reducing systemic inflammation in old mice would shift the microbiome composition to that more similar of a young control treated mouse. Without, highly elevated levels of TNF, we predicted that Humira-treated old mice would experience reduced microbial dysbiosis within the gut.

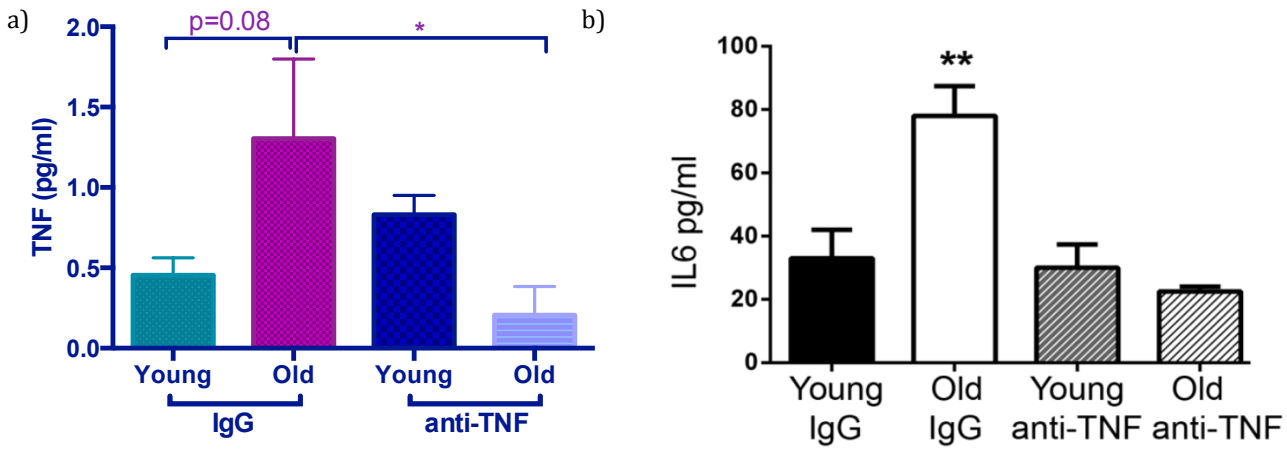

Figure 24: Anti-TNF results in a significant reduction of systemic inflammation in old mice.
Young (n=6) and old (n=6) mice were treated with anti-TNF (Humira) or an IgG control intraperitoneally. Plasma A) TNF and B) IL-6 levels were measured following drug treatment using a Luminex assay. Statistical significance was determined using multiple *t* test where appropriate. *P* = 0.05 was considered significant.

Examining the taxa summary plots indicates these changes more specifically (Figure 25A). We found that anti-TNF therapy was able to reverse some of the key changes observed in old wild-type mice. Specifically, anti-TNF therapy in old mice resulted in increases in the number of OTUs representing the *Bacteroides, Adlercreutzia, Peptococcaceae, Coriobacteriaceae* and *Subdoligranulum* groups and decreases in the number of OTUs belonging to the *Roseburia* and *Anaerofustis* groups (Table 1 and 2). Examining the β-diversity using a Principle Coordinate Analyses plot revealed that although Humira-treated mice did not cluster closely with young controls, they did have a microbial composition that was different from old control mice (Figure 25B). These data suggest that reducing systemic inflammation by

administering anti-TNF therapy does change the composition of the fecal microbiome.

a)

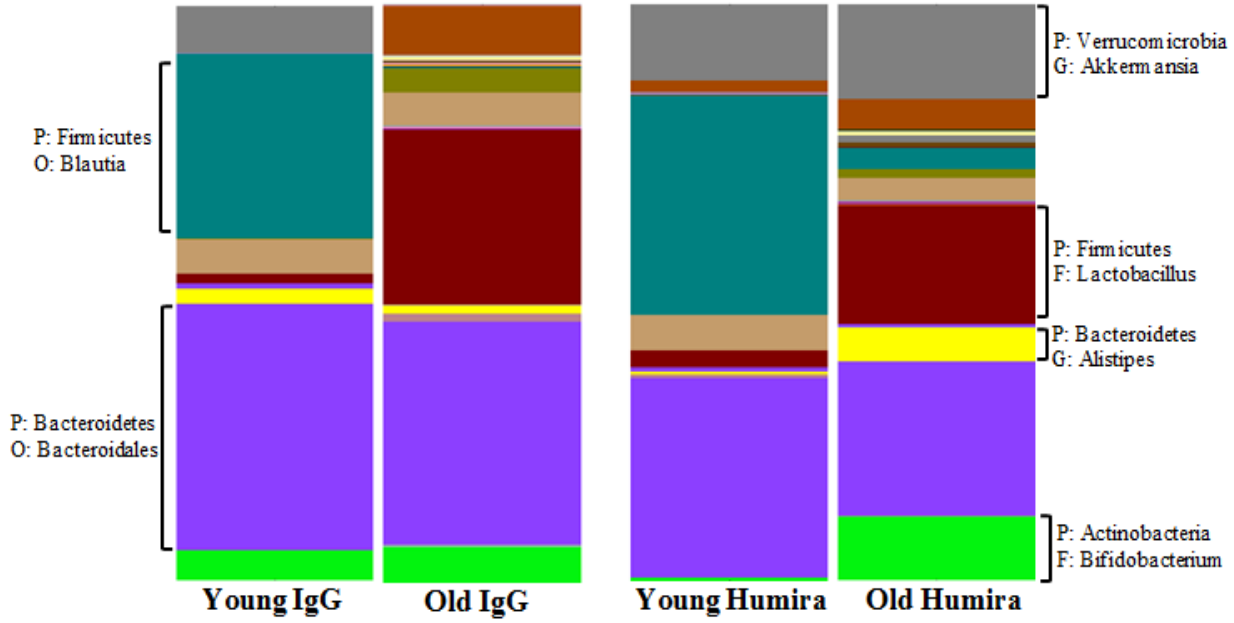

b)

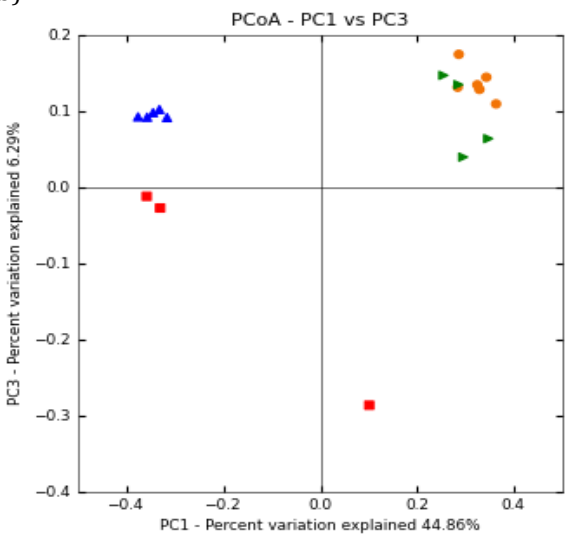

Figure 25: Treatment with anti-TNF alters the fecal microbiome of old WT mice.
Mice were injected intraperitoneally with an IgG control or anti-TNF (Humira) at 40ug/g for a period of 2.5 weeks. Fecal pellets were collected at the end of injections from young (<3mo) and old (>18mo) IgG control treated or Humira treated mice and bacterial communities were examined to determine the differences between groups. A) The averaged taxa summary plots of all the samples within the particular group [n=3-5/group]. The bacterial groups are labeled according to the highest assigned taxonomic group. The height of the bar represents the relative abundance of the associated genus within young and old mice. Most abundant genera are labeled on the group. B) Communities clustered using Principal coordinate analyses (PCoA) of the Bray Curtis distance matrix. Each point represents one sample and is differentiated by

colour to indicate their group. Plots represent the microbial composition as indicated by the β-diversity between each fecal pellet sample. Green = Young IgG treated; Blue = Old IgG treated; Orange = Young Humira treated; Red = Old Humira treated.

Examining whether the old TNFKO microbiome is protective against age-associated inflammation

Our data thus far has suggested that the old microbiome is associated with increased age-associated inflammation and decreased in gut barrier integrity. Furthermore, we have shown that the onset of these changes with age is directly or indirectly mediated by the elevated levels of TNF in old mice. Furthermore, old $TNF^{-/-}$ mice experienced reduced microbial dysbiosis with age in comparison to their wild-type counterparts. This led us to hypothesize that the reduction in microbial dysbiosis in old $TNF^{-/-}$ mice may help prevent some of the negative changes seen with age (ie. increased systemic inflammation, decreased barrier integrity, changes in the myeloid cell lineage).

In order to test this hypothesis, we administered the old wild-type or old $TNF^{-/-}$ fecal microbiota to young germ-free mice using the fecal gavage technique (n = 7-8 mice/group). Following six weeks of colonization, we did not observe any changes in systemic inflammation as measured by plasma levels of TNF (Figure 26A) or IL-6 (Figure 26B).

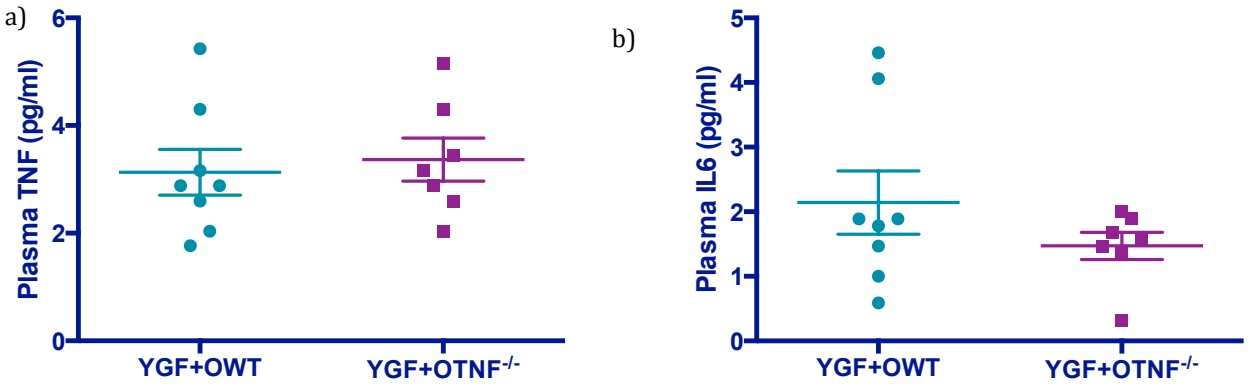

Figure 26: Colonized young germ-free mice with the old TNF$^{-/-}$ mouse microbiome does not result in reduced systemic inflammation.
Young germ-free mice were colonized with either the old wildtype (OWT) or old TNF$^{-/-}$ (OTNF$^{-/-}$) mouse microbiome (n = 8 mice/group) via the fecal gavage method. Following six weeks of colonization, systemic inflammation was measured using a Luminex assay. No differences in plasma levels of A) TNF or B) IL-6 were observed. Statistical significance was determined using unpaired t-tests where appropriate.

Furthermore, when we examined changes in permeability throughout the entire intestinal tract, we did not observe any changes in permeability between the young germ-free mice colonized with the old wildtype or old TNF$^{-/-}$ microbiota (Figure 27A). No difference in paracellular permeability was observed in the colon as well (Figure 27B). Finally, examining the myeloid cells present in these colonized germ-free revealed that colonized with the old TNF$^{-/-}$ microbiome resulted in a significant reduction of Ly6C^{high} monocytes in the colon of young germ-free mice (Figure 28A). However, we did not observe an overall systemic reduction of Ly6C^{high} monocytes in the blood (Figure 28B). This preliminary data suggests that although the composition of the old TNF$^{-/-}$ microbiome appears to reduce the recruitment of

Ly6C^{high} monocytes to the gut, it is not sufficient to completely reverse the outcomes of age-associated inflammation.

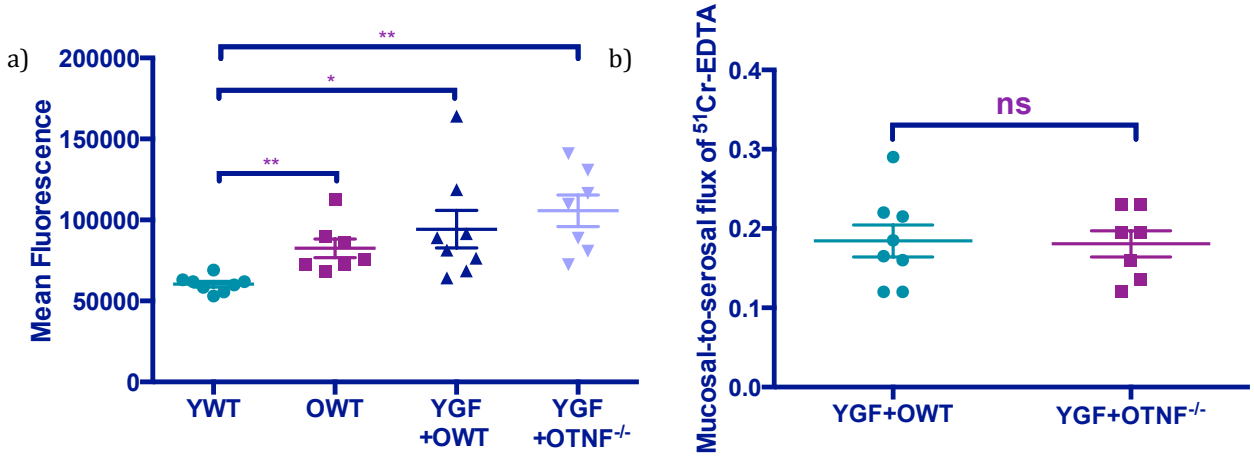

Figure 27: Colonization of young germ-free mice with the old TNF$^{-/-}$ mouse microbiome does not result in improved barrier integrity.
Young germ-free mice were colonized with either the old wildtype or old TNF$^{-/-}$ mouse microbiome (n = 8 mice/group) via the fecal gavage method. No differences were observed in A) overall intestinal permeability using the FITC-dextran gavage and in the B) paracellular permeability in the colon. For FITC-dextran gavages, mice were fasted for four hours prior to oral gavage with FITC-dextran at a concentration of 80 mg/mL. Four hours after the gavage, mice were bled and the mean fluorescence was quantified in whole blood. For Ussing chamber studies, a portion of the distal colon was removed from the mouse and mounted on the chamber in order to study permeability changes within the colon. Values are the mean +/- SEM of samples within each category. Statistical significance was determined using unpaired t-tests where appropriate.

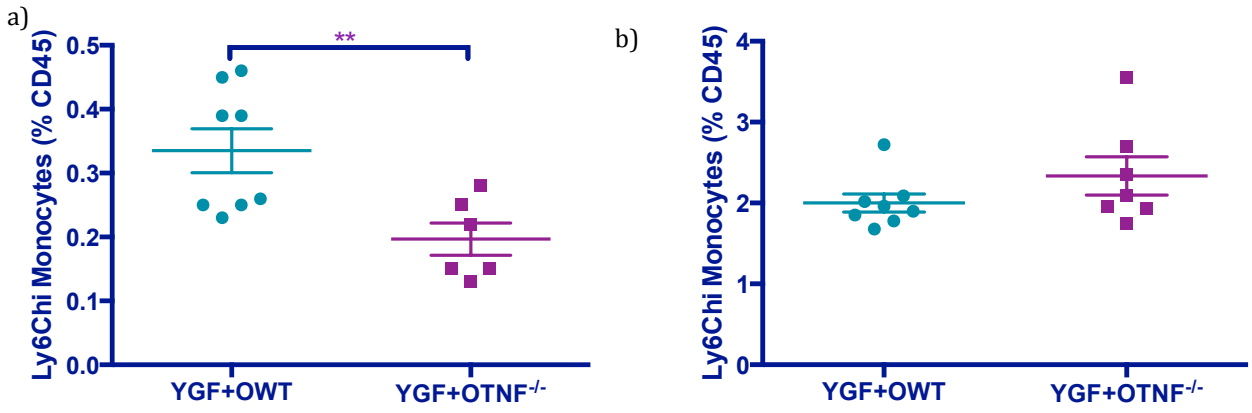

Figure 28: Ly6C^{high} monocytes are significantly reduced in the colon of young germ-free mice colonized with the old TNF$^{-/-}$ mouse microbiome, but not within the blood.
Young germ-free mice were colonized with either the old wildtype or old TNF$^{-/-}$ mouse microbiome (n = 8 mice/group) via the fecal gavage method. Following six weeks of colonization, the abundance of Ly6C^{high} monocytes was quantified using flow cytometry. The Ly6C^{high} monocyte population was significantly reduced in the A) colon but B) not in the blood. Ly6C^{high} monocytes were gated in the live cell population as CD45^{+} CD3^{-} CD11b^{+} SSC^{lo} CD64^{-} Ly6C^{+high} cells. Values are the mean +/- SEM of samples within each category. Statistical significance was determined using multiple t-tests where appropriate. P<0.05 was considered to be significant.

DISCUSSION

Although originally known for it's ability to induce cytotoxicity and necrosis in tumors, TNF is now known to be a pleiotropic cytokine (148, 150). This is because of its diverse inflammatory roles in infection, injury, and cancer (148). In many models of disease, ablation of TNF or TNF signalling has been shown to improve outcomes. For example, reducing the systemic levels of TNF using anti-TNF therapy has shown to slow down disease progression and reduce pathology in cases of inflammatory bowel diseases (IBD), rheumatoid arthritis and ankylosing spondylitis (151). We and others have observed that the elderly experience low-grade chronic

inflammation which is characterized by increased levels of systemic TNF (11, 71, 152).

The major findings outlined in this chapter were that old $TNF^{-/-}$ mice are protected from systemic increases in IL-6, decrease in the colonic barrier integrity, and as well, have reduced recruitment of $Ly6C^{high}$ monocytes in the colon. Furthermore, anti-TNF therapy administration speaks to the reversibility of these changes in old. The conclusion from these studies was that increases in TNF contribute to age-associated changes observed in old mice.

Changes to the composition of the gut microbiome have been associated with increased TNF levels and increased intestinal permeability (153). For example, in obesity studies, mice that were fed a high fat diet had decreased transepithelial resistance and expression of tight junction proteins, in addition to increased expression TNF mRNA in the colon (153). This inflammatory intestinal environment was associated with specific gut microbiome changes as well. In particular, a negative correlation between gut integrity and *Lactobacillus* abundance, and a positive correlation between gut integrity and *Oscillibacter* was observed in obese mice (153). Key changes in the microbiota have also been identified in other TNF-mediated inflammatory conditions. Specifically, in rheumatoid arthritis (RA) patients, microbiome studies have revealed alterations in bacteria belonging to the *Lactobacillus* communities and have elevated levels of *Prevotella*, a bacteria that is often associated with inflammatory conditions (154). These studies have begun to

identify the specific microbiome changes occurring in the gut in response to the chronic exposure to TNF.

Our $TNF^{-/-}$ mice are protected from increases in paracellular permeability within their colons. The role of TNF in modulating intestinal epithelial barrier function has been studied extensively in the past (155–159). Intestinal inflammation leads to the increased recruitment of immune cells in the gut. These immune cells produce extensive amounts of pro-inflammatory cytokines including TNF, IL-6 and INF-y (157). Increased expression of these cytokines in the gut can lead to re-modelling of the apical junctional complex, comprised of tight junctions and adherens (157). Disruption of the gut barrier integrity by the influx of cytokines is proposed to occur independently of apoptosis (157). *In vitro* studies completed in Caco-2 intestinal epithelial monolayers have shown that treatment with TNF for 24 hours resulted in reduced transepithelial resistance and increased paracellular permeability (159). TNF treatment also resulted in the reduced expression of the tight junction protein occludin (159). Therefore, the general consensus is that TNF modulates the intestinal gut barrier by remodelling tight junction proteins during times of inflammation. Although the mechanism behind has not been fully elucidated, the current understanding is that TNF causes in increase in the myosin light chain kinase (MLCK) protein expression (156, 160). This increase has been correlated to reducing tight junction permeability in *in vitro* models. Furthermore, this process is regulated by the activation of the NF-κB pathway, as inhibition of this pathway prevented the increased transcription of MLCK by TNF and ultimately reversed the changes in permeability as well (156). Clinical studies examining the effect of TNF on inducing barrier

integrity changes have further supported the *in vitro* data. Specifically, in models of IBD, anti-TNF therapy has been shown to reduce intestinal inflammation and permeability as well (156). In fact, concentrations between 1-10ng/ml in humans is sufficient to cause an increase in intestinal tight junction permeability (156, 161).

The increased concentration of TNF observed in old mice has been linked to immunosenesence in our laboratory. We have previously shown that old mice are impaired in their ability to clear *S. pneumoniae* colonization from the nasal tract effectively (57, 96). Interestingly, colonization of old $TNF^{-/-}$ mice with *S. pneumoniae* resulted in significantly fewer CFUs within the nasal wash in comparison to their old wild-type counterparts (96). We have suggested that the elevated levels of TNF in old mice impair monocyte development and ultimately result in reduced bacterial clearance. TNF has the ability to regulate inflammatory responses as it can initiate acute inflammation upon identifying a pathogen and is also able to aid in the recovery process (150). Because of it's multi-functional roles, excessive inflammation measured by the levels of systemic TNF can alter the balance of its functions and lead to immune dysfunction, as seen in the elderly.

In models of atherosclerosis, high levels of plasma TNF in the elderly were positively correlated with the development of atherosclerosis (104). Interestingly, when the elderly cohort from this study was divided into two groups based on whether they were TNF-low or TNF-high, it was observed that individuals who fell in the TNF-high category had an even greater risk of developing disease (104). Finally, reducing inflammation via the use of TNF knockout mice or with the use of

anti-TNF therapy results in improved tumor immunotherapy responses in aged mice (162). Administering tumor immunotherapy to old wild-type mice often results in lethal toxicities and tissue pathology. It is hypothesized that the increased inflammation in old mice causes excessive inflammatory responses to the treatment, ultimately resulting in even worse outcomes in these mice. This was further supported by that fact that depletion of macrophages prior to administering the treatment resulted in improved outcomes. Put together, when aged TNF knockout mice or anti-TNF therapy was used, increased longevity and decreased pathology was observed (162).

To summarize, our data suggests that much of the age-associated changes observed in old mice are modulated by the lifelong exposure to TNF. Moving forward, it would be beneficial to examine ways to reduce systemic levels of TNF in the elderly. This may be an effective strategy towards decelerating the onset of gut microbial dysbiosis and limit structural damages in order to help promote health aging in these individuals.

Chapter 6. Discussion

Immunosenescence renders the elderly population at a higher risk of experiencing infections and age-related diseases. Although the mechanisms behind immunosenescence have not been completely characterized, others and we have proposed that changes in the gut microbiome composition with age contribute to changes in gut physiology and ultimately impact the host's immune responses. In Chapter 3 of this thesis, we have attempted to characterize the physiological, immunological and microbiome changes occurring in young and old SPF mice. By doing so, we were first able to identify the key differences found with age. Then, in Chapter 4, we focused on determining what component of the aging process contributes to immune dysfunction observed in old mice. Specifically, we aimed to determine whether it was the age of the mouse, or the composition of the microbiome that led to these changes. Finally, in Chapter 5, we narrowed down the component of that drives age-associated inflammation. We found that TNF is a major contributing factor to age-associated inflammation in old mice. The ultimate goal of this thesis was to determine the casual relationship between gut microbial dysbiosis and immune dysfunction in old mice.

The cycle of inflamm-aging in old mice

One of the biggest challenges in studying inflammation in old mice is determining its etiology. Although we are aware that such changes occur with age, we are unclear about what the root cause of this inflammation is. We have suggested that changes in the gut microbiome can result in immune dysfunction with age. However, immune dysfunction in the elderly is a cumulative effect of increases in

systemic inflammation, changes in intestinal permeability and phenotypic and functional changes in the myeloid cells. These changes ultimately contribute back to causing even more inflammation in the elderly. Eventually, this becomes a downward spiraling phenomenon that continues to progress with age. As a result, it is difficult to determine which change in the elderly begins this vicious cycle that results in inflamm-aging in old mice.

We have suggested that changes in the gut microbiome are one of the first steps to starting this cycle. Data supporting this is seen in the analysis of our naïve old germ-free mice. Without the burden of the old microbiome, we found that old germ-free mice did not experience increased systemic inflammation, decreased intestinal barrier integrity and as well do not show changes in the myeloid cell populations within the bone marrow, blood and colon. Furthermore, when young germ-free mice are colonized with the old microbiota, we observed changes that were similar to that seen in old SPF mice. In particular, they have increased circulating levels of TNF, have increased paracellular permeability within their colons and as well, have an increase in the number of Ly6C^{high} monocytes within circulation and in their colon. Therefore, although these recipient germ-free mice were not aged, we were able to begin the cycle resulting in inflamm-aging by simply providing them with the composition of the old gut microbiome.

Impact of gut microbiome on health in the elderly

The presence of the gut microbiome has long been implicated in the health of individuals. In fact, in 1989, Dr. Strachan invented the "hygiene hypothesis," which

he described as the increase in the incidence of allergic diseases as a result of a decrease in the number of infections experienced throughout childhood (163). This concept has now been broadened to suggest that early microbial exposure is important in shaping robust immune responses and preventing allergic and skin atopic diseases. The hygiene hypothesis further suggests that the early exposure to bacteria and endotoxins can help prime the gut microbiome to later help fight infectious diseases. For example, it has been shown that probiotics (typically made of lactic acid producing bacteria like *Lactobacillus* and *Bifidobacterium*) are able to prime the intestinal microbiome to maintain a healthy state and promote barrier integrity. This contributes to protection against atopic, allergic and infectious diseases (163).

Exposure to bacteria during early life is important in maintaining health. However, changes to the microbiome during the later stages of life, as seen in the elderly, can have detrimental effects on health as well. The data presented in Chapter 3 provides evidence for changes in the gut microbiome composition with age. Examining the beta-diversity of young and old mice reveal that old mice cluster distinctly on a PCoA plot when compared to their young SPF controls. Furthermore, examining the bacterial changes at the genus level reveal specific changes that may be contributing to the increased inflammation observed with age. Then in Chapter 4, we were able to show that the composition of the old microbiome is sufficient to induce systemic inflammation, decreases in intestinal barrier integrity and changes in the phenotype of myeloid cells. Put together, all of these changes occurring as a

result of gut microbial dysbiosis with age may be ultimately contributing to immunosenescence in the elderly.

Proof of concept studies have shown that manipulating the composition of the microbiome can exacerbate disease conditions in certain states or work as a therapeutic (164). For example, studies examining the link between obesity and the microbiome have shown that humanized germ-free mice that received a microbiome composition from obese individuals resulted in increased adiposity (165). In contrast, several studies have also shown that treatment of gastrointestinal abnormalities or *Clostridium difficile* infections can be substantially improved by administering probiotics or by completing fecal transplantations (164). These studies show that strategically manipulating the microbiome can function as a therapeutic in diseased states.

As we age and develop from infancy into old age, so does our microbiome (166). Although several studies have characterized the gut microbiome throughout childhood, particularly because of its role in developing robust immune responses, very few have examined in detail the changes that occur with age. The changes to the composition of our gut microbiome can alter host immune responses, affecting the health and longevity of the elderly. In general, the gut microbiome of elderly individuals is characterized with reduced diversity and stability (167). However, with regards the specific changes, a lot of variability is observed. A number of factors such as age, nationality, geographic location and health status impact the specific microbial changes in the elderly. Some of the most common changes observed with

age include a decrease in "protective" bacteria like *Faecalibacterium prausnitzii* and *bifidobacteria*. These bacteria are known to have anti-inflammatory functions in the gut. Decreased abundance of these groups have often been associated with frail or hospitalized elderly (167). However, even with regards to these changes, variability has been observed in the literature. Other changes observed with age are the general increase in facultative anaerobes, like streptococci, staphylococci, enterococci, and enterobacteria. These bacterial groups, commonly referred to as pathobionts, are commonly found in the healthy GI tract but can also function as a pathogen during a diseased state (167).

Driving force of gut microbial dysbiosis with age

In chapter 4, we have shown a causal link between the composition of the old microbiome and some of the pathophysiology observed with age. Colonizing young germ-free mice with the old microbiome resulted in increased systemic inflammation, decreased barrier integrity and alterations in the phenotype of myeloid cells when compared to young germ-free mice colonized with the young microbiome. Since the age of these mice were all the same, the main difference between the two groups was the composition of the microbiome. Thus, we were able to conclude that the composition of the old microbiome is sufficient to induce these changes. However, we did not study what factors in the aged mice might be driving the changes in the gut microbiome. It has been suggested that the onset of gut microbial dysbiosis with age occurs as a result of the deterioration of the immune

system along with the reduction in motility in the gastrointestinal tract. These changes result in the loss of homeostasis in the gut microbiome.

Briefly, during a healthy state, homeostasis is maintained within the gut microbiome and mechanisms are in place to prevent unnecessary immune responses against the host microbiome. In particular, the microbiome is abundant in the upper portion of the mucus layer and is located away from the epithelial surface to avoid interactions with the immune system (168). In particular enterocytes play a crucial role in limiting the interactions between the host microbiome and the immune system by producing anti-microbial peptides and mucin. As a result, inflammation is kept at a minimum and the environment subsequently promotes tolerance signals, further promoting an anti-inflammatory state (90, 167). However, during an inflamed state, as seen with age, reduced production of IgA, anti-microbial peptides and mucus results in the failure in maintaining the microbiome away from the epithelial surface (167). The close proximity of enterocytes and the microbiome results in increased activation of the immune system. This ultimately results in an elevated pro-inflammatory status in the gut. An inflamed state then promotes the outgrowth of pathobionts, which contributes to microbial dysbiosis with age (167).

Once gut microbial dysbiosis is triggered in the elderly, it initiates a number of pathologies observed with age. We found that the composition of the old microbiome results in a decrease in gut barrier integrity. Decreases in barrier integrity can have profound effects on the health of old mice. In fact, in models of aging using Drosophila, loss in gut integrity has been shown to be a more effective

predictor of mortality than age itself (169). Furthermore, recent studies have shown that changes in the composition of the gut microbiome can lead to immune activation and can dictate the changes in barrier function (170). The increase in immune activation caused by microbial dysbiosis is one of the major contributing factors towards decreased barrier function. In fact, it has been shown that the resulting increase in the expression of inflammatory signaling pathways contributes to increases in intestinal permeability and accelerated mortality in aged Drosophila (170).

Targeting TNF as a potential therapeutic

Increases in TNF are one of the major hallmarks of "inflamm-aging." Throughout Chapters 3 and 4, we determined that old mice have increased circulating levels of TNF and this increase is mainly mediated by the composition of the old microbiome. In Chapter 5, we focused specifically on determining the impact of TNF on age-associated inflammation. We found that the key myeloid producers of TNF, monocytes and macrophages, are altered with age. Specifically, we observed an increase in the Ly6C^{high} monocyte population in the bone marrow, blood and colon of old SPF mice, which were largely driven by the composition of the aged microbiome. This was supported by the fact that old germ-free mice did not experience these changes. Furthermore, we found functional differences in the colonic macrophage populations of old SPF mice. Macrophages isolated from old mice constitutively produce increased amounts of TNF when compared to those isolated from young mice. Moreover, macrophages isolated from old mice revealed a

hyper-inflammatory response towards stimulation with a bacterial product. These data suggest that changes in the myeloid cell populations with age contribute to the amount of TNF produced in old mice. In fact, by reducing the levels of circulating TNF using transgenic mice or anti-TNF therapy, we were able to rescue some of the pathologies observed with age. These data suggest that targeting the reduction of TNF may be one avenue to help promote healthy aging in the elderly.

Data from our studies and others have shown that removing TNF is associated with reducing inflammation and altering the composition of the gut microbiome (171). As a result, identifying the changes occurring in a $TNF^{-/-}$ mouse microbiome and implementing them in elderly individuals may be one potential avenue to reducing systemic inflammation with age. $TNF^{-/-}$ mice have been observed to have significantly reduced alpha diversity when compared to their wildtype counterparts (171). Furthermore, similar to what we have shown, the *Firmicutes* to *Bacteroidetes* ratio is elevated in wildtype mice in comparison to $TNF^{-/-}$ mice. Examining microbial changes at the genus level reveal that $TNF^{-/-}$ mice tend to have an increase in a number of beneficial bacteria like *Ruminococcus*, *Turicibacter*, and unclassified *Ruminococcus.* Our aged $TNF^{-/-}$ mice also do not have a decrease in the number of OTUs representing the *Akkermansia* and *Blautia* genera in old $TNF^{-/-}$ mice. Another potential method to reduce the circulating abundance of TNF with age, is by completing regular exercise. In the recent literature, a strong link has been formed between diet and exercise and inflammation. As a result, this may be a potential route to explore as a therapeutic (172, 173). Put together, directly or indirectly

altering the aged gut microbiome composition to reduce intestinal inflammation may be a promising strategy to reduce age-associated inflammation and potentially reverse some of the pathologies observed in the elderly.

Limitations in using a mouse model of aging for microbiome studies

We have utilized a mouse model to study the changes observed with age. Specifically, we have utilized young (<3 months old) and old (>18 months old) SPF and germ-free mice. Although mouse models of aging are effective methods for studying human aging, there are still drawbacks that must be addressed. Especially when examining microbiome changes with age, it is important to minimize the variability between subjects. Ideally, we would like to use human subjects for these studies but there are some limitations that prevent us from doing so. The intra- and interindividual heterogeneity observed in humans limits the interpretations that can be made about changes in the gut microbiome (164). By using mice, we are able to control for factors like genetics, diet (enabling is to minimize changes associated with obesity), residence, social interactions, drug administrations and gender. Since many studies have shown that changes in any of these factors can impact the composition of the gut microbiome, it is important to keep all of these factors stable so that we can solely determine the impact of the age of the mouse on the composition of its microbiome (174–176). Although we are able to control for a number of these variables, there are still some differences that we inevitability experience. In fact, even after controlling for all of the above mentioned variables,

variation between mice can result from interindividual changes, cage effects and genetics (164).

In order to determine the casual effects of the gut microbiome in age-associated inflammation, we utilized germ-free mice. Germ-free mice allow us to conventionalize mice with a unique gut microbiome composition and determine casual links between the microbiome and health outcomes (164). Although there are a number of ways to complete this, including at birth (by transferring embryos into a potential recipient), immediately following birth (germ-free pups can be fostered by another mouse), or by administering bacteria to germ-free mice at a later time point (via oral gavage, intrarectal gavage or by co-housing) (164). We have chosen to conventionalize our young and old germ-free mice with either the young or old gut microbiota using the co-housing method to prevent inducing stress in our old mice. With this method, germ-free mice are able to acquire the donor microbiome via coprophagy or by grooming themselves or their littermates (164). In order to optimize successful microbiota transfer and minimize variation, we minimized handing of the mice, maximized the number of cages used (to limit cage-effects), collected fecal samples to study the variations of the gut microbiome composition throughout colonization, standardize the diet and housing conditions and co-house germ-free and SPF mice for an extended period of time (164). Although germ-free mice allow us to study the direct casual relationship between the microbiome and changes with age, there are still flaws that must be addressed as germ-free mice have defects in the development of gut-associated lymphoid tissues, and have

defects in immune responses (164). Furthermore, although these mice do not contain any live bacteria, they may still be exposed to microbial products (from their food and water sources), that may contribute to the development of some host responses (164, 177). Therefore, it is important to keep these limitations in mind when extrapolating these results into a human population.

Concluding Remarks

The purpose of the work presented in this thesis was to determine the effect of gut microbial dysbiosis on immune dysfunction with age. We have demonstrated that the composition of the gut microbiome contributed to increases in systemic inflammation, intestinal permeability and phenotypic changes in the myeloid cell populations with age. The findings from this study are crucial to identifying the effects of age-associated microbial dysbiosis on immune function and will contribute to unraveling alternatives to protect the elderly from such infections. We have suggested two major interventions to improving health in the elderly. This includes either directly reducing age-associated inflammation or reversing gut microbial dysbiosis to indirectly promote health in the elderly. Future directions for this study could involve examining whether the young microbiome is protective against infectious diseases. Although we briefly studied the impact of the microbiome composition against *S. pneumoniae* colonization, this needs to be repeated and studied in greater detail. These studies will ultimately indicate whether the microbiome in aged mice is driving the immune dysfunction and impaired bacterial clearance with age. The over-arching goal of our research is to characterize and identify the etiologies of age-associated pathologies in the elderly. By targeting these changes, we can help promote healthy aging and longevity in the elderly population.

Works Cited

1. **Wroe PC**, **Finkelstein JA**, **Ray GT**, **Linder JA**, **Johnson KM**, **Rifas-Shiman S**, **Moore MR**, **Huang SS**. 2012. Aging population and future burden of pneumococcal pneumonia in the United States. J Infect Dis **205**:1589–92.
2. **Wiener, J., Tilly J**. 2002. Population ageing in the United States of America: implications for public programmes. Int J Epidemiol **31**:776–81.
3. **Huang SS**, **Johnson KM**, **Ray GT**, **Wroe P**, **Lieu TA**, **Moore MR**, **Zell ER**, **Linder JA**, **Grijalva CG**, **Metlay JP**, **Finkelstein JA**. 2011. Healthcare utilization and cost of pneumococcal disease in the United States. Vaccine **29**:3398–3412.
4. **Gruver AL**, **Hudson LL**, **Sempowski GD**. 2007. Immunosenescence of ageing. J Pathol.
5. **Gerritsen J**, **Smidt H**, **Rijkers GT**, **De Vos WM**. 2011. Intestinal microbiota in human health and disease: The impact of probiotics. Genes Nutr.
6. **Schiffrin EJ**, **Morley JE**, **Donnet-Hughes A**, **Guigoz Y**. 2010. The inflammatory status of the elderly: The intestinal contribution. Mutat Res - Fundam Mol Mech Mutagen.
7. **Aw D**, **Silva AB**, **Palmer DB**. 2007. Immunosenescence: Emerging challenges for an ageing population. Immunology.
8. **Montoya a**, **Mody L**. 2011. Common infections in nursing homes: a review of current issues and challenges. Aging health **7**:889–899.
9. **De Martinis M**, **Franceschi C**, **Monti D**, **Ginaldi L**. 2006. Inflammation markers predicting frailty and mortality in the elderly. Exp Mol Pathol.
10. **Krabbe KS**, **Pedersen M**, **Bruunsgaard H**. 2004. Inflammatory mediators in the elderly. Exp Gerontol.
11. **Thevaranjan, N., Puchta, A., Naidoo, A., Szamosi, J., Verschoor, C., Loukov, D., Schenck, L., Jury, J., Foley, K., Schertzer, J., Larche, M., Davidson, D., Surette, M., Verdu, E., Bowdish D**. New evidence of Metchnikoff's hypothesis of aging: microbiota drive age-associated immune impairment. J Exp Med.
12. **De Martinis M**, **Franceschi C**, **Monti D**, **Ginaldi L**. 2005. Inflamm-ageing and lifelong antigenic load as major determinants of ageing rate and longevity. FEBS Lett.
13. **Roubenoff R**, **Harris TB**, **Abad LW**, **Wilson PW**, **Dallal GE**, **Dinarello C a**. 1998. Monocyte cytokine production in an elderly population: effect of age and inflammation. J Gerontol A Biol Sci Med Sci **53**:M20–6.
14. **Barbara JA**, **Van ostade X**, **Lopez A**. 1996. Tumour necrosis factor-alpha (TNF-alpha): the good, the bad and potentially very effective. Immunol Cell Biol **74**:434–443.
15. **Bradley JR**. 2008. TNF-mediated inflammatory disease. J Pathol.
16. **Lechleitner M**, **Herold M**, **Dzien-Bischinger C**, **Hoppichler F**, **Dzien a**. 2002. Tumour necrosis factor-alpha plasma levels in elderly patients with Type 2 diabetes mellitus-observations over 2 years. Diabet Med **19**:949–53.

17. **D'Argenio V**, **Salvatore F**. 2015. The role of the gut microbiome in the healthy adult status. Clin Chim Acta **451**:97–102.
18. **Kelly JR**, **Kennedy PJ**, **Cryan JF**, **Dinan TG**, **Clarke G**, **Hyland NP**. 2015. Breaking down the barriers: the gut microbiome, intestinal permeability and stress-related psychiatric disorders. Front Cell Neurosci **9**:392.
19. **Suzuki T**. 2013. Regulation of intestinal epithelial permeability by tight junctions. Cell Mol Life Sci **70**:631–59.
20. **Makki K**, **Froguel P**, **Wolowczuk I**. 2013. Adipose tissue in obesity-related inflammation and insulin resistance: cells, cytokines, and chemokines. ISRN Inflamm **2013**:139239.
21. **Stanley TL**, **Zanni M V.**, **Johnsen S**, **Rasheed S**, **Makimura H**, **Lee H**, **Khor VK**, **Ahima RS**, **Grinspoon SK**. 2011. TNF-α antagonism with etanercept decreases glucose and increases the proportion of high molecular weight adiponectin in obese subjects with features of the metabolic syndrome. J Clin Endocrinol Metab **96**.
22. **Raman K**, **Chong M**, **Akhtar-Danesh G-G**, **D'Mello M**, **Hasso R**, **Ross S**, **Xu F**, **Paré G**. 2013. Genetic markers of inflammation and their role in cardiovascular disease. Can J Cardiol **29**:67–74.
23. **Meier J**, **Sturm A**. 2009. The intestinal epithelial barrier: Does it become impaired with age?, p. 240–245. *In* Digestive Diseases.
24. **Valentini L**, **Ramminger S**, **Haas V**, **Postrach E**, **Werich M**, **Fischer A**, **Koller M**, **Swidsinski A**, **Bereswill S**, **Lochs H**, **Schulzke J-D**. 2014. Small intestinal permeability in older adults. Physiol Rep **2**:e00281.
25. **Saltzman JR**, **Kowdley K V**, **Perrone G**, **Russell RM**. 1995. Changes in small-intestine permeability with aging. J AmGeriatrSoc **43**:160–164.
26. **Beaumont DM**, **Cobden L**, **WL S**, **Laker MF**, **James OFW**. 1987. Passive and active carbohydrate absorption by the ageing gut. Age Ageing **16**:294–300.
27. **Schuijt TJ**, **van der Poll T**, **de Vos WM**, **Wiersinga WJ**. 2013. The intestinal microbiota and host immune interactions in the critically ill. Trends Microbiol.
28. **Cash HL**, **Hooper LV**. 2005. Commensal bacteria shape intestinal immune system development. ASM News **71**:77–83.
29. **Voreades N**, **Kozil A**, **Weir TL**. 2014. Diet and the development of the human intestinal microbiome. Front Microbiol **5**.
30. **Faith JJ**, **Guruge JL**, **Charbonneau M**, **Subramanian S**, **Seedorf H**, **Goodman AL**, **Clemente JC**, **Knight R**, **Heath AC**, **Leibel RL**, **Rosenbaum M**, **Gordon JI**. 2013. The long-term stability of the human gut microbiota. Science **341**:1237439.
31. **Peterson CT**, **Sharma V**, **Elm??n L**, **Peterson SN**. 2015. Immune homeostasis, dysbiosis and therapeutic modulation of the gut microbiota. Clin Exp Immunol.
32. **Claesson MJ**, **Jeffery IB**, **Conde S**, **Power SE**, **O'Connor EM**, **Cusack S**, **Harris HMB**, **Coakley M**, **Lakshminarayanan B**, **O'Sullivan O**, **Fitzgerald GF**, **Deane J**, **O'Connor M**, **Harnedy N**, **O'Connor K**, **O'Mahony D**, **van Sinderen D**,

Wallace M, **Brennan L**, **Stanton C**, **Marchesi JR**, **Fitzgerald AP**, **Shanahan F**, **Hill C**, **Ross RP**, **O'Toole PW**. 2012. Gut microbiota composition correlates with diet and health in the elderly. Nature **488**:178–184.

33. **Hawrelak JA**, **Myers SP**. 2004. The causes of intestinal dysbiosis: A review. Altern Med Rev.
34. **Hopkins MJ**, **Sharp R**, **Macfarlane GT**. 2001. Age and disease related changes in intestinal bacterial populations assessed by cell culture, 16S rRNA abundance, and community cellular fatty acid profiles. Gut **48**:198–205.
35. **Liévin-Le Moal V**, **Servin AL**. 2006. The front line of enteric host defense against unwelcome intrusion of harmful microorganisms: Mucins, antimicrobial peptides, and Microbiota. Clin Microbiol Rev.
36. **Tiihonen K**, **Ouwehand AC**, **Rautonen N**. 2010. Human intestinal microbiota and healthy ageing. Ageing Res Rev **9**:107–116.
37. **Hooper L V.** 2004. Bacterial contributions to mammalian gut development. Trends Microbiol.
38. **Estes JD**, **Harris LD**, **Klatt NR**, **Tabb B**, **Pittaluga S**, **Paiardini M**, **Barclay GR**, **Smedley J**, **Pung R**, **Oliveira KM**, **Hirsch VM**, **Silvestri G**, **Douek DC**, **Miller CJ**, **Haase AT**, **Lifson J**, **Brenchley JM**. 2010. Damaged intestinal epithelial integrity linked to microbial translocation in pathogenic simian immunodeficiency virus infections. PLoS Pathog **6**:49–50.
39. **Williams S**. 2014. Gnotobiotics. Proc Natl Acad Sci U S A **111**:1661.
40. **Martin, Rebeca; Bermúdez-Humarán, Luis; Langella P**. 2016. Gnotobiotic Rodents: An In Vivo Model for the Study of Microbe–Microbe Interactions. Front Microbiol **7**.
41. **Round JL**, **Mazmanian SK**. 2009. The gut microbiota shapes intestinal immune responses during health and disease. Nat Rev Immunol **9**:313–23.
42. **Janeway CA**, **Travers P**, **Walport M**, **Shlomchik M**. 2001. Immunobiology: The Immune System In Health And Disease, p. 892. *In* immuno biology 5.
43. **Jung C**, **Hugot J-P**, **Barreau F**. 2010. Peyer's Patches: The Immune Sensors of the Intestine. Int J Inflam **2010**:823710.
44. **Bain CC**, **Mowat AMI**. 2014. The monocyte-macrophage axis in the intestine. Cell Immunol **291**:41–48.
45. **Bain CC**, **Mowat AM**. 2014. Macrophages in intestinal homeostasis and inflammation. Immunol Rev.
46. **Bain CC**, **Bravo-Blas A**, **Scott CL**, **Gomez Perdiguero E**, **Geissmann F**, **Henri S**, **Malissen B**, **Osborne LC**, **Artis D**, **Mowat AM**. 2014. Constant replenishment from circulating monocytes maintains the macrophage pool in the intestine of adult mice. Nat Immunol **15**:929–37.
47. **Yang J**, **Zhang L**, **Yu C**, **Yang X-F**, **Wang H**. 2014. Monocyte and macrophage differentiation: circulation inflammatory monocyte as biomarker for inflammatory diseases. Biomark Res **2**:1.
48. **Zigmond E**, **Varol C**, **Farache J**, **Elmaliah E**, **Satpathy AT**, **Friedlander G**, **Mack M**, **Shpigel N**, **Boneca IG**, **Murphy KM**, **Shakhar G**, **Halpern Z**, **Jung S**.

2012. Ly6Chi Monocytes in the Inflamed Colon Give Rise to Proinflammatory Effector Cells and Migratory Antigen-Presenting Cells. Immunity **37**:1076–1090.

49. **Mcl Mowat, A., Bain C**. 2011. Mucosal Macrophages in Intestinal Homeostasis and Inflammation. J Innate Immunol **3**:550–564.
50. **Henriques-Normark B**, **Tuomanen EI**. 2013. The pneumococcus: Epidemiology, microbiology, and pathogenesis. Cold Spring Harb Perspect Med **3**.
51. **Krone CL**, **Trzciński K**, **Zborowski T**, **Sanders EAM**, **Bogaert D**. 2013. Impaired Innate Mucosal Immunity in Aged Mice Permits Prolonged Streptococcus pneumoniae Colonization. Infect Immun **81**:4615–4625.
52. **Bogaert D**, **De Groot R**, **Hermans PWM**. 2004. Streptococcus pneumoniae colonisation: The key to pneumococcal disease. Lancet Infect Dis.
53. **Syrjänen RK**, **Kilpi TM**, **Kaijalainen TH**, **Herva EE**, **Takala a K**. 2001. Nasopharyngeal carriage of Streptococcus pneumoniae in Finnish children younger than 2 years old. J Infect Dis **184**:451–459.
54. **Regev-Yochay G**, **Raz M**, **Dagan R**, **Porat N**, **Shainberg B**, **Pinco E**, **Keller N**, **Rubinstein E**. 2004. Nasopharyngeal carriage of Streptococcus pneumoniae by adults and children in community and family settings. Clin Infect Dis **38**:632–639.
55. **Watt JP**, **O'Brien KL**, **Katz S**, **Bronsdon M a.**, **Elliott J**, **Dallas J**, **Perilla MJ**, **Reid R**, **Murrow L**, **Facklam R**, **Santosham M**, **Whitney CG**. 2004. Nasopharyngeal versus oropharyngeal sampling for detection of pneumococcal carriage in adults. J Clin Microbiol **42**:4974–4976.
56. **Janssens J**, **Krause K**. 2004. Review Pneumonia in the very old **4**:112–124.
57. **Thevaranjan N**, **Whelan FJ**, **Puchta A**, **Ashu E**, **Rossi L**, **Surette MG**, **Bowdish DME**. 2016. *Streptococcus pneumoniae* colonization disrupts the microbial community within the upper respiratory tract of aging mice. Infect Immun IAI.01275–15.
58. **Puchta, A, Naidoo, A, Verschoor C, Loukov D, Thevaranjan N, Nguyen P, Loeb M, Xing Z, Kobzik L, Larché M BD**. 2015. TNF drives monocyte dysfunction with age and results in impaired anti- pneumococcal immunity. PLOS Pathog **In revisio**:In Press.
59. **Verdu EF**, **Huang X**, **Natividad J**, **Lu J**, **Blennerhassett PA**, **David CS**, **McKay DM**, **Murray JA**. 2008. Gliadin-dependent neuromuscular and epithelial secretory responses in gluten-sensitive HLA-DQ8 transgenic mice. Am J Physiol Gastrointest Liver Physiol **294**:G217–225.
60. **Pinier M**, **Fuhrmann G**, **Galipeau HJ**, **Rivard N**, **Murray JA**, **David CS**, **Drasarova H**, **Tuckova L**, **Leroux J-C**, **Verdu EF**. 2012. The copolymer P(HEMA-co-SS) binds gluten and reduces immune response in gluten-sensitized mice and human tissues. Gastroenterology **142**:316–325.e1–12.
61. **Galipeau HJ**, **Wiepjes M**, **Motta J-P**, **Schulz JD**, **Jury J**, **Natividad JM**, **Pinto-Sanchez I**, **Sinclair D**, **Rousset P**, **Martin-Rosique R**, **Bermudez-Humaran L**,

Leroux JC, **Murray JA**, **Smecuol E**, **Bai JC**, **Vergnolle N**, **Langella P**, **Verdu EF**. 2014. Novel Role of the Serine Protease Inhibitor Elafin in Gluten-Related Disorders. Am J Gastroenterol **109**:748–756.

62. **Whelan FJ**, **Verschoor CP**, **Stearns JC**, **Rossi L**, **Luinstra K**, **Loeb M**, **Smieja M**, **Johnstone J**, **Surette MG**, **Bowdish DME**. 2014. The loss of topography in the microbial communities of the upper respiratory tract in the elderly. Ann Am Thorac Soc **11**:513–521.
63. **Stearns JC**, **Davidson CJ**, **McKeon S**, **Whelan FJ**, **Fontes ME**, **Schryvers AB**, **Bowdish DME**, **Kellner JD**, **Surette MG**. 2015. Culture and molecular-based profiles show shifts in bacterial communities of the upper respiratory tract that occur with age. ISME J **9**:1246–59.
64. **Martin M**. 2011. Cutadapt removes adapter sequences from high-throughput sequencing reads. EMBnet.journal **17**:10.
65. **Masella AP**, **Bartram AK**, **Truszkowski JM**, **Brown DG**, **Neufeld JD**. 2012. PANDAseq: paired-end assembler for illumina sequences. BMC Bioinformatics **13**:31.
66. **Caporaso JG**, **Kuczynski J**, **Stombaugh J**, **Bittinger K**, **Bushman FD**, **Costello EK**, **Fierer N**, **Peña AG**, **Goodrich JK**, **Gordon JI**, **Huttley G a**, **Kelley ST**, **Knights D**, **Koenig JE**, **Ley RE**, **Lozupone C a**, **McDonald D**, **Muegge BD**, **Pirrung M**, **Reeder J**, **Sevinsky JR**, **Turnbaugh PJ**, **Walters W a**, **Widmann J**, **Yatsunenko T**, **Zaneveld J**, **Knight R**. 2010. QIIME allows analysis of high-throughput community sequencing data. Nat Methods **7**:335–336.
67. **Whitehead JC**, **Hildebrand BA**, **Sun M**, **Rockwood MR**, **Rose RA**, **Rockwood K**, **Howlett SE**. 2014. A clinical frailty index in aging mice: Comparisons with frailty index data in humans. Journals Gerontol - Ser A Biol Sci Med Sci **69**:621–632.
68. **Weisser SB**, **van Rooijen N**, **Sly LM**. 2012. Depletion and Reconstitution of Macrophages in Mice. J Vis Exp 5–11.
69. **Howcroft, T., Campisi, J., Louis, G., Smith, M., Wise, B., Wyss-Coray, T., Augustine, A., McElhaney, J., Kohanski, R., Sierra F**. 2013. The role of inflammation in age-related disease. Aging (Albany NY) **5**:84–93.
70. **Mogensen TH**. 2009. Pathogen recognition and inflammatory signaling in innate immune defenses. Clin Microbiol Rev.
71. **Franceschi C**, **Campisi J**. 2014. Chronic inflammation (Inflammaging) and its potential contribution to age-associated diseases. Journals Gerontol - Ser A Biol Sci Med Sci.
72. **Yao X**, **Li H**, **Leng SX**. 2011. Inflammation and Immune System Alterations in Frailty. Clin Geriatr Med.
73. **Jackson M**, **Jeffery IB**, **Beaumont M**, **Bell JT**, **Clark AG**, **Ley RE**, **O'Toole PW**, **Spector TD**, **Steves CJ**. 2016. Signatures of early frailty in the gut microbiota. Genome Med **8**:8.
74. **Van Tongeren SP**, **Slaets JPJ**, **Harmsen HJM**, **Welling GW**. 2005. Fecal microbiota composition and frailty. Appl Environ Microbiol **71**:6438–6442.

75. **Langille M**, **Meehan CJ**, **Koenig JE**, **Dhanani AS**, **Rose RA**, **Howlett SE**, **Beiko RG**. 2014. Microbial shifts in the aging mouse gut. Microbiome **2**:50.
76. **Aartsma-Rus A**, **van Putten M**. 2014. Assessing functional performance in the mdx mouse model. J Vis Exp e51303.
77. **Roubenoff R**. 2000. Sarcopenia: a major modifiable cause of frailty in the elderly. J Nutr Health Aging **4**:140–2.
78. **Shreiner AB**, **Kao JY**, **Young VB**. 2015. The gut microbiome in health and in disease. Curr Opin Gastroenterol **31**:69–75.
79. **Yatsunenko T**, **Rey F**, **Manary M**. 2012. Human gut microbiome viewed across age and geography. Nature **486**:222–7.
80. **Lozupone CA**, **Stombaugh J**, **Gonzalez A**, **Ackermann G**, **Wendel D**, **V??zquez-Baeza Y**, **Jansson JK**, **Gordon JI**, **Knight R**. 2013. Meta-analyses of studies of the human microbiota. Genome Res **23**:1704–1714.
81. **Verschoor CP**, **Naidoo A**, **Wallace JG**, **Johnstone J**, **Loeb M**, **Bramson JL**, **Bowdish DME**. 2014. Circulating Muramyl Dipeptide Is Negatively Associated with Interleukin-10 in the Frail Elderly. Inflammation **38**:272–277.
82. **Shulman RJ**, **Jarrett ME**, **Cain KC**, **Broussard EK**, **Heitkemper MM**. 2014. Associations among gut permeability, inflammatory markers, and symptoms in patients with irritable bowel syndrome. J Gastroenterol **49**:1467–1476.
83. **Gupta, Jalaj., Nebreda A**. 2014. Analysis of Intestinal Permeability in Mice. Cell Biol **4**.
84. **An G**, **Wei B**, **Xia B**, **McDaniel JM**, **Ju T**, **Cummings RD**, **Braun J**, **Xia L**. 2007. Increased susceptibility to colitis and colorectal tumors in mice lacking core 3-derived O-glycans. J Exp Med **204**:1417–1429.
85. **Anderson JM**, **Vanitallie CM**. 1995. Tight Junctions and the Molecular-Basis For Regulation Of Paracellular Permeability. Am J Physiol Liver Physiol **32**:G 467–G 475.
86. **Anderson JM**, **Van Itallie CM**. 2009. Physiology and function of the tight junction. Cold Spring Harb Perspect Biol.
87. **O'Brien, A., McClung, J., Kapral F**. 1978. Increased tissue conductance and ion transport in guinea pig ileum after exposure to staphylococcus aureus delta-toxin in vitro. Infect Immun **21**:102–113.
88. **Araya RE**, **Jury J**, **Bondar C**, **Verdu EF**, **Chirdo FG**. 2014. Intraluminal administration of poly I:C causes an enteropathy that is exacerbated by administration of oral dietary antigen. PLoS One **9**.
89. **Kau AL**, **Ahern PP**, **Griffin NW**, **Goodman AL**, **Gordon JI**. 2011. Human nutrition, the gut microbiome and the immune system. Nature **474**:327–36.
90. **Round JL**, **Mazmanian SK**. 2009. The gut microbiota shapes intestinal immune responses during health and disease. Nat Rev Immunol **9**:313–323.
91. **Cader MZ**, **Kaser A**. 2013. Recent advances in inflammatory bowel disease: mucosal immune cells in intestinal inflammation. Gut **62**:1653–64.
92. **Macia L**, **Thorburn AN**, **Binge LC**, **Marino E**, **Rogers KE**, **Maslowski KM**, **Vieira AT**, **Kranich J**, **Mackay CR**. 2012. Microbial influences on epithelial

integrity and immune function as a basis for inflammatory diseases. Immunol Rev.
93. **Arpaia, N., Rudensky A**. 2014. Microbial metabolites control gut inflammatory responses. Proc Natl Acad Sci U S A **111**:2058–2059.
94. **Lissner D**, **Schumann M**, **Batra A**, **Kredel LI**, **Kuhl AA**, **Erben U**, **May C**, **Schulzke JD**, **Siegmund B**. 2015. Monocyte and M1 Macrophage-induced Barrier Defect Contributes to Chronic Intestinal Inflammation in IBD. Inflamm Bowel Dis **21**:1297–1305.
95. **Sartor RB**. 2008. Microbial Influences in Inflammatory Bowel Diseases. Gastroenterology **134**:577–594.
96. **Puchta A, Naidoo A, Verschoor C, Loukov D, Thevaranjan N, Mandur T, Nguygen P, Jordana M, Loeb M, Xing Z, Kobzik L, Larche M BD**. TNF drives monocyte dysfunction with age and results in impaired anti-pneumococcal immunity. PLoS Pathog In Press.
97. **Franceschi C**, **Bonafè M**, **Valensin S**, **Olivieri F**, **De Luca M**, **Ottaviani E**, **De Benedictis G**. 2000. Inflamm-aging. An evolutionary perspective on immunosenescence. Ann N Y Acad Sci **908**:244–254.
98. **Bruunsgaard H**, **Andersen-Ranberg K**, **Jeune B**, **Pedersen AN**, **Skinhøj P**, **Pedersen BK**. 1999. A high plasma concentration of TNF-alpha is associated with dementia in centenarians. J Gerontol A Biol Sci Med Sci **54**:M357–64.
99. **Michaud M**, **Balardy L**, **Moulis G**, **Gaudin C**, **Peyrot C**, **Vellas B**, **Cesari M**, **Nourhashemi F**. 2013. Proinflammatory cytokines, aging, and age-related diseases. J Am Med Dir Assoc.
100. **Bruunsgaard H**, **Ladelund S**, **Pedersen AN**, **Schroll M**, **Jørgensen T**, **Pedersen BK**. 2003. Predicting death from tumour necrosis factor-alpha and interleukin-6 in 80-year-old people. Clin Exp Immunol **132**:24–31.
101. **Goldstein DR**. 2010. Aging, imbalanced inflammation and viral infection. Virulence **1**:295–298.
102. **Jenny N**. 2012. Inflammation in aging: cause, effect, or both? Discov Med **13**:451–460.
103. **Evrin PE**, **Nilsson SE**, **Oberg T**, **Malmberg B**. 2005. Serum C-reactive protein in elderly men and women: association with mortality, morbidity and various biochemical values. Scand J Clin Lab Invest **65**:23–31.
104. **Bruunsgaard H**, **Skinhøj P**, **Pedersen AN**, **Schroll M**, **Pedersen BK**. 2000. Ageing, tumour necrosis factor-alpha (TNF-alpha) and atherosclerosis. Clin Exp Immunol **121**:255–60.
105. **Brinkley TE**, **Leng X**, **Miller ME**, **Kitzman DW**, **Pahor M**, **Berry MJ**, **Marsh AP**, **Kritchevsky SB**, **Nicklas BJ**. 2009. Chronic inflammation is associated with low physical function in older adults across multiple comorbidities. Journals Gerontol Ser A-Biological Sci Med Sci **64**:455–461.
106. **Murad K**, **Kitzman DW**. 2012. Frailty and multiple comorbidities in the elderly patient with heart failure: Implications for management. Heart Fail Rev.

107. **Sergio G**. 2008. Exploring the complex relations between inflammation and aging (inflamm-aging): Anti-inflamm-aging remodelling of inflamm- aging, from robustness to frailty. Inflamm Res.
108. **Ryall JG**, **Schertzer JD**, **Lynch GS**. 2008. Cellular and molecular mechanisms underlying age-related skeletal muscle wasting and weakness. Biogerontology.
109. **Brooks S V**, **Faulkner JA**. 1994. Skeletal muscle weakness in old age: underlying mechanisms. Med Sci Sports Exerc **26**:432.
110. **Katz D**, **Hollander D**, **Said HM**, **Dadufalza V**. 1987. Aging-associated increase in intestinal permeability to polyethylene glycol 900. Dig Dis Sci **32**:285–288.
111. **Tran L**, **Greenwood-Van Meerveld B**. 2013. Age-associated remodeling of the intestinal epithelial barrier. Journals Gerontol - Ser A Biol Sci Med Sci **68**:1045–1056.
112. **K??hl AA**, **Erben U**, **Kredel LI**, **Siegmund B**. 2015. Diversity of intestinal macrophages in inflammatory bowel diseases. Front Immunol.
113. **Jiang C**, **Ting AT**, **Seed B**. 1998. PPAR-g agonists inhibit production of monocyte inflammatory cytokines. Nature **391**:82–86.
114. **Willing, B., Pal, V., Proctor S**. 2016. Koch's postulates, microbial dysbiosis and inflammatory bowel disease. Clin Microbiol Infect doi: 10.1016/j.cmi.2016.04.018.
115. **Sartor RB**, **Mazmanian SK**. 2012. Intestinal Microbes in Inflammatory Bowel Diseases. Am J Gastroenterol Suppl **1**:15–21.
116. **Yang Y**, **Jobin C**. 2014. Microbial imbalance and intestinal pathologies: connections and contributions. Dis Model Mech **7**:1131–1142.
117. **Biagi E**, **Nylund L**, **Candela M**, **Ostan R**, **Bucci L**, **Pini E**, **Nikkïla J**, **Monti D**, **Satokari R**, **Franceschi C**, **Brigidi P**, **de Vos W**. 2010. Through ageing, and beyond: Gut microbiota and inflammatory status in seniors and centenarians. PLoS One **5**.
118. **Guigoz Y**, **Doré J**, **Schiffrin EJ**. 2008. The inflammatory status of old age can be nurtured from the intestinal environment. Curr Opin Clin Nutr Metab Care **11**:13–20.
119. **Collado MC**, **Derrien M**, **Isolauri E**, **De Vos WM**, **Salminen S**. 2007. Intestinal integrity and Akkermansia muciniphila, a mucin-degrading member of the intestinal microbiota present in infants, adults, and the elderly. Appl Environ Microbiol **73**:7767–7770.
120. **Everard A**, **Belzer C**, **Geurts L**, **Ouwerkerk JP**, **Druart C**, **Bindels LB**, **Guiot Y**, **Derrien M**, **Muccioli GG**, **Delzenne NM**, **de Vos WM**, **Cani PD**. 2013. Cross-talk between Akkermansia muciniphila and intestinal epithelium controls diet-induced obesity. Proc Natl Acad Sci U S A **110**:9066–71.
121. **Schneeberger M**, **Everard A**, **Gómez-Valadés AG**, **Matamoros S**, **Ramírez S**, **Delzenne NM**, **Gomis R**, **Claret M**, **Cani PD**. 2015. Akkermansia muciniphila inversely correlates with the onset of inflammation, altered adipose tissue metabolism and metabolic disorders during obesity in mice. Sci Rep **5**:16643.

122. **Reunanen J**, **Kainulainen V**, **Huuskonen L**, **Ottman N**, **Belzer C**, **Huhtinen H**, **de Vos WM**, **Satokari R**. 2015. Akkermansia muciniphila Adheres to Enterocytes and Strengthens the Integrity of the Epithelial Cell Layer. Appl Environ Microbiol **81**:3655–62.
123. **Pang WW**, **Price EA**, **Sahoo D**, **Beerman I**, **Maloney WJ**, **Rossi DJ**, **Schrier SL**, **Weissman IL**. 2011. Human bone marrow hematopoietic stem cells are increased in frequency and myeloid-biased with age. Proc Natl Acad Sci U S A **108**:20012–7.
124. **Chambers SM**, **Shaw CA**, **Gatza C**, **Fisk CJ**, **Donehower LA**, **Goodell MA**. 2007. Aging hematopoietic stem cells decline in function and exhibit epigenetic dysregulation. PLoS Biol **5**:1750–1762.
125. **Mohanty S**, **Joshi SR**, **Ueda I**, **Wilson J**, **Blevins TP**, **Siconolfi B**, **Meng H**, **Devine L**, **Raddassi K**, **Tsang S**, **Belshe RB**, **Hafler DA**, **Kaech SM**, **Kleinstein SH**, **Trentalange M**, **Allore HG**, **Shaw AC**. 2015. Prolonged proinflammatory cytokine production in monocytes modulated by interleukin 10 after influenza vaccination in older adults, p. 1174–1184. *In* Journal of Infectious Diseases.
126. **Askenase MH**, **Han SJ**, **Byrd AL**, **MoraisdaFonseca D**, **Bouladoux N**, **Wilhelm C**, **Konkel JE**, **Hand TW**, **Lacerda-Queiroz N**, **Su X zhuan**, **Trinchieri G**, **Grainger JR**, **Belkaid Y**. 2015. Bone-Marrow-Resident NK Cells Prime Monocytes for Regulatory Function during Infection. Immunity **42**:1130–1142.
127. **Netea MG**, **Quintin J**, **Van Der Meer JWM**. 2011. Trained immunity: A memory for innate host defense. Cell Host Microbe.
128. **Quintin J**, **Saeed S**, **Martens JHA**, **Giamarellos-Bourboulis EJ**, **Ifrim DC**, **Logie C**, **Jacobs L**, **Jansen T**, **Kullberg BJ**, **Wijmenga C**, **Joosten LAB**, **Xavier RJ**, **Van Der Meer JWM**, **Stunnenberg HG**, **Netea MG**. 2012. Candida albicans infection affords protection against reinfection via functional reprogramming of monocytes. Cell Host Microbe **12**:223–232.
129. **Cheng S-C**, **Quintin J**, **Cramer RA**, **Shepardson KM**, **Saeed S**, **Kumar V**, **Giamarellos-Bourboulis EJ**, **Martens JHA**, **Rao NA**, **Aghajanirefah A**, **Manjeri GR**, **Li Y**, **Ifrim DC**, **Arts RJW**, **van der Meer BMJW**, **Deen PMT**, **Logie C**, **O'Neill LA**, **Willems P**, **van de Veerdonk FL**, **van der Meer JWM**, **Ng A**, **Joosten LAB**, **Wijmenga C**, **Stunnenberg HG**, **Xavier RJ**, **Netea MG**. 2014. mTOR- and HIF-1 -mediated aerobic glycolysis as metabolic basis for trained immunity. Science (80-) **345**:1250684–1250684.
130. **Nicholas D**, **Tang H**, **Zhang Q**, **Rudra J**, **Xu F**, **Langridge W**, **Zhang K**. 2015. Quantitative Proteomics Reveals a Role for Epigenetic Reprogramming During Human Monocyte Differentiation. Mol Cell Proteomics **14**:15–29.
131. **Fink RI**, **Kolterman OG**, **Griffin J**, **Olefsky JM**. 1983. Mechanisms of insulin resistance in aging. J Clin Invest **71**:1523–1535.
132. **Basu R**, **Breda E**, **Oberg AL**, **Powell CC**, **Man CD**, **Basu A**, **Vittone JL**, **Klee GG**, **Arora P**, **Jensen MD**, **Toffolo G**, **Cobelli C**, **Rizza RA**. 2003. Mechanisms of the age-associated deterioration in glucose tolerance: Contribution of alterations

in insulin secretion, action, and clearance. Diabetes **52**:1738–1748.
133. **Lerman-Garber I**, **Rosales-Calderón M**. 2010. Changes in glucose tolerance in elderly. Rev Investig Clin organo del Hosp Enfermedades la Nutr **62**:312–317.
134. **Stout RW**. 1994. Glucose tolerance and ageing. J R Soc Med **87**:608–9.
135. **Lebovitz HE**. 2001. Insulin resistance: Definition and consequences. Exp Clin Endocrinol Diabetes **109**.
136. **Mackowiak PA**. 2013. Recycling metchnikoff: probiotics, the intestinal microbiome and the quest for long life. Front public Heal **1**:52.
137. **Dinh DM**, **Volpe GE**, **Duffalo C**, **Bhalchandra S**, **Tai AK**, **Kane A V.**, **Wanke CA**, **Ward HD**. 2015. Intestinal Microbiota, microbial translocation, and systemic inflammation in chronic HIV infection, p. 19–27. *In* Journal of Infectious Diseases.
138. **Brenchley JM**, **Price DA**, **Schacker TW**, **Asher TE**, **Silvestri G**, **Rao S**, **Kazzaz Z**, **Bornstein E**, **Lambotte O**, **Altmann D**, **Blazar BR**, **Rodriguez B**, **Teixeira-Johnson L**, **Landay A**, **Martin JN**, **Hecht FM**, **Picker LJ**, **Lederman MM**, **Deeks SG**, **Douek DC**. 2006. Microbial translocation is a cause of systemic immune activation in chronic HIV infection. Nat Med **12**:1365–1371.
139. **Dillon SM**, **Lee EJ**, **Kotter C V**, **Austin GL**, **Dong Z**, **Hecht DK**, **Gianella S**, **Siewe B**, **Smith DM**, **Landay AL**, **Robertson CE**, **Frank DN**, **Wilson CC**. 2014. An altered intestinal mucosal microbiome in HIV-1 infection is associated with mucosal and systemic immune activation and endotoxemia. Mucosal Immunol **7**:983–94.
140. **Marchetti G**, **Tincati C**, **Silvestri G**. 2013. Microbial translocation in the pathogenesis of HIV infection and AIDS. Clin Microbiol Rev **26**:2–18.
141. **Platt AM**, **Bain CC**, **Bordon Y**, **Sester DP**, **Mowat AM**. 2010. An independent subset of TLR expressing CCR2-dependent macrophages promotes colonic inflammation. J Immunol **184**:6843–54.
142. **Rivollier A**, **He J**, **Kole A**, **Valatas V**, **Kelsall BL**. 2012. Inflammation switches the differentiation program of Ly6Chi monocytes from antiinflammatory macrophages to inflammatory dendritic cells in the colon. J Exp Med **209**:139–55.
143. **Varol C**, **Vallon-Eberhard A**, **Elinav E**, **Aychek T**, **Shapira Y**, **Luche H**, **Fehling HJ**, **Hardt WD**, **Shakhar G**, **Jung S**. 2009. Intestinal Lamina Propria Dendritic Cell Subsets Have Different Origin and Functions. Immunity **31**:502–512.
144. **Bain CC**, **Scott CL**, **Uronen-Hansson H**, **Gudjonsson S**, **Jansson O**, **Grip O**, **Guilliams M**, **Malissen B**, **Agace WW**, **Mowat a M**. 2013. Resident and pro-inflammatory macrophages in the colon represent alternative context-dependent fates of the same Ly6Chi monocyte precursors. Mucosal Immunol **6**:498–510.
145. **Ueda Y**, **Kayama H**, **Jeon SG**, **Kusu T**, **Isaka Y**, **Rakugi H**, **Yamamoto M**, **Takeda K**. 2010. Commensal microbiota induce LPS hyporesponsiveness in

colonic macrophages via the production of IL-10. Int Immunol **22**:953–962.
146. **Balzola F**, **Bernstein C**, **Ho GT**, **Lees C**. 2010. Inducible Foxp3 + regulatory T-cell development by a commensal bacterium of the intestinal microbiota: Commentary. Inflamm Bowel Dis Monit.
147. **Du Z**, **Hudcovic T**, **Mrazek J**, **Kozakova H**, **Srutkova D**, **Schwarzer M**, **Tlaskalova-Hogenova H**, **Kostovcik M**, **Kverka M**. 2015. Development of gut inflammation in mice colonized with mucosa-associated bacteria from patients with ulcerative colitis. Gut Pathog **7**:32.
148. **Tracey KJ**, **Cerami A**. 1994. Tumor necrosis factor: a pleiotropic cytokine and therapeutic target. Annu Rev Med **45**:491–503.
149. **Zhou, C., Irani, R., Dai, Y., Blackwell, S., Hicks, M., Ramin, S., Kellems, R., & Xia Y**. 2011. Autoantibody-Mediated IL-6–Dependent Endothelin-1 Elevation Underlies Pathogenesis in a Mouse Model of Preeclampsia. J Immunol **186**.
150. **Marino MW**, **Dunn A**, **Grail D**, **Inglese M**, **Noguchi Y**, **Richards E**, **Jungbluth A**, **Wada H**, **Moore M**, **Williamson B**, **Basu S**, **Old LJ**. 1997. Characterization of tumor necrosis factor-deficient mice. Proc Natl Acad Sci **94**:8093–8098.
151. **Ali T**. 2013. Clinical use of anti-TNF therapy and increased risk of infections. Drug Healthc Patient Saf **5**:79.
152. **Hinojosa E**, **Boyd AR**, **Orihuela CJ**. 2009. Age-associated inflammation and toll-like receptor dysfunction prime the lungs for pneumococcal pneumonia. J Infect Dis **200**:546–554.
153. **Lam YY**, **Ha CWY**, **Campbell CR**, **Mitchell AJ**, **Dinudom A**, **Oscarsson J**, **Cook DI**, **Hunt NH**, **Caterson ID**, **Holmes AJ**, **Storlien LH**. 2012. Increased gut permeability and microbiota change associate with mesenteric fat inflammation and metabolic dysfunction in diet-induced obese mice. PLoS One **7**.
154. **Brusca SB**, **Abramson SB**, **Scher JU**. 2014. Microbiome and mucosal inflammation as extra-articular triggers for rheumatoid arthritis and autoimmunity. Curr Opin Rheumatol **26**:101–7.
155. **Gibson PR**. 2004. Increased gut permeability in Crohn's disease: is TNF the link? Gut **53**:1724–1725.
156. **Ye D**, **Ma I**, **Ma TY**. 2006. Molecular mechanism of tumor necrosis factor-alpha modulation of intestinal epithelial tight junction barrier. Am J Physiol Gastrointest Liver Physiol **290**:G496–504.
157. **Bruewer M**, **Nusrat A**, **Luegering A**, **Kucharzik T**, **Parkos CA**, **Madara JL**, **Hopkins AM**. 2003. Proinflammatory cytokines disrupt epithelial barrier function by apoptosis-independent mechanisms. J Immunol **171**:6164–6172.
158. **Al-Sadi R**, **Guo S**, **Ye D**, **Ma TY**. 2013. TNF-α modulation of intestinal epithelial tight junction barrier is regulated by ERK1/2 activation of Elk-1. Am J Pathol **183**:1871–1884.
159. **Cui W**, **Li LX**, **Sun CM**, **Wen Y**, **Zhou Y**, **Dong YL**, **Liu P**. 2010. Tumor necrosis factor alpha increases epithelial barrier permeability by disrupting tight junctions in Caco-2 cells. Braz J Med Biol Res **43**:330–337.

160. **Ma TY**, **Boivin MA**, **Ye D**, **Pedram A**, **Said HM**. 2005. Mechanism of TNF-{alpha} modulation of Caco-2 intestinal epithelial tight junction barrier: role of myosin light-chain kinase protein expression. Am J Physiol Gastrointest Liver Physiol **288**:G422–30.
161. **Gitter a H**, **Bendfeldt K**, **Schmitz H**, **Schulzke JD**, **Bentzel CJ**, **Fromm M**. 2000. Epithelial barrier defects in HT-29/B6 colonic cell monolayers induced by tumor necrosis factor-alpha. Ann N Y Acad Sci **915**:193–203.
162. **Bouchlaka MN**, **Sckisel GD**, **Chen M**, **Mirsoian A**, **Zamora AE**, **Maverakis E**, **Wilkins DEC**, **Alderson KL**, **Hsiao H-H**, **Weiss JM**, **Monjazeb AM**, **Hesdorffer C**, **Ferrucci L**, **Longo DL**, **Blazar BR**, **Wiltrout RH**, **Redelman D**, **Taub DD**, **Murphy WJ**. 2013. Aging predisposes to acute inflammatory induced pathology after tumor immunotherapy. J Exp Med **210**:2223–37.
163. **Bloomfield SF**, **Stanwell-Smith R**, **Crevel RWR**, **Pickup J**. 2006. Too clean, or not too clean: The Hygiene Hypothesis and home hygiene. Clin Exp Allergy.
164. **Laukens D**, **Brinkman BM**, **Raes J**, **De Vos M**, **Vandenabeele P**. 2015. Heterogeneity of the gut microbiome in mice: guidelines for optimizing experimental design. FEMS Microbiol Rev fuv036.
165. **Harley ITW**, **Karp CL**. 2012. Obesity and the gut microbiome: Striving for causality. Mol Metab.
166. **Clemente JC**, **Ursell LK**, **Parfrey LW**, **Knight R**. 2012. The impact of the gut microbiota on human health: An integrative view. Cell.
167. **Biagi E**, **Candela M**, **Turroni S**, **Garagnani P**, **Franceschi C**, **Brigidi P**. 2013. Ageing and gut microbes: Perspectives for health maintenance and longevity. Pharmacol Res.
168. **Duerkop BA**, **Vaishnava S**, **Hooper L V.** 2009. Immune Responses to the Microbiota at the Intestinal Mucosal Surface. Immunity.
169. **Rera M**, **Clark RI**, **Walker DW**. 2012. Intestinal barrier dysfunction links metabolic and inflammatory markers of aging to death in Drosophila. Proc Natl Acad Sci U S A **109**:21528–33.
170. **Clark RI**, **Salazar A**, **Yamada R**, **Fitz-Gibbon S**, **Morselli M**, **Alcaraz J**, **Rana A**, **Rera M**, **Pellegrini M**, **Ja WW**, **Walker DW**. 2015. Distinct Shifts in Microbiota Composition during Drosophila Aging Impair Intestinal Function and Drive Mortality. Cell Rep **12**:1656–1667.
171. **Jones-Hall YL**, **Kozik A**, **Nakatsu C**. 2015. Ablation of tumor necrosis factor is associated with decreased inflammation and alterations of the microbiota in a mouse model of inflammatory bowel disease. PLoS One **10**.
172. **Hemarajata P**, **Versalovic J**. 2013. Effects of probiotics on gut microbiota: mechanisms of intestinal immunomodulation and neuromodulation. Therap Adv Gastroenterol **6**:39–51.
173. **Corridoni D**, **Pastorelli L**, **Mattioli B**, **Locovei S**, **Ishikawa D**, **Arseneau KO**, **Chieppa M**, **Cominelli F**, **Pizarro TT**. 2012. Probiotic bacteria regulate intestinal epithelial permeability in experimental ileitis by a TNF-dependent mechanism. PLoS One **7**.

174. **Graf D**, **Di Cagno R**, **Fåk F**, **Flint HJ**, **Nyman M**, **Saarela M**, **Watzl B**. 2015. Contribution of diet to the composition of the human gut microbiota. Microb Ecol Health Dis **26**:26164.
175. **Jernberg C**, **Löfmark S**, **Edlund C**, **Jansson JK**. 2010. Long-term impacts of antibiotic exposure on the human intestinal microbiota. Microbiology.
176. **DiBaise JK**, **Frank DN**, **Mathur R**. 2012. Impact of the Gut Microbiota on the Development of Obesity: Current Concepts. Am J Gastroenterol Suppl **1**:22–27.
177. **Coates M**. 1975. Gnotobiotic animals in research: their uses and limitations. Lab Anim **9**:275–282.

Appendix I.

Streptococcus pneumoniae Colonization Disrupts the Microbial Community within the Upper Respiratory Tract of Aging Mice

Netusha Thevaranjan, Fiona J. Whelan, Alicja Puchta, Eta Ashu, Laura Rossi, Michael G. Surette, Dawn M. E. Bowdish

Published in *Infection and Immunity.* 2016; 84(4): 906-16

AMERICAN SOCIETY FOR MICROBIOLOGY | Infection and Immunity

Streptococcus pneumoniae Colonization Disrupts the Microbial Community within the Upper Respiratory Tract of Aging Mice

Netusha Thevaranjan,[a,b,c] Fiona J. Whelan,[d,e] Alicja Puchta,[a,b,c] Eta Ashu,[a,b,c] Laura Rossi,[d] Michael G. Surette,[c,d,e,f] Dawn M. E. Bowdish[a,b,c]

Department of Pathology and Molecular Medicine, McMaster University, Hamilton, Canada[a]; McMaster Immunology Research Centre, McMaster University, Hamilton, Canada[b]; Michael G. DeGroote Institute for Infectious Disease Research, McMaster University, Hamilton, Canada[c]; Farncombe Family Digestive Health Research Institute, McMaster University, Hamilton, Canada[d]; Department of Biochemistry and Biomedical Sciences, McMaster University, Hamilton, Canada[e]; Department of Medicine, McMaster University, Hamilton, Canada[f]

Nasopharyngeal colonization by the Gram-positive bacterium *Streptococcus pneumoniae* is a prerequisite for pneumonia and invasive pneumococcal diseases. Colonization is asymptomatic, involving dynamic and complex interplay between commensals, the host immune system, and environmental factors. The elderly are at an increased risk of developing pneumonia, which might be due to changes in the respiratory microbiota that would impact bacterial colonization and persistence within this niche. We hypothesized that the composition of the upper respiratory tract (URT) microbiota changes with age and subsequently can contribute to sustained colonization and inefficient clearance of *S. pneumoniae*. To test this, we used a mouse model of pneumococcal colonization to compare the composition of the URT microbiota in young, middle-aged, and old mice in the naive state and during the course of colonization using nasal pharyngeal washes. Sequencing of variable region 3 (V3) of the 16S rRNA gene was used to identify changes occurring with age and throughout the course of *S. pneumoniae* colonization. We discovered that age affects the composition of the URT microbiota and that colonization with *S. pneumoniae* is more disruptive of preexisting communities in older mice. We have further shown that host-pathogen interactions following *S. pneumoniae* colonization can impact the populations of resident microbes, including *Staphylococcus* and *Haemophilus*. Together, our findings indicate alterations to the URT microbiota could be detrimental to the elderly, resulting in increased colonization of *S. pneumoniae* and decreased efficiency in its clearance.

Streptococcus pneumoniae colonizes the mucosal surfaces of the upper respiratory tract (URT), which includes the nose, nasal cavity, pharynx, and larynx (1). Although colonization within the nasal passage often is asymptomatic, access to the airways can result in pneumonia, with further dissemination causing invasive pneumococcal disease (i.e., otitis media, bacteremia, and meningitis) (1, 2). Previous studies analyzing the nasopharyngeal culture of 1,704 samples, including children and adults from the same population, revealed that 53% of children carried *S. pneumoniae* within the nasopharyngeal tract as opposed to only 4 to 11% that were adult carriers (3–5). Furthermore, *S. pneumoniae* carriage rates positively correlate with age in young children and then begin to drop in adults (3, 6, 7). These results have been confirmed in epidemiological studies conducted in several locations around the world (7–9).

Despite having significantly lower carriage rates than children (3, 10), colonization within the upper respiratory tract of elderly individuals often leads to the progression and development of pneumonia and invasive pneumococcal disease (11–13). Pneumonia in particular affects elderly individuals approximately four times more often than individuals under the age of 65 (14). The elderly account for approximately 60% of the hospitalizations caused by pneumococcal pneumonia in the United States (15). Since colonization is a prerequisite for infection, the microbe-microbe interactions that contribute to sustaining colonization or promoting expansion must be further studied to understand disease progression in elderly patients.

Using Illumina sequencing of the 16S rRNA gene, we characterized the URT microbiome in young (10 to 14 weeks), middle-aged (12 to 14 months), and old (18 to 22 months) mice in the naive state and throughout the course of nasopharyngeal colonization with *Streptococcus pneumoniae*. We show that the composition of the URT microbiome differs in the naive state between young, middle-aged, and old mice. Old mice are unable to clear bacterial colonization as effectively as their young counterparts. We observed a number of interspecies interactions between *S. pneumoniae* and the existing mouse microbiome (e.g., *Staphylococcus*) that have been reported previously only in experimental models (16–24). In particular, *Streptococcus* interacted competitively with *Staphylococcus* and synergistically with *Haemophilus*. This study begins to characterize how aging impacts bacterial colonization, which will ultimately explain the progression of upper respiratory tract infections in the elderly.

Received 9 October 2015 **Returned for modification** 12 November 2015
Accepted 6 January 2016

Accepted manuscript posted online 19 January 2016

Citation Thevaranjan N, Whelan FJ, Puchta A, Ashu E, Rossi L, Surette MG, Bowdish DME. 2016. *Streptococcus pneumoniae* colonization disrupts the microbial community within the upper respiratory tract of aging mice. Infect Immun 84:906–916. doi:10.1128/IAI.01275-15.

Editor: A. Camilli

Address correspondence to Dawn M. E. Bowdish, bowdish@mcmaster.ca.

Supplemental material for this article may be found at http://dx.doi.org/10.1128/IAI.01275-15.

MATERIALS AND METHODS

Mice. C57BL/6 female mice were from The Jackson Laboratory and were housed under specific-pathogen-free (SPF) conditions at the McMaster Central Animal Facility. The animals were assigned to three groups: 10- to 14-week-old mice (young), 12- to 14-month-old mice (middle-aged), and 18- to 22-month-old mice (old) ($n = 72$ total). Within each age group, mice were sacrificed at various time points throughout pneumococcal colonization (at day 0, 3, 14, and 21) in order to obtain nasopharyngeal washes (25). Mice that reached the endpoint prematurely were found to have bacteria in the lungs or spleens and were not used in this study. In general, <5% of young mice and 20 to 25% of old mice were euthanized prematurely (26). All procedures were performed in accordance with the McMaster Animal Research Ethics Board guidelines.

Murine model of pneumococcal colonization and nasopharyngeal wash preparation. Mice were colonized with 10^7 CFU of a clinical strain of *S. pneumoniae*, P1547 (serotype 6A), obtained from Jeff Weiser (NYU School of Medicine) as described previously (27, 28). The bacteria were grown in tryptic soy broth medium (Life Technologies) at 37°C and 5% CO_2 until cultures reached log phase, with an optical density at 600 nm (OD_{600}) of between 0.45 and 0.55 (27). Anesthetized mice were euthanized by exsanguination. The trachea was expanded and a small incision was made 2 cm above the lungs. Briefly, 1-ml syringes containing 350 μl of sterilized phosphate-buffered saline (PBS) attached to a 26-gauge needle were connected to a 4-cm PE-20 polyethylene tube. The syringe was inserted into the trachea and tied off using a silk suture (Ethicon), and the contents used to wash the nares were collected in 1.5-ml flat-top microtubes (Diamed) (28). Nasal washes then were collected at day 0 (young, $n = 5$; middle-aged, $n = 4$; old, $n = 7$), 3 (young, $n = 6$; middle-aged, $n = 5$; old, $n = 5$), 14 (young, $n = 9$; middle-aged, $n = 6$; old, $n = 4$), and 21 (young, $n = 4$; middle-aged, $n = 3$; old, $n = 4$) after colonization with *Streptococcus pneumoniae* as previously described (28).

PCR amplification of the 16S rRNA gene. DNA extraction and 16S variable region 3 (V3) amplification were carried out as described in our recent studies of human nasal swabs (8, 29). The primers were based on the method described in Bartram et al., except the barcodes were incorporated into the forward primer (30).

Briefly, each PCR mixture contained the following in order to amplify V3 of the 16S rRNA gene by PCR: 5 μl of 10× buffer (Life Technologies), 1.5 μl of $MgCl_2$ (50 mM) (Life Technologies), 1 μl of deoxynucleoside triphosphate (dNTP) (10 mM) (Invitrogen), 2 μl of bovine serum albumin (BSA) (10 mg/ml made in pure water and irradiated for 30 min) (Life Technologies), 5 μl of V3F primer (1 μM) (27), 5 μl of V3R primer (1 μM) (27), 0.5 μl of *Taq* polymerase (Life Technologies), and 200 ng of DNA. The reaction then was run for 30 cycles (94°C for 2 min, 94°C for 30 s, 50°C for 30°C, 72°C for 30 s), with a final polymerization step at 72°C for 10 min (Eppendorf). The products were separated by electrophoresis in a 2% agarose gel and visualized under a UV transilluminator light, and the products corresponding to the amplified V3 (~300 bp) were excised and purified using standard gel extraction kits (Qiagen).

Illumina sequencing and processing. Samples were sent to the McMaster DNA Sequencing Facility and sequenced using an Illumina MiSeq per the manufacturer's instructions. The completed run was demultiplexed with Illumina's Casava software. The resulting sequenced data were processed as previously described (8, 29). Briefly, Cutadapt was used to trim the forward and reverse paired-end reads at the opposing primers for input into PANDAseq for assembly (31, 32). Sequences were organized into operational taxonomic units (OTUs) with a clustering threshold of 97% using AbundantOTU+ (33). Single-sequence OTUs (singletons) were removed prior to all analyses using Quantitative Insights into Microbial Ecology (QIIME) (34). All beta diversity plots were generated in R using the Phyloseq package and taxonomic summaries (34). A total of 10,312,391 paired-end reads were observed from the sequencing data (with a minimum of 1,193 reads and a maximum of 347,295 reads). This gave an average of 132,210 counts per sample with a standard deviation of 77,464. These counts corresponded to 7,100 unique OTUs observed within the samples.

Quantitative PCR. Real-time PCR (quantitative PCR [qPCR]) was used to assess the total bacterial load and *lytA* abundance using a previously published protocol (8, 35). Briefly, levels of *S. pneumoniae* in the nasal wash samples using GoTaq qPCR master mix (Promega, WI, USA) and an ABI StepOnePlus (Applied Biosystems, CA, USA) according to the manufacturer's instructions. Forward and reverse primers used for 16S rRNA were the following: 341Fwd, 5′-CCTACGGGAGGCAGCAG-3′; 518Rev, 5′-ATTACCGCGGCTGCTGG-3′ (36). Forward and reverse primers used to measure *lytA* were the following: Fwd, 5′-AGTACCAGT TGCCGTCTGTG-3′; Rev, 5′-AAATGGGGCATTAGCCGTGA-3′. *lytA* levels were found to accurately represent CFU, which were previously quantitated and published (26).

Statistics. Unless otherwise mentioned in the figure legend, statistical significance was determined by unpaired *t* tests (two-tailed) or a one-way analysis of variance (ANOVA). Data were analyzed with Prism (version 6; GraphPad). Statistical significance of groups by β-diversity (Bray-Curtis) was determined using permutational ANOVA (PERMANOVA) in R phyloseq (37). This was calculated using the ADONIS function, which conducts a permutational multivariate analysis of variance within the samples using distance matrices. Statistical significance was defined as a P value of 0.05.

RESULTS

Upper respiratory microbial communities differ between young, middle-aged, and old mice. The composition of the microbial community in nasopharyngeal washes from 10-week-old, 12-month-old, and 20-month-old naive mice were compared. There was no detectable difference in total bacterial load between age groups, as measured by qPCR of the 16S rRNA gene (246 ± 106 pg in young mice, 168 ± 38 pg in middle-aged mice, and 379 ± 384 pg in old mice). In order to determine if the composition of the nasopharyngeal tract microbial community changed with age, the β-diversity metric, calculated based on the Bray-Curtis distance, was visualized using a principal coordinate analysis (PCoA) plot (Fig. 1A). Under Bray-Curtis calculations, the samples are statistically different by age ($P = 0.04$) (Fig. 1A; also see Table S1 in the supplemental material).

Taxonomic summaries prior to colonization indicate that the most abundant phyla are *Firmicutes*, *Proteobacteria*, *Bacteroidetes*, and *Actinobacteria* (Fig. 1B). The *Proteobacteria* are present at a relative abundance of 41.9% in young mice but only 27.9% in old mice. In contrast, young mice contain a significantly lower abundance of *Bacteroidetes* (9.7%) than old mice (19.5%). All three age groups contain comparable levels of *Firmicutes* (young, 44.0%; middle aged, 44.6%; old, 45.2%), and young and old mice had comparable levels of *Actinobacteria* (young, 2.1%; middle aged, 7.2%; old, 4.1%).

Old mice do not effectively clear nasopharyngeal colonization. We next determined whether old mice differed in their ability to clear pneumococcal colonization. Mice were intranasally inoculated with *Streptococcus pneumoniae* and were monitored up to 21 days (25). The pneumococcal autolysin gene *lytA* was measured by qPCR to quantitate the levels of *S. pneumoniae* present in nasal wash samples over the course of the colonization (Fig. 2A). As expected, *lytA* was not detectable at day 0. Peak levels of *S. pneumoniae* occurred at day 3 postcolonization in young and middle-aged mice. Levels of *S. pneumoniae* decreased in young mice by 14 days postcolonization, and most mice had levels of *S. pneumoniae* that were below the limit of detection by day 21, consistent with their ability to clear pneumococcal colonization. In contrast,

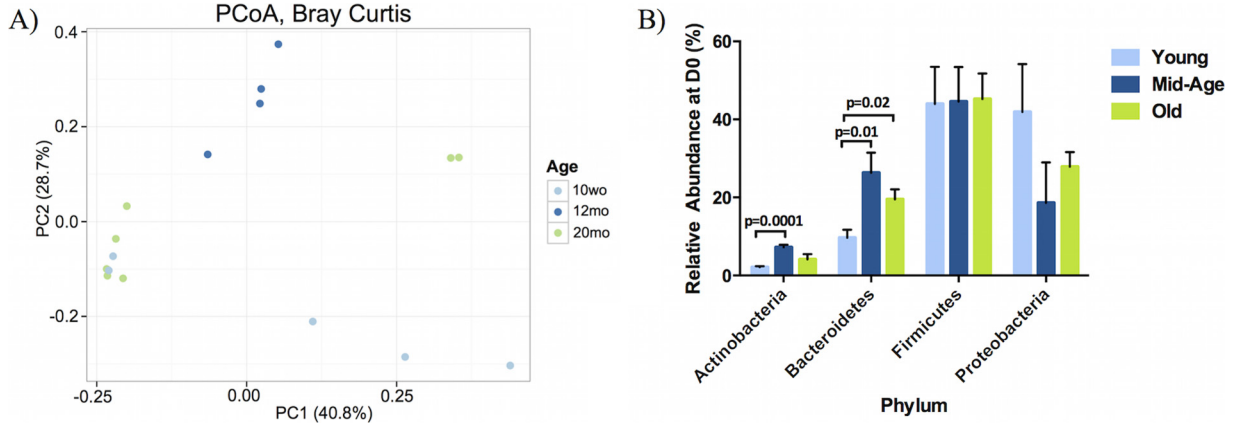

FIG 1 16S rRNA sequencing of nasopharyngeal washes from young, middle-aged, and old mice under naive conditions reveal significant differences within the overall bacterial composition and specific phyla. Bacterial communities were examined under naive conditions to examine the differences between age groups. (A) Communities clustered using principal coordinate analyses (PCoA) of the Bray-Curtis distance matrix. Each point represents one sample and is differentiated by color to indicate the age of the mouse. Plots represent the microbial composition as indicated by the β-diversity between each nasal wash sample. Clustering was observed between the young, middle-aged, and old mice before colonization was statistically significant by PERMANOVA. (B) The four most abundant phyla present in young, middle-aged, and old mice under naive conditions were quantified within the young, middle-aged, and old samples prior to pneumococcal colonization (young, 10 weeks old [10wo], $n = 5$; middle-aged, 12 months old [12mo], $n = 4$; old, 20 months old [20mo], $n = 7$). Values are the means ± standard errors of the means (SEM) of samples within each category. Statistical significance was determined using multiple *t* tests where appropriate ($n = 3$ to 9/group). A *P* value of <0.05 was considered significant. D0, day zero.

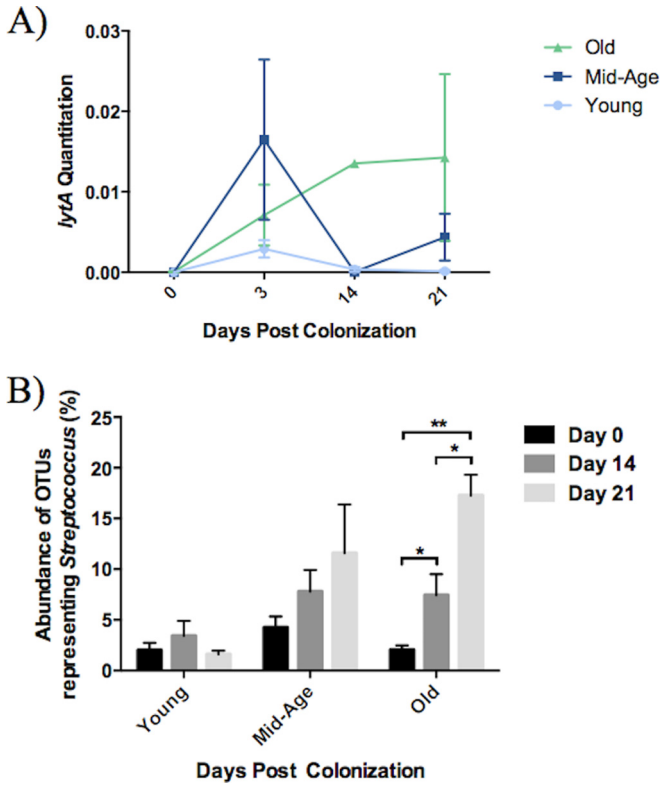

FIG 2 Old mice do not effectively clear nasopharyngeal colonization of *S. pneumoniae*. *S. pneumoniae* clearance was examined within young, middle-aged, and old mice using *lytA* expression (A) and the OTUs representing the *Streptococcus* genus (B). *lytA* expression was measured in nasal wash samples of these mice using quantitative PCR. All samples were normalized to the total bacterial load, which was measured by 16S rRNA gene quantitative PCR. Relative abundances of *Streptococcus* in the nasal microbiome were calculated from all OTUs associated with the *Streptococcus* genus within each sample. Values are the means ± SEM of samples within each category. Statistical significance was determined using multiple *t* tests where appropriate ($n = 3$ to 9/group). A *P* value of <0.05 was considered significant.

lytA levels peak around day 14 in old mice and persist through to day 21 of colonization. At day 21, nasal washes from old mice have considerably higher levels of *S. pneumoniae* than young mice.

Furthermore, the abundance of OTUs representing the streptococci decreased to very low levels by day 21 in young mice (approximately 1.6% of OTUs). However, this was not seen in the elderly mice. Unlike the young, the elderly mice had a high relative abundance of streptococci at day 21 postcolonization (approximately 17.3% of OTUs) (Fig. 2B). It is important to note that OTUs corresponding to the *Streptococcus* genus include all streptococci and are not specific to *S. pneumoniae*. In fact, the OTUs representing the streptococci include a wide array of species, and some of the abundant OTUs assigned to this genus are phylogenetically similar to our bacterium of interest, *S. pneumoniae* (see Fig. S1 in the supplemental material).

Nasopharynx microbial communities respond differently to pneumococcal colonization with age. The microbial communities for the nasal wash samples at days 3, 14, and 21 postcolonization were compared to baseline conditions (day 0) (Fig. 1A and 3). Clustering of samples between the age groups was evident at days 3 and 21 postcolonization, suggesting that the microbial communities of mice within the same age group respond similarly to the introduction of *S. pneumoniae* (Fig. 3A and C). Specifically, 3 days postcolonization, the young, middle-aged, and old microbiota cluster according to their specific age group as visualized using the Bray-Curtis distance metric (Fig. 3A; also see Table S1 in the supplemental material). By day 21, this clustering becomes more distinct between the three age groups, suggesting that the bacterial communities present within young and old mice are distinctly separate after 21 days of colonization (Fig. 3C; also see Fig. S1).

Taxonomic summaries of microbial communities within the nasopharynx of these mice indicated that the proportion of the four most abundant phyla, *Proteobacteria*, *Firmicutes*, *Bacteroidetes*, and *Actinobacteria*, changed during the course of pneumococcal colonization (Fig. 3). *Proteobacteria* comprised the ma-

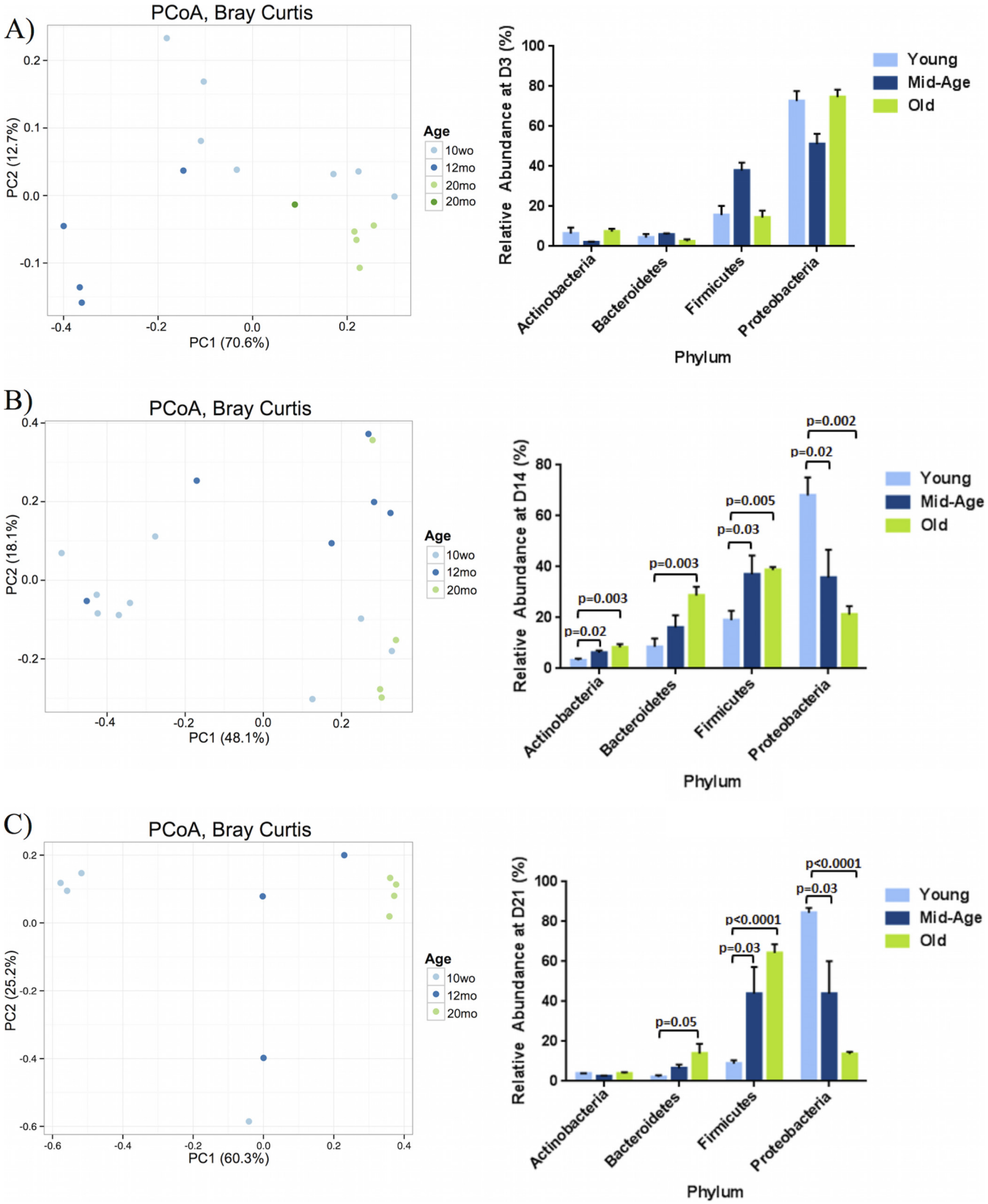

FIG 3 During colonization, the microbial community changes with age. Principal coordinate analyses (PCoA) plots showing the similarity of the aging URT microbiome postpneumococcal colonization as well as relative abundance plots of the four most abundant phyla were analyzed at day 3 (A), day 14 (B), and day 21 (C) postcolonization. β-Diversity measures were completed using Bray-Curtis calculations and visualized using PCoA. The age groups of the samples are indicated by the designated color. The distance between each of the samples reflects how similar their microbiomes are to one another. Statistical analyses were completed using PERMANOVA. The results are summarized in Table S1 in the supplemental material. The panels on the right represent the mean relative abundances of each phyla within each sample ± SEM of samples within each category. Statistical significance was determined using multiple *t* test where appropriate ($n = 3$ to 9/group). $P < 0.05$ was considered significant.

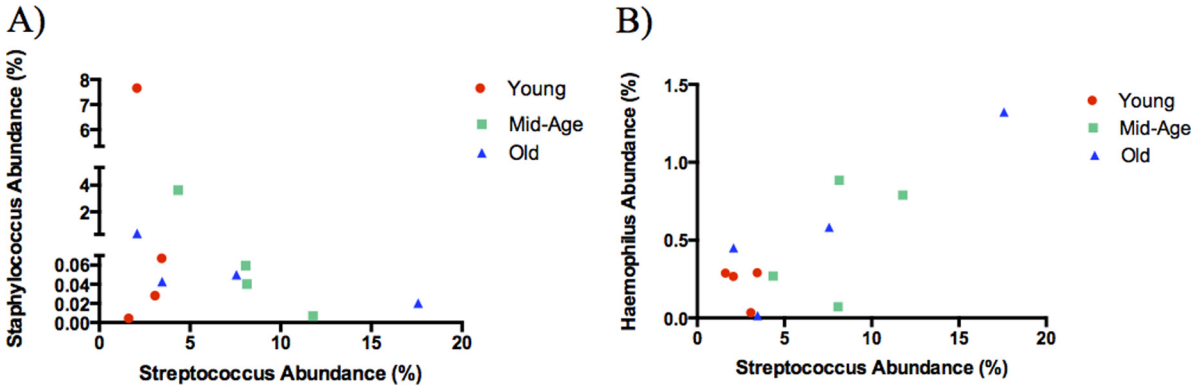

FIG 4 *Staphylococcus* decreases while *Haemophilus* increases in proportion to *Streptococcus* during nasopharyngeal colonization. Relative abundances of OTUs representing *Staphylococcus* (A) or *Haemophilus* (B) in correlation to OTUs representing *Streptococcus*. Each data point within an age group represents the average abundance within nasopharyngeal washes at day 0, 3, 14, or 21 postcolonization ($n = 3$ to 9/group). The age groups of the samples are indicated by color.

jority of the nasal microbiota within young mice prior to colonization (Fig. 1B), and this was relatively consistent across the course of colonization (Fig. 3). In fact, immediately after colonization at day 3, the OTUs representing *Proteobacteria* increased from about 40% to 72% relative abundance, and this was maintained throughout colonization until clearance at day 21 (Fig. 3A). The relative abundances of *Proteobacteria* within young mice were comparable at day 14 postcolonization (68%) and were slightly elevated at day 21 (84.4%) (Fig. 3B). In contrast, although levels of *Proteobacteria* were elevated in old mice at day 3 postcolonization (74.7%), they continued to decrease throughout colonization, comprising about 21.2% of OTUs by day 14 and only 13.6% by day 21 (Fig. 3C). In fact, by day 21, old mice contained significantly lower levels ($P < 0.0001$) of OTUs representing the *Proteobacteria* phylum compared to the levels present at day 3 (Fig. 3C; also see Fig. S2 in the supplemental material).

It was evident that the abundant OTUs within the *Firmicutes* phylum (which includes *S. pneumoniae*) were similar between all three age groups at baseline (young, 44%; middle-aged, 44.6%; old, 45.2%) (Fig. 1B). However, within the day 3, 14, and 21 microbiota, there was a decrease in relative abundance of OTUs within the *Firmicutes* phylum in young mice (day 3, 15.7%; day 14, 19%; day 21, 8.8%) and an increase within the old mice (day 3, 14.3%; day 14, 38.7%; day 21, 64.3%) (Fig. 3C). In fact, by day 21, there is a significantly greater abundance of OTUs ($P < 0.0001$) representing *Firmicutes* within the old mice relative to the young and middle-aged samples (see Fig. S2B in the supplemental material).

The abundance of bacterial groups within the URT is altered throughout colonization. The presence of *Streptococcus pneumoniae*, *Staphylococcus aureus*, and *Haemophilus influenzae* in the nasopharynx previously has been shown to influence subsequent colonization (19). In particular, *S. pneumoniae* and *S. aureus* appear to have an antagonistic relationship, while *S. pneumoniae* and *H. influenzae* demonstrate a synergistic relationship to promote cocolonization within this microbial niche (17, 18, 20, 21). To further investigate these interactions in a natural community, we examined how existing populations of *Staphylococcus* and *Haemophilus* are altered following *S. pneumoniae* colonization. Prior to colonization (day 0), there is a higher abundance of *Staphylococcus* than *Streptococcus* within the URT. However, throughout colonization with *S. pneumoniae*, the abundance of OTUs representing *Staphylococcus* appears to decrease as the abundance of *Streptococcus* increases (Fig. 4A). This trend is particularly evident within the middle-aged and old mice, as the abundance of *Streptococcus* within their nasopharyngeal washes continues to increase throughout colonization. In contrast, the interaction with *Haemophilus* appeared to be synergistic, as the relative abundance of *Streptococcus* throughout colonization was mirrored by the increased abundance of *Haemophilus* (Fig. 4B). These results support previously published data indicating that colonization with *S. pneumoniae* can greatly influence the survival and growth of the existing residents within the environment.

Microbial communities do not return to their baseline composition following *S. pneumoniae* colonization. In order to further examine the resolution phase of colonization, the microbiota was examined at days 14 and 21. Taxon summary plots illustrate that the introduction of *S. pneumoniae* alters the existing bacterial composition, and these changes continue to progress throughout colonization, as examined at the phylum level (see Fig. S3 in the supplemental material) and even more specifically at the genus level (Fig. 5). The microbial communities of mice colonized with *S. pneumoniae* did not return to baseline composition, as the day 21 microbial communities contained differing abundances of bacterial groups compared to baseline conditions (Fig. 5A and C). Young mice maintained high levels of *Proteobacteria* throughout colonization with *S. pneumoniae*. Although the role of *Proteobacteria* within the URT still remains unclear, some studies have shown its presence to be quite common within this niche (38).

Examining the mice following colonization with *S. pneumoniae* revealed similar results, as this introduction altered the abundance of existing bacteria within the community (Tables 1 to 3). Indeed, the introduction of *S. pneumoniae* led to the reduction of certain bacterial groups below the level of detection. The most frequently observed genera showing considerable changes upon colonization were examined in greater detail. These included *Streptococcus*, *Haemophilus*, *Staphylococcus*, *Clostridium*, and *Escherichia*. In young mice, *Streptococcus* OTUs appeared to increase slightly until day 14 and then decreased by day 21 (Table 1). The middle-aged and old mice contained a higher abundance of *Streptococcus* OTUs that continued to increase until day 21 (Tables 2 and 3). There was a 2-fold increase in the *Streptococcus* OTU abundance between day 3 and day 21 in the middle-aged mice and an 11-fold increase in the old mice. Bacterial genera such as *Haemophilus* tended to briefly increase throughout colonization in all

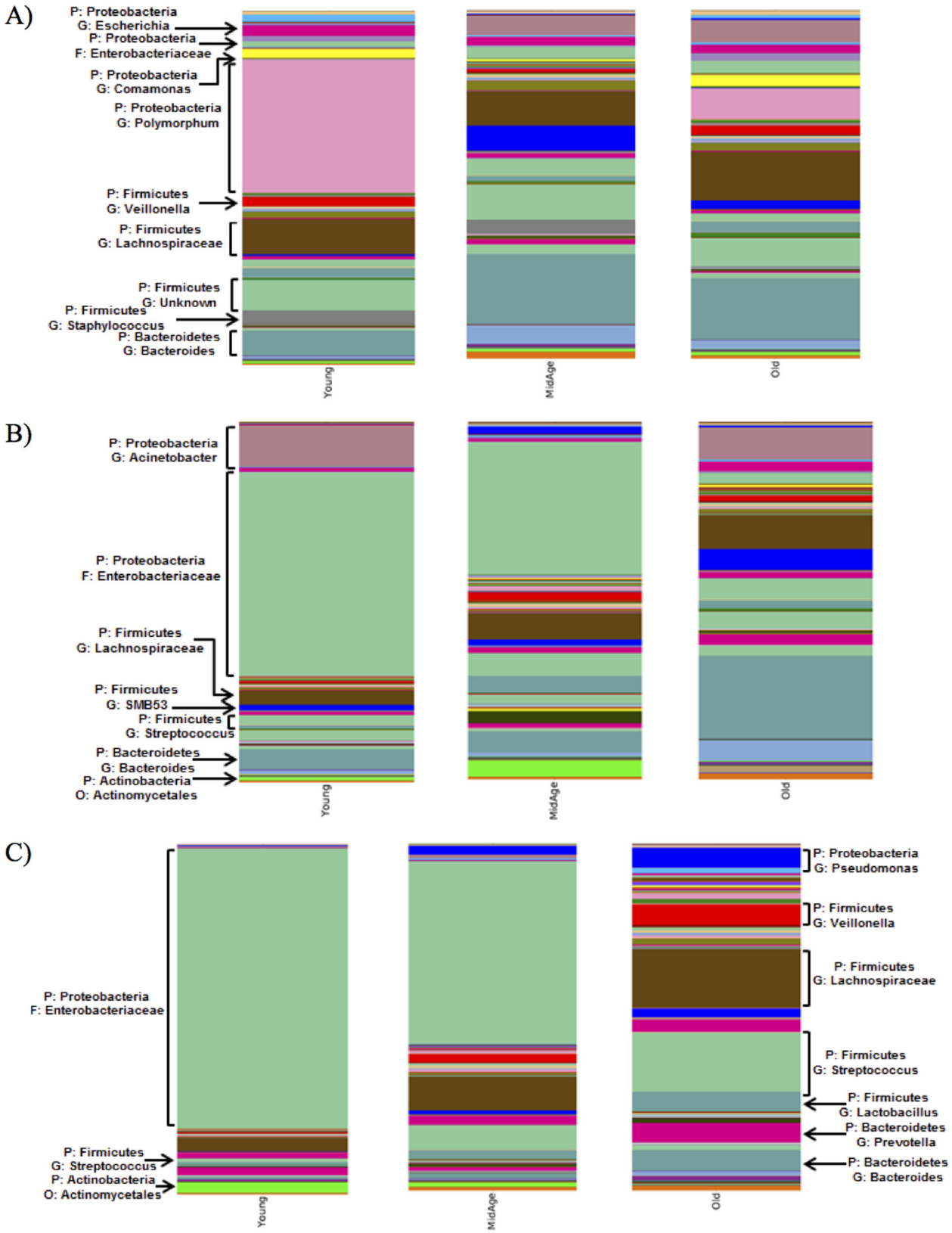

FIG 5 Bacterial communities within the URT microbiome diverge significantly from precolonization levels. Shown is an averaged taxon summary plot of all samples within a particular group ($n = 3$ to 9/group). The bacterial groups are labeled according to phylum and then specified to the highest assigned taxonomic group. The height of the bar represents the relative abundance of the associated genus within the day 0 (control) mice (A) and day 14 (B) and day 21 (C) postcolonization mice. The most abundant genera are labeled on the group.

TABLE 1 Genera most affected by *S. pneumoniae* within the young URT microbiome[a]

PHYLUM	FAMILY	GENUS	Day 3	Day 14	Day 21
Firmicutes	Streptococcaceae	***Streptococcus***	1.01	1.41	-0.435
Proteobacteria	Pasteurellaceae	***Haemophilus***	-0.23	0.04	0.04
Firmicutes	Staphylococcaceae	***Staphylococcus***	-15.05	-14.38	-17.15
Firmicutes	Clostridiaceae	***Clostridium***	-0.2	-0.144	-0.2
Proteobacteria	Enterobacteriaceae	***Escherichia***	-2.26	-2.26	-3.305
Proteobacteria	Moraxellaceae	***Moraxella***	-0.065	-0.054	-0.065
Proteobacteria	Moraxellaceae	***Acinetobacter***	0.03	10.9	-0.045
Firmicutes	Clostridiaceae	***Blautia***	-3.23	-2.78	-2.905
Firmicutes	Veillonellaceae	***Veillonella***	-2.813	-1.98	-2.405
Proteobacteria	Comamonadaceae	***Comamonas***	-2.757	-2.64	-2.765
Proteobacteria	Enterobacteriaceae	***Leclercia***	7.73	5.48	9.06
Proteobacteria	Pseudomonadaceae	***Pseudomonas***	-0.007	-0.02	0.335

[a] Shown are the differences that occur compared to baseline conditions (day 0) in young mice within each genus. Regions shaded in green indicate an increase from baseline conditions, while regions shaded in red indicate a decrease from baseline conditions.

three age groups, whereas *Escherichia* remained constant at low levels postcolonization. Taken together, these data indicated that even if the host is able to clear the pneumococcal infection, their microbiota do not necessarily return to preinfection state, which might ultimately determine future responses to secondary infections from resident or newly acquired infections.

DISCUSSION

Nasopharyngeal colonization is a prerequisite for pneumonia or invasive pneumococcal disease (39). In young adults, colonization is cleared within 3 to 6 weeks due to adequate immune control, and the bacteria rarely translocate from the nasopharynx. As a result, disease is rare (3). However, despite the low carriage rates in the elderly (8, 40), *Streptococcus pneumoniae* is the most common cause of pneumonia in this cohort (41–43). Furthermore, vaccination of older adults does not reduce pneumonia and leads to only a trivial reduction in invasive pneumococcal disease (44, 45). Since *S. pneumoniae* colonization is influenced by the composition of the nasopharyngeal microbiome, we hypothesized that age-related microbial dysbiosis influences the kinetics of pneumococcal colonization.

Within the upper respiratory tract (URT), *Streptococcus pneu-*

TABLE 2 Genera most affected by *S. pneumoniae* within the middle-aged URT microbiome[a]

PHYLUM	FAMILY	GENUS	Day 3	Day 14	Day 21
Firmicutes	Streptococcaceae	***Streptococcus***	3.78	3.83	7.53
Proteobacteria	Pasteurellaceae	***Haemophilus***	-0.15	0.633	0.55
Firmicutes	Staphylococcaceae	***Staphylococcus***	1.17	-7.93	-11.78
Firmicutes	Clostridiaceae	***Clostridium***	-0.075	0.075	-0.075
Proteobacteria	Enterobacteriaceae	***Escherichia***	-0.51	-0.96	-2.03
Proteobacteria	Moraxellaceae	***Moraxella***	-0.03	-0.03	-0.03
Proteobacteria	Moraxellaceae	***Acinetobacter***	-8.84	-8.833	-8.333
Firmicutes	Clostridiaceae	***Blautia***	-1.87	-1.33	-0.88
Firmicutes	Veillonellaceae	***Veillonella***	-0.765	1.945	3.205
Proteobacteria	Comamonadaceae	***Comamonas***	-0.57	-0.233	-0.283
Proteobacteria	Enterobacteriaceae	***Leclercia***	5.325	2.625	3.395
Proteobacteria	Pseudomonadaceae	***Pseudomonas***	0.16	1.4	3.7

[a] Shown are the differences that occur compared to baseline conditions (day 0) in middle-aged mice within each genus. Regions shaded in green indicate an increase from baseline conditions, while regions shaded in red indicate a decrease from baseline conditions.

TABLE 3 Genera most affected by *S. pneumoniae* within the elderly URT microbiome[a]

PHYLUM	FAMILY	GENUS	Day 3	Day 14	Day 21
Firmicutes	Streptococcaceae	***Streptococcus***	1.4	5.72	15.72
Proteobacteria	Pasteurellaceae	***Haemophilus***	-0.437	0.143	0.893
Firmicutes	Staphylococcaceae	***Staphylococcus***	-6.83	-5.55	-9.98
Firmicutes	Clostridiaceae	***Clostridium***	-0.214	-0.064	-0.214
Proteobacteria	Enterobacteriaceae	***Escherichia***	-2.43	0	-2.33
Proteobacteria	Moraxellaceae	***Moraxella***	-0.129	-0.129	-0.129
Proteobacteria	Moraxellaceae	***Acinetobacter***	-4.75	5.81	-4.94
Firmicutes	Clostridiaceae	***Blautia***	-4.39	-2.28	-1.905
Firmicutes	Veillonellaceae	***Veillonella***	-2.87	-1.09	3.355
Proteobacteria	Comamonadaceae	***Comamonas***	-3.44	-2.84	-2.89
Proteobacteria	Enterobacteriaceae	***Leclercia***	7.45	-1.465	-2.315
Proteobacteria	Pseudomonadaceae	***Pseudomonas***	-0.094	0.036	5.636

[a] Shown are the differences that occur compared to baseline conditions (day 0) in old mice within each genus. Regions shaded in green indicate an increase from baseline conditions, while regions shaded in red indicate a decrease from baseline conditions.

moniae can reside as an asymptomatic commensal or a pathogen, resulting in invasive pneumococcal disease (46). As a result of this dual role, a combination of factors within this microbial niche determines how it behaves. Inter- and intraspecies competition between *S. pneumoniae* and members of the upper respiratory tract microbiome contribute to the ability of *S. pneumoniae* to establish colonization, the ability of the host to mount a robust antibacterial response, and the expression of virulence factors required to establish disease (47–51). For example, by sensing peptides released by neighboring bacterial species, *S. pneumoniae* stops replication, initiates a stress response (including the induction of competence), and becomes more adept at maintaining pneumococcal colonization in mouse models (52). Many clinical studies in children demonstrate that pneumococcal carriage is positively associated with *Haemophilus influenzae* carriage but negatively associated with the carriage of *Staphylococcus aureus* (17, 23). Furthermore, adults who had more diverse nasal microbiota with a lower number of dominant species, such as *Corynebacterium*, were more likely to be natural *S. pneumoniae* carriers and more likely to become experimentally colonized by the pneumococcus (53). Our previous study of nursing home elderly found that the nasal microbiome had more diverse species and a lower percentage of protective *Corynebacterium* (8), which mimics the colonization-permissive phenotype of the previous study (53). Thus, the composition of the URT microbiome in youth and young adulthood contributes to the ability of *S. pneumoniae* to establish colonization and, ultimately, infection.

A previous study examining the bacterial profiles of the adult nostril and oropharynx niches in humans revealed a few dominant phyla within each region. Specifically, the nostril bacteria were comprised of *Firmicutes* and *Actinobacteria*, while the oropharynx bacteria were comprised of *Firmicutes*, *Proteobacteria*, and *Bacteroidetes* (54–58). Despite the genus- and species-level differences that exist between humans and mice, we observed similar characteristics in our murine URT microbiome at the phylum level. Furthermore, healthy adults are reported to have an inverse correlation between *Firmicutes* and *Actinobacteria* within the nasal microbiota (55). This trend was observed within our murine model as well, further revealing the similarities within the two communities.

It is well documented that the gut microbiota changes with age (59–61), and it appears that this may correlate with changes in health (60); however, there are fewer studies on how the airway microbiota changes with age (8) and whether these changes influence the ability of *S. pneumoniae* to establish colonization. We have shown that the microbial communities of the URT are significantly different with age under steady-state conditions, consistent with a previous report (62). Thus, we sought to further examine the impact of these differences within the old mice on their ability to allow *S. pneumoniae* colonization and persistence. *S. pneumoniae* colonization is reported to be influenced by the presence of its community members, including *Haemophilus influenzae* and *Staphylococcus aureus*. Since both of these genera are present within the murine URT microbiome, this model allows us to study the natural interactions between *S. pneumoniae* and the nasopharyngeal microbiota community members.

We examined the changes in the microbial community that occur within the URT following colonization with *S. pneumoniae*, at least some of which are due to immunosenescence. Antibacterial immunity is impaired in the elderly due to complex changes in innate and adaptive immunity called immunosenescence (63–65). As an example, we have identified that age-related changes in monocytes impair the nasopharyngeal clearance of *S. pneumoniae* (26). Others have demonstrated that immunity in the lung is impaired because Toll-like receptor (TLR) expression and signaling decreases with age, and this impairs macrophage responses to *S. pneumoniae* (66). Similarly, the quality of the adaptive antipneumococcal antibodies also have been demonstrated to decrease with age, demonstrating that the adaptive immune response also is impaired (67, 68). The extent to which immunosenescence impairs the maintenance of commensal and microbial communities is not known.

In our mouse model, young mice were able to return to precolonization levels of the streptococci. However, this was not mirrored in the middle-aged and old mice. PCoA plots reveal that young, middle-aged, and old mice cluster within their own age groups following colonization, as shown in a previous publication (62). This trend becomes more distinct by day 21, suggesting that the bacterial community present in each age group responds similarly to colonization. Also, throughout colonization, old mice have an increased abundance of OTUs representing the *Firmicutes* phylum, which includes *S. pneumoniae*. Tolerance to commensal bacteria is a key contributor in initiating an immune response against pathogenic bacteria. It has been proposed that changes occurring at the upper respiratory tract barrier within the elderly result in the inability of commensal residents to differentiate between commensal and pathogenic species, ultimately resulting in alterations within innate host defense mechanisms and ineffective bacterial clearance with age (1). Specifically, inhibitors of the NF-κB pathway have been shown to be elevated at the respiratory epithelium in old mice. This increase might be inhibiting the initiation of proinflammatory signaling pathways during bacterial infection and could result in either a more tolerogenic response or a delayed immune response in old mice (1).

Host-pathogen interactions within the nasopharyngeal niche can impact resident microbes. Our data recapitulate experimental models of *S. pneumoniae* competition or cooperation with other members of the microbiome. We observe that the streptococci appeared to have a competitive interaction with resident *Staphylococcus* and a synergistic relationship with *Haemophilus*, as has been described previously (16–18, 21). It is proposed that the inverse relationship with *Staphylococcus* is a form of bacterial interference (16, 17, 19). It has been suggested that the hydrogen peroxide produced by *S. pneumoniae* inhibits a variety of competing organisms in the aerobic environment of the URT, including *Staphylococcus* (16, 17, 20). Contrary to *S. pneumoniae*'s interaction with *Staphylococcus*, *Haemophilus* facilitates *S. pneumoniae*'s survival, as shown in previous studies using nasopharyngeal samples of children between 0 and 35 months of age (23). Although the exact mechanisms are unclear, it has been suggested that this phenomenon is related to the downregulation of pneumococcal autolysis and fratricide genes, as well as an increase in pneumococcal biofilm formation (19, 23, 24). As a result, there is decreased production of pneumococcal cell wall hydrolase and a subsequent decrease in pneumococcal lysis during the presence of *Haemophilus influenzae*. Our observations suggest that the composition of the natural mouse microbiome influences the effectiveness of experimental colonization. Whether this is a factor contributing to differences in susceptibility between mouse strains is not known.

This study examined how age may affect the composition of the microbial community during *S. pneumoniae* colonization and, in turn, how this phenomenon can play a role in either the clearance or proliferation of a pathogenic species. The overall trends from this study revealed that the elderly mice were not able to clear *S. pneumoniae* as effectively as the young mice, as they maintained high levels of bacteria even 21 days postcolonization. Characterizing the URT and determining factors driving pneumococcal colonization are important, as pneumonia is a frequently occurring and costly disease in the elderly. Using these data, we can understand the relationship between the aging system and its impact on bacterial colonization to help create alternatives to protect the elderly from age-associated infections.

ACKNOWLEDGMENTS

We thank Mark McDermott for critical reading of the manuscript and Jenn Stearns for helpful discussions and suggestions on the analyses. We also thank Michelle Shah and Christine King for their contributions and helpful suggestions during the Illumina library preparations and sequencing.

This work was funded by grants from the Canadian Institutes of Health Research (CIHR) to D.M.E.B. A.P. was supported by an Ontario Graduate Scholarship. N.T. was supported by an Early Researcher Award from the Ontario Ministry of Research and Innovation. Work in the Bowdish laboratory is supported by the McMaster Immunology Research Centre (MIRC) and the M. G. DeGroote Institute for Infectious Disease Research (IIDR). M.G.S. and D.M.E.B. are supported by the CIHR and hold Canada Research Chairs.

FUNDING INFORMATION

Ontario Graduate Scholarship provided funding to Alicja Puchta. Canada Research Chairs (Chaires de Recherche du Canada) provided funding to Michael G. Surette and Dawn M. E. Bowdish. Gouvernement du Canada | Canadian Institutes of Health Research (CIHR) provided funding to Michael G. Surette and Dawn M. E. Bowdish. Ministry of Research and Innovation (Ontario Ministry of Research and Innovation) provided funding to Dawn M. E. Bowdish.

This work was funded by grants from the Canadian Institutes of Health Research (CIHR) to D.M.E.B. A.P. was supported by an Ontario Graduate Scholarship. N.T. was supported by an Early Researcher Award from the Ontario Ministry of Research and Innovation. Work in the Bowdish laboratory is supported by the McMaster Immunology Research Centre (MIRC) and the M. G. DeGroote Institute for Infectious Disease Research (IIDR). M.G.S. and D.M.E.B. are supported by the CIHR and hold Canada Research Chairs.

REFERENCES

1. **Krone CL, Trzciński K, Zborowski T, Sanders EAM, Bogaert D.** 2013. Impaired innate mucosal immunity in aged mice permits prolonged Streptococcus pneumoniae colonization. Infect Immun **81:**4615–4625. http://dx.doi.org/10.1128/IAI.00618-13.
2. **Diavatopoulos DA, Short KR, Price JT, Wilksch JJ, Brown LE, Briles DE, Strugnell RA, Wijburg OL.** 2010. Influenza A virus facilitates Streptococcus pneumoniae transmission and disease. FASEB J **24:**1789–1798. http://dx.doi.org/10.1096/fj.09-146779.
3. **Regev-Yochay G, Raz M, Dagan R, Porat N, Shainberg B, Pinco E, Keller N, Rubinstein E.** 2004. Nasopharyngeal carriage of Streptococcus pneumoniae by adults and children in community and family settings. Clin Infect Dis **38:**632–639. http://dx.doi.org/10.1086/381547.
4. **Hamaluba M, Kandasamy R, Ndimah S, Morton R, Caccamo M, Robinson H, Kelly S, Field A, Norman L, Plested E, Thompson BAV, Zafar A, Kerridge SA, Lazarus R, John T, Holmes J, Fenlon SN, Gould KA, Waight P, Hinds J, Crook D, Snape MD, Pollard AJ.** 2015. A cross-sectional observational study of pneumococcal carriage in children, their parents, and older adults following the introduction of the 7-valent pneumococcal conjugate vaccine. Medicine (Baltimore, MD) **94:**e335. http://dx.doi.org/10.1097/MD.0000000000000335.
5. **Watt JP, O'Brien KL, Katz S, Bronsdon MA, Elliott J, Dallas J, Perilla MJ, Reid R, Murrow L, Facklam R, Santosham M, Whitney CG.** 2004. Nasopharyngeal versus oropharyngeal sampling for detection of pneumococcal carriage in adults. J Clin Microbiol **42:**4974–4976. http://dx.doi.org/10.1128/JCM.42.11.4974-4976.2004.
6. **Le Polain de Waroux O, Flasche S, Prieto-Merino D, Edmunds WJ.** 2014. Age-dependent prevalence of nasopharyngeal carriage of Streptococcus pneumoniae before conjugate vaccine introduction: a prediction model based on a meta-analysis. PLoS One **9:**e86136. http://dx.doi.org/10.1371/journal.pone.0086136.
7. **Abdullahi O, Nyiro J, Lewa P, Slack M, Scott JAG.** 2008. The descriptive epidemiology of Streptococcus pneumoniae and Haemophilus influenzae nasopharyngeal carriage in children and adults in Kilifi district, Kenya.

Pediatr Infect Dis J **27:**59–64. http://dx.doi.org/10.1097/INF.0b013e31814da70c.
8. **Whelan FJ, Verschoor CP, Stearns JC, Rossi L, Luinstra K, Loeb M, Smieja M, Johnstone J, Surette MG, Bowdish DME.** 2014. The loss of topography in the microbial communities of the upper respiratory tract in the elderly. Ann Am Thorac Soc **11:**513–521. http://dx.doi.org/10.1513/AnnalsATS.201310-351OC.
9. **Almeida ST, Nunes S, Santos Paulo AC, Valadares I, Martins S, Breia F, Brito-Avô A, Morais A, de Lencastre H, Sá-Leão R.** 2014. Low prevalence of pneumococcal carriage and high serotype and genotype diversity among adults over 60 years of age living in Portugal. PLoS One **9:**e90974. http://dx.doi.org/10.1371/journal.pone.0090974.
10. **Nuorti JP, Butler JC, Crutcher JM, Guevara R, Welch D, Holder P, Elliott JA.** 1998. An outbreak of multidrug-resistant pneumococcal pneumonia and bacteremia among unvaccinated nursing home residents. N Engl J Med **338:**1861–1868. http://dx.doi.org/10.1056/NEJM199806253382601.
11. **Krone CL, Wyllie AL, van Beek J, Rots NY, Oja AE, Chu MLJN, Bruin JP, Bogaert D, Sanders EAM, Trzciński K.** 2015. Carriage of Streptococcus pneumoniae in aged adults with influenza-like-illness. PLoS One **10:**e0119875. http://dx.doi.org/10.1371/journal.pone.0119875.
12. **Perez-Trallero E, Marimon JM, Larruskain J, Alonso M, Ercibengoa M.** 2011. Antimicrobial susceptibilities and serotypes of Streptococcus pneumoniae isolates from elderly patients with pneumonia and acute exacerbation of chronic obstructive pulmonary disease. Antimicrob Agents Chemother **55:**2729–2734. http://dx.doi.org/10.1128/AAC.01546-10.
13. **Stupka JE, Mortensen EM, Anzueto A, Restrepo MI.** 2009. Community-acquired pneumonia in elderly patients. Aging Health **5:**763–774. http://dx.doi.org/10.2217/ahe.09.74.
14. **Janssens J, Krause K.** 2004. Pneumonia in the very old. Lancet Infect Dis **4:**112–124. http://dx.doi.org/10.1016/S1473-3099(04)00931-4.
15. **Wroe PC, Finkelstein JA, Ray GT, Linder JA, Johnson KM, Rifas-Shiman S, Moore MR, Huang SS.** 2012. Aging population and future burden of pneumococcal pneumonia in the United States. J Infect Dis **205:**1589–1592. http://dx.doi.org/10.1093/infdis/jis240.
16. **Bosch AATM, Biesbroek G, Trzcinski K, Sanders EAM, Bogaert D.** 2013. Viral and bacterial interactions in the upper respiratory tract. PLoS Pathog **9:**e1003057. http://dx.doi.org/10.1371/journal.ppat.1003057.
17. **Regev-Yochay G, Dagan R, Raz M, Carmeli Y, Shainberg B, Derazne E, Rahav G, Rubinstein E.** 2004. Association between carriage of Streptococcus pneumoniae and Staphylococcus aureus in children. JAMA **292:**716–720. http://dx.doi.org/10.1001/jama.292.6.716.
18. **Margolis E, Yates A, Levin BR.** 2010. The ecology of nasal colonization of Streptococcus pneumoniae, Haemophilus influenzae and Staphylococcus aureus: the role of competition and interactions with host's immune response. BMC Microbiol **10:**59. http://dx.doi.org/10.1186/1471-2180-10-59.
19. **Shiri T, Nunes MC, Adrian PV, Van Niekerk N, Klugman KP, Madhi SA.** 2013. Interrelationship of Streptococcus pneumoniae, Haemophilus influenzae and Staphylococcus aureus colonization within and between pneumococcal-vaccine naïve mother-child dyads. BMC Infect Dis **13:**483. http://dx.doi.org/10.1186/1471-2334-13-483.
20. **Regev-Yochay G, Trzcinski K, Thompson CM, Malley R, Lipsitch M.** 2006. Interference between Streptococcus pneumoniae and Staphylococcus aureus: in vitro hydrogen peroxide-mediated killing by Streptococcus pneumoniae. J Bacteriol **188:**4996–5001. http://dx.doi.org/10.1128/JB.00317-06.
21. **Quintero B, Araque M, van der Gaast-de Jongh C, Escalona F, Correa M, Morillo-Puente S, Vielma S, Hermans PWM.** 2011. Epidemiology of Streptococcus pneumoniae and Staphylococcus aureus colonization in healthy Venezuelan children. Eur J Clin Microbiol Infect Dis **30:**7–19. http://dx.doi.org/10.1007/s10096-010-1044-6.
22. **Murphy TF.** 2006. Otitis media, bacterial colonization, and the smoking parent. Clin Infect Dis **42:**904–906. http://dx.doi.org/10.1086/500942.
23. **Chien YW, Vidal JE, Grijalva CG, Bozio C, Edwards KM, Williams JV, Griffin MR, Verastegui H, Hartinger SM, Gil AI, Lanata CF, Klugman KP.** 2012. Density interactions between Streptococcus pneumoniae, Haemophilus influenzae and Staphylococcus aureus in the nasopharynx of young Peruvian children. Pediatr Infect Dis J **32:**72–73.
24. **Tikhomirova A, Kidd SP.** 2013. Haemophilus influenzae and Streptococcus pneumoniae: living together in a biofilm. Pathog Dis **69:**114–126. http://dx.doi.org/10.1111/2049-632X.12073.
25. **Puchta A, Verschoor CP, Thurn T, Bowdish DME.** 2014. Characterization of inflammatory responses during intranasal colonization with Streptococcus pneumoniae. J Vis Exp **2014:**e50490.
26. **Puchta A, Naidoo A, Verschoor CP, Loukov D, Thevaranjan N, Mandur TS, Nguyen PS, Jordana M, Loeb M, Xing Z, Kobzik L, Larche MJ, Bowdish DM.** 2015. TNF drives monocyte dysfunction with age and results in impaired anti-pneumococcal immunity. PLoS Pathog **12:**e1005368.
27. **Siegel SJ, Tamashiro E, Weiser JN.** 2015. Clearance of pneumococcal colonization in infants is delayed through altered macrophage trafficking. PLoS Pathog **11:**e1005004. http://dx.doi.org/10.1371/journal.ppat.1005004.
28. **Dorrington MG, Roche AM, Chauvin SE, Tu Z, Mossman KL, Weiser JN, Bowdish DME.** 2013. MARCO is required for TLR2- and Nod2-mediated responses to Streptococcus pneumoniae and clearance of pneumococcal colonization in the murine nasopharynx. J Immunol **190:**250–258. http://dx.doi.org/10.4049/jimmunol.1202113.
29. **Stearns JC, Davidson CJ, McKeon S, Whelan FJ, Fontes ME, Schryvers AB, Bowdish DME, Kellner JD, Surette MG.** 2015. Culture and molecular-based profiles show shifts in bacterial communities of the upper respiratory tract that occur with age. ISME J **9:**1246–1259. http://dx.doi.org/10.1038/ismej.2014.250.
30. **Bartram AK, Lynch MDJ, Stearns JC, Moreno-Hagelsieb G, Neufeld JD.** 2011. Generation of multimillion-sequence 16S rRNA gene libraries from complex microbial communities by assembling paired-end Illumina reads. Appl Environ Microbiol **77:**3846–3852. http://dx.doi.org/10.1128/AEM.02772-10.
31. **Martin M.** 2011. Cutadapt removes adapter sequences from high-throughput sequencing reads. EMBnet J **17:**10. http://dx.doi.org/10.14806/ej.17.1.200.
32. **Masella AP, Bartram AK, Truszkowski JM, Brown DG, Neufeld JD.** 2012. PANDAseq: paired-end assembler for Illumina sequences. BMC Bioinformatics **13:**31. http://dx.doi.org/10.1186/1471-2105-13-31.
33. **Ye Y.** 2010. Identification and quantification of abundant species from pyrosequences of 16S rRNA by consensus alignment. Proc IEEE Int Conf Bioinformatics Biomed **2010:**153–157. http://dx.doi.org/10.1109/BIBM.2010.5706555.
34. **Caporaso JG, Kuczynski J, Stombaugh J, Bittinger K, Bushman FD, Costello EK, Fierer N, Peña AG, Goodrich JK, Gordon JI, Huttley GA, Kelley ST, Knights D, Koenig JE, Ley RE, Lozupone CA, McDonald D, Muegge BD, Pirrung M, Reeder J, Sevinsky JR, Turnbaugh PJ, Walters WA, Widmann J, Yatsunenko T, Zaneveld J, Knight R.** 2010. QIIME allows analysis of high-throughput community sequencing data. Nat Methods **7:**335–336. http://dx.doi.org/10.1038/nmeth.f.303.
35. **Carvalho MDGS, Tondella ML, McCaustland K, Weidlich L, McGee L, Mayer LW, Steigerwalt A, Whaley M, Facklam RR, Fields B, Carlone G, Ades EW, Dagan R, Sampson JS.** 2007. Evaluation and improvement of real-time PCR assays targeting lytA, ply, and psaA genes for detection of pneumococcal DNA. J Clin Microbiol **45:**2460–2466. http://dx.doi.org/10.1128/JCM.02498-06.
36. **Sauder LA, Engel K, Stearns JC, Masella AP, Pawliszyn R, Neufeld JD.** 2011. Aquarium nitrification revisited: Thaumarchaeota are the dominant ammonia oxidizers in freshwater aquarium biofilters. PLoS One **6:**e23281. http://dx.doi.org/10.1371/journal.pone.0023281.
37. **McMurdie PJ, Holmes S.** 2014. Waste not, want not: why rarefying microbiome data is inadmissible. PLoS Comput Biol **10:**e1003531. http://dx.doi.org/10.1371/journal.pcbi.1003531.
38. **Park H, Shin JW, Park S-G, Kim W.** 2014. Microbial communities in the upper respiratory tract of patients with asthma and chronic obstructive pulmonary disease. PLoS One **9:**e109710. http://dx.doi.org/10.1371/journal.pone.0109710.
39. **Bogaert D, De Groot R, Hermans PWM.** 2004. Streptococcus pneumoniae colonisation: the key to pneumococcal disease. Lancet Infect Dis **4:**144–154. http://dx.doi.org/10.1016/S1473-3099(04)00938-7.
40. **Ridda I, Macintyre CR, Lindley R, McIntyre PB, Brown M, Oftadeh S, Sullivan J, Gilbert GL.** 2010. Lack of pneumococcal carriage in the hospitalised elderly. Vaccine **28:**3902–3904. http://dx.doi.org/10.1016/j.vaccine.2010.03.073.
41. **Ahmed AE, Nicholson KG, Nguyen-Van-Tam JS.** 1995. Reduction in mortality associated with influenza vaccine during 1989-90 epidemic. Lancet **346:**591–595. http://dx.doi.org/10.1016/S0140-6736(95)91434-X.
42. **File TM.** 2003. Community-acquired pneumonia. Lancet **362:**1991–2001. http://dx.doi.org/10.1016/S0140-6736(03)15021-0.
43. **Polverino E, Dambrava P, Cillóniz C, Balasso V, Marcos MA, Esquinas**

C, Mensa J, Ewig S, Torres A. 2010. Nursing home-acquired pneumonia: a 10 year single-centre experience. Thorax **65:**354–359. http://dx.doi.org/10.1136/thx.2009.124776.

44. **Rudnick W, Liu Z, Shigayeva A, Low DE, Green K, Plevneshi A, Devlin R, Downey J, Katz K, Kitai I, Krajden S, Ostrowska K, Richardson D, Richardson S, Sarabia A, Silverman M, Simor AE, Tyrrell G, McGeer A.** 2013. Pneumococcal vaccination programs and the burden of invasive pneumococcal disease in Ontario, Canada, 1995-2011. Vaccine **31:**5863–5871. http://dx.doi.org/10.1016/j.vaccine.2013.09.049.
45. **Leventer-Roberts M, Feldman BS, Brufman I, Cohen-Stavi CJ, Hoshen M, Balicer RD.** 2015. Effectiveness of 23-valent pneumococcal polysaccharide vaccine against invasive disease and hospital-treated pneumonia among people aged ≥65 years: a retrospective case-control study. Clin Infect Dis **60:**1472–1480.
46. **Bogaert D, Keijser B, Huse S, Rossen J, Veenhoven R, van Gils E, Bruin J, Montijn R, Bonten M, Sanders E.** 2011. Variability and diversity of nasopharyngeal microbiota in children: a metagenomic analysis. PLoS One **6:**e17035. http://dx.doi.org/10.1371/journal.pone.0017035.
47. **Lijek RS, Luque SL, Liu Q, Parker D, Bae T, Weiser JN.** 2012. Protection from the acquisition of Staphylococcus aureus nasal carriage by cross-reactive antibody to a pneumococcal dehydrogenase. Proc Natl Acad Sci U S A **109:**13823–13828. http://dx.doi.org/10.1073/pnas.1208075109.
48. **Lijek RS, Weiser JN.** 2012. Co-infection subverts mucosal immunity in the upper respiratory tract. Curr Opin Immunol **24:**417–423. http://dx.doi.org/10.1016/j.coi.2012.05.005.
49. **Lysenko ES, Lijek RS, Brown SP, Weiser JN.** 2010. Within-host competition drives selection for the capsule virulence determinant of streptococcus pneumoniae. Curr Biol **20:**1222–1226. http://dx.doi.org/10.1016/j.cub.2010.05.051.
50. **Marks LR, Davidson BA, Knight PR, Hakansson AP.** 2013. Interkingdom signaling induces Streptococcus pneumoniae biofilm dispersion and transition from asymptomatic colonization to disease. mBio **4:**1–13. http://dx.doi.org/10.3391/mbi.2013.4.1.01.
51. **Lysenko ES, Ratner AJ, Nelson AL, Weiser JN.** 2005. The role of innate immune responses in the outcome of interspecies competition for colonization of mucosal surfaces. PLoS Pathog **1:**0003–0011.
52. **Hathaway LJ, Bättig P, Reber S, Rotzetter JU, Aebi S, Hauser C, Heller M, Kadioglu A, Mühlemann K.** 2014. Streptococcus pneumoniae detects and responds to foreign bacterial peptide fragments in its environment. Open Biol **4:**130224. http://dx.doi.org/10.1098/rsob.130224.
53. **Cremers AJ, Zomer AL, Gritzfeld JF, Ferwerda G, van Hijum SA, Ferreira DM, Shak JR, Klugman KP, Boekhorst J, Timmerman HM, de Jonge MI, Gordon SB, Hermans PW.** 2014. The adult nasopharyngeal microbiome as a determinant of pneumococcal acquisition. Microbiome **2:**44. http://dx.doi.org/10.1186/2049-2618-2-44.
54. **Gao Z, Kang Y, Yu J, Ren L.** 2014. Human pharyngeal microbiome may play a protective role in respiratory tract infections. Genomics Proteomics Bioinformatics **12:**144–150. http://dx.doi.org/10.1016/j.gpb.2014.06.001.
55. **Lemon KP, Klepac-Ceraj V, Schiffer HK, Brodie EL, Lynch SV, Kolter R.** 2010. Comparative analyses of the bacterial microbiota of the human nostril and oropharynx. mBio **1:**e00129-10. http://dx.doi.org/10.1128/mBio.00129-10.
56. **Pei Z, Bini EJ, Yang L, Zhou M, Francois F, Blaser MJ.** 2004. Bacterial biota in the human distal esophagus. Proc Natl Acad Sci U S A **101:**4250–4255. http://dx.doi.org/10.1073/pnas.0306398101.
57. **Spor A, Koren O, Ley R.** 2011. Unravelling the effects of the environment and host genotype on the gut microbiome. Nat Rev Microbiol **9:**279–290. http://dx.doi.org/10.1038/nrmicro2540.
58. **Hibbing ME, Fuqua C, Parsek MR, Peterson SB.** 2010. Bacterial competition: surviving and thriving in the microbial jungle. Nat Rev Microbiol **8:**15–25. http://dx.doi.org/10.1038/nrmicro2259.
59. **O'Sullivan O, Coakley M, Lakshminarayanan B, Conde S, Claesson MJ, Cusack S, Fitzgerald AP, O'Toole PW, Stanton C, Ross RP.** 2013. Alterations in intestinal microbiota of elderly Irish subjects post-antibiotic therapy. J Antimicrob Chemother **68:**214–221. http://dx.doi.org/10.1093/jac/dks348.
60. **Claesson MJ, Jeffery IB, Conde S, Power SE, O'Connor EM, Cusack S, Harris HMB, Coakley M, Lakshminarayanan B, O'Sullivan O, Fitzgerald GF, Deane J, O'Connor M, Harnedy N, O'Connor K, O'Mahony D, van Sinderen D, Wallace M, Brennan L, Stanton C, Marchesi JR, Fitzgerald AP, Shanahan F, Hill C, Ross RP, O'Toole PW.** 2012. Gut microbiota composition correlates with diet and health in the elderly. Nature **488:**178–184. http://dx.doi.org/10.1038/nature11319.
61. **Claesson MJ, Cusack S, O'Sullivan O, Greene-Diniz R, de Weerd H, Flannery E, Marchesi JR, Falush D, Dinan T, Fitzgerald G, Stanton C, van Sinderen D, O'Connor M, Harnedy N, O'Connor K, Henry C, O'Mahony D, Fitzgerald AP, Shanahan F, Twomey C, Hill C, Ross RP, O'Toole PW.** 2011. Composition, variability, and temporal stability of the intestinal microbiota of the elderly. Proc Natl Acad Sci U S A **108**(Suppl): 4586–4591. http://dx.doi.org/10.1073/pnas.1000097107.
62. **Krone CL, Biesbroek G, Trzciński K, Sanders EAM, Bogaert D.** 2014. Respiratory microbiota dynamics following Streptococcus pneumoniae acquisition in young and elderly mice. Infect Immun **82:**1725–1731. http://dx.doi.org/10.1128/IAI.01290-13.
63. **Lexau CA, Lynfield R, Danila R, Pilishvili T, Facklam R, Farley MM, Harrison LH, Schaffner W, Reingold A, Bennett NM, Hadler J, Cieslak PR, Whitney CG.** 2005. Changing epidemiology of invasive pneumococcal disease among older adults in the era of pediatric pneumococcal conjugate vaccine. JAMA **294:**2043–2051. http://dx.doi.org/10.1001/jama.294.16.2043.
64. **El-Solh AA, Sikka P, Ramadan F, Davies J.** 2001. Etiology of severe pneumonia in the very elderly. Am J Respir Crit Care Med **163:**645–651. http://dx.doi.org/10.1164/ajrccm.163.3.2005075.
65. **Palmer LB, Albulak K, Fields S, Filkin AM, Simon S, Smaldone GC.** 2001. Oral clearance and pathogenic oropharyngeal colonization in the elderly. Am J Respir Crit Care Med **164:**464–468. http://dx.doi.org/10.1164/ajrccm.164.3.2008149.
66. **Hinojosa E, Boyd AR, Orihuela CJ.** 2009. Age-associated inflammation and Toll-like receptor dysfunction prime the lungs for pneumococcal pneumonia. J Infect Dis **200:**546–554. http://dx.doi.org/10.1086/600870.
67. **Cremers AJH, Lut J, Hermans PWM, Meis JF, de Jonge MI, Ferwerda G.** 2014. Avidity of antibodies against infecting pneumococcal serotypes increases with age and severity of disease. Clin Vaccine Immunol **21:**904–907. http://dx.doi.org/10.1128/CVI.00147-14.
68. **Nicoletti C, Borghesi-Nicoletti C, Yang XH, Schulze DH, Cerny J.** 1991. Repertoire diversity of antibody response to bacterial antigens in aged mice. II. Phosphorylcholine-antibody in young and aged mice differ in both VH/VL gene repertoire and in specificity. J Immunol **147:**2750–2755.

Appendix II.

New evidence of Metchnikoff's hypothesis of aging: microbiota drive age-associated immune impairment

Netusha Thevaranjan*, Alicja Puchta*, Avee Naidoo, J. C. Szamosi, Chris P. Verschoor, Dessi Loukov, Louis P Schenck, Jennifer Jury, Kevin Foley, Jonathan Schertzer, Maggie J. Larché, Donald J. Davidson, Michael G. Surette, Elena F Verdú, and Dawn M.E. Bowdish

In Review: Journal of Experimental Medicine

New evidence of Metchnikoff's hypothesis of aging: microbiota drive age-associated immune impairment

Netusha Thevaranjan[1-3,7], Alicja Puchta[1-3,7], Avee Naidoo[1-3], J. C. Szamosi[4], Chris P. Verschoor[1-3], Dessi Loukov, Louis P Schenck[3,4], Jennifer Jury[4], Kevin Foley, Jonathan Schertzer, Maggie J. Larché[5], Donald J. Davidson[6], Michael G. Surette[3,4], Elena F Verdú[4], and Dawn M.E. Bowdish[1-3,†]

Affiliations:

[1]Department of Pathology and Molecular Medicine, McMaster University, Hamilton, ON, Canada.
[2]McMaster Immunology Research Centre, McMaster University, Hamilton, ON, Canada.
[3]Michael G. DeGroote Institute for Infectious Disease Research, McMaster University, Hamilton, ON, Canada.
[4]Farncombe Family Digestive Health Research Institute, McMaster University, Hamilton, ON, Canada.
[5]Department of Medicine, McMaster University, Hamilton, ON, Canada
[6]University of Edinburgh / MRC Centre for Inflammation Research, Queen's Medical Research Institute, Edinburgh EH16 4TJ, Scotland, UK
[7]These authors contributed equally to this work.

Corresponding Author Contact: [†]Dawn M.E. Bowdish

Pathology and Molecular Medicine
McMaster University
1200 Main Street West, MDCL-4020
Hamilton, ON L8N 3Z5
Email: bowdish@mcmaster.ca
Phone: 905-525-9140, ext. 22313

Running Title: Microbiota drives age-associated inflammation

Abstract: In 1901, Elie Metchnikoff hypothesized that the ill health that accompanies aging occurred because the intestinal microbiota. He believed, and we have now demonstrated that, bacterial products pass through the intestinal barrier, activate macrophages and cause systemic inflammation. We demonstrated that germ-free mice live longer, healthier lives than their WT counterparts and are protected from age-associated inflammation and macrophage dysfunction. Co-housing germ-free mice with old, but not young, mice increased levels of pro-inflammatory cytokines in the blood, demonstrating the role of microbial dysbiosis in driving age-associated inflammation. In TNF knockout mice, which are protected from age-associated inflammation, microbial dysbiosis does not occur. Furthermore age-related microbial dysbiosis can be reversed by reducing levels of the cytokine TNF using anti-TNF therapy. These data suggest that reversing the microbial dysbiosis that occurs with age may be a viable strategy for reducing age-associated inflammation and the morbidity that accompanies it.

Introduction

Metchnikoff proposed that tissue destruction and senescence was a consequence of chronic systemic inflammation due to increased permeability in the colon and the escape of bacteria and their products(Metchnikoff, 1907). He believed that these bacterial products drove the activation of phagocytes, resulting in inflammation that led to the deterioration of surrounding tissues. Metchnikoff had remarkable foresight: his identification of the microbiota of the gut as a community whose composition could be altered, and his belief that bacterial products or "toxins" could alter health and behavior have since been proven experimentally(Cryan and Dinan, 2012; Gevers et al., 2012). Metchnikoff's theory that declining health with age is caused by systemic inflammation due to exposure to bacterial components from the gut has been hypothesized by others(Biagi et al., 2010; Franceschi and Campisi, 2014; Guigoz et al., 2008), but until now, has not been experimentally validated.

Chronic inflammation caused by increased mucosal barrier permeability and microbial translocation (defined as the translocation of microbes and/or their products from the mucosal compartment to the circulation without overt bacteremia) has been implicated in the increased systemic inflammation and accelerated immunosenescence observed in HIV patients(Appay et al., 2007; Brenchley et al., 2006). Aging is also characterized by a state of chronic, low-grade, systemic inflammation(Franceschi et al., 2000). Higher than average levels of age-associated inflammation are a strong predictor of overall ill-health, development of chronic inflammatory conditions, and all-cause mortality in the elderly. High levels of age-associated inflammation also influence susceptibility to pneumococcal infection, and are a predictor of disease severity and survival(Antunes et al., 2002; Yende et al., 2005). Although age-associated inflammation clearly influences the aging process, it is unclear why levels of cytokines in the tissues and circulation increase with age. It has been theorized that gradual, cumulative, sub-clinical tissue damage occurs with age, increasing the burden of tissue repair and resulting in increasing background levels of pro-inflammatory cytokine production(Franceschi et al., 2000); however, the experimental evidence which would definitively prove this hypothesis is lacking.

Although it has been demonstrated that gut microbial composition correlates with levels of circulating cytokines and markers of health in the elderly(Claesson et al., 2012), it is not known whether this is merely correlative or whether the gut microbiota is a driver of age-associated inflammation. Herein, we report that, in agreement with Metchnikoff's theory of aging, microbial translocation occurs with age due to increased permeability in the intestinal tract. We demonstrate that microbial products enter the bloodstream in aged mice where they trigger systemic inflammation (i.e. elevated levels of serum IL-6). Chronic exposure to inflammation alters macrophage function, rendering these cells poor bacterial killers, but potent producers of inflammatory cytokines, and ultimately contributing to age-associated inflammation. By colonizing aged germ-free mice, which do not have age-associated inflammation until they are colonized with microbiota from aged SPF mice, we demonstrate that the microbiota, and specifically age-associated microbial dysbiosis drives the inflammation that accompanies aging.

TNF drives age-associated defects in macrophage function

We found that after normalizing for differences in bacterial uptake between mice, resident

peritoneal (Fig 1A) and bone marrow derived (Fig 1B) macrophages from old wild-type (WT) mice (18-22 mo) were impaired in their ability to kill *Streptococcus pneumoniae* as compared to those from young WT (10-14 wk) mice. Following internalization, bacterial lysis was observable in macrophages from young mice, but reduced or delayed in old mice (Suppl Fig 1A). Maturation markers on macrophages from young and old mice were expressed at equal levels, indicating that differences observed with age were not due to altered differentiation or maturity (data not shown).

Levels of pro-inflammatory cytokines such as IL6 and TNF in the circulation and tissues increase with age, both in humans and mice(Bouchlaka et al., 2013; Franceschi et al., 2007). In keeping with previous reports, levels of TNF and IL6 in the circulation (Fig 1C &D) and IL6 in the lungs (Fig 1E) were found to be higher in older mice. Peribronchiolar cellular infiltration was observed in the lungs of old mice in the absence of stimulation or overt infection (Fig 1F). In addition, *ex vivo* lung tissue slices (Fig 1G) or whole blood (Fig 1H) from old mice produced higher baseline levels of IL6 than young mice and were hyper-reactive when stimulated with *S. pneumoniae* or LPS, respectively, demonstrating significantly enhanced pro-inflammatory responses to live bacterial and bacterial products. This phenotype was also observed using bone marrow derived macrophages from old mice, which produced more IL6 following stimulation with LPS or *S. pneumoniae* compared to young mice (Figure 1I).

It has been frequently observed that individuals with higher levels of age-associated inflammation are at increased risk of both developing, and dying from *S. pneumoniae* infection(Antunes et al., 2002; Yende et al., 2005). Furthermore, infusion of TNF into mice impairs anti-pneumococcal immunity and increases levels of *S. pneumoniae* in experimental models(Hinojosa et al., 2009). We therefore hypothesized that the chronically elevated levels of TNF that occur with age could have a direct effect on macrophage-mediated killing of *S. pneumoniae*. Exogenous addition of TNF (10 ng/ml) to culture media was indeed found to reduce bacterial killing by macrophages from young or old mice (Fig 2A), replicating the defective killing phenotype of macrophages from old mice in cells from young mice.

Since acute exposure to TNF impaired macrophage killing of *S. pneumoniae*, we postulated that chronic age-associated inflammation, characterized by high systemic levels of TNF, might underpin the defects we observed in macrophage anti-bacterial function. In contrast to wild-type animals, aged TNF knockout (KO) mice did not have greater levels of IL6 in the circulation in the steady state (Fig 2B) and when LPS was added to whole blood, old mice did not produce higher amounts of IL6 than the stimulated blood of young mice (Fig 2C). Constitutive IL-6 production was not affected by age in TNF KO lung slices (Fig 2D) and pulmonary cellular infiltrates were not observed in old mice, demonstrating protection from inflammation in the lungs (Fig 2E) Finally, bone marrow derived macrophages from old TNF KO mice did not have the impaired pneumococcal killing observed in WT mice (Fig 2F). Thus, age-associated inflammation, and more specifically, chronic exposure to TNF, contributes to changes in macrophage function, resulting in decreased *S. pneumoniae* killing capacity.

Intestinal permeability and levels of circulating bacterial products increase with age

Although our data demonstrated that the presence of TNF promoted systemic inflammation and impaired macrophage function, the cause of increased TNF production with age was unclear. Based on Metchnikoff's hypothesis that bacterial components from the gut microbiota could cause systemic inflammation, we investigated whether increased intestinal permeability and translocation of bacterial products occurred in aged mice.

Intestinal permeability was measured in WT mice (3, 12, 15 and 18 month old), by performing oral gavages with 3-5kDa FITC-labelled dextran and measuring translocation of fluorescence into the plasma and was found to significantly increase with age (Fig 3A). We next assessed whether this was due to altered paracellular and/or passive permeability in the ileum and colon of young and old WT mice. Although there were no gross differences in intestinal architecture (Fig 3B), paracellular permeability was higher in the colons of old mice (Fig 3C), as determined by mucosal-to-serosal flux by using ^{51}chromium-EDTA (^{51}Cr-EDTA). Consistent with evidence of increased permeability in the colon, where bacterial numbers are highest, plasma levels of the bacterial cell wall component muramyl dipeptide (MDP) were also significantly higher in old WT mice as compared to young mice (Fig 3D). Thus, increased leakiness of

the gut is a consequence of aging.

Germ-free mice are protected from age-associated inflammation and dysregulated macrophage function

The central postulate of Metchnikoff's theory of aging is that the microbiome drives age-associated inflammation and macrophage dysfunction. If the increase in circulating microbial products is a driving force in age-associated inflammation and mortality, we reasoned that germ-free (GF) mice, which have no detectable MDP in the circulation (data not shown), nor age-associated increase in intestinal permeability (Fig 4A), would be protected. Aging GF mice lived longer than their specific pathogen free (SPF) WT counterparts (Fig. 4B), similar to what has been previously shown in germ-free mice (Gordon and Pesti, 1971) and rats (Snyder et al., 1990). These GF mice were protected from age-associated inflammation, lacking the high circulatiing IL6 levels found in old control animals (Fig 4C). They also did not have peribronchiolar cellular infiltrates in their lungs (Fig 4D) or increased levels of IL6 in the lungs (Fig 4E) compared to young germ-free mice. Furthermore, baseline and LPS-induced IL6 in the whole blood was not age dependent in GF mice, in contrast to the significantly enhanced inflammatory phenotype in old SPF WT mice (Fig. 4F). Finally, bone marrow derived macrophages from old GF mice did not have impaired *S. pneumoniae* killing capacity (Fig. 4G) or produce more IL6 than young GF mice either basally or after stimulating responses with LPS *ex vivo* (Fig. 4H). These data demonstrate that chronic age-associated inflammation requires the presence of a microbiome.

The composition of the microbial community influences intestinal permeability and age-associated inflammation

We envisioned two possibilities that could explain how the microbiome drives age-associated inflammation. In the first, the presence of any microbiota, even a minimal microbiota, could become metabolically costly and over time, result in increased intestinal permeability. The second hypothesis was that microbial dysbiosis occurs with age to drive increased intestinal permeability.

To test the first hypothesis, (i.e. whether a low-diversity microbial community was sufficient to drive age-associated inflammation), mice with a minimal microbiome were used. Mice were colonized with the altered Schaedler flora (ASF) and bred for two generations during which time their microbiota diversified naturally as previously described(Slack et al., 2009). Similar to old SPF WT mice, old ASF-derived mice had greater intestinal permeability (Fig. 5A), higher levels of plasma IL6 (Fig. 5B) and higher IL6 production in whole blood following PBS or LPS stimulation (Fig. 5C) than in young mice. Despite having a minimal microbiota these mice also experienced age-related microbial dysbiosis (Fig 5D).

Although our data demonstrated that colonization with a microbiota of initially limited diversity was sufficient to elicit age-associated changes in permeability and inflammation, we next investigated whether the microbial composition might have altered with aging and whether there was any effect of differential microbial composition on phenotypes. Similar to what others have reported, we found that there were changes in the composition of the microbiome of the SPF mice with age (Table 1, Fig 6A) including the orders *Bacteroidales, Clostridiales* and *Erysipelotrichales* (Claesson et al., 2011; Mariat et al., 2009). To determine whether this age-associated dysbiosis could increase age-associated inflammation, young and old germ-free mice were colonized, via co-housing, with microbiota from either young or old SPF mice. The microbial dysbiosis that was evident in the fecal microbiota of the donor mice was maintained in the colonized recipient mice over the timecourse of this study (Fig 6A). After a minimum of 6 wks, changes in paracellular permeability were assessed in the colonized mice. The paracellular permeability was measured from all the germ-free mice colonized with the microbiota sourced from old mice (n=23 total, n=11 young mice + n=12 old mice) compared to young microbiota (n=13, n=6 young mice +n=7 old mice). Microbiota sourced from old mice significantly increased paracellular permeability (Fig 6B). The age of the host did influence the development of paracellular permeability since young germ-free mice colonized with old microbiota had a greater increase in paracellular permability than old mice In contrast to the paracellular permeability, the age of the host contributed to levels of circulating TNF. (Fig 6D). Young GF mice that were colonized with old SPF microbiota had higher levels plasma TNF than those recolonized with young SPF microbiota (Fig 6E) indicating that the specific composition of the

aging microbial community contributes to age-associated inflammation but this is exentuatedin the old mice (Fig 6E). These data indicate that the composition of the aged microbiome is a stronger driver of intestinal permeability than the age of the host but that other age-related changes in the host predispose to systemic inflammation.

Age-associated inflammation contributes to susceptibility to *Streptococcus pneumoniae* infection (Puchta et al., 2016) (Antunes et al., 2002; Yende et al., 2005). To determine if age-related microbial dysbiosis alters responses to *S. pneumoniae,* young germ-free mice were colonized with young and old microbiota and intranasally colonized with *S. pneumoniae* . Although there was no difference in intranasal CFUs (Fig 6G), there was an increase in cellular inflammation as measured by $Ly6C^{high}$ inflammatory monocytes (Fig 6F), a response which we have previously shown becomes dysregulated with age (Puchta et al., 2016).

Age-associated inflammation drives microbial dysbiosis

Our data demonstrate that gut microbiota and/or age-related microbial dysbiosis can lead to increased gut permeability with age and result in age-associated inflammation. However, since expression of TNF, has been shown to increase intestinal permeability *in vitro*(Soderholm et al., 2004) , and anti-TNF treatment can alter intestinal permeability *in vivo*(Noth et al., 2012) we also considered the possibility that age-associated increases in TNF could exacerbate intestinal permeability and subsequent release of bacterial products. We hypothesised that if age-associated increases in TNF promoted increased intestinal permeability, old TNF KO mice would be protected and would not have higher levels of circulating bacterial components than young TNF KO mice. Consistent with this, intestinal barrier function in old TNF KO mice was equivalent to young TNF KO mice, young SPF WT mice and to young or old germ-free mice (Fig 6A) and circulating levels of MDP in these mice did not increase with age (Fig 6B) demonstrating a critical role for inflammation. Although TNF is proposed to alter permeability in epithelial barriers, the mechanism remains unclear. We hypothesized that TNF may be a driver of microbial dysbiosis. We therefore compared the extent to which the intestinal microbiota diverged in old TNF KO mice compared to young TNF KO mice, and contrasted this to the divergence observed in WT controls. In contrast to the clear divergence that occurs in WT mice with aging, TNF KO mice did indeed have less dramatic changes with aging and did not demonstrate clear separation between old and young intestinal microbiome (Fig 6C, Table 1). To further evaluate the potential of TNF to induce changes to the intestinal microbiome, young and old WT mice were treated with the anti-TNF drug Humira for 2 weeks, which reduced TNF levels in old mice to below the limit of detection (data not shown). Anti-TNF but not an IgG control altered the composition of the intestinal microbiota of old mice (Fig 7D) but had virtually no effect on the composition of the faecal microbiota of young mice, indicating that the microbiota can be manipulated by altering the inflammatory status of the host. Specific changes observed during anti-TNF treatment are described in Table 2. Despite altering microbiome, Humira had no measurable effect on intestinal permeability, as measured by translocation of FITC-dextran (data not shown), indicating that these changes to the composition of the intestinal microbiota were not a consequence of altered TNF levels having any direct effect on intestinal permeability. Although these experiments do not rule out a role for age-associated increases in TNF driving intestinal permeability by directly altering intestinal barrier function, they do demonstrate a critical role for TNF in the development of age-associated microbial dysbiosis, intestinal permeability and translocation of bacterial products to drive accelerated age-associated inflammation and impaired cellular antimicrobial function, a model for which is presented in Fig 8.

Discussion

Age-associated inflammation is a strong risk factor for overall mortality in this population. In fact, individuals having higher than age-average levels of inflammatory markers are more likely to be hospitalized(de Gonzalo-Calvo et al., 2012a), have higher all-cause mortality rates(Giovannini et al., 2011), be frail(Leng et al., 2007), be less independent(de Gonzalo-Calvo et al., 2012b) and are more likely to have a variety of late-life diseases(Artz et al., 2014; Bruunsgaard et al., 1999; Bruunsgaard et al., 2000; Ershler and Keller, 2000; Kuhlmann et al., 2013; Luciano et al., 2012; Nerpin et al., 2012).

Age-associated inflammation has also been shown to increase susceptibility to pneumococcal infection(Yende et al., 2013; Yende et al., 2005), and is associated with increased disease severity and decreased survival from pneumococcal infection in older adults(Antunes et al., 2002; Reade et al., 2009). Despite the clinical importance of age-associated inflammation, the etiological factors that lead to its development have not been identified. This study demonstrates *in vivo*, for the first time, that age-associated inflammation and microbial dysbiosis drive intestinal permeability and translocation of bacterial components, further fueling inflammation and impairing cellular antibacterial function. These data specifically implicate the critical importance of TNF and the gut microbiome, and highlight possible new strategies to address age-associated impairment of anti-bacterial immunity and increased overall mortality from pneumococcal infection in the elderly.

In humans transient endotoxemia occurs naturally after ingestion of high fat meals, vigorous exercise and in many diseases(Kelly et al., 2012). Microbial translocation has been shown to occur in HIV patients due to a loss of immune control at the gut mucosa and this translocation leads to a state of "immune activation" and systemic inflammation that is reminiscent of what is observed in normal aging(Brenchley et al., 2006). This increase in chronic inflammation correlates with early mortality, which is often due to premature development of "diseases of age" such as cardiovascular disease(Sandler et al., 2011). In simian models of HIV, translocation of bacterial products is a precursor of immune activation and macrophage dysfunction(Estes et al., 2010). In these models reducing levels of circulating LPS by chelation with the drug sevelamer prevents immune dysfunction, systemic inflammation and, most relevant to our study, reduces intestinal permeability implying that bacterial translocation is a driver of intestinal permeability, rather than a readout of intestinal damage(Kristoff et al., 2014). These data are consistent with our model in which both germ-free and TNF KO mice (which do not have increased levels of circulating bacterial products) are protected from age-associated inflammation. Unlike the germ-free mice, which are protected by virtue of not being exposed to bacteria, the TNF mice may be protected because they do not undergo microbial dysbiosis with age, which we demonstrate confers intestinal permeability (Fig 5E) and systemic inflammation in the context of the aged host (Fig 5D). This may be an evolutionarily conserved component of the aging process since intestinal permeability has been demonstrated to increase with age, to precede systemic inflammation and to be a marker of premature death in *Drosophila*(Rera et al., 2012).

Metchnikoff made careful observations that in acute inflammation macrophage-mediated phagocytosis seemed to be impaired. In examining autopsy samples of elderly brains he noticed tissue macrophages seemed to be associated with areas of damage and hypothesized that their presence might do more harm than good. He also observed that the integrity of the gut changed with age and concluded that "It is indubitable, therefore, that the intestinal microbes or their poisons may reach the system generally and bring harm to it."(Metchnikoff, 1907) He believed that this macrophage "intoxification" had systemic effects and led to deterioration of even distal tissues. Our observations are consistent with his as we observe an increase in circulating bacterial products as our WT mice age and evidence of systemic and distal inflammation. This systemic inflammation appears to have profound effects on macrophage function that begin during myelopoiesis as macrophages derived from bone marrow precursors in the absence of the aging microenvironment are also hyper-inflammatory and have poor killing capacity. Although Metchnikoff imagined that loss of macrophage function was a result of age-associated inflammation, he did not predict that they may also contribute to the global inflammatory state. In fact is appears as though both aged monocytes (Puchta et al., 2016) and macrophages (Mirsoian et al., 2014) contribute to chronic inflammation as their depletion reduces levels of inflammatory cytokines.

Consistent with our findings that the gut microbiota can also influence systemic (i.e. lung) inflammation and tissue damage, it has shown that increased circulating bacterial toxins result in reduced tight junction gene expression and lethal pulmonary damage following fecal transplantation(Ji et al., 2014). The authors suggest that these changes may occur following overgrowth of gut microbes and/or threshold production of bacterial products, resulting in their systemic translocation, increased

inflammation, and ensuing pulmonary endothelial damage. The bacterial taxa that were mainly implicated in this pathogenicity were members of Clostridia, which others have also demonstrated have distinct abundance patterns in the aging gut microbial community(Claesson et al., 2011; Claesson et al., 2012). Furthermore, some members of this group are known to produce toxins with pathogenic properties that can induce systemic inflammation (Solomon, 2013) and changes in permeability in both the intestinal mucosa(Goldstein et al., 2009)and alveolar endothelium(Geny et al., 2007). Whether enrichment or depletion of specific members of the Clostridia contributes to systemic inflammation or alterations in tissue permeability with age remains to be determined.

Although it has been suggested that changes in the microbiota might drive the ills of aging, determining cause and effect has been challenging. Numerous studies that have demonstrated that there are characteristic changes in gut microbial communities in elderly humans(Claesson et al., 2011; Makivuokko et al., 2010; Mariat et al., 2009; Zwielehner et al., 2009) and that these changes correlate with health status in the elderly population(Bartosch et al., 2004; Claesson et al., 2012). Furthermore, alterations of the gut microbiota appear to improve immune function in the elderly. For example, oral supplementation with *Bifidobacterium* increased lymphocyte proportions in the circulation, improved the anti-tumoricidal activity of natural killer cells and restored phagocytosis in peripheral blood mononuclear cells and neutrophils(Gill et al., 2001a; Gill et al., 2001b). Interestingly, these benefits were most strongly evident in individuals 70 years of age and older, as well as those individuals who demonstrated the greatest degree of cellular immunosenescence. Furthermore, dysbiosis in HIV patients, which shows many parallels to that which occurs in the elderly (including decreased *Bifidobacteria* frequency and increased clusters of *Clostridium*) has been shown to shift following prebiotic administration. This led to a decrease in the overall degree of microbial translocation and ultimately improved immune cell function(Gori et al., 2011). The microbial communities of the elderly gut appear to be strongly influenced by diet(Claesson et al., 2012) and dietary interventions designed to restore a robust microbiome may improve anti-bacterial immunity in the by reducing age-associated inflammation and macrophage immunosenescence.

Although manipulation of the microbiota may improve health in the elderly, until now it has not been clear whether microbial dysbiosis is a driver of immune dysfunction. For example it has been demonstrated that gut microbial composition correlates with levels of circulating cytokines and markers of health in the elderly(Claesson et al., 2012), but not whether the microbiome drives these changes. Our data demonstrate that microbial dysbiosis occurs with age, even in a minimal microbiota, and these changes are sufficient to promote age-associated inflammation. Interestingly there may be a causal relationship between age-associated inflammation and microbial dysbiosis since we found that TNF KO mice had a less divergent microbiome with age and treatment with anti-TNF altered the microbial communities of aged mice. Further experiments will need to be performed to determine if it is the loss of beneficial members of the microbial community, overgrowth of harmful members or a shift in metabolism that contributes to this phenomenon.

Metchnikoff had great faith that the appropriate controlled experiments could be performed to demonstrate that manipulation of the intestinal microbiome would extend life. Until that time he suggested "… those who wish to preserve their intelligence as long as possible and to make their cycle of life as complete and as normal as possible under present conditions, must depend on general sobriety and on habits conforming to the rules of rational hygiene." The experiments he envisioned remain to be performed, and until they are the only reliable ways to reduce age-associated inflammation, delay the onset of inflammatory diseases and prolong life are a sensible diet(Fontana and Hu, 2014; Fontana and Klein, 2007) and exercise (Lee et al., 1995). For those of us less inclined to live a lifestyle of "general sobriety", targeting age-associated inflammation may provide an attractive alternative.

Experimental Procedures

Animals

Female wild-type C57BL/6 mice (originally from Jackson Laboratories), were bred in house. To protect from age-related obesity, aging SPF mice (and corresponding young controls) are fed with a low protein diet Teklad Irradiated Global 14% protein Maintenance Diet and provided with an exercise wheel. The average weight of a young SPF mouse (8-14 wks) is this study is 20g+/-1g and the old SPF mice (18-22 mo) are on average, 27g+/-2.5g. The percent body fat for the young SPF/WT mice was (11.3%+/-2.5%) and for the old mice was (25%+/-4.4%). Pathogen-free status of mice within the aging colony was confirmed in mice through constitutive monitoring of sentinel mice and specific testing of fecal samples for common mouse pathogens. All of the animals that were used were sex-matched to their controls and maintained in the same animal room, with the exception of germ-free and ASF mice (all C57BL/6), which were bred in the Gnotobiotic Facility of McMaster. All mice were housed in pathogen-free conditions in accordance with Institutional Animal Utilization protocols approved by McMaster University's Animal Research Ethics Board as per the recommendations of the Canadian Council for Animal Care.

Adalimumab (HUMIRA, Abbott Laboratories), a humanized anti-TNF antibody, or the human IgG isotype control diluted in sterile saline were administered to mice. A dose of 40 ug per gram of body weight was given intraperitoneally in a volume of 200 µl every other day, for a period of 3 weeks to young and old WT mice.

Streptococcus pneumoniae (clinical isolate P1547, 1 x 10^7 CFUs) was added intranasally to un-anaesthetized mice as in(Puchta et al., 2014). Bacteria were enumerated and numbers of circulating monocytes were quantified as in (Puchta et al., 2016).

Histology

Histopathological analysis was carried out on samples from the lungs of old WT, TNF KO and germ-free mice, and their young controls. Upon collection, lungs were formalin-inflated and these, alongside formalin fixed spleens, were paraffin-embedded. Tissue blocks were cut into 5-µm sections that were stained with hematoxylin-eosin (HE). The slides were blinded/coded and the colon epithelial architecture and inflammation were histologically scored, as adapted from (1), using the following system: tissue architectural changes: 0, normal; 1, blebbing; 2, loss of epithelium; 3, complete loss of crypt architecture; and inflammation: 0, normal; 1, increased number of inflammatory cells in lamina propria; 2, increased number of inflammatory cells in submucosa; 3, dense inflammatory cell mass, but not transmural in nature; 4, transmural inflammation. The average score for all mice was 0 for both inflammation and epithelial cell architectural changes. Images were acquired with a Leica DM LB2 microscope at a magnification of 20X and captured using a Leica DFC 280 camera.

Measurement of cytokine production

For circulating levels of cytokines, blood samples from naive animals were collected into heparin, and spun at 15000 x *g* for 5 minutes. 100 µl of plasma was then collected, and IL6 levels assayed using ELISA as per the manufacturer's direction (eBioscience). To measure the TNF and IL6 cytokine concentrations within the plasma samples of the colonized germ-free mice, Milliplex immunoassay Kits were used and completed as recommended by the manufacturer's instructions (Millipore, Etobicoke, ON). For whole blood stimulation studies, 100 µl of whole blood samples collected in heparin from young and old WT, TNF KO and germ-free mice were stimulated with 100 ng/ml of LPS, or left unstimulated. Samples were incubated for 24 hours at 5% CO_2 and 37°C, then centrifuged at 15000 *x g* for 5 minutes. 50 µl of plasma samples were assayed for the presence of IL6 using ELISA. To measure constitutive levels IL6 in the lung, right lobe samples of lung were mechanically homogenized in 500 µl of PBS and assayed by ELISA. To measure inducible cytokine production in lung tissue, lungs were perfused with low melt agarose and sliced into 10 micron sections.. 3 slices were cultured in 1 ml of media for 24 hours; supernatants were then removed and assayed for IL6 production using 100 µl of sample ELISA. To measure cytokine production by bone marrow macrophages, 3.5 x 10^5 mature bone-marrow-derived macrophages were seeded in a 24-well tissue culture-grade plate (Fisher) in 1.5 ml of media and allowed

24 hours to recover. Cells were then stimulated with either 100 ng/ml of LPS, whole heat-killed P1547 at an MOI of 50 or 50 µl of media control. Supernatants were collected at 24 hours post-stimulation. Levels of TNF or IL6 were measured by ELISA.

Macrophage culture

Bone marrow derived-macrophages were isolated according to previously published methods(*60*) and differentiated in the presence of L929 conditioned media for 8 days as per standard protocols. After 8 days the cells were incubated with 4 mg/ml lidocaine (Sigma) for 15 minutes at 4°C and gently lifted using a cell lifter. Cells were then centrifuged, counted and re-suspended in medium at a concentration appropriate for measurement of cytokine production, bacterial uptake, flow cytometry or bacterial killing assays. Macrophage maturation was assessed by flow cytometry using APC-conjugated anti-F4/80, PE-conjugated anti-Ly6G or -CCR2, FITC-conjugated Ly6C, eFluor 450-conjugated CD45 and PE-Cy7-conjugated CD11b, or corresponding isotype controls. PRR expression was measured using anti-TLR4-FITC, anti-TLR2-PE-Cy7 and anti-CD14-PerCpCy5.5 (eBioscience), as well as anti-MARCO-PE (RND systems)

Bacterial killing assays

To measure macrophage killing of *S. pneumoniae,* 5 x 10^5 bone marrow derived macrophages were pre-incubated with an MOI of 10 bacteria per macrophage for 60 minutes at 37°C with gentle inversion as outlined above to allow for internalization of bacteria. Samples were then washed with PBS three times to remove unbound bacteria and bacterial killing was measured over the course of 120 min. The number of bacteria remaining after washing (t = 0 min) were normalized to 100%. At 30, 60, 90 and 120 min the macrophages were lysed by osmotic rupture in distilled H_2O for 15 min and viable CFUs were determined by culturing of supernatants on TS agar plates as described above. To visualize *S. pneumoniae* uptake by macrophages, TRITC labelled bacteria were incubated with bone marrow derived macrophages for 2h at an MOI of 200. Cells were fixed and stained using an anti-beta actin antibody (Cell Signaling). Images were acquired at 40X magnification using an inverted Zeiss LSM510 laser confocal microscope.

In vitro and in vivo permeability

Sections of colon and ileum were excised, opened along the mesenteric border, and mounted in Ussing chambers (World Precision Instruments, Sarasota, Florida). Recordings were performed as described in detail before(*61–63*). Briefly, tissues were allowed to equilibrate for 15-25 min before baseline values for potential difference (PD) and short circuit current (Isc) were recorded. Tissue conductance (G) was calculated by Ohm's law using the PD and Isc values. Mucosal to serosal flux of the small inert probe (360 Da) ^{51}-*chromium*-ethylenediaminetetraacetic acid (^{51}Cr-EDTA) was used to assess paracellular permeability. After equilibration, time zero samples were taken from the serosal buffer and 6µCi/ml ^{51}CR-EDTA was added to the mucosal compartment. A "hot sample" was taken from the mucosal buffer then samples were then taken every 30 minutes from the serosal buffer for 2 hours and counted in a liquid scintillation counter (Beckman). Counts from each 30 mins were averaged and compared to the "hot sample"(100%). Data expressed as mucosal-to-serosal flux (%flux/cm^2/hr). Each sample was completed in duplicates.

For non-terminal studies, tracer FITC-labeled dextran (4kDa; Sigma-Aldrich) was used to assess *in vivo* intestinal permeability. Mice were deprived of food 4 h prior to and both food and water 4 h following an oral gavage using 200 µl of 0.8 mg/ml FITC-dextran. Blood was retro-orbitally collected after 4 h, and fluorescence intensity was measured on fluorescence plates using an excitation wavelength of 493nm and an emission wavelength of 518 nm.

MDP Detection Bioassay

HEK293T cells stably were transfected with mNod2 (a kind gift from Dr. Jonathan Schertzer) and pNifty2-SEAP plasmids (Invivogen) to create a reporter system. Binding of the intracellular mNod2 receptor with its ligand, MDP, results in downstream activation and translocation of NF**κ**B. Activation of this transcription factor leads to SEAP expression via the ELAM proximal promoter, which is detected via

absorbance spectroscopy. Plates were seeded with cells 24 hours prior to addition of heat-inactivated mouse plasma, diluted 1 in 200 in HEK Blue Detection Media (Invivogen) to a final volume of 200 µl, in a 96-well plate format. Readings were performed at 630nm, 24 hours subsequent to stimulation.

Germ-free Mouse Recolonization

For recolonization studies, young and old germ-free mice were transferred to individually ventilated racks and co-housed with either a young or old mouse. The mice were left undisturbed for two week following the start of the colonization and then maintained for a minimum of 6 weeks at which point fecal pellets were collected for microbiome analysis (as described below), plasma cytokines were assayed and intestinal permeability was measured as described above.

Bacterial profiling by deep sequencing analysis of 16S rRNA with Illumina

Fecal pellets were collected and the V3 region of the 16S rRNA gene was amplified by PCR as in (Bartram et al., 2011; Stearns et al., 2015; Whelan et al., 2014). Briefly, each 50 µl PCR reaction mixture contained 1.5 mM of $MgCl_2$ (50mM), 200 µM dNTPs, 4 mM of BSA, 25 pmol of each primer, 1U of Taq polymerase (Life Technologies), and 200 ng of DNA. The reaction was then run for 30 cycles (94°C for 2 minutes, 94°C for 30 seconds, 50°C for 30°C, 72°C for 30 seconds), with a final polymerization step at 72°C for 10 minutes (Eppendorf). The products were separated by electrophoresis in 2% agarose gel, and visualized under a UV transilluminator and the products corresponding to the amplified V3 region (~300 base pairs) were excised and purified using standard gel extraction kits (Qiagen). Illumina sequencing and initial quality control were carried out by the MOBIX - McMaster Genome Center (McMaster University). Custom, in-house Perl scripts were developed to process the sequences after Illumina sequencing(Whelan et al., 2014). Briefly, Cutadapt was used to trim the forward and reverse paired-end reads at the opposing primers for input into PANDAseq for assembly (Martin, 2011) (Masella et al., 2012). Mismatches and ambiguous base attributions in the assembly from specific set of paired - end sequences were discarded. Operational taxonomic units (OTUs) were picked using AbundantOTU+ and taxonomy - assigned using the Ribosomal Database Project (RDP) classifier against the Greengenes reference database (Ye, 2011). Single sequence OTUs (singletons) were removed prior to all analyses using Quantitative Insights into Microbial Ecology (QIIME) (Caporaso et al., 2010).

Statistics

Unless otherwise mentioned in the figure legend, statistical significance was determined by two-way analysis of variance with Fischer's post-test and unpaired *t* tests (two tailed). Statistical significance was defined as a *p* value of 0.05. All data were analyzed with Prism (Version 6; GraphPad). Microbiome changes were analyzed with Quantitative Insights into Microbial Ecology (QIIME) software using principal component analysis as measured by Bray-Curtis. The Chi-squared of the likelihood ratio test in phyloseq DESeq2 was used to determine differences between groups as in (McMurdie and Holmes, 2013). Differences between specific OTUs were determined using Welch's unequal variances *t*-test.

Author contributions: AP, NT, DJD, MGS, EFV, DMEB designed the experiments. AP, NT, AN, CPV, JJ performed experiments. AP, NT, AN, CPV, JCS, EV, MS, DMEB analyzed the data. MJL provided reagents and expertise. AP, NT, DJD, MGS, DMEB wrote the manuscript.

Acknowledgements: AP was supported by an Ontario Graduate Scholarship. CPV was supported by a fellowship from the Canadian Thoracic Society. AN was supported by a scholarship from the CIHR. NT was supported by an Early Researcher Award from the Ontario Ministry of Research and Innovation. This work was funded by grants from the Canadian Institutes of Health Research (CIHR) to DMEB. EFV is

supported by CIHR (MOP 123282). EV, MGS and DMEB are supported by the CIHR and hold Canada Research Chairs. Work in the Bowdish laboratory is supported by the McMaster Immunology Research Centre (MIRC) and the M.G. DeGroote Institute for Infectious Disease Research (IIDR). DJD is an MRC Senior Research Fellow (G1002046). The authors would like to thank Kate Manners, and Laura Rossi for isolation and preparation of DNA for microbiome analysis..

References

Antunes, G., S.A. Evans, J.L. Lordan, and A.J. Frew. 2002. Systemic cytokine levels in community-acquired pneumonia and their association with disease severity. *Eur Respir J* 20:990-995.

Appay, V., J.R. Almeida, D. Sauce, B. Autran, and L. Papagno. 2007. Accelerated immune senescence and HIV-1 infection. *Exp Gerontol* 42:432-437.

Artz, A.S., Q.L. Xue, A. Wickrema, C. Hesdorffer, L. Ferrucci, J.M. Langdon, J.D. Walston, and C.N. Roy. 2014. Unexplained anaemia in the elderly is characterised by features of low grade inflammation. *Br J Haematol* 167:286-289.

Bartosch, S., A. Fite, G.T. Macfarlane, and M.E. McMurdo. 2004. Characterization of bacterial communities in feces from healthy elderly volunteers and hospitalized elderly patients by using real-time PCR and effects of antibiotic treatment on the fecal microbiota. *Appl Environ Microbiol* 70:3575-3581.

Bartram, A.K., M.D. Lynch, J.C. Stearns, G. Moreno-Hagelsieb, and J.D. Neufeld. 2011. Generation of multimillion-sequence 16S rRNA gene libraries from complex microbial communities by assembling paired-end illumina reads. *Appl Environ Microbiol* 77:3846-3852.

Biagi, E., L. Nylund, M. Candela, R. Ostan, L. Bucci, E. Pini, J. Nikkila, D. Monti, R. Satokari, C. Franceschi, P. Brigidi, and W. De Vos. 2010. Through ageing, and beyond: gut microbiota and inflammatory status in seniors and centenarians. *PLoS One* 5:e10667.

Bouchlaka, M.N., G.D. Sckisel, M. Chen, A. Mirsoian, A.E. Zamora, E. Maverakis, D.E. Wilkins, K.L. Alderson, H.H. Hsiao, J.M. Weiss, A.M. Monjazeb, C. Hesdorffer, L. Ferrucci, D.L. Longo, B.R. Blazar, R.H. Wiltrout, D. Redelman, D.D. Taub, and W.J. Murphy. 2013. Aging predisposes to acute inflammatory induced pathology after tumor immunotherapy. *J Exp Med* 210:2223-2237.

Brenchley, J.M., D.A. Price, T.W. Schacker, T.E. Asher, G. Silvestri, S. Rao, Z. Kazzaz, E. Bornstein, O. Lambotte, D. Altmann, B.R. Blazar, B. Rodriguez, L. Teixeira-Johnson, A. Landay, J.N. Martin, F.M. Hecht, L.J. Picker, M.M. Lederman, S.G. Deeks, and D.C. Douek. 2006. Microbial translocation is a cause of systemic immune activation in chronic HIV infection. *Nat Med* 12:1365-1371.

Bruunsgaard, H., K. Andersen-Ranberg, B. Jeune, A.N. Pedersen, P. Skinhoj, and B.K. Pedersen. 1999. A high plasma concentration of TNF-alpha is associated with dementia in centenarians. *J Gerontol A Biol Sci Med Sci* 54:M357-364.

Bruunsgaard, H., P. Skinhoj, A.N. Pedersen, M. Schroll, and B.K. Pedersen. 2000. Ageing, tumour necrosis factor-alpha (TNF-alpha) and atherosclerosis. *Clin Exp Immunol* 121:255-260.

Caporaso, J.G., J. Kuczynski, J. Stombaugh, K. Bittinger, F.D. Bushman, E.K. Costello, N. Fierer, A.G. Pena, J.K. Goodrich, J.I. Gordon, G.A. Huttley, S.T. Kelley, D. Knights, J.E. Koenig, R.E. Ley, C.A. Lozupone, D. McDonald, B.D. Muegge, M. Pirrung, J. Reeder, J.R. Sevinsky, P.J. Turnbaugh, W.A. Walters, J. Widmann, T. Yatsunenko, J. Zaneveld, and R. Knight. 2010. QIIME allows analysis of high-throughput community sequencing data. *Nat Methods* 7:335-336.

Claesson, M.J., S. Cusack, O. O'Sullivan, R. Greene-Diniz, H. de Weerd, E. Flannery, J.R. Marchesi, D. Falush, T. Dinan, G. Fitzgerald, C. Stanton, D. van Sinderen, M. O'Connor, N. Harnedy, K. O'Connor, C. Henry, D. O'Mahony, A.P. Fitzgerald, F. Shanahan, C. Twomey, C. Hill, R.P. Ross, and P.W. O'Toole. 2011. Composition, variability, and temporal stability of the intestinal microbiota of the elderly. *Proc Natl Acad Sci U S A* 108 Suppl 1:4586-4591.

Claesson, M.J., I.B. Jeffery, S. Conde, S.E. Power, E.M. O'Connor, S. Cusack, H.M. Harris, M. Coakley, B. Lakshminarayanan, O. O'Sullivan, G.F. Fitzgerald, J. Deane, M. O'Connor, N. Harnedy, K. O'Connor, D. O'Mahony, D. van Sinderen, M. Wallace, L. Brennan, C. Stanton, J.R. Marchesi, A.P. Fitzgerald, F. Shanahan, C. Hill, R.P. Ross, and P.W. O'Toole. 2012. Gut

555 microbiota composition correlates with diet and health in the elderly. *Nature* 488:178-184.
556 Cryan, J.F., and T.G. Dinan. 2012. Mind-altering microorganisms: the impact of the gut microbiota on
557 brain and behaviour. *Nat Rev Neurosci* 13:701-712.
558 de Gonzalo-Calvo, D., B. de Luxan-Delgado, P. Martinez-Camblor, S. Rodriguez-Gonzalez, M.
559 Garcia-Macia, F.M. Suarez, J.J. Solano, M.J. Rodriguez-Colunga, and A. Coto-Montes. 2012a.
560 Chronic inflammation as predictor of 1-year hospitalization and mortality in elderly population.
561 *Eur J Clin Invest* 42:1037-1046.
562 de Gonzalo-Calvo, D., B. de Luxan-Delgado, S. Rodriguez-Gonzalez, M. Garcia-Macia, F.M. Suarez,
563 J.J. Solano, M.J. Rodriguez-Colunga, and A. Coto-Montes. 2012b. Interleukin 6, soluble tumor
564 necrosis factor receptor I and red blood cell distribution width as biological markers of
565 functional dependence in an elderly population: a translational approach. *Cytokine* 58:193-198.
566 Ershler, W.B., and E.T. Keller. 2000. Age-associated increased interleukin-6 gene expression, late-life
567 diseases, and frailty. *Annu Rev Med* 51:245-270.
568 Estes, J.D., L.D. Harris, N.R. Klatt, B. Tabb, S. Pittaluga, M. Paiardini, G.R. Barclay, J. Smedley, R.
569 Pung, K.M. Oliveira, V.M. Hirsch, G. Silvestri, D.C. Douek, C.J. Miller, A.T. Haase, J. Lifson,
570 and J.M. Brenchley. 2010. Damaged intestinal epithelial integrity linked to microbial
571 translocation in pathogenic simian immunodeficiency virus infections. *PLoS Pathog*
572 6:e1001052.
573 Fontana, L., and F.B. Hu. 2014. Optimal body weight for health and longevity: bridging basic, clinical,
574 and population research. *Aging Cell* 13:391-400.
575 Fontana, L., and S. Klein. 2007. Aging, adiposity, and calorie restriction. *JAMA* 297:986-994.
576 Franceschi, C., M. Bonafe, S. Valensin, F. Olivieri, M. De Luca, E. Ottaviani, and G. De Benedictis.
577 2000. Inflamm-aging. An evolutionary perspective on immunosenescence. *Ann N Y Acad Sci*
578 908:244-254.
579 Franceschi, C., and J. Campisi. 2014. Chronic inflammation (inflammaging) and its potential
580 contribution to age-associated diseases. *J Gerontol A Biol Sci Med Sci* 69 Suppl 1:S4-9.
581 Franceschi, C., M. Capri, D. Monti, S. Giunta, F. Olivieri, F. Sevini, M.P. Panourgia, L. Invidia, L.
582 Celani, M. Scurti, E. Cevenini, G.C. Castellani, and S. Salvioli. 2007. Inflammaging and anti-
583 inflammaging: a systemic perspective on aging and longevity emerged from studies in humans.
584 *Mech Ageing Dev* 128:92-105.
585 Geny, B., H. Khun, C. Fitting, L. Zarantonelli, C. Mazuet, N. Cayet, M. Szatanik, M.C. Prevost, J.M.
586 Cavaillon, M. Huerre, and M.R. Popoff. 2007. Clostridium sordellii lethal toxin kills mice by
587 inducing a major increase in lung vascular permeability. *Am J Pathol* 170:1003-1017.
588 Gevers, D., R. Knight, J.F. Petrosino, K. Huang, A.L. McGuire, B.W. Birren, K.E. Nelson, O. White,
589 B.A. Methe, and C. Huttenhower. 2012. The Human Microbiome Project: a community
590 resource for the healthy human microbiome. *PLoS Biol* 10:e1001377.
591 Gill, H.S., K.J. Rutherfurd, and M.L. Cross. 2001a. Dietary probiotic supplementation enhances natural
592 killer cell activity in the elderly: an investigation of age-related immunological changes. *J Clin*
593 *Immunol* 21:264-271.
594 Gill, H.S., K.J. Rutherfurd, M.L. Cross, and P.K. Gopal. 2001b. Enhancement of immunity in the
595 elderly by dietary supplementation with the probiotic Bifidobacterium lactis HN019. *Am J Clin*
596 *Nutr* 74:833-839.
597 Giovannini, S., G. Onder, R. Liperoti, A. Russo, C. Carter, E. Capoluongo, M. Pahor, R. Bernabei, and
598 F. Landi. 2011. Interleukin-6, C-reactive protein, and tumor necrosis factor-alpha as predictors
599 of mortality in frail, community-living elderly individuals. *J Am Geriatr Soc* 59:1679-1685.
600 Goldstein, J., W.E. Morris, C.F. Loidl, C. Tironi-Farinati, B.A. McClane, F.A. Uzal, and M.E.
601 Fernandez Miyakawa. 2009. Clostridium perfringens epsilon toxin increases the small intestinal
602 permeability in mice and rats. *PLoS One* 4:e7065.
603 Gordon, H.A., and L. Pesti. 1971. The gnotobiotic animal as a tool in the study of host microbial

relationships. *Bacteriol Rev* 35:390-429.
Gori, A., G. Rizzardini, B. Van't Land, K.B. Amor, J. van Schaik, C. Torti, T. Quirino, C. Tincati, A. Bandera, J. Knol, K. Benlhassan-Chahour, D. Trabattoni, D. Bray, A. Vriesema, G. Welling, J. Garssen, and M. Clerici. 2011. Specific prebiotics modulate gut microbiota and immune activation in HAART-naive HIV-infected adults: results of the "COPA" pilot randomized trial. *Mucosal Immunol* 4:554-563.
Guigoz, Y., J. Dore, and E.J. Schiffrin. 2008. The inflammatory status of old age can be nurtured from the intestinal environment. *Curr Opin Clin Nutr Metab Care* 11:13-20.
Hinojosa, E., A.R. Boyd, and C.J. Orihuela. 2009. Age-associated inflammation and toll-like receptor dysfunction prime the lungs for pneumococcal pneumonia. *J Infect Dis* 200:546-554.
Ji, Y., S. Sun, J.K. Goodrich, H. Kim, A.C. Poole, G.E. Duhamel, R.E. Ley, and L. Qi. 2014. Diet-induced alterations in gut microflora contribute to lethal pulmonary damage in TLR2/TLR4-deficient mice. *Cell Rep* 8:137-149.
Kelly, C.J., S.P. Colgan, and D.N. Frank. 2012. Of microbes and meals: the health consequences of dietary endotoxemia. *Nutr Clin Pract* 27:215-225.
Kristoff, J., G. Haret-Richter, D. Ma, R.M. Ribeiro, C. Xu, E. Cornell, J.L. Stock, T. He, A.D. Mobley, S. Ross, A. Trichel, C. Wilson, R. Tracy, A. Landay, C. Apetrei, and I. Pandrea. 2014. Early microbial translocation blockade reduces SIV-mediated inflammation and viral replication. *J Clin Invest* 124:2802-2806.
Kuhlmann, A., I.S. Olafsdottir, L. Lind, J. Sundstrom, and C. Janson. 2013. Association of biomarkers of inflammation and cell adhesion with lung function in the elderly: a population-based study. *BMC Geriatr* 13:82.
Lee, I.M., C.C. Hsieh, and R.S. Paffenbarger, Jr. 1995. Exercise intensity and longevity in men. The Harvard Alumni Health Study. *JAMA* 273:1179-1184.
Leng, S.X., Q.L. Xue, J. Tian, J.D. Walston, and L.P. Fried. 2007. Inflammation and frailty in older women. *J Am Geriatr Soc* 55:864-871.
Luciano, M., R. Mottus, J.M. Starr, G. McNeill, X. Jia, L.C. Craig, and I.J. Deary. 2012. Depressive symptoms and diet: their effects on prospective inflammation levels in the elderly. *Brain Behav Immun* 26:717-720.
Makivuokko, H., K. Tiihonen, S. Tynkkynen, L. Paulin, and N. Rautonen. 2010. The effect of age and non-steroidal anti-inflammatory drugs on human intestinal microbiota composition. *Br J Nutr* 103:227-234.
Mariat, D., O. Firmesse, F. Levenez, V. Guimaraes, H. Sokol, J. Dore, G. Corthier, and J.P. Furet. 2009. The Firmicutes/Bacteroidetes ratio of the human microbiota changes with age. *BMC Microbiol* 9:123.
Martin, M. 2011. Cutadapt removes adapter sequences from high-throughput sequencing reads. *2011* 17:
Masella, A.P., A.K. Bartram, J.M. Truszkowski, D.G. Brown, and J.D. Neufeld. 2012. PANDAseq: paired-end assembler for illumina sequences. *BMC Bioinformatics* 13:1-7.
McMurdie, P.J., and S. Holmes. 2013. phyloseq: an R package for reproducible interactive analysis and graphics of microbiome census data. *PLoS One* 8:e61217.
Metchnikoff, E. 1907. The Prolongation of Life: Optimistic Studies. G. P. Putnam's Sons
Mirsoian, A., M.N. Bouchlaka, G.D. Sckisel, M. Chen, C.C. Pai, E. Maverakis, R.G. Spencer, K.W. Fishbein, S. Siddiqui, A.M. Monjazeb, B. Martin, S. Maudsley, C. Hesdorffer, L. Ferrucci, D.L. Longo, B.R. Blazar, R.H. Wiltrout, D.D. Taub, and W.J. Murphy. 2014. Adiposity induces lethal cytokine storm after systemic administration of stimulatory immunotherapy regimens in aged mice. *J Exp Med* 211:2373-2383.
Nerpin, E., J. Helmersson-Karlqvist, U. Riserus, J. Sundstrom, A. Larsson, E. Jobs, S. Basu, E. Ingelsson, and J. Arnlov. 2012. Inflammation, oxidative stress, glomerular filtration rate, and

albuminuria in elderly men: a cross-sectional study. *BMC Res Notes* 5:537.
Noth, R., E. Stuber, R. Hasler, S. Nikolaus, T. Kuhbacher, J. Hampe, B. Bewig, S. Schreiber, and A. Arlt. 2012. Anti-TNF-alpha antibodies improve intestinal barrier function in Crohn's disease. *J Crohns Colitis* 6:464-469.
Puchta, A., A. Naidoo, C.P. Verschoor, D. Loukov, N. Thevaranjan, T.S. Mandur, P.S. Nguyen, M. Jordana, M. Loeb, Z. Xing, L. Kobzik, M.J. Larche, and D.M. Bowdish. 2016. TNF Drives Monocyte Dysfunction with Age and Results in Impaired Anti-pneumococcal Immunity. *PLoS Pathog* 12:e1005368.
Puchta, A., C.P. Verschoor, T. Thurn, and D.M. Bowdish. 2014. Characterization of inflammatory responses during intranasal colonization with Streptococcus pneumoniae. *J Vis Exp* e50490.
Reade, M.C., S. Yende, G. D'Angelo, L. Kong, J.A. Kellum, A.E. Barnato, E.B. Milbrandt, C. Dooley, F.B. Mayr, L. Weissfeld, and D.C. Angus. 2009. Differences in immune response may explain lower survival among older men with pneumonia. *Crit Care Med* 37:1655-1662.
Rera, M., R.I. Clark, and D.W. Walker. 2012. Intestinal barrier dysfunction links metabolic and inflammatory markers of aging to death in Drosophila. *Proc Natl Acad Sci U S A* 109:21528-21533.
Sandler, N.G., H. Wand, A. Roque, M. Law, M.C. Nason, D.E. Nixon, C. Pedersen, K. Ruxrungtham, S.R. Lewin, S. Emery, J.D. Neaton, J.M. Brenchley, S.G. Deeks, I. Sereti, and D.C. Douek. 2011. Plasma levels of soluble CD14 independently predict mortality in HIV infection. *J Infect Dis* 203:780-790.
Slack, E., S. Hapfelmeier, B. Stecher, Y. Velykoredko, M. Stoel, M.A. Lawson, M.B. Geuking, B. Beutler, T.F. Tedder, W.D. Hardt, P. Bercik, E.F. Verdu, K.D. McCoy, and A.J. Macpherson. 2009. Innate and adaptive immunity cooperate flexibly to maintain host-microbiota mutualism. *Science* 325:617-620.
Snyder, D.L., M. Pollard, B.S. Wostmann, and P. Luckert. 1990. Life span, morphology, and pathology of diet-restricted germ-free and conventional Lobund-Wistar rats. *J Gerontol* 45:B52-58.
Soderholm, J.D., C. Streutker, P.C. Yang, C. Paterson, P.K. Singh, D.M. McKay, P.M. Sherman, K. Croitoru, and M.H. Perdue. 2004. Increased epithelial uptake of protein antigens in the ileum of Crohn's disease mediated by tumour necrosis factor alpha. *Gut* 53:1817-1824.
Solomon, K. 2013. The host immune response to Clostridium difficile infection. *Ther Adv Infect Dis* 1:19-35.
Stearns, J.C., C.J. Davidson, S. McKeon, F.J. Whelan, M.E. Fontes, A.B. Schryvers, D.M. Bowdish, J.D. Kellner, and M.G. Surette. 2015. Culture and molecular-based profiles show shifts in bacterial communities of the upper respiratory tract that occur with age. *ISME J* 9:1246-1259.
Whelan, F.J., C.P. Verschoor, J.C. Stearns, L. Rossi, K. Luinstra, M. Loeb, M. Smieja, J. Johnstone, M.G. Surette, and D.M. Bowdish. 2014. The loss of topography in the microbial communities of the upper respiratory tract in the elderly. *Ann Am Thorac Soc* 11:513-521.
Yende, S., K. Alvarez, L. Loehr, A.R. Folsom, A.B. Newman, L.A. Weissfeld, R.G. Wunderink, S.B. Kritchevsky, K.J. Mukamal, S.J. London, T.B. Harris, D.C. Bauer, and D.C. Angus. 2013. Epidemiology and long-term clinical and biologic risk factors for pneumonia in community-dwelling older Americans: analysis of three cohorts. *Chest* 144:1008-1017.
Yende, S., E.I. Tuomanen, R. Wunderink, A. Kanaya, A.B. Newman, T. Harris, N. de Rekeneire, and S.B. Kritchevsky. 2005. Preinfection systemic inflammatory markers and risk of hospitalization due to pneumonia. *Am J Respir Crit Care Med* 172:1440-1446.
Zwielehner, J., K. Liszt, M. Handschur, C. Lassl, A. Lapin, and A.G. Haslberger. 2009. Combined PCR-DGGE fingerprinting and quantitative-PCR indicates shifts in fecal population sizes and diversity of Bacteroides, bifidobacteria and Clostridium cluster IV in institutionalized elderly. *Exp Gerontol* 44:440-446.

Tables:

Table 1. OTUs that were significantly changed in old SPF and TNF KO mice

Increased

Family	Genus	# of OTUs (WT)	Old>Young (WT)	Old>Young (TNF KO)	# of OTUs (TNF KO)
Ruminococcaceae	*Ruminococcus*	6	****	NS	7
Lachnospiraceae	*Clostridium*	34	****	a **	34
Ruminococcaceae	*Clostridium*	14	****	NS	16
Prevotellaceae	*Prevotella*	39	**	**	44
Erysipelotrichaceae	*Allobaculum*	54	****	*	60
Lachnospiraceae	Many identified	354	*	a *	343
Bifidobacteriaceae	*Bifidobacterium*	17	***	**	17
Ruminococcaceae	*Oscillospira*	54	****	NS	56
Lactobacillaceae	*Lactobacillus*	53	***	a****	57
Bacteroidaceae	*Bacteroides*	52	**	***	71
Coriobacteriaceae	*Adlercreutzia*	22	***	NS	23
Peptococcaceae	Not identified	14	*	NS	15
Catabacteriaceae	Not identified	51	****	a**	65
Coriobacteriaceae	Not identified	14	***	NS	14

[a]OTUs that were significantly decreased in Old TNF KO mice are underlined

Decreased

Family	Genus	# of OTUs (WT)	Old<Young (WT)	Old<Young (TNF KO)	# of OTUs (TNF KO)
Rikenellaceae	*Alistipes*	48	**	NS	52
Verrucomicrobiaceae	*Akkermansia*	41	****	[b] *	49
Lachnospiraceae	*Blautia*	11	****	[b]*	10

[b]OTUs that were significantly increased in OLD TNF KO mice are underlined

707

708 Table 2: OTUs altered by anti-TNF treatment in old mice

Family	Genus	Old>Young	Decreased by anti-TNF treatment
Erysipelotrichaceae	Not identified	****	NS
Ruminococcaceae	*Ruminococcus*	****	NS
Lachnospiraceae	*Clostridium*	****	NS
Ruminococcaceae	*Clostridium*	****	NS
Prevotellaceae	*Prevotella*	**	NS
Erysipelotrichaceae	*Allobaculum*	****	NS
Lachnospiraceae	Many identified	*	NS
Bifidobacteriaceae	*Bifidobacterium*	***	NS
Ruminococcaceae	*Oscillospira*	****	NS
Lactobacillaceae	*Lactobacillus*	***	NS
Bacteroidaceae	*Bacteroides*	**	*
Coriobacteriaceae	*Adlercreutzia*	***	*
Peptococcaceae	Not identified	*	**
Catabacteriaceae	Not identified	****	* (Increased)
Coriobacteriaceae	Not identified	***	*
Ruminococcaceae	*Subdoligranulum*	NS	*

Decreased

Family	Genus	Old<Young	Increased by anti-TNF treatment
Rikenellaceae	*Alistipes*	**	NS
Verrucomicrobiaceae	*Akkermansia*	****	NS
Lachnospiraceae	*Blautia*	****	NS
Lachnospiraceae	*Roseburia*	NS	*
Eubacteriaceae	*Anaerofustis*	NS	*

709

710

Figures

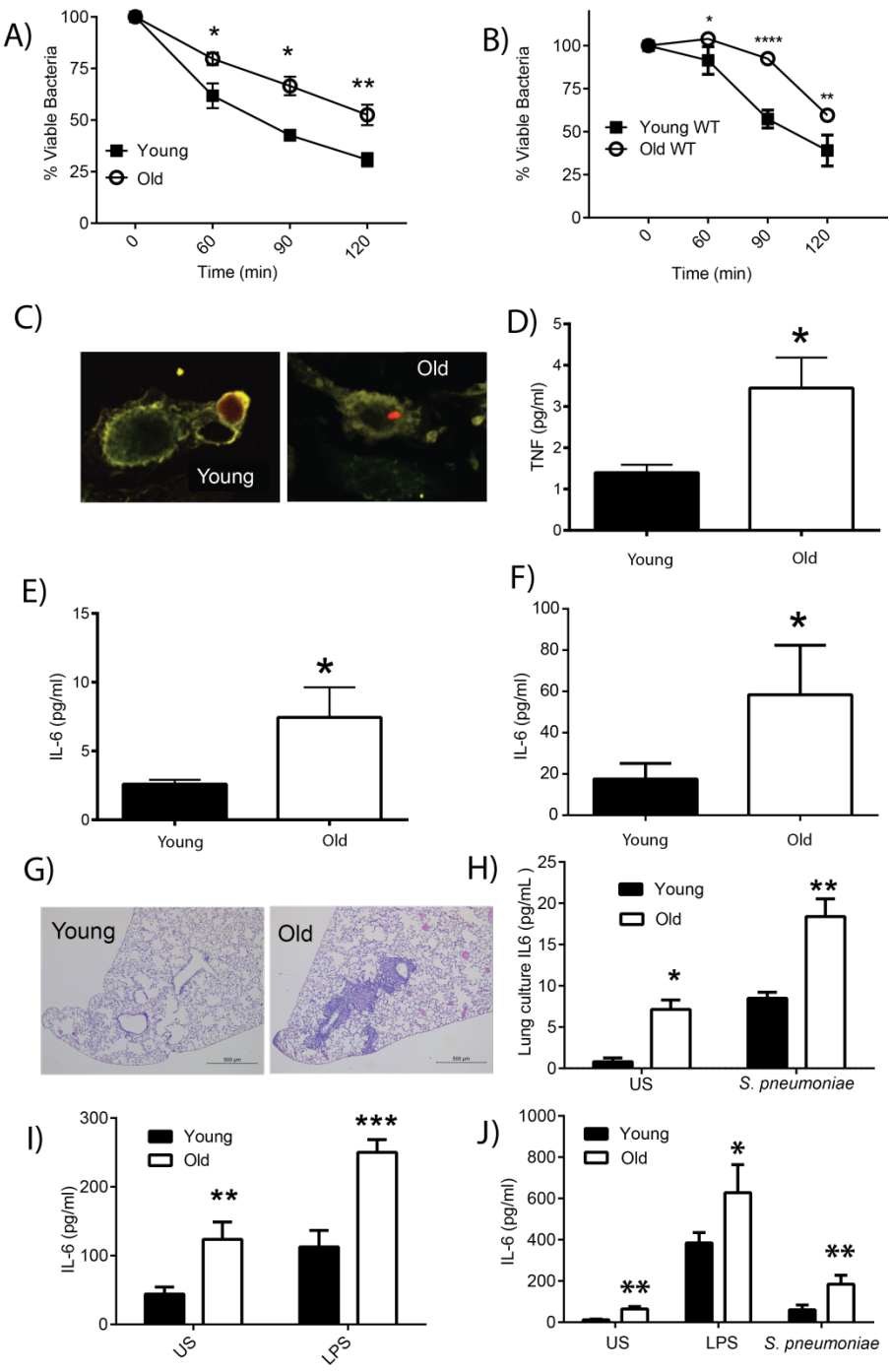

Figure 1. Hyper-inflammatory responses occur with age. A) Killing of *S. pneumoniae* by resident peritoneal macrophages isolated from young and old mice (n = 5). (**B**) Killing of *S. pneumoniae* by bone-marrow derived macrophages from young and old C57Bl/6 mice (n = 6). (C) Intact TRITC-labelled *S. pneumoniae* was observed in macrophages derived from old mice but not young up to 4 hours post infection. Levels of TNF (**D**) and IL6**(E)** were higher in the plasma of old mice as was (**F**) IL6 in slices of whole lung homogenates from old mice (**G**) H&E stain of formalin-fixed histological sections from the lungs of young and old WT mice at 5X magnification. One representative image is at least 5 biological replicates. (**H**) Lung slices were processed from the lungs of young and old mice and cultured in media. IL6 production was subsequently measured in the supernatant at 4 hours following stimulation with heat-

killed *S. pneumoniae* or PBS control (n = 3, representative of 2 independent experiments). (**I**) IL6 production in the whole blood of young and old WT mice following stimulation with LPS or a vehicle control (PBS)(n = 5 to 9). **(J)** IL6 production from macrophages derived from young and old mice following 24-hour stimulation with a vehicle control (PBS), LPS, or *S. pneumoniae* as measured by ELISA (n = 6). Results represent mean ± SEM. Statistical significance was determined using the Mann-Whitney test or two-way ANOVA with Fisher's post-test where appropriate. $p < 0.05$ is indicated by *; $p < 0.005$ by ** and $p < 0.0005$ by ***.

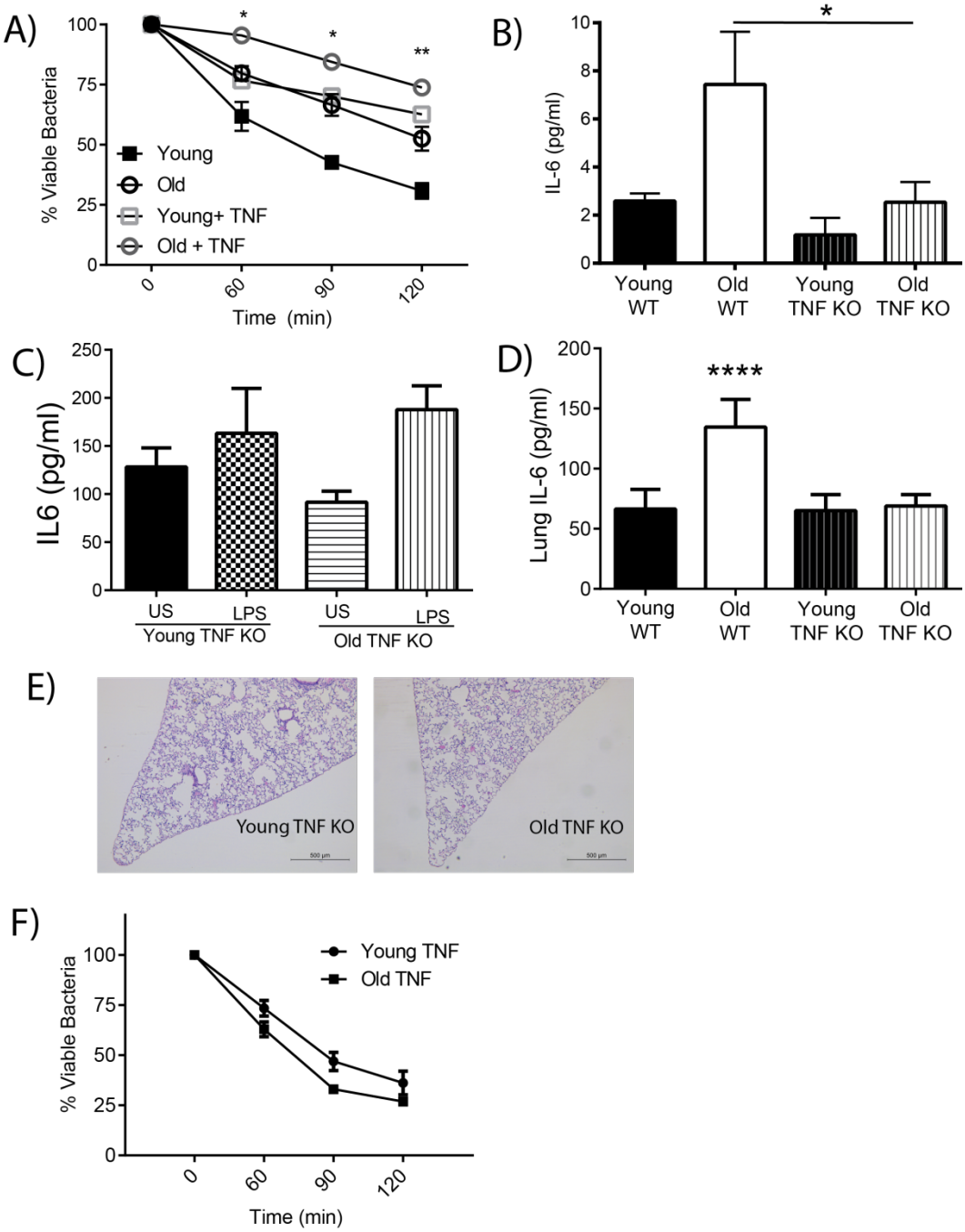

Figure 2. Chronic exposure to TNF contributes to hyper-inflammatory responses and tissue damage that occur with age. A) Young and old murine bone marrow macrophage-mediated killing of *S. pneumoniae* is decreased in the presence of 10 ng/ml of exogenous TNF (n = 5). **(B)** Unlike old WT mice, old TNF KO mice do not have increased levels of plasma IL6 (n=3-10 mice per group, one of two independent experiments shown) **(C)** IL6 production in the whole blood of young and old TNF KO mice

following stimulation with LPS or a vehicle control (PBS) demonstrates that old TNF KO mice do not have hyper-inflammatory responses to LPS(n = 5). (**D**) IL6 levels as detected by ELISA in whole lung tissue homogenates were no higher in old TNF KO mice than young TNF mice (n=3). (**E**) H&E stain of formalin-fixed histological sections of lungs of young and old TNF KO mice (20X magnification, one representative of 3). (**F**) Bone marrow derived macrophages from young and old TNF KO mice do not differ in their ability to kill *S. pneumoniae* (n = 5). Results represent pooled data and are shown as mean ± SEM. Statistical significance was determined using the Mann-Whitney test or two-way ANOVA with Fisher's post-test where appropriate. $p < 0.05$ is indicated by *; $p < 0.005$ by ** and $p < 0.0005$ by ***.

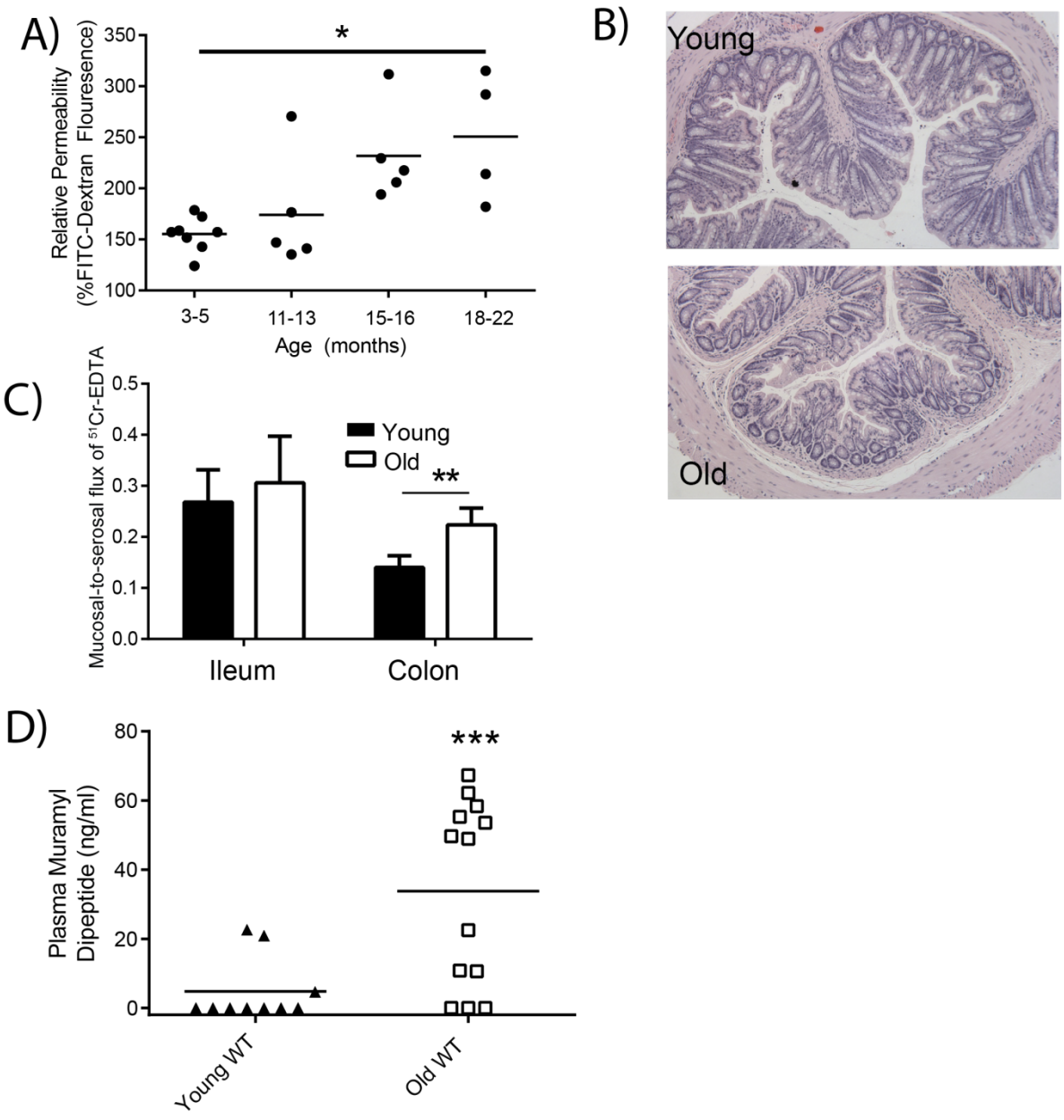

Figure 3. Old mice have more permeable colons and increased levels of bacterial products in the circulation. (**A**) Intestinal permeability of aging mice (3, 12, 15 and 18 months old) as measured by FITC-dextran translocation to the circulation following oral gavage (n = 4-8) and was found to increase significantly with age ($p<0.007$, one way ANOVA). **(B)** Colons of young and old mice do not have detectable changes in either epithelial architecture or inflammatory infiltrate when measured as described in the Materials and Methods. (**C**) Mucosal-to-serosal flux of ^{51}Cr-EDTA as measured in Ussing chambers was used to measure the paracellular permeability of ileums and colons from young and old WT

mice (n = 6 to 12). (**D)** Circulating muramyl dipeptide (MDP) in the plasma of young and old WT mice as measured by NOD-NF-κB promotor bioassay. Significant changes shown are relative to young WT mice. Statistical significance was determined using the Mann-Whitney test or two-way ANOVA with Fisher's post-test where appropriate. $p < 0.05$ is indicated by *; $p < 0.005$ by ** and $p < 0.0005$ by ***.

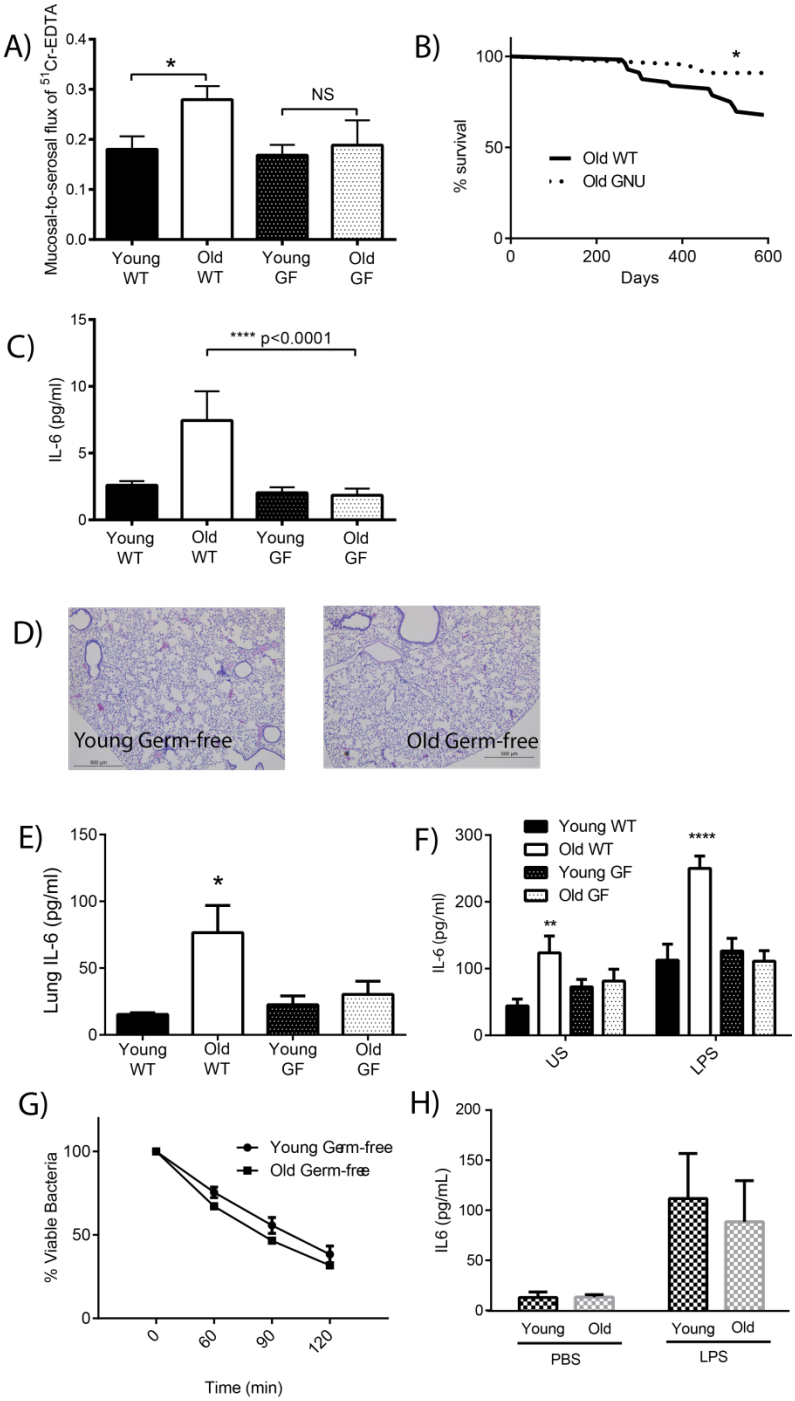

Figure 4. Germ-free mice do not develop age-associated inflammation or macrophage defects, and have improved longevity. (A) Mucosal-to-serosal flux of ^{51}Cr-EDTA as measured in Ussing chambers was used to measure the paracellular permeability of the colons from young and old germ free mice (n = 5

to 8). There was no significant increase in permeability in old germ free mice. **(B)** Survival analysis showing all-cause mortality of WT and GF mice up to 600 days of life. Differences in the survival curves were analyzed by Log-rank (Mantel-Cox) test. **(C)** Plasma cytokines are not higher than young germ free mice and are lower than WT SPF mice (*n* = 3 to 5). **(D)** Histological analysis of lung sections stained with H&E from young and old germ-free mice do not indicate any increased leukocyte infiltration with age (20X magnification; one representative image of at least three mice). **(E)** IL6 levels in the lung homogenates of old germ free mice are not higher than young WT or young germ-free mice **(F)** IL6 production in the whole blood of young and old WT SPF and GF mice following stimulation with LPS or a vehicle control (PBS). Old germ free mice do not have higher levels than young WT SPF or young germ free mice(*n* = 5 to 9). Significant changes shown are relative to young WT mice. **(G)** Macrophages from young and old germ-free mice do not differ in their ability to kill *S. pneumoniae* (*n* = 3). Results represent the mean ± SEM of 3 biological replicates. **(H)** Bone marrow derived macrophages from old germ free mice do no not have decreased killing or produce more IL6 following stimulation with LPS or a vehicle control (PBS) in macrophages from young GF mice (*n* = 5). Statistical significance was determined using the Mann-Whitney test or two-way ANOVA with Fisher's post-test where appropriate. $p < 0.05$ is indicated by *; $p < 0.005$ by ** and $p < 0.0005$ by ***.

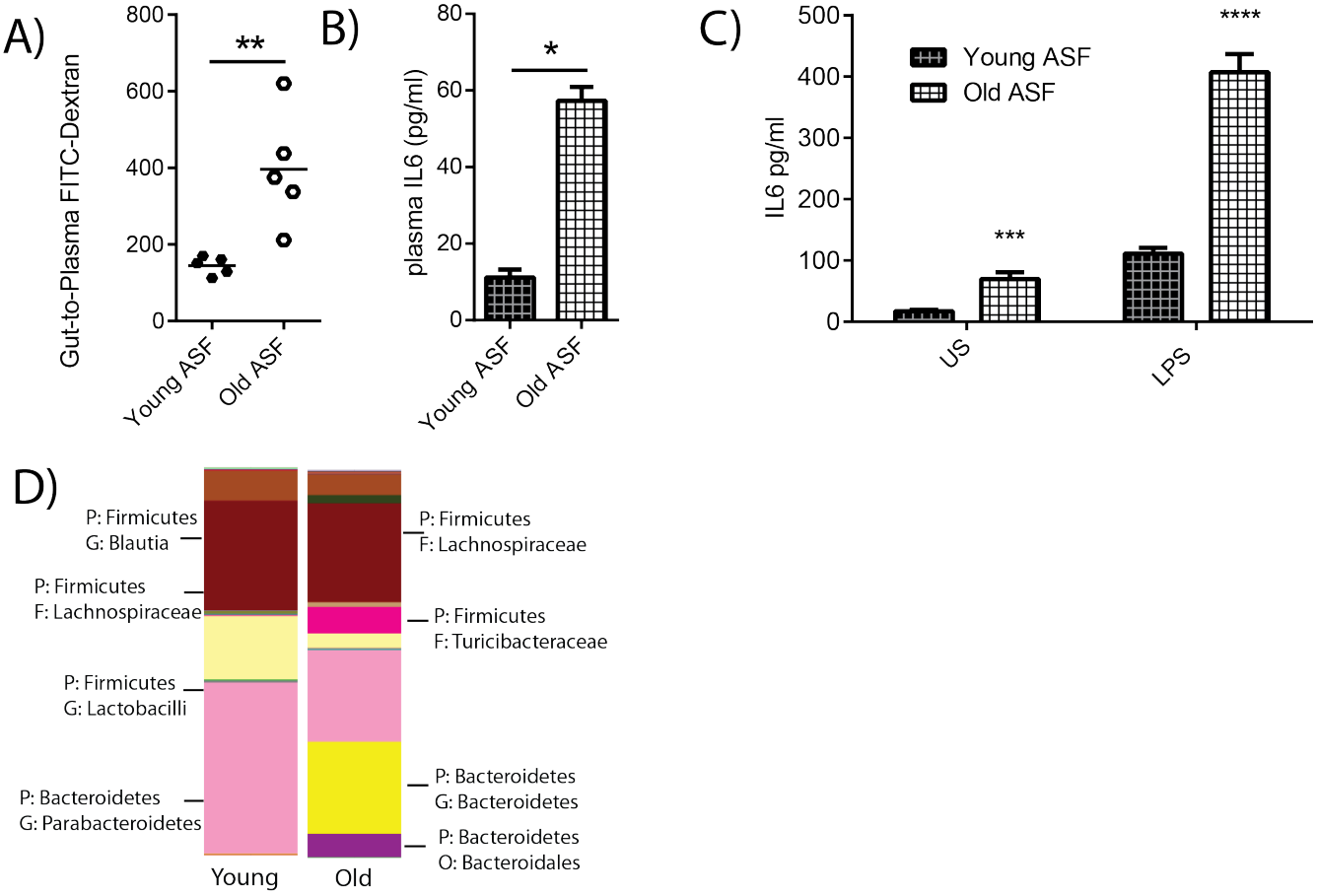

Figure 5. Microbial dysbiosis occurs in response to a minimal microbiota.**(A)** Mice with a minimal ASF-derived microbiota were aged and their intestinal permeability was measured via FITC-dextran oral gavage assay (n = *5*). Old ASF mice had higher intestinal permeability than young ASF mice in addition to higher levels of **(B)** plasma IL6. **(C)** IL6 production after LPS stimulation in whole blood was higher in old ASF mice (n=3). (D) Taxa summary of microbiota of young and old ASF mice indicate that age-related microbial dysbiosis occurs. Statistical significance was determined using the Mann-Whitney test or two-

way ANOVA with Fisher's post-test where appropriate. $p < 0.05$ is indicated by *; $p < 0.005$ by ** and $p < 0.0005$ by ***.

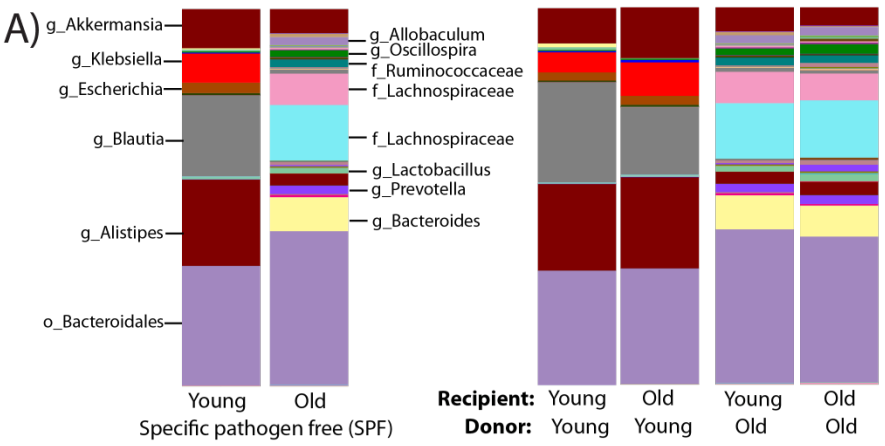

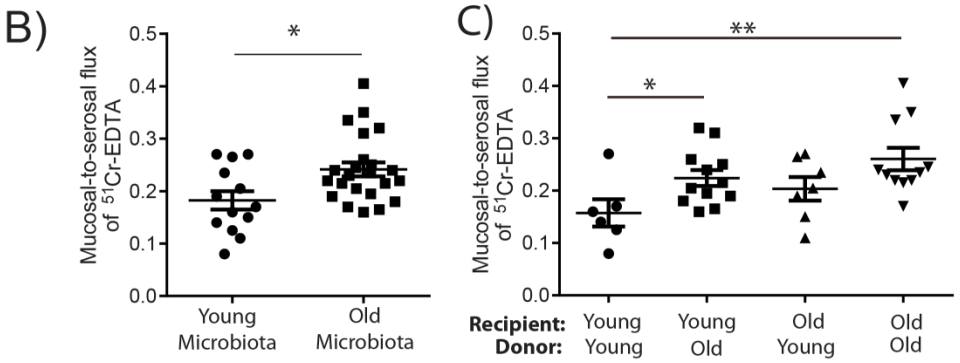

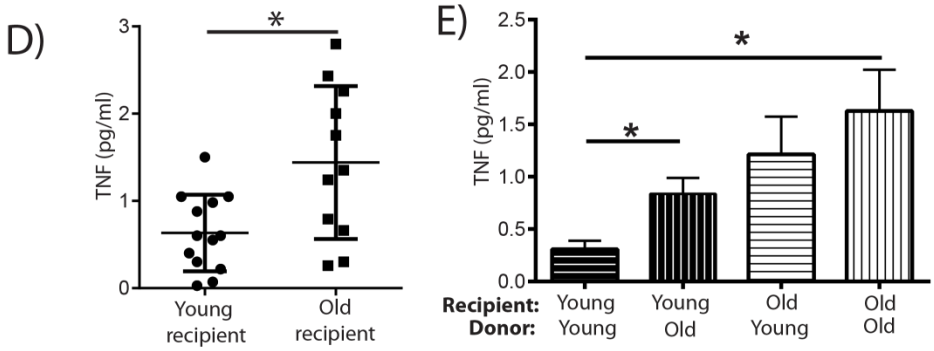

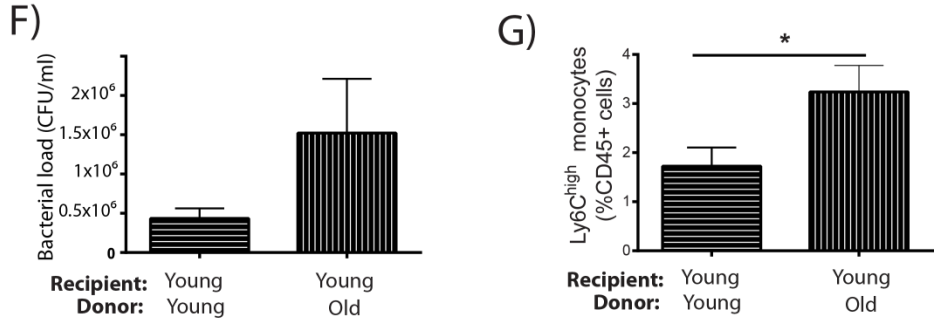

Serum cytokines here

Figure 6. **Age-associated inflammation is dependent on the composition of the intestinal microbial community. (A) The composition of the young and old microbiota is retained upon transfer to young or old germ free mice. (B)** Paracellular permeability was measured in germ-free mice colonized with young and old microbiota (n=6-8 mice per group). There was a statistically significant increase in paracellular permeability in mice colonized with old microbiota (n=23 total, n=11 young mice + n=12 old mice) compared to young microbiota (n=13, n=6 young mice +n=7 old mice). Age-related microbial dysbiosis and host age contribute to intestinal permeability. Colonization of young germ-free mice with old microbiota increased (C) paracellular permeability compared to those colonized with young microbiota ($p<0.05$). Although there was a trend towards old mice colonized with old microbiota having higher paracellular permeability than old mice colonized with young microbiota, this was not significant. (n=6-8 mice per group). (D(E) (F)Young germ-free mice colonized with young (n=6)and old (n=8) microbiota were intranasally colonized with *S. pneumoniae.* Although bacterial loads in the nasopharynx were not different between mice colonized with young and old microbiota cellular inflammation as measured by increased inflammatory/Ly6C^{high} monocytes (F), and serum cytokines (G) were significantly higher in mice colonized with the old microbiota..Bars represent the mean +/- SEM. Significance was determined by an unpaired t test. $p < 0.05$ is indicated by *; $p < 0.005$ by **.

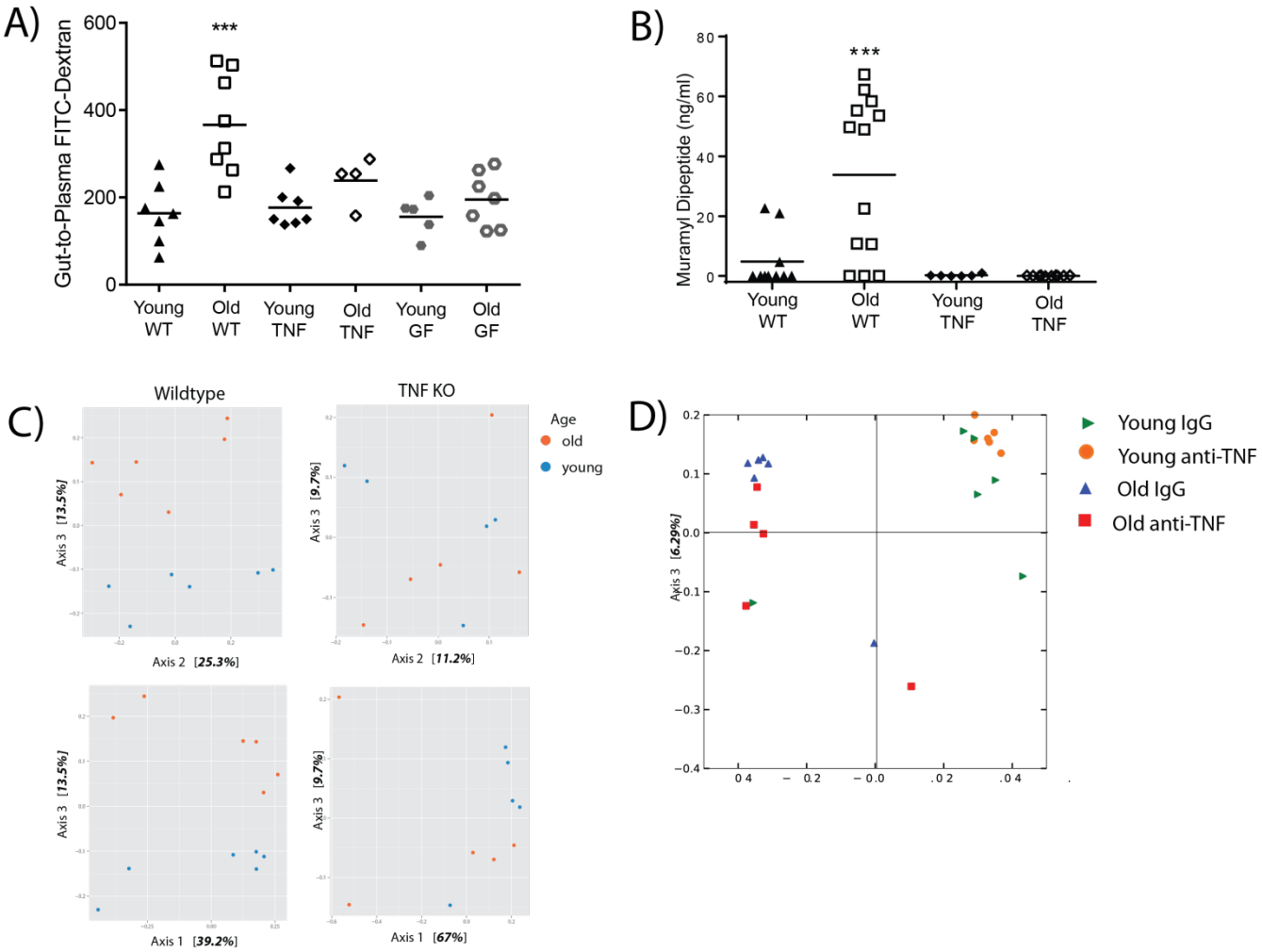

Figure 7. Microbial dysbiosis occurs with age and inflammation. (A) Intestinal permeability, as measured by plasma FITC-dextran following oral gavage, and was increased in old WT/SPF but not old TNF KO or old germ-free mice. **(B)** Circulating muramyl dipeptide (MDP) is increased in old SPF WT mice. Old TNF KO and germ-free (GF) mice are not significantly different from young SPF mice (n = 5 to 10). GF mice do not have any detectable MDP in the circulation. **(C)** Principal coordinate analysis based on Bray-Curtis demonstrates that the microbial communities of old WT mice diverge from young mice but this is not the case in old TNF KO mice. Chi-squared of the likelihood ratio test in DESeq2 shows old and young microbiomes are significantly different ($p < 0.001$). **(D)**Anti-TNF (Adalimumab) or a human IgG isotype control were administered at a dose of 50ng/g of body weight every other day for two weeks. Principal co-ordinate analysis was used to visualize differences in the microbial communities after 2 weeks of anti-TNF treatment. Anti-TNF treatment altered the composition of the fecal microbiota of old but not young mice.

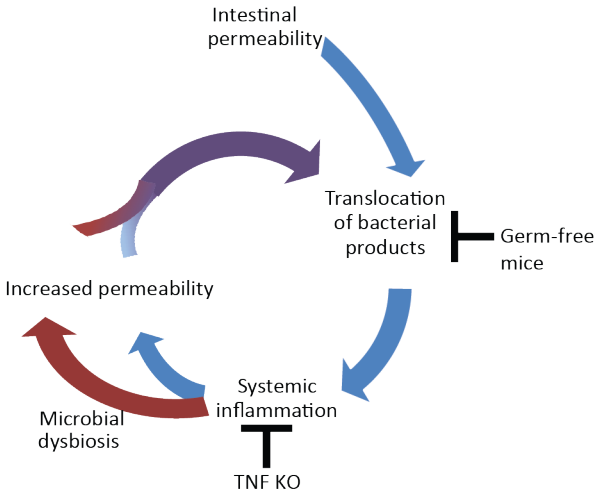

Figure 8. Proposed model of gut-microbe dependent induction of age-associated inflammation. Basal translocation of microbial products occurs throughout life; however with age, these induce an inflammatory response, which contributes to microbial dysbiosis. Microbial dysbiosis increases intestinal permeability which increases intestinal permeability and bacterial translocation. This feed-forward process increases with age.

Supplementary Figure 1.

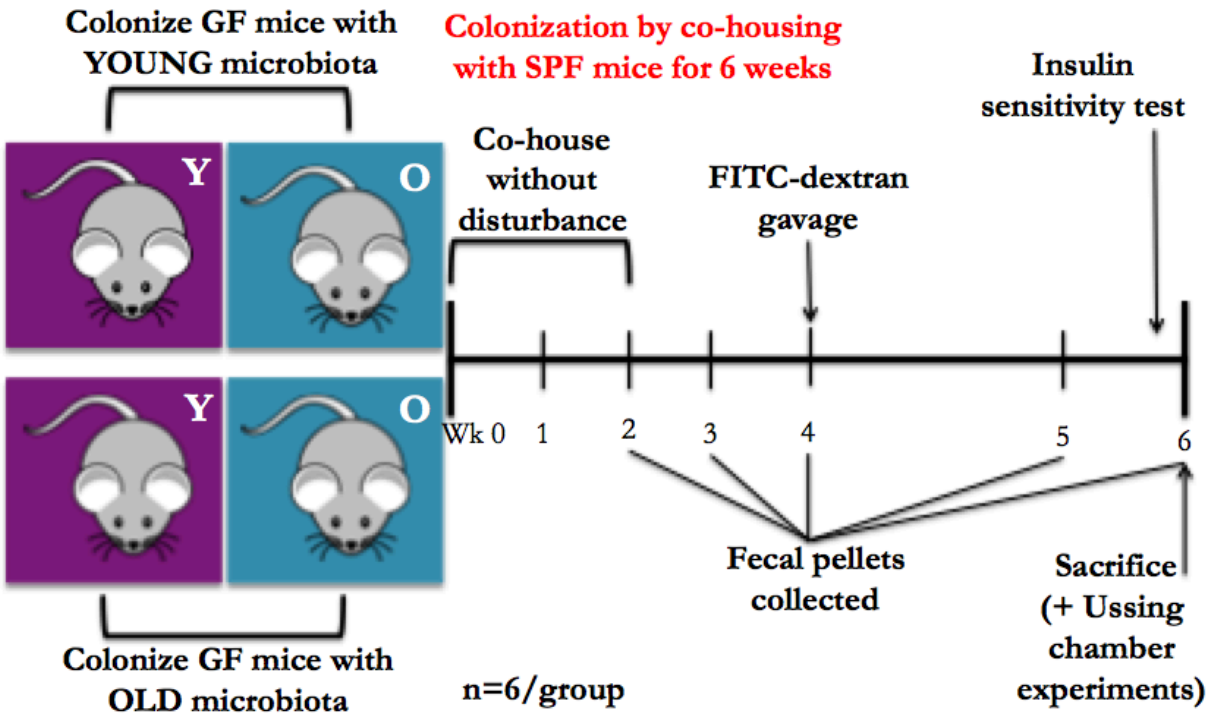

The experimental design for germ-free colonization experiments. Briefly, young and old germ-free mice are colonized with either the young or old microbiota via the co-housing method. Mice are co-housed without disturbance for a total of two weeks. Following the two weeks, fecal pellets are collected on a weekly basis until the point of sacrifice. After four weeks of initial co-housing, a FITC-dextran gavage is performed. Approximiately 5.5 weeks of colonization, an insulin sensitivity test is performed. Sacrifice, tissue collection and analysis occur six weeks after colonization.

Supplementary Figure 2.

Dilutions for staining colonic cells

Antibody	Fluorophore	Dilution	Laser
Zombie	APC efluor 780	1/250	Red
CD3	APC efluor 780	1/100	Red
CD45	Pacific Blue	1/75	Violet
CD11b	PerCP Cy5.5	1/200	Blue
CD64	APC	1/100	Red
MHCII	AF700	1/100	Red
Ly6C	FITC	1/300	Blue
CCR2	PE	1/50	Blue
F4/80	BV605	1/100	Violet
TNF	BV650	1/50	Violet
IL-6	PerCP efluor 710	1/50	Blue
IL-10	PE/Dazzle 594	1/50	Blue

Dilutions for staining blood and lung cells

Antibody	Fluorophore	Dilution	Laser
CD45	Pacific Blue	1/75	Violet
CD11b	PECy7	1/400	Blue
Ly6C	FITC	1/400	Blue
CCR2	PE	1/50	Blue
F4/80	APC	1/250	Red
CD3	AF700	1/100	Red
CD19	AF700	1/100	Red
NK1.1	AF700	1/100	Red
IL-6	PerCP eFluor710	1/50	Blue
TNF	BV650 (Qdot605 or eF650NC)	1/50	Violet

Supplementary Figure 3.

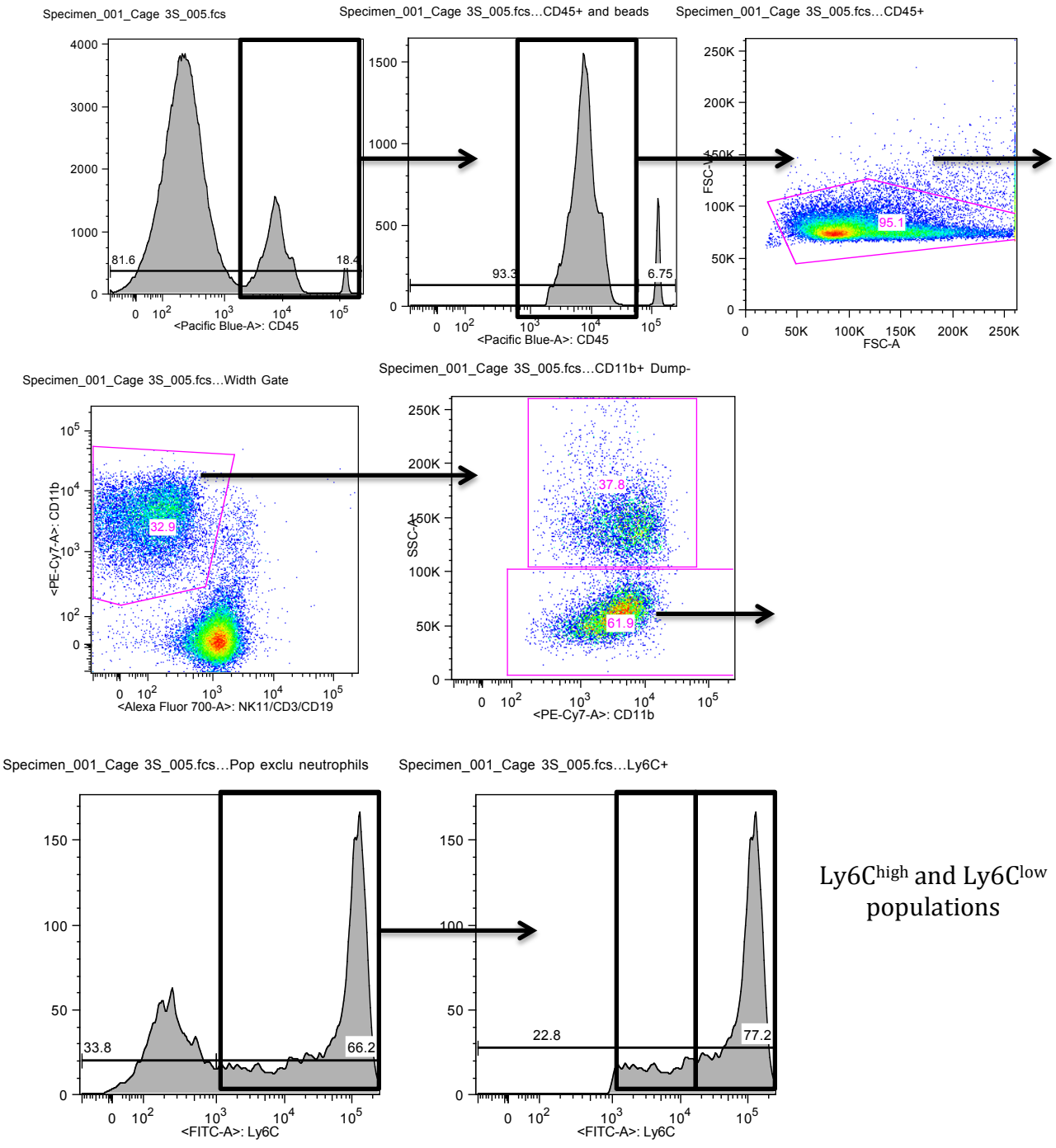

Ly6C^{high} and Ly6C^{low} populations

Gating strategy for the identification of Ly6C^{high} monocytes in the blood.

Supplementary Figure 4.

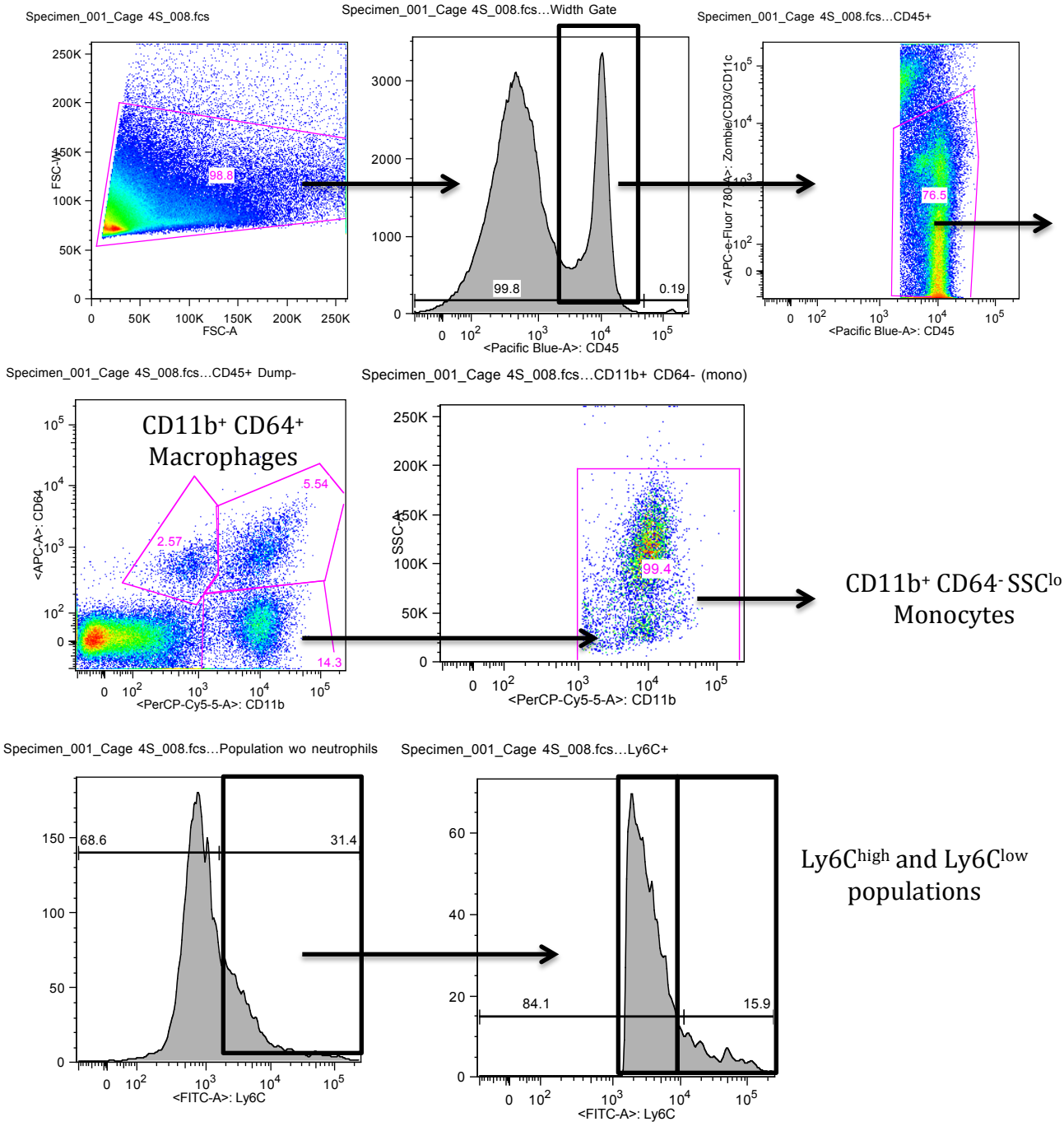

Gating strategy to differentiate between macrophages and monocytes in the colon.

Supplementary Figure 5[1,2].

INTEGUMENT	
Alopecia	Hair loss due to age-related balding and/or barbering (fur trimming)
Loss of fur colour	Change in fur colour from black to grey or brown
Dermatitis	Inflammation, overgrooming, barbering or scratching causing skin erosion. Can result in open sores anywhere on the body
Loss of whiskers	Loss of vibrisse (whiskers) due to aging and/or whisker trimming
Coat condition	Ruffled fur and/or matted fur. Ungroomed appearance. Coat does not look smooth, sleek, and shiny
PHYSICAL/MUSCULOSKELETAL	
Tumors	Development of tumors or masses anywhere on the body
Distended abdomen	Enlarged abdomen. May be due to tumor growth, organ enlargement, or intraperitoneal fluid accumulation
Kyphosis	Exaggerated outward curvature of the lower cervical/ thoracic vertebral column. Hunched back or posture.
Tail stiffening	Tail appears stiff, even when animal is moving in the cage. Tail does not wrap freely when stroked
Gait disorders	Lack of coordination in movement including hopping, wobbling, or uncoordinated gait. Wide stance. Circling or weakness
Tremor	Involuntary shaking at rest or during movement
Forelimb grim	A decline in forelimb grip strength
Body condition score	Visual signs of muscle wasting or obesity based on the amount of flesh covering bony protuberances
OCULAR/ NASAL	
Cataracts	Clouding of the lens of the eye. An opaque spot in the center of the eye
Corneal opacity	Development of white spots on the cornea. Cloudy cornea
Eye discharge/swelling	Eyes are swollen or bulging (exopthalmia). They may exhibit abnormal secretions and/or crusting
Microphthalmia	Eyes are small and/or sunken. May involve one or both eyes
Vision loss	Vision loss, indicated by failure to reach toward the ground

[1] Whitehead JC, Hildebrand BA, Sun M, et al. A Clinical Frailty Index in Aging Mice: Comparisons With Frailty Index Data in Humans. *The Journals of Gerontology Series A: Biological Sciences and Medical Sciences*. 2014;69(6):621-632. doi:10.1093/gerona/glt136.

[2] Aartsma-Rus, A., van Putten, M. Assessing Functional Performance in the *Mdx* Mouse Model. *J. Vis. Exp.* (85), e51303, doi:10.3791/51303 (2014).

	when lowered by the tail
Menace reflex	Rapid eye blink and closure of the palpebral fissure in response to a nontactile visual threat to the eye. Measures of the integrity of the entire visual pathway including cortical components
Nasal discharge	Signs of abnormal discharge from the nares
DIGESTIVE/ UROGENITAL	
Malocclusions	Incisor teeth are uneven or overgrown. Top teeth grow back into the roof of the mouth or bottom teeth are long and easily seen
Rectal prolapse	Protrusion of the rectum just below the tail
Vaginal/uterine /penile prolapse	Vagina or uterus protrudes through the vagina and vulva. Penus cannot reenter the penile sheath
Diarrhea	Feces on the walls of the home cage. Bedding adheres to feces in cage. Feces, blood, or bedding around the rectum
RESPIRATORY	
Breathing rate/depth	Difficulty breathing (dyspnea), pulmonary congestion (rales) and/or rapid breathing (tachypnea)
DISCOMFORT	
Mouse grimace scale	Measure of pain/discomfort based on facial expression. Assessment of five facial features: orbital tightening, nose bulge, cheek bulge, ear position (drawn back), or whisker change (either backward or forward)
Piloerection	Involuntary bristling of the fur due to sympathetic nervous system activation
OTHER	
Temperature	Increase or decrease in body temperature
Weight	Increase or decrease in body weight
MUSCLE STRENGTH	
Cage hang test	Measure of muscle strength by hanging mice upside down on a wire rack. The length of time which a mouse can hold on indicates their muscle strength.

Modified clinical signs of frailty measured in young and old mice. Table modified from Whitehead et al., 2014 and van Putten et al., 2011 (1, 2). Each measure in the frailty score is scored with either a 0, 0.5, or 1 to indicate how severe that change is. The values are added in order to determine the overall frailty score of a mouse. Each cage hang test was completed in triplicates. Maximum time was indicated if mice were able to hold on for 60 seconds.